DYNAMIC ANALYSIS OF THE 'CUT-AND-COVER' TYPE UNDERGROUND NUCLEAR REACTOR CONTAINMENT

HUSSEIN WAHBA MOHAMED
EL-TAHAN

DYNAMIC ANALYSIS OF THE 'CUT-AND-COVER' TYPE UNDERGROUND NUCLEAR REACTOR CONTAINMENT

by

Hussein Wahba Mohamed El-Tahan, B.Sc.

A Thesis submitted in partial fulfillment
of the requirements for the degree of
Master of Engineering

Faculty of Engineering and Applied Science
Memorial University of Newfoundland

August 1977

St. John's Newfoundland, Canada

To My Parents

ABSTRACT

Nonlinear dynamic structure-medium interaction for 'cut-and-cover' type underground nuclear reactor containments is studied for earthquake excitation. The structure considered is a reinforced concrete containment for a 1100 - MWe power plant buried in a dense sand medium. The analysis has been carried out using the recently developed computer programmes: LUSH (plane-strain finite element), and SHAKE (one-dimensional wave propagation analysis). The high frequency ranges, which must be considered in the study of soil-structure interaction for nuclear power plants, and the nonlinear soil behaviour during strong earthquakes are adequately taken into account in this study.

Parametric studies for the response of the containment and the surrounding medium are carried out for: 1) containment shape (high horseshoe, flat horseshoe and semi-circular roof-vertical walls), 2) relative stiffness of the containment and the medium, 3) depth of burial of the containment (shallow, intermediate and deep embedments), 4) relative stiffness of the medium and filling material (original fill, loose sand, stabilized sand and reinforced earth), 5) thickness of the backfill jackets (10ft. and 70ft.), 6) isolation of the containment using energy absorbing jackets around the containment (polyurethane foam and foamed concrete), and 7) type of surrounding medium (sand and rock). Comparative studies are presented for rock vs. sand siting and aboveground vs. underground siting in sand.

The response values determined are: i) time history of acceleration, displacement and stresses, ii) maximum stresses and maximum accelerations, and iii) acceleration response spectra. Plotting of these results using the CALCOMP Plotter involved writing of twelve computer

programmes.

The results indicate that: i) The high horseshoe shape is the best among the three shapes considered decreasing the containment stresses by 10-20%, ii) Flexible containments are better than rigid ones, iii) Successive reductions in containment stresses to 67% of the initial values are associated with each additional 70ft. embedment depth, iv) The relative stiffness of the filling material and the medium has the most significant effect on the response. The lower the modulus of elasticity of the filling material, the greater is the reduction in the containment and medium stresses. A filling material with stiffness 30% lower than that of the medium, reduces the stresses by 30% in the containment, and about 20% in the medium, v) Using a jacket of energy absorbing material (polyurethane foam) in a sand medium reduces the containment and medium stresses by 65% and 40% respectively, vi) A reduction in the containment stresses of about 20% is achieved using a reinforced earth jacket, vii) Increasing the width of the backfill side-cover increases the stresses in the containment and the medium, viii) The response values of the medium near the containment are considerably affected by the interaction. The interaction effect is larger for aboveground siting, and ix) A containment in the sand medium is subjected to dynamic loading higher than that for a rock medium.

Recommendations are made for further studies to account for more realistic modelling and material behaviour, and more complex plant configuration and structural details.

ACKNOWLEDGEMENT

The author is very grateful to his supervisor, Dr. D.V. Reddy, Professor of Engineering and Applied Science, for his excellent guidance, encouragement, and continous support with the provision of extensive reference material during the course of the research, and for his careful review of the manuscript. Working with Professor Reddy will always be remembered as an opportunity and a most rewarding experience.

The author wishes to express his appreciation to Dean R.T. Dempster for his help and keen interest evinced to support this investigation.

The generous financial support offered by Memorial University of Newfoundland is gratefully acknowledged. Special thanks are due to Dean Aldrich, School of Graduate Studies, and Professor El-Hawary, Chairman, Graduate Studies Committee, for their constant advice and encouragement.

Mr. G. Somerton of N.L.C.S. (Newfoundland and Labrador Computer Services) provided valuable help in computerized plotting, and Professor T.W. Kierans evinced keen interest with input of ideas and literature.

Finally, the author wishes to specially thank his wife for her help in preparing the data for the computer programmes and the CALCOMP plotter, and her continuous encouragement, understanding and patience.

The computing costs were supported in part by NRC Research Grant No. A 8119.

TABLE OF CONTENTS

Page

Page

Page

LIST OF TABLES

LIST OF FIGURES

Figure | Page

NOTATION

$\{A\}$	The amplification function
E	The elasticity modulus
G	The shear modulus
G_{max}	The shear modulus at small strains
G^*	The complex shear modulus
h_{max}	Maximum vertical element size
h_f	The highest frequency contained in the input motion record (Hz)
Im ( )	The imagenary part of
$[K]$	The stiffness matrix
k_o	The coefficient of lateral pressure at rest
k_{2max}	The shear modulus parameter
KINT	The interpolation coefficient in frequency domain
$[M]$	The mass matrix (lumped or consistent)
$\{m\}$	The load vector corresponding to $\ddot{y} = 1$
N	Number of points in the digitized input motion record
Re ( )	The real part of
$\{U\}$	The displacement amplitudes
$\{u\}$	Relative displacements of nodal points
v_s	Shear wave velocity
w	Material density (pcf)
$\ddot{Y}$	Amplitude of the hormonic acceleration
$\ddot{y}(t)$	The given input acceleration
β	The damping ratio
Δt	Time interval of the digitized input motion

λ_s	Wave length of the shortest wave
ω	Frequency (rad/sec)
$\sigma'_m(y)$	The effective mean normal stress at depth y
σ'_v	The effective vertical pressure
ν	Poisson's ratio

CHAPTER I

INTRODUCTION

1.1 General

Underground siting has been suggested as an effective alternative to the aboveground siting in view of the "inherent general reduction to complexity of seismic amplification, benefits of structural and biological integrity, and possibilities of urban siting, ecological considerations, reduced effects on the landscape, ability to design three-dimensionally, seperation of component facilities, support capability to equipment, reduced power transmission costs, increased number of acceptable units and power capability from a single location, and reduction of decommissioning problems" (Reddy and Kierans [75]).

The problem of analysing large underground nuclear reactor containments to resist dynamic excitation by nuclear explosions or earthquakes is of considerable interest. In contrast to aboveground siting, engineers are restricted, to a certain extent, by a lack of adequate literature and limited actual experiences (only four small underground nuclear reactors have been constructed, all in Europe). The 'cut-and-cover' technique is of considerable importance specially for central Europe as only this concept can contribute to a solution of the siting problems.

1.2 Statement of the Problem

The purpose of this investigation is to analyse the nonlinear dynamic response of the 'cut-and-cover' type underground nuclear reactor containments to earthquake excitation taking into consideration the soil

nonlinear behaviour, and to study the effect of containment geometry, burial depth, and 'filling material' properties.

Acceleration time histories and response spectra, and displacements and stresses, are obtained and plotted using the CALCOMP plotter.

1.3 Layout

Chapter I presents a general description of the problem.

Chapter II reviews the literature on underground nuclear reactor containments with emphasis on the 'cut-and-cover' concept.

Chapter III presents the analysis procedure, modelling and the response of free field and soil-structure systems. The methods used to determine the values of all the parameters needed for the analysis, including the details of the finite element model, are discussed in detail.

Chapter IV presents parametric studies and the results obtained for variable geometry of the containment, depth of burial, relative stiffness of the medium and the filling material, thickness of the backfill jackets, isolation of the containment using energy absorbing jackets, and the type of the surrounding medium. Comparative studies are also presented for rock vs. sand siting and aboveground vs. underground siting.

Chapter V compares the results obtained in Chapter III and IV. The conclusions from this investigation and recommendations for further research are presented at the end of this chapter.

Appendix A presents listings of sample plotting programmes written to plot the results of this investigation using the CALCOMP plotter.

Appendix B presents brief descriptions of the programmes used in the analyses (LUSH and SHAKE).

CHAPTER II

REVIEW OF LITERATURE

2.1 General

Underground and underwater sitings have been suggested as possible alternatives to surface siting to provide increased containment protection; this study deals with underground siting. The concept of the underground siting of nuclear reactors for power generation is not new; in the mid-1950's Beck [8] carried out studies to evaluate the potential for underground siting. In Europe, a total of four nuclear reactors have been located underground, the details of which have been described by Watson, Kammer, Lange, Selzer and Beck [98]. Studies on the underground siting of large nuclear power plants are under way in the U.S.A., Sweden, Norway, and Switzerland. A cut-and-cover nuclear reactor is being designed for Israel and there is considerable interest in the same concept in other countries like West Germany.

2.2 Underground Siting Concept

Since 1958 several studies have been conducted into the feasibility of placing nuclear power plants underground. Most of these studies deal with the concept of placing a large size reactor in a covern excavated in massive rock. United Engineers Inc. [97] have summarized the feasibility studies carried out by Refs. 8 and 98, Blake et al [13], United Engineers and Acres Inc. [96], Swiger [89], Chester [21], Smernoff [87], Rogers [77], Norsk [67], Oak Ridge National Laboratory [70], Holmes and Narver Co. [43], and Brekke and Glass [15]. The general conclusions made in these reports and a comparison between these studies are listed in

Table 1. A summary of the assessment studies of underground siting (with emphasis on the 'cut-and-cover' concept) which have been carried out by Kröger and Altes [53] is presented in Table 2. The discussion of the advantages and disadvantages of the underground siting by Crowley [29] and Buclin [16], based on field experience and practical problems, is of considerable interest. The conclusions are that the underground siting concept should receive greater attention in siting consideration, research and development. Reddy and Kierans [75] have summarized the advantage of the underground nuclear reactors as follows:

"(1) Potential improvement in containment fail-safeness by virtue of the protection of several hundred feet of media impervious to radioactivity notwithstanding functional penetrations.

(2) Reduction of structural change from deliberate or accidental damage due to

(a) military attacks;
(b) nuclear or other blasts;
(c) vandalism; and
(d) air and sea vehicle impacts and explosions.

(3) Improvement in plant configuration by the ability to design three-dimensionally as opposed to surface structure two-dimensionally.

(4) Separation of component facilities such as containment structure and turbine plant structure.

(5) Current exploratory techniques for the location of an underground site involving tunnels and shafts will expose faults. This is not so in the case of surface siting which may involve the risk of an undetected hidden fault in or close to an alluvium covered surface site.

(6) The surrounding medium provides three-dimensional support capability to functional structures such as a turbine-generator system and allows for the bracing of secondary equipment over the full height.

(a) Power transmission costs and construction periods may be reduced by location close to load centers.
(b) Savings in buildings, substructures and foundations.
(c) Excavated rock can be used as construction material.
(d) No holdups in construction schedule due to adverse weather.

(8) Use of a single underground site with provision for multiple units involving increased power capability would be more economical than a surface site with limitations on size and number of units. There would be a general reduction of decommissioning problems due to more effective isolation.

(9) Systems and technology of cooling arrangements are essentially the same as for surface plants with modifications needed only in configuration and control".

2.2.1 Alternate Underground Concepts

Fig. 2.1 presents the configuration given by Ref. 53, and described in Ref. 97, as follows:

i) Surface Mounded Type [21]: A plant constructed at ground level with backfill material mounded around the structure.

ii) Cut-and-Cover in Soil or Rock: A plant constructed in open cut excavation in an unconsolidated soil [13] or in rock [89] subsequently backfilled over the containment to the ground surface.

iii) Underground in Rock [96]: A plant constructed in a covern excavated at depth in rock, either in a hillside or below general grade level.

Kierans, Reddy, and Heale [51] have described the basic types of underground openings in rock and soil (Fig. 2.2).

2.2.2 Cut-and-Cover Type

Cut-and-Cover type underground nuclear reactor containments are suitable for siting in soils and weak rock. The cut-and-cover concept can be used in any geological formation and sometimes it is the only configuration which can contribute to a solution of siting problems under the natural environmental conditions of many regions like central Europe and specially Germany. Ref. 13 indicated that not only is the cut-and-cover technique feasible and suitable for all reactor types, but also appears to introduce little additional cost while accomplishing the objective of confinement of radioactivity most effectively (by controlling the permeability of the filling material).

Fig. 2.3 presents the semi-embedment and the total embedment configurations proposed by Ref. 53 as alternative concepts for the cut-and-cover

type underground reactor containments.

2.2.2.1 Construction

The construction technique of the cut-and-cover reactors does not propose any extensive modifications of plant design so that most of the experience acquired to date with aboveground plants can be transferred to the new situation [53]. According to the present state-of-the-art, slurry trenches and freezing techniques may be used for the vertical walls of the excavation [54].

2.3 Seismic Loading

2.3.1 General

The determination of the response of any structure to earthquake excitation is complicated by the dependence on a large number of factors, such as nature and intensity of the earthquake, structural details (shape, thickness ...etc.), construction materials, siting (aboveground or underground), and the surrounding medium (rock or soil).

2.3.2 Effect of Depth

Theoretical studies carried out by Krishna and Arya [52] indicate that displacements are greater in soft soil than in rock. However, it is possible that for a large soil layer a great deal of the energy would be absorbed in the subsoil layers and the motion felt at the surface could be small. Observations of the El Centro Earthquake revealed that if the thickness of the clay layer had been only 30 ft., rather than 100 ft., the maximum acceleration could have been about 0.5 to 0.6g instead of 0.13g [97]. The results of the measurements during earthquakes in Japan show that the underground acceleration is 1/2 to 1/3

that at the surface, while at similar depths there is little difference in displacement between the surface and underground [97]. Similar observations were obtained by Saita and Suzuki [80]. Nasu [66] has observed that the amplification of earthquake motion aboveground, compared to that in a tunnel 500 ft. below the ground surface decreases as the period of the earthquake increases. Ref. 75 indicated that the seismic loading on an underground structure located in a rock continuum is not affected by the amplification of body (P and S) and surface (L) waves due to soil layers. Glass [38] indicated that "when the cavity is located deeper than about one quarter wave length from the surface, the structure is not affected by the doubling of displacement amplitude which occurs upon reflection of body waves at the earth's surface".

2.3.3 Type of Medium

It has been noticed during all strong earthquakes that within the same locality even similar structures suffer unequal damage. Structures on, or in rock usually suffer the least (Tandon [91] and Kanai [49]), while those on loose soil or on the surface suffer the worst damage (Okamoto [71] and Kanai [50]).

In the study carried out by Ref. 91, on seismic intensity for foundations on the soil surface and on rock, for the Assam Earthquake, it has been found that the intensities experienced in rock are far less than those of soil foundations. During the Anjar Earthquake of 1956, the eastern portions of the town of Bhuj, in which the buildings were founded on alluvium, suffered extensive damage, while the western portion of the town founded on rock suffered very little damage. Ref. 97 pointed out that soft soil amplifies the motion due to its low density and stiffness (elasticity modulus). A detailed study by Mithal and Srivastava [63] indicated that areas with compact, massive and consolidated

rocks, and dense and compact boulder strata with low water content, behave as stable masses during earthquakes.

2.3.4 Tunnel Damage During Earthquakes

Experiments carried out by Bulson [17] on square tubes buried in compacted sand and subjected to static and dynamic (blast) loadings indicated that "although flexible structures have definite advantages statically, rigid tunnels might be more suited to the carrying of dynamic loads".

Ref. 71 has made an extensive study of tunnel damage due to the earthquake loading in Japan. The findings of this study are: i) for the same type of medium, the damage ratio is higher in tunnel sectors with thick lining than in sections with thin lining, ii) regardless of the type of medium, the damage ratio is also higher in thick linings, and iii) the damage ratio is higher for tunnels with poor ground geology. The conclusions from the study indicate that the safety of a tunnel at the time of an earthquake is influenced by the conditions of the natural ground, and that when these conditions are poor, they cannot be overcome by an increase in the lining thickness.

2.3.5 Conclusion

Generally, displacements, accelerations, and velocities are higher at the ground surface than those below it. Structures in, or on a weak medium, will be subjected to larger seismic effects than those for a relatively stiff medium. Although it is thought that an increase of lining thickness can better resist seismic forces, in some cases, it results in an increase in seismic stresses producing a reverse effect. However, the deep underground siting concept offers definite seismic

load reduction.

2.4 Analysis

As this investigation is restricted to 'cut-and-cover' type nuclear reactor containments in soil, the review of analytical procedures discussed in this section will be confined to soil siting.

Analyses for underground siting in rock have been presented in many references. Ref. 75 presented comprehensive review with extensive bibliography. Static analyses have been presented by Sigvaldason [86], Benson, Kierans and Sigvaldason [9], Yu and Coates [102], Kulhawy [57-59], Ghaboussi and Ranken [37], Chang, Nair and Karwoski [20], Ghaboussi, Wilson and Isenberg [36], and Ref. 2. Dynamic Analyses have been carried out by Blakey [14], Moselhi [64], Sheha [70], Heale and Reddy [41], Reddy and Heale [74], Murthy and Reddy [65], and Forrestal, Reddy and Herrmann [35].

2.4.1 Static Analysis

Compared to the relatively new field of geotechnical engineering, the earth-structure interaction problem is very old. The limitations of the Coulomb [28] and Rankine [73] theories in determining the resultant of earth pressure acting on a simple retaining wall are due to high idealization of the soil and the wall; besides, the deformation of the wall cannot be obtained.

Information about wall deformation associated with more realistic conditions has been obtained only through experimental work such as that of Terzaghi [92-94], Rowe and Peaker [79], and James and Bransby [48]. Elastic analyses (Hetenyi [42] and Finn [34]) and limit theories (Hansen [40], Drucker [32] and Sokolovski [88]) have been developed to

account for the effect of wall deformations. For underground structures, Burns [18] developed a theory for an elastic cylinder in an isotropic linearly elastic field loaded by a uniform static surface pressure. Allgood [3, 4] simplified the equations governing elastic behaviour and indicate their applicability to design if proper effective soil moduli are used. In view of the limitations of the above analytical solutions in simulating real problems (e.g. real material behaviour, foundation deformation and the effect of construction sequence), empirical and semi-empirical technique are generally used to design many earth support systems other than retaining walls. Peck [72] and Deere, Monsees and Schmidt [31] have updated the available empirical techniques in the case of lined tunnels.

Atkinson and Cairncross [6] studied the stability of a shallow unlined circular tunnel supported by a uniform internal pressure using theory of plasticity. Neglecting the soil self-weight, they obtained relatively simple solution for the particualr case of a uniform pressure applied at the soil surface. The solution obtained is of limited use in evaluating the stability of tunnels in real soils whose self-weight may itself cause instability in tunnels. To investigate this problem further, Atkinson, Brown and Potts [7] carried out a series of laboratory tests on unlined circular tunnels in dense sand. The results indicated that the stability of a tunnel in dense sand is approximately independent of its depth.

With the advent of the high-speed computer and the rapid development of numerical method of analysis, the finite element method proves to be one of the most powerful numerical techniques for the stress analysis of complex structural systems because of its ability to simulate realistic

soil or rock behaviour and complicated boundary conditions and construction sequences. Clough [23] presented a state-of-the-art report on the application of the finite element method to earth-structure interaction in which he concluded that the finite element method is "an analytical tool which can realistically simulate almost any class of earth-structure interaction problem". The finite element programmes developed by Wilson [99, 100] and Farhoomand [33] have been modified and used by Nossier and Takahashi [68] to study the behaviour of buried cylinders in soil and the effectiveness of backpacking due to static and dynamic surface loadings. Bjerrum, Frimann and Duncan [12] have presented a state-of-the-art report on earth pressure on flexible structures in which the behaviour of anchored sheet pile walls has been examined in the light of model tests, field observations, theoretical analyses and the finite element method.

2.4.2 Dynamic Analysis

2.4.2.1 General

External dynamic excitations for totally embedded structures are from ground motion due to nuclear blasts or natural earthquakes. Comparison of earthquake and blast-induced ground motion presented in Ref. 75 indicate remarkable similarity in the character, intensity, duration, frequency content and spectral shapes of the two motions.

Allgood [5] presented a summary of the available knowledge of soil-structure interaction as it pertains to facilities that provide protection from nuclear weapons effects. Howard, Ibàñez and Smith [44] presented a review and evaluation of the design standards and the analytical and experimental methods used in the seismic design of

nuclear power plants.

Various factors that affect the seismic loading on aboveground and underground structures are discussed in detail in Sec. 2.3.

2.4.2.2 Methods of Analysis

Four different analytical procedures can be used for soil-structure interaction problems. Analytical and semi-analytical solutions, the lumped parameter method, and the finite element method.

Analytical and semi-analytical methods available up to the present time (1977) are applicable only for simple geometry and loading (e.g. Yoshihara, Robinson and Merritt [101], Dawkins [30], Ali-Akbarian [2], Novak and Beredugo [69], and Tajimi [90]). Therefore, they are not practical for the complex configuration of a cut-and-cover structure in media with varying properties.

2.4.2.2.1 Lumped Parameter Method

Soil-structure interaction is represented by a system of lumped masses, springs and dashpots whose constants may be determined from the elastic half-space theory (e.g. Bielak [11] and Ref. 69). The applicability of this approach to soil-structure interaction of the underground structure, specially the 'cut-and-cover' type, seems to be very limited because i) available solutions for large media have only been derived for horizontally layered media configurations, ii) impedance functions have been derived only for simple foundations [44], and iii) it is difficult to simulate the surrounding medium and filling material. Hall and Kissenpfennig [39] presented a comparative study on the responses of deeply embedded foundations obtained by the finite element and the lumped parameter analyses and concluded that 'complex soil sites where

the soils are not horizontal layered must normally be analysed using the finite element approach'.

2.4.2.2.2 Finite Element Method

The finite element method offers a powerful tool in interaction problems involving foundation embedment, soil media with non-horizontal layers and other geometric irregularities, and the coupling between adjacent structures.

The solution of soil-structure interaction problems by the finite element method currently follows one of the two alternatives: i) solution with the structure and soil coupled as a single large model, or ii) solution using the sub-structure approach. Ref. 44 indicated that "due to the substructure method of separately performing modal extraction on the soil and the super structure, and then performing a coupled analysis using modal synthesis, there are apparent cost advantages to the technique for the large dynamic model often required for nuclear power systems".

Three numerical methods are used in the solution of the equations of motion; modal analysis, direct integration and the complex response (transform) method [62]. In contrast to the modal analysis method, the complex response and the direct integration methods permit using variable damping in each element.

Although the finite element method is capable of solving non-linear three-dimensional dynamic analysis problems, analyses carried out to date have been mainly two-dimensional for reasons of economy and computer size. Investigations carried out by Luco and Hadijian [61] have indicated that it is not possible to obtain a two-dimensional

representation which approximates both the dynamic stiffness and the radiation damping of the three-dimensional model, and that two-dimensional models for analysis of nuclear power plants lead to underestimation of the maximum response. Ref. 83 pointed out that errors up to 20-30% may occur due to the two-dimensional analysis of three-dimensional systems. Berger, Lysmer and Seed [10] indicated that good agreement between two and three-dimensional models of the response for points below the soil surface.

Analysis of the soil-structure interaction using the finite element method assumes that the motions in the system are generated by shear waves travelling upward. Ref. 83 indicated that while this assumption is a potential source of error, it is consistent with the normal simplification of complex engineering analysis purpose; and it is a reasonable representation of the actual conditions. Ref. 44 indicated that non-vertically travelling seismic waves may be significant in some cases.

2.4.2.2.3 Finite Element Modelling

Ref. 61 indicated that extreme care must be taken in modelling the actual soil-structure system with a two-dimensional finite element for dynamic analysis. Model dimension, mesh size, and soil properties should be carefully chosen to simulate the actual system properly.

(a) Boundaries

To overcome the problem of reflection at rigid boundaries, Ref. 14 carried out the analysis of an underground cavity subjected to a short-duration step pulse of few milliseconds so that the wave does not reflect from the boundary before the analysis ends. For longer time

durations, Kuhlemeyer [56] and Castellani [19] used viscous absorbing (transmitting) boundaries. Ref. 54 used displaced boundaries to simulate an infinite space. Ref. 62 indicated that if the soil damping is high (12% or more), energy radiating outwards from the vicinity of the structure is absorbed quickly, and the free field conditions are developed within a distance of 2 to 2 1/2 times the model depth. Other studies [61], based on continuum and finite element comparisons, indicated that placement of the boundary at 4 to 6 times the foundation width is required.

(b) Mesh Size

In applying the finite element approach to dynamic problems, the element size should be small compared to the wave length. A fine mesh is required to achieve adequate frequency transmission capability within the frequency band of interest. Investigations carried out by Costantino and Lufiano [26] indicated that the mesh must be able to transmit two or more times the required upper frequency of interest to enable adequate computation of motion. To simulate the propagation of waves adequately, Kuhlemeyer and Lysmer [55] proposed an empirical formula that the element size should not be larger than 1/4 or preferably 1/8 of the shortest wave length. Ref. 62 suggested that a value of 1/5 the shortest wave length gives acceptable results. Comparison of the results of the finite element analysis for fine and coarse meshes, and wave propagation analysis carried out by Ref. 83 indicate that while the fine mesh gave the same response spectra as that of the wave propagation, the spectral values for the coarse mesh were less than those of the fine mesh and wave propagation, especially at high frequencies.

A typical procedure often used in finite element analyses uses coarse elements away from the structure to minimize the number of degrees of freedom in the mesh. Costantino, Miller and Lufrano [27] pointed out that "these coarse elements are opaque to the higher frequencies transmitted through the finer elements, i.e., higher frequencies will be transmitted back into the mesh. Thus, the coarse elements will act as conventional boundaries at the higher frequencies thereby eliminating any advantages thought to be gained by the coarse elements".

(c) Dynamic Material Properties

Material properties required for the finite element analysis are damping ratios, shear moduli, unit weight and Poisson's ratio. Soil non-linear behaviour during strong earthquakes can be accounted for, in an approximate manner, using "the equivalent linear method", described by Idriss, Dezfulian and Seed [45], and based on experimental data collected from resonant column or triaxial test data for cyclic loading conditions [82].

Material damping is commonly introduced by defining Rayleigh damping matrix as a linear combination of the mass and stiffness matrices. According to this approach, the damping ratio, β, is frequency dependent; has large value at high and low frequencies and hence modes of vibrations at high and low frequencies are damped out. This can be a serious limitation in the analysis of structures containing critical equipment with high frequency characteristics such as nuclear power plants [83]. Recent development to eliminate this effect have been described by Ref. 62 by using a complex modulus, G*, defined as

$$G^* = G(1-2\beta^2 + 2i\beta\sqrt{1-\beta^2}) \quad \ldots\ldots\ldots\ldots\ldots\ldots\ldots\ldots\ldots\ldots\ldots\ldots \quad 2.1$$

where G = shear modulus. Ref. 39 indicated that the controlled damping, calculated according to Eqn 2.1, agrees very well with the measured values.

Ref. 83 studied the free field response of a layered soil using wave propagation analysis and the finite element method with i) controlled damping, and ii) Rayleigh damping. The results indicate that while the response spectra of the wave propagation analysis and the finite element method using controlled damping were the same, the results of the finite element method using Rayleigh damping were very different from those of the wave propagation analysis. This implies that the high frequency components are damped out when using the frequency dependent Rayleigh damping.

The above discussion indicates that the analysis of soil-structure interaction using the equivalent linear method and the controlled damping ratios (complex moduli) seems to lead to more realistic response values.

2.4.2.3 Finite Difference Approach

Ref. 44 pointed out that finite difference methods offer a powerful potential numerical tool for treating wave propagation/soil-structure interaction problems in the seismic analysis of nuclear containment structures and are also completely general with respect to media constitutive properties. However, these methods have received little attention to date by analysts dealing with soil-structure interaction problems in nuclear power plant design in spite of their "higher computational efficiency than finite element methods for certain classes

of dynamic problems" [44]. A two-dimensional axisymmetric finite difference computer programme - AFTON [95] - has been developed and used by Agbabian-Jackson Associates [1] to examine the transient response of non-uniform axisymmetric structures embedded in layered media when subjected to uniform transient pressure pulses.

Table 3 presents a brief comparison between finite difference, finite element, and continuum methods presented in Ref. 1.

2.5 Review of the Previous Work

Investigations carried out on the dynamic analysis of cut-and-cover type underground nuclear reactor containments are presented in some detail in this section.

An initial study was carried out by Blake, Karpenko, McCauley and Walter [13] for a cut-and-cover type underground nuclear reactor containment. The study was based on a postulated 1100-MWe power plant containment constructed in an open pit in soil and then backfilled with selected material. The backfill was chosen for its well-defined low permeability so that it will confine, within a small envelope, any radioactivity release that might result from a rupture of the containment. The containment foundation was placed 340 ft. below the ground level. The soil cover was 160 ft. so as to provide a nominal 70-psia static overburden pressure to balance the internal design pressure. The reinforced concrete containment, with steel lining, studied had a semi-circular roof of a diameter of 130 ft. and vertical walls 90 ft. high. The seismic and overburden effects on the containment were determined

using finite element analysis. The finite element model was 500 ft. deep and the side boundaries were placed 500 ft. from the axis of symmetry. Two types of loading were considered: an overburden loading and horizontal earthquake loading. The stresses in the medium and the containment were obtained from static and dynamic analyses. The results indicated that the static overburden loading produces stresses much greater than those produced by the earthquake loading. Analyses were made to verify containment after a catastrophic reactor accident followed by failure of the containment structure. Since the proposed method of excavation permits selection of backfill materials, a good selection of low permeability fill results in preventing radioactive releases in even the worst cases of nuclear accident. The conclusions from this study were: i) the additional costs of undergrounding are negligible, ii) harmful radiation can be confined, iii) no new technology is required, and iv) static loading produces greater stresses in the containment compared to earthquake loading.

Moselhi [64] studied the response of an underground cavity in rock to a step pulse plane wave. The cavity was lined with a 1 inch thick steel lining. Parametric studies were carried out on the shape of the containment, isolation of the structure using energy absorbing material, and properties of the backfill for a cut-and-cover type structure. The plane-strain finite element model was 42' long and 38' deep. The structure used for the cut-and-cover had a semi-circular roof and vertical walls. The model boundaries were of the rigid type and the duration of the analysis was confined to 3 milliseconds to restrict

the analysis to the time period before the first wave reached the nearest boundary.

For the cut-and-cover structure, normal and heavy weight concrete - each with 3 different elastic moduli - were used as backfill. The results of the effect of the density and the stiffness on the structure and the medium response indicated that neither the density of the filling material nor its stiffness as separate values can greatly affect the internal forces in the structure, but a proper combination of the values of the two properties can lead to a significant reduction in the straining actions of the structure and the stresses in the medium. The results of the analysis of the underground cavity indicated that the high horseshoe shape is the best. A reduction, as high as 80%, in the stresses in the crown element of the structure was achieved by isolating the structure using energy absorbing material.

Kröger, Altes, Escherich, and Kasper [54] used LUSH to study the effect of embedment depth of the containment on the soil-structure interaction. Three configurations were used: aboveground, semi-embedment and total embedment. A pressurized water reactor (1300-MWe) of Kraftwerkunion-design served as a reference plant for which a cut-and-cover plant design was to be developed. Three different acceleration time histories, derived from actual measurements and from artificial synthesis, were used to simulate earthquake excitation. The results of the analysis indicate that i) the three acceleration time histories give different peak stresses due to different spectral intensities, but the acceleration patterns, as functions of depth, are similar.

They do not change significantly even with variations in the dynamic shear modulus and critical damping of the soil layers, ii) high shear moduli and low damping ratios give larger stresses, iii) the acceleration patterns are strongly influnced by the thickness of the soil layer between the rigid base and the foundation of the containment. This phenomenon is independent of the level of the embedment, iv) in general, the embedded containment is less stressed than the aboveground one, and v) the shift of maximum response towards higher frequencies, for increasing depth of embedment, was confirmed by this study.

2.6 Summary

A review of the underground concepts, factors affecting seismic loading on the structure, analysis procedures, and previous work on the cut-and-cover type underground nuclear reactor containments have been presented. Additional literature reviews are presented in Chapters III and IV.

CHAPTER III

PROBLEM FORMULATION

3.1 General Description

The state-of-the-art for underground siting lags considerably behind that for aboveground siting. As indicated in Chapter II, there are many questions that have yet to be answered in the underground siting concept. This project attempts to answer some of these questions by a study of the dynamic response of cut-and-cover type underground nuclear reactor containments, subjected to earthquake or blast-type excitation.

The structure considered is a reinforced concrete containment for a 1100-MWe power plant buried in dense sand medium. The containment structure, excavation and back fill for a typical case are shown in Fig. 3-1(a). The profile of the site and the soil properties are shown in Fig. 3-1(b).

3.2 Computer Programmes Used in the Analyses

In the analyses described herein, computations were made using the recently developed programmes that permit the use of variable shear moduli and variable damping in the soil. The free field response and the response of the soil-structure system were determined by the plane strain finite element programme, LUSH, developed by Lysmer, Udaka, Seed and Huang [62]. The nonlinear soil properties are taken into account in LUSH by a combination of the equivalent linear method described by Ref. 45, and the method of complex response with complex moduli developed in Ref. 62. The latter method makes it possible to use different

damping properties for each element of the finite element model. The high frequency ranges, which must be consdiered in the study of soil-structure interaction for nuclear power plants, are also taken into consideration in this approach.

The free field response obtained by the finite element method using LUSH was checked using the computer programme, SHAKE, developed by Schnabel, Lysmer and Seed [81]. SHAKE is based on a one-dimensional vertical wave propagation method for horizontal soil layers taking the non-linear soil properties into account.

The equations of motion of a soil-structure system, excited by earthquake, and their solution using the two-dimensional plane strain finite element programme, LUSH, are described in the following sections. Brief descriptions of LUSH and SHAKE are presented in Appendix B.

3.3 Analytical Procedure

3.3.1 Equations of Motion

The equations of motion for undamped vibrations of a soil-structure finite element system, excited by earthquake, can be written as

$$[M]\{\ddot{u}\} + [K]\{u\} = - \{m\}\ddot{y}(t) \quad \ldots\ldots\ldots\ldots\ldots\ldots \quad 3.1$$

where

$\{u\}$ = the nodal point displacements relative to the fixed base,

$[K]$ = the stiffness matrix,

$[M]$ = the mass matrix (lumped or consistent),

$\ddot{y}(t)$ = the given input acceleration at the rigid base with the horizontal and vertical components:

$$h(t) = C_h \cdot \ddot{y}(t)$$
$$v(t) = C_v \cdot \ddot{y}(t) \qquad \ldots\ldots\ldots\ldots\ldots\ldots\ldots\ldots 3.2$$

in which C_h and C_v are scaler constants, and

$\{m\}$ = the load vector corresponding to $\ddot{y} = 1$ related to the mass matrix $[M]$ through

$$\{m\} = [M](C_h\{V_h\} + C_v\{V_v\}) \qquad \ldots\ldots\ldots\ldots\ldots\ldots 3.3$$

in which $V_h = \begin{Bmatrix} 1 \\ 0 \\ . \\ . \\ . \\ 0 \\ 1 \end{Bmatrix}$ and $V_v = \begin{Bmatrix} 0 \\ 1 \\ . \\ . \\ . \\ 0 \\ 1 \end{Bmatrix}$

As each nodal point has two degrees of freedom, all the above vectors have the dimension NF = 2 x the number of free nodal points, and the matrices [M] and [K] have the dimension NF*NF.

3.3.2 Response to Harmonic Input Motion

The method of complex response [62], in its basic form, assumes that the input motion is harmonic with the frequency ω (radian/sec.)

$$\ddot{y}(t) = \ddot{Y}.e^{i\omega t} \qquad \ldots\ldots\ldots\ldots\ldots\ldots\ldots\ldots 3.4$$

where the amplitude $\ddot{Y}$ may be complex. This implies that the response is also harmonic

$$\{u\} = \{U\} \cdot e^{i\omega t} \qquad \ldots\ldots\ldots\ldots\ldots\ldots\ldots\ldots 3.5$$

where $\{U\}$ is a constant, perhaps a complex vector. Substitution of

of Eqn. 3.5 into the equations of motion 3.1 gives

$$([K] - \omega^2 [M]) \{U\} = -\ddot{Y} \cdot \{m\} \quad \ldots\ldots\ldots\ldots\ldots\ldots\ldots\ldots \quad 3.6$$

which is nothing but a set of linear equations in the unknowns {U}. Eqn. 3.6 can be solved by Gaussian elimination if ω is not a natural frequency of the system, and the time-dependent response {u} follows Eqn. 3.5 which provides the complex response to the complex input motion in Eqn. 3.4. Since the real part of the output corresponds to the real part of the input, the response to

$$\ddot{y}(t) = \mathrm{Re}(\ddot{Y} \cdot e^{i\omega t}) = \mathrm{Re}(\ddot{Y}) \cos \omega t - \mathrm{Im}(\ddot{Y}) \sin \omega t \quad \ldots\ldots\ldots \quad 3.7$$

is

$$u(t) = \mathrm{Re}(\{U\} \cdot e^{i\omega t}) = \mathrm{Re}\ \{U\} \cos \omega t - \mathrm{Im}\ \{U\} \sin \omega t \quad \ldots\ldots \quad 3.8$$

3.3.3 Damped Vibrations

Viscous damping can be considered in the method of complex response by using complex moduli in the formulation of the stiffness matrix [K]. Ref. 62 shows that by application to a simple damped oscillator, the use of the complex shear modulus

$$G^* = G(1-2\beta^2 + 2i\beta \sqrt{1-\beta^2}) \quad \ldots\ldots\ldots\ldots\ldots\ldots \quad 3.9$$

will lead to the exactly the same amplitudes as nodal analysis with a uniform damping ratio, β. This approach enables representation of variable damping by using different values of G and β in each element.

3.3.4 Response to Actual Earthquake

Actual earthquake motions are not harmonic. However, if the motion

is input as a digitized record with N points, at time intervals Δt, it can be decomposed into N/2+1 harmonics of complex amplitudes, $\ddot{Y}_s$, and frequencies

$$\omega_s = \frac{2\pi s}{N.\Delta t}, \quad s = 0, 1, \ldots\ldots \frac{N}{2} \qquad \ldots\ldots 3.10$$

The computation of the complex amplitudes from the given real values is most conveniently made by a superfast algorithm known as the "Fast Fourier Transform" by Cooley and Tukey [24].

Having decomposed the earthquake motion into harmonic motions, Eqs. 3.6 have to be solved N/2+1 times for each value of the (N/2+1) frequency. In view of linear viscoelastic behaviour, the complete solution can be obtained by simple superposition as follows:

$$\{u(t)\} = \mathrm{Re} \sum_{s=0}^{N/2} \{U\}_s \, e^{i\omega_s t} \qquad \ldots\ldots 3.11$$

3.3.5 Solution of the Equation of Motion

The computer programme LUSH solves Eqn. 3.6 using the Method of Complex Response [62]. In order to save computation time, the required number of solutions to Eqn. 3.6 can be reduced according to the maximum frequency used in the analysis, and the value of the interpolation factor in the frequency domain. Usually, the input motion contains frequencies as high as 100 Hz which are usually not of interest and can be neglected. Thus Eqs. 3.6 have to be solved for only frequencies less than the maximum required frequency (8-25 Hz).

The number of required solutions can be further reduced by interpolation in the frequency domain. Suppose Eqn. 3.6 is written in the form

$$([K] - \omega^2[M])\ \{A\} = -\ \{m\} \quad \text{..... 3.12}$$

The components of {A} are called amplification functions with smooth functional dependence on ω. $\{A\}_s$ can be evaluated at, say, every fourth frequency ω_s, s = 0, 4, 8, ..., and then the intermediate amplification functions can be obtained by interpolation. The actual number of interpolated points which can be used without the introduction of significant errors should be determined by trial and error as shown in the analysis described herein.

Having determined all the amplification functions, $\{A\}_s$, s = 0, 1, ... N/2, either by solution of Eqns. 3.12 with interpolation, or by setting them equal to zero above the cut-off frequency, the displacements at the times k.Δt are determined from

$$\{U\}_k = \text{Re} \sum_{s=0}^{N/2} (\{A\}_s \cdot \ddot{Y}_s)\, e^{i\omega_s k\Delta t}, \quad k = 0, 1, N-1 \quad \text{..... 3.13}$$

which can be evaluated by the Inverse Fast Fourier transform method.

3.3.6 Soil Non-Linear Behaviour

The above solution is applicable only to linear viscoelastic systems but large shear deformations which occur in soils during strong earthquakes introduce significant non-linear effects. This problem has been solved in LUSH using the equivalent linear method by Ref. 45. According to this method, an approximate nonlinear solution can be obtained by a linear analysis provided the stiffness and damping used in the analysis are compatible with the effective shear strain amplitudes at all points of the system. Data on strain-compatible soil properties

published by Seed and Idriss [82] is provided within subroutine CURV52 of LUSH. The strain-compatible soil properties are obtained by an iteration procedure using the 'one-dimensional column study' described below.

3.3.7 One-Dimensional Column Study

The free field response to the horizontal component of input motion can be determined by application of LUSH to a single column of rectangular elements representing the soil layers in the free field. If all nodal points are allowed to move only in the horizontal direction, and if the element dimensions are small enough (as described in Sec. 3.4.4.1), the model will simulate the vertical propagation of shear waves in the free field, and iteration will lead to the nonlinear response of the model in the free field.

3.4 Modelling

3.4.1 General Description

The containment structure is placed in an open pit in 3 horizontal layers of sand of total depth of 500' followed by a semi-infinite rock layer. The side boundaries are placed 1010' from the structure centre line. Because of symmetry, only one half of the soil-structure system is studied after introducing boundary conditions compatible with the horizontal input motion. A typical finite element discretization of the soil-structure system is shown in Fig. 3.2. Details of the element disceretization of the containment structure is shown in Fig. 3.3.

3.4.2 Factors Affecting Computation Time

Execution time, actual CPU and equivalent CPU times required for one run by the programme LUSH are functions of many parameters, including

a) the geometry of the finite element mesh (total number of elements and band width of the stiffness matrix), b) duration and time step of the input motion, c) maximum frequency used in the analysis, d) number of iterations on soil properties, and e) the interpolation coefficient in the frequency domain. Special care should be given in numbering nodal points and choosing the dimensions of the finite element model, element size, maximum frequency and the interpolation coefficient in order to save computer time. After all possible minimizations of computer time and storage, the analysis of a typical case needed 1100K computer storage, 53 min. actual CPU time and about 13 hrs. equivalent CPU. The computer time would have been increased to at least 8 times the above values if all the above parameters had not been carefully chosen.

In the following sections, the procedures followed to determine all the parameters needed in the analysis are described.

3.4.3 Model Dimensions

The overall dimensions of the finite element mesh influence the response of the structure due to the action of the waves reflecting from the boundaries. As discussed in Chapter II, this problem can be overcome either by the use of energy absorbing boundaries or by the use of a sufficiently extensive mesh. LUSH uses the latter approach. For aboveground nuclear plant structures, it has been found that if the material damping in the soil is relatively high (approx. 12% of critical), energy radiating outwards from the vicinity of the structure is absorbed relatively quickly, and free field conditions are developed within a distance of approximately 2 to 2 1/2 times the depth of the

model away from the structure [62]. In the analysis described herein, the side boundaries of the model are placed 1010' away from the centre line of the structure.

The rigid base should be placed below the foundation of the structure at a distance greater than or equal to the width of the structure [62]. In the model considered, the rigid base is placed 150' below the structure foundation for a structure width of 95'.

The check on the adequacy of the extent of the mesh was made for each case studied by comparing the computed motion at an ample distance from the structure with the free field motion obtained from the one-dimensional column studies at the same elevation as explained in Sec. 3.5.

3.4.4 Details of the Finite Element Mesh

3.4.4.1 Size of the Elements

The choice of element size in the finite element mesh for cases where high frequency effects are important needs careful control. Element sizes should be small compared to the wave length of shear waves propagating through the model. Large elements are unable to transmit motion with high frequencies and corresponding short wave lengths. Because a significant part of the earthquake motion corresponds to vertical wave propagation, the vertical size of the element is very important. As indicated in Chapter II, Ref. 55 proposed an empirical rule that the vertical element size should not be larger than one-quarter, or preferably, one-eighth of the wave length of motion. For analysis using LUSH, Ref. 62 suggests a maximum vertical element size, h_{max}, as follows:

$$h_{max} = \frac{1}{5} \lambda_s = \frac{1}{5} \frac{V_s}{f_{max}} \quad \ldots\ldots\ldots\ldots\ldots\ldots\ldots\ldots \quad 3.14$$

where λ_s is the wave length of the shortest wave, V_s is the shear wave velocity in the element, and f_{max} is the highest frequency of the analysis. The guideline given by Eqn. 3.14, is followed in this study to determine the vertical element sizes. Because the shear wave velocity in each element is dependent on the strain-compatible shear modulus of the element, which in turn is dependent on the element strain and the depth of the element from the ground surface, the maximum vertical element size varies from one element to the other (Fig. 3.24).

The variable vertical element sizes are determined by trail and error using the one-dimensional column study analysis, as described in section 3.5. The adequacy of the selected mesh size is further checked by comparing the results of the one-dimensional column studies using LUSH with the solution obtained using SHAKE [81]. SHAKE computes the free field response using continuum (wave propagation) theory, thus eliminating the errors introduced by discretization. Comparisons of maximum accelerations, maximum shear stresses and acceleration response spectra obtained for the free field response using LUSH and SHAKE are presented in Figs. 3.4, 3.5, and 3.6 respectively.

The vertical element sizes of the two dimensional finite element mesh (soil-structure system) were chosen using the results of the one-dimensional column studies described above. Ref. 62 indicates that the computed response is less sensitive to the horizontal element size, which can be chosen several times larger than the vertical element size. However, care must be taken to avoid very elongated elements (in the horizontal direction) in the vicinity of the structure as indicated by

Idriss and Sadigh [47]. The analysis carried out by Ref. 47 used small aspect ratios (typically 3-4) in the vicinity of the structure; higher aspect ratios farther away from the structure have been used.

In the studies presented herein, the horizontal element size is chosen to have aspect ratios of about 3 near the structure and higher values near the side boundaries as shown in Fig. 3.2. The basic model has 508 nodal points and 498 elements (449 soil elements and 49 concrete elements).

3.4.4.2 Numbering the Nodal Points

Since the computation time for LUSH increases porportionally with the square of the band width of the stiffness matrix, great care is required in numbering the nodal points of the finite element mesh of the soil-structure system in order to minimize the band width. Also, a high degree of refinement in modelling the containment structure will result in an increase of band width and, thus, an increase in the execution time [47]. Extensive care has been taken in numbering the nodal points in the soil structure system, and many trials were made to get the least possible value of the band width in each model (as low as 40).

3.4.4.3 Boundary Conditions

If the finite element model is symmetrical, only one half of the structure can be analyzed using the appropriate boundary conditions, described in Ref. 62, to simulate the input motion and the horizontal soil layers outside the vertical boundaries. In the cases studied herein, the model is symmetrical and the input motion is horizontal. Therefore, one half of the soil-structure system was studied and all the nodal points at the vertical boundaries were allowed to move only in the

horizontal direction to simulate the horizontal motion of the points in the free field due to the vertical wave propogation.

3.4.5 Interpolation Coefficient KINT

As discussed in Section 3.3.5, considerable saving in computation time can be achieved by interpolation of the transfer function in the frequency domain. The controlling parameter used in LUSH is the interpolation control number, KINT, which is an integer number with values of power of 2 (1, 2, 8, ... etc.). For example, if the KINT value chosen is eight, every eighth point of the amplification functions will be computed from Eqn. 3.12 and the remaining values will be obtained by interpolation. Ref. 62 suggests typical values of KINT as 4, 8 or 16. In the analysis carried out by Ref. 47 using LUSH, it has been found that values of 16 in some cases and 8 in the others are acceptable for the analysis. To determine the highest value of KINT acceptable for the analysis carried out in this study, one-dimensional column studies were carried out using values of 4, 8, 16 and 32. Comparisons of acceleration response spectra at nodal point 11 and the maximum accelerations in the soil profile using the above values of KINT, as shown in Figs. 3.7 and 3.8, indicate the maximum acceptable value to be 16.

3.4.6 Maximum Frequency

A most important decision to be made is the choice of the maximum frequency to be included in the analysis. This frequency will, more than anything else, influence the accuracy, the finite element dimensions and the cost of the analysis. The computation time is proportional to the maximum frequency considered during the analysis, furthermore, smaller elements are required for high frequency analysis. It has been

shown that the computation time is proportional to at least the fourth power of the maximum frequency [62]. Hence, it is very important not to consider frequencies higher than those that are absolutely necessary. Ref. 47 pointed out that typical frequency values of 15 to 25 Hz are used in the soil-structure analysis involving nuclear power plants, and that most interaction effects between the structure and the surrounding soil would involve frequencies well below 20 Hz. Taking the above factors into account for this analysis, it was decided to retain frequencies up to 20 Hz as used by Ref. 47. To save some computer time, lower values of maximum frequency (10 and 15 Hz) have been used for the initial steps of the iterative procedure.

3.4.7 Dynamic Properties of Soil

The basic material properties to be specified for each element using LUSH are: the unit weight, Poisson's ratio and shear modulus at small strains (10^{-4}%). In addition, estimates of the strain-compatible values of shear modulus and the damping ratios in each element are needed to take into account nonlinear soil behaviour.

The shear modulus at small strains in an element at depth y, below the ground surface, is obtained using the modulus parameter K_{2max} and the following equation:

$$G_{max}(y) = 1000\ K_{2max}\ [\sigma'_m(y)]^{\frac{1}{2}} \quad \ldots\ldots\ldots\ldots\ldots\ldots\ldots\ 3.15$$

in which

G_{max} = the shear modulus at small strain in lb/ft^2,

$\sigma'_m(y)$ = effective mean normal stress in lb/ft^2 at depth y which can be obtained from the equation

$$\sigma'_m(y) = \frac{(1 + 2K_0)}{3} \sigma'_v(y) \quad \text{..... 3.16}$$

K_0 is the coefficeint of lateral pressure at rest,

and σ'_v is the effective vertical pressure at depth y. Values of Poisson's ratio, unit weight, K_0 and K_{2max} for each soil layer are shown in Fig. 3.1.b.

Initial estimation of the strain-compatible soil properties to be used in the soil-structure model was obtained by an iterative procedure using the one-dimensional column study. These values were considered as initial soil properties (shear modulus and fractional damping) in the finite element model. The actual compatible moduli and damping ratios for the soil in the soil-structure interaction analysis were determined within a few iterations (typically one to three). Strain-compatible damping and modulus values obtained by the one-dimensional column study are shown in Figs. 3.9a and 3.9b.

3.4.8 Input Motion

The finite element analysis requires a base motion for excitation of the two-dimensional model. Because the control motion is typically specified at some point in the free field, it is necessary to determine the motion that would have to develop in an underlying rock-like formation to produce the specified motions at the control point [83]. This can be accomplished by using SHAKE.

As SHAKE was not available at the commencement of the work, the base motion of the sample problem in QUAD-4 by Idriss, Lysmer, Hwang and Seed [46] was chosen as the base motion of the finite element model. The base motion in Ref. 46 was due to the acceleration time history recorded at Taft during the 1952 Kern County earthquake. When SHAKE

became available, it was used to check the free field response obtained by LUSH. The time history, acceleration spectrum and Fourier spectrum for the computed base motion using SHAKE are shown in Figs. 3.10, 3.11, and 3.12 respectively.

3.4.8.1 Time Interval

The time interval of the digitized acceleration values should be small enough to ensure that the earthquake record contains frequencies higher than the maximum frequency used in the analysis. The highest frequency contained in the record, h_f, is

$$h_f = 1/2\Delta t \quad \ldots\ldots\ldots\ldots\ldots\ldots\ldots\ldots \quad 3.17$$

As the input motion is digitized at a time interval, $\Delta t = 0.01$ sec., the highest frequency is $1/2 \times 0.01 = 50$ Hz which is higher than the chosen maximum frequency (20 Hz). Then the time interval of the earthquake record is small enough to obtain frequencies higher than the maximum frequency.

3.4.8.2 Input Motion Duration and Quiet Zone

In order to simulate the finite duration of actual earthquakes, it is necessary to introduce a "quiet zone" at the end of each cycle to allow sufficient time for the viscous damping of the system to attenuate the response before the commencement of the next cycle. Ref. 62 states that because soil damping is high, the quiet zone usually needs to be only a few seconds long. The number of trailing zeros required depends on the frequency characteristics and the damping of the system; it must be determined by trial and error using the one-dimensional column study. The number of zeros is considered sufficient

if the output motions are attenuated within the period of the motion. It has been found from the results of column studies, shown in Figs. 3.13 to 3.17, that a quiet zone of 3 sec. length is sufficient to attenuate the motion.

As the total number of the digitized earthquake values for analysis using LUSH must be a power of two (1024, 2048, 4096, ... etc.), it was decided to use 2048 points including 348 zeros which means that the total duration of the earthquake is 20.48 sec. including 3.48 sec. quite zone.

The base motion was considered horizontal with a maximum acceleration of 0.15g.

3.5 Numerical Illustrations

This section presents numerical illustrations for a) the free field response of sand medium using the one-dimensional column study, b) the effect of the vertical size of the element on the transmission of the vertically propagating shear waves in the free field, and c) the response of the soil-structure system for a typical model.

3.5.1 The Free Field Response

The free field response of the sand medium has been obtained by the one-dimensional finite element column study using LUSH and checked by the wave propagation analysis using SHAKE. The modelling is shown in Figs. 3.18(i) and 3.19. The strain-compatible soil properties (shear moduli and damping ratios), used in the finite element analysis, are presented in Figs. 3.9a and 3.9b. The strain-compatible soil properties were determined as described in section 3.4.7 in four iterations. Comparisons of the maximum horizontal accelerations, maximum

shear stresses and response spectra, obtained by SHAKE and LUSH, are presented in Figs. 3.4, 3.5 and 3.6. Time histories of the displacements, accelerations and shear stresses, and acceleration spectra at different depths are presented in Figs. 3.13 to 3.17 and 3.20. Plots of the maximum shear stresses, maximum shear strains and shear wave velocities are presented in Figs. 3.21, 3.22 and 3.23.

3.5.2 Effect of Element Size on the Transmission of the Vertically propagating shear waves

Vertical element sizes for the one-dimensional column studies were determined by trial and error using a simple mesh with a constant element height of 15 ft. (Fig. 3.18ii) as the initial mesh to determine the minimum number of elements. This has been achieved by choosing the maximum element size that satisfies Eqn. 3.14. Comparison of the maximum element heights, computed from Eqn. 3.14, and the chosen element heights for the free field response (Mesh No. 1 Fig. 3.18) is presented in Fig. 3.24. The free field response obtained using this mesh was checked using SHAKE as explained in section 3.4.4.1. However, to study the effect of element size on the transmission of the vertically propagating shear waves in the medium, and on the free field response, the responses with two other meshes, of constant element heights of 15 and 20 ft., (Fig. 3.18) were compared to the variable element size mesh used before. Comparisons of i) the maximum shear stresses, ii) the maximum horizontal accelerations, and iii) acceleration spectra at the ground surface and at a depth of 40 ft. for the three meshes, shown in Fig. 3.18, are presented in Figs. 3.25, 3.26 and 3.27-3.28 respectively.

The results indicate that the spectral accelerations for meshes Nos. 1 and 2, are in close agreement at depths greater than 40 ft.,

and those of meshes, Nos. 2 and 3, at the ground surface. The spectral accelerations of meshes, Nos. 2 and 3, are less than those for mesh No. 1 for frequencies higher than 10 Hz at both locations. This means that elements with heights larger than those specified by Eqn. 3.14, and plotted in Fig. 3.24, are not able to transmit shear waves with short wave lengths (high frequencies).

3.5.3 Soil-Structure Interaction For a Typical Case

Selected results for the typical case, shown in Fig. 3.1a, and comparisons of the response of the soil-structure system and the free field are presented in this section. The finite element representation of the soil-structure system for this case is shown in Fig. 3.2. The strain-compatible soil properties to account for the soil non-linear behaviour were determined as described in section 3.4.7. The maximum principal stresses in the containment and the maximum horizontal and vertical accelerations in the soil and containment are presented in Figs. 3.29, 3.30 and 3.31. Time histories of the horizontal acceleration and the displacement at the middle of the containment floor are presented in Figs. 3.32 and 3.33. Plots of the maximum horizontal accelerations, the maximum shear stresses, and the acceleration spectra at different depths (Fig. 3.34) are presented in Figs. 3.35 to 3.39. Comparisons of the maximum horizontal accelerations and the maximum shear stresses in the soil near the containment, and in the free field are presented in Figs. 3.40 and 3.41. The accelerations and stresses in the soil at the model boundaries and in the free field are presented in Figs. 3.42 and 3.43.

The results indicate that i) the maximum shear stresses, the maximum

horizontal accelerations, and the maximum spectral accelerations in the soil near the structure are less than those in the free field, and ii) the boundaries are sufficiently far to reach the free field response.

3.6 Summary

The analysis procedure, modelling and the response of the free field and the soil-structure system are presented. The methods used to determine the values of all the parameters needed for the analyses, including the details of the finite element model, are discussed in detail.

The response of a typical model is presented to illustrate the results that can be obtained for each model. Because of the large number of the results that can be obtained in each case, the comparison presentation is restricted to a few characteristic values. The maximum principal stresses in the containment, maximum shear stresses and accelerations in the soil near the containment, and the acceleration spectra at two points in the containment are the only values compared in the parametric studies presented in Chapter IV.

CHAPTER IV

PARAMETRIC STUDIES

4.1 General

Parametric studies are described for a) the most convenient shape and depth of burial of the containment structure for earthquake resistance, b) effects of the density, stiffness and side thickness of the backfill material on the structure-medium interaction, c) the effect of the relative stiffnesses of the containment and the medium on the structure-medium interaction, and d) isolation of the containment structure from the surrounding medium using a soft energy absorbing material.

4.2 Shape of the Containment Structure

Studies carried out by Ref. 98 and Szechy [22] indicated the horseshoe shape to be the most suitable for an underground cavity under static loading conditions. For a blast type of dynamic loading, Ref. 64 found the horseshoe shape to be the best among four different shapes, and the high horseshoe shape to be better than the flat horseshoe from the viewpoint of stresses in the lining of the underground cavity.

To find out the best containment shape for earthquake resistance, three different shapes of the same area were investigated (Fig. 4.1) i) semi-circular roof with vertical walls, ii) high horseshoe with rise-to-span ratio of 1/2, and iii) flat horseshoe with rise-to-span ratio of 1/4. To compare the high horseshoe with the vertical walled and cylindrical roof shape, the analyis was carried out for the two shapes, with the backfill properties the same as those of the medium. Maximum

principal stresses in each containment are presented in Figs. 4.3 and 4.4. Comparisons of i) the maximum principal stresses in the containments, ii) the maximum shear stresses in the soil at a vertical plane 40 ft. away from the containment, iii) the maximum horizontal accelerations in the soil at a vertical plane 70ft. away from the containment, and iv) the acceleration spectra at the centre of the foundation, and at the mid-point of the wall for each shape are presented in Figs. 4.5, 4.6 and 4.7-4.8 respectively. The results indicate the horseshoe shape to be better than the one with semi-circular roof and vertical walls.

In order to determine the better rise-to-span ratio for the horseshoe shape, analysis was carried out for the flat and the high horseshoe shapes covered by loose sand as backfill (Fig. 4.1). The plots of maximum principal stresses for the high and flat horseshoe structures are presented in Figs. 4.9 and 4.10. Comparisons of i) the maximum shear stresses in the soil at a vertical plane 40 ft. away from the structure, ii) the maximum horizontal accelerations in the soil at a vertical plane 10 ft. away from the structure, and iii) the acceleration spectra at mid-span of the wall and the foundation centre are presented in Figs. 4.11, 4.12 and 4.13-4.14 respectively.

The results indicate that while the stresses in the flat horseshoe structure are slightly less than those for the high horseshoe, the stresses in the soil medium near the flat containment are slightly higher than those near the high containment. However, the saving in the cost of the structure due to small reduction in stresses for the high horseshoe shape is very small compared to the additional cost of the excavation for the flat horseshoe shape (Fig. 4.1). Therefore, the rest of the studies were restricted to the high horseshoe shape. For

simplicity, the high horseshoe shape will be referred to in the following parametric study as the containment.

4.3 Stiffness of the Containment Structure

The dynamic response of any structure is dependent on its stiffness. For an ordinary structure subjected to a certain load, the stresses will be reduced by 50% to 75% if the dimensions of its sections are doubled. For an underground structure subjected to earthquake excitation, an increase of the structure thickness will decrease structural deformations, thereby increasing the load exerted by the soil on the structure. On the other hand, the thickness increase in the structure will reduce the stresses in the structure. But this increases the load on the structure and thereby the stresses. To determine the net effect of increasing the containment thickness, the analysis was carried out for the high horseshoe containment shown in Fig. 4.1ii by increasing the thickness of the arch walls and arch roof from 5 ft. to 10 ft. keeping the floor thickness (10 ft.) unchanged. Comparisons of the results for the thin and thick containment structures are presented in Figs. 4.15 to 4.19.

The results show that while doubling the wall and roof thickness reduces the stresses in the walls and roof of the structure by only 15%, it increases the stresses in the floor of the structure and in the soil by nearly the same amount which implies that the soil loading on the structure has been increased by additional thickness.

4.4 Depth of Burial

As discussed in Chapter II, underground siting provides protection against natural and man-caused damage to structures and reduction of the

seismic motion. Ref. 98 pointed out that the depth of burial in rock must be sufficient to prevent cracks from opening the surface under the influence of increased cavity pressure following a reactor loss-of-coolant accident. Results of the analysis carried out by Ref. 98 for an underground horseshoe cavity in rock suggested depths of cover of 150-200 ft. In the analysis carried out by Ref. 13 for a cut-and-cover containment in soil, it has been found that the depth required to provide a static overburden pressure to balance the internal pressure is 150 ft. The experience in mining and transportation fields suggest deep soil locations as preferable to surface soil locations to provide the additional protection from harmful radiation in the event of a seismic incident or a major internal accident [75]. Ref. 54 pointed out that protection against conventional weapons requires a coverage of soil of 25-60 ft. with a superimposed shield plate made of concrete.

To investigate the effect of the depth of burial of the structure on its response to earthquake excitations, analysis was carried out for three values of the depth of soil cover of 70, 150 and 220 ft. (Fig. 4.20). Comparisons of the maximum principal stresses and the maximum horizontal and vertical accelerations in the structure for the three cases are presented in Figs. 4.21 and 4.22a-4.22b. Comparisons of i) maximum shear stresses in the soil at vertical plane 40 ft. away from the structure, and ii) acceleration spectra at the roof centre, the mid-point of the wall and the floor centre of the structure, are presented in Figs. 4.23, and 4.24, 4.25 and 4.26 respectively.

The results show reduction in maximum principal stresses in the containment, the maximum shear stresses in the soil and the maximum

accelerations in the containment due to the increase of the depth of burial.

4.5 Backfill

As shown in Chapter II, the effect of backfill material for actual containments has not been studied adequately. This section discusses the investigation of the effect of backfill properties and the thickness of side cover on the soil-structure interaction. The term "jacket" is used to refer to the part of the filling material between the walls of the structure and the vertical edges of the excavations and the cover over structure up to certain height. The materials used for the study are: a) same material as the original medium to fill the whole pit, b) loose sand with thin (10 ft.) and thick (70 ft.) side covers, c) jackets of stabilized sand with thin and thick side covers, and d) a reinforced earth jacket. The configurations and properties of the filling materials used for the analysis are shown in Figs. 4.27, 4.28 and 4.29.

Comparisons of the response of the soil-structure system to earthquake excitation for the above cases of filling materials are presented in the following sections.

4.5.1 Original and Loose Backfill

Original and loose backfills for the configuration shown in Fig. 4.27i were studied. Comparisons of i) maximum principal stresses in the structure, ii) maximum shear stresses in the soil at a distance of 40 ft. away from the structure, iii) maximum horizontal accelerations in soil at a vertical plane 70 ft. away from the structure, and iv) the acceleration spectra at the mid-point of the wall and at the floor centre

of the containment are presented in Figs. 4.30, 4.31, 4.32 and 4.33-4.34.

The results indicate that both the maximum stresses in the soil and the containment are reduced for filling material softer than the medium.

4.5.2 Loose and Stabilized Jackets

The effect of the density and stiffness of the backfill material on the response of the soil-structure system was studied by comparing the behaviour of a stabilized sand fill with that of a loose backfill (Figs. 4.27 and 4.28). The comparative values of i) maximum principal stresses in the containment, ii) maximum shear stresses in the soil, iii) maximum acceleration in the soil, and iv) acceleration spectra at two locations in the containment are presented in Figs. 4.35 to 4.39 for thin jackets, and Figs. 4.40 to 4.44 for thick jackets.

The results indicate that in both cases (thin and thick jackets), the maximum principal stresses and accelerations in the containment and the maximum shear stresses and accelerations in the soil for the case of loose fill are less than those for the stabilized fill.

4.5.3 Effect of Jacket Thickness (Loose and Stabilized)

Figs. 4.45 to 4.49 and 4.50 to 4.54 show response comparisons for loose (thick vs. thin) and stabilized (thick vs. thin) jackets - principal stresses in the structure, maximum shear stresses and accelerations in the soil, and acceleration spectra at two points in the structure.

The results indicate the maximum stresses and accelerations in the structure and in the soil for thin jackets to be less than those for the thick jackets.

4.5.4 Reinforced Earth Jacket

Reinforced earth implies the use of strong bars, rods, fibres or nets that are embedded in soil to provide additional load-carrying strength. The bonding between the soil and the ties is developed through friction. The concept of strengthening the soil with added rods or fibres is not new and it is now extensively used in the construction of retaining walls. Reinforced earth walls constructed, to date, have mainly used thin galvanized steel strips for the ties and materials such as plastics, various fabrics, lightweight steel panels and precast concrete blocks for the outerskin, which is required to maintain the integrity of the sand and the outside face. Experimental and analytical (FEM) studies on the static and dynamic behaviour of reinforced earth structures carried out by Lee, Adams and Vangheron [60], Richardson and Lee [76], Romstad, Herrmann and Shen [78] and Shen, Romstad and Herrmann [85] are of considerable interest.

The case shown in Fig. 4.29 has been studied to determine the effect of introducing a reinforced earth jacket around the containment structure on soil-structure interaction. The properties of the soil jacket were modified to account for the weight and stiffness of the reinforcing bars. Rigid ties were provided at the edges of the elements in the jacket area to simulate the reinforcing bars as shown in Fig. 4.29ii.

The walls of the structure were considered adequate to act as the outer skin. The results in Figs. 4.55 to 4.60 indicate that the reinforced earth reduces the maximum stresses and accelerations in the containment and in the soil near it.

4.6 Isolation of the Structure

Stresses in underground structures subjected to dynamic loadings (nuclear blast or earthquake excitation) can be greatly reduced by using a soft, elastic energy absorbing material between the structure and the surrounding medium. This isolating material is easily deformed to absorb the energy produced by the exciting load, i.e. acting almost like a rubber ring protecting the structure from any disturbance in the surrounding medium. On the othe hand, a crushable material could be used for the same purpose. In this case when the stresses in the isolating material reach the crushing strength, no more load will be transmitted to the structure through the medium.

The concept of reducing the stresses in an underground cylindrical pipes by isolating the pipe with polyurethane foam, studied by Costantino and Mariano [25], indicates the beneficial effect of the isolation layer in reducing the liner-shell membrane forces and bending moments. The studies of Ref. 64 indicated that a surrounding medium of soft, energy absorbing material (considered by Ref. 25) reduces by about 80% the liner membrane forces and bending moments.

To study the effect of isolating the containment structure, two different materials were used to isolate the structure: a) closed cell polyurethane foam and b) foamed light weight concrete. The results for each case are presented in the following sections.

4.6.1 Isolation Using Polyurethane Foam

The structure was isolated by a 10 ft. thick jacket of polyurethane foam. The configuration and properties of the isolation material are shown in Fig. 4.61i.

The effect of the polyurethane foam on the maximum stresses and accelerations in the containment and the soil, and the computed acceleration spectra at two points in the structure are presented in Figs. 4.62 to 4.67.

The results show considerable reduction in the maximum principal stresses and accelerations in the containment, and the maximum shear stresses and accelerations in the soil.

4.6.2 Isolation Using Foamed Concrete

The configuration and properties of the foamed concrete jacket are shown in Fig. 4.61b. The effect of the foamed concrete jacket on the maximum stresses in the structure and the soil is presented in Figs. 4.68 and 4.69. A comparison of the maximum principal stresses in the structure for foamed concrete and polyurethane foam jackets is presented in Fig. 4.70. The effect of the foamed concrete jacket on the maximum horizontal acceleration in the soil and the acceleration spectra at two points in the containment structure are presented in Figs. 4.71, 4.72 and 4.73.

The results indicate that compared to loose fill, the foam concrete jacket in a sand medium increases the maximum stresses in the structure and the maximum stresses and accelerations in the soil.

4.7 Effect of Medium Stiffness

In order to study the effect of the stiffness of the medium on structure-medium interaction, and the response of the structure-medium system to earthquake excitation, the finite element model for the sand medium, described in Chapter III, was used to study the response in a rock medium. The structure was isolated by a jacket of foamed concrete

with the same configuration as that shown in Fig. 4.6lii.

4.7.1 The Free Field Response

The free field response has been obtained using the one-dimensional column study using LUSH, and checked by the results obtained using SHAKE. Comparisons of the maximum stresses, strains and acceleration spectra in the free field, obtained by LUSH and SHAKE, are presented in Figs. 4.74, 4.75 and 4.76 respectively.

Comparisons of the free field response of the rock and sand media are presented in Figs. 4.77 to 4.82. The time-histories of horizontal accelerations, shear stresses and horizontal displacements at a depth of 44 ft. in the rock free field are presented in Figs. 4.83, 4.84 and 4.85 respectively.

The results indicate the stresses, accelerations and spectral values to be higher in rock than in sand media. The peak spectral values occur at higher frequencies in rock than in sand. But displacements are the same in both cases.

4.7.2 Rock-Structure Interaction

A comparative study of the responses of the structure medium system (stresses and accelerations in the containment and in the medium, and acceleration spectra at two locations in the containment) for sand and rock media are presented in Figs. 4.86, 4.87, 4.88, 4.89 and 4.90-4.91 respectively.

The results indicate that for a structure in a rock medium the stresses (structure) are lower, and accelerations (structure and rock) are higher compared to a structure in a sand medium. In contradistinction to a sand medium, the stresses and the spectral accelerations

in rock are higher occurring at higher frequencies.

4.8 Summary

Parametric studies have been presented in this chapter for a) shape and stiffness of the containment, b) depth of burial, c) backfill material, d) isolation of the structure, and e) stiffness of the medium. Comparative studies have been discussed briefly for each case and the results will be discussed in greater detail in Chapter V.

CHAPTER V

DISCUSSION AND CONCLUSIONS

5.1 General

The results of the free field response and the soil-structure interaction, presented in Chapter III, and the results of the parametric studies, presented in Chapter IV, are discussed. The cases considered are: i) the free field response obtained by the one-dimensional finite element column study using LUSH, and the continuum (wave propagation) solution using SHAKE, for rock and sand media, ii) containment geometry (containment shape and thickness of the containment walls and roof), iii) burial depth, iv) properties of the backfill (4 different filling materials and two types of energy absorbing jackets), and v) medium-structure interaction for rock and sand media.

5.2 The Free Field Response

The free field responses obtained by finite element analysis using LUSH are very close to those obtained by the wave propagation analysis using SHAKE for both rock and sand media (Figs. 3.4 to 3.6 and 4.74 to 4.76). This implies that the parameters used in finite element analysis (element sizes and the interpolation coefficient) have been adequately chosen.

The results in Figs. 4.77 to 4.82 show that i) Maximum shear stresses in the sand medium increase from the ground surface down to a depth of 75 ft., then remain constant down to the rigid base (at 500 ft.), while they increase in the rock medium with the depth, ii) The maximum horizontal accelerations in the sand medium are approximatly

uniform from the rigid base up to the 200 ft. depth, and then increase towards the surface, while in the rock medium, they increase from the base towards the ground surface, iii) Spectral accelerations (from the response spectrum) decrease with depth in both sand and rock media and the frequency of the peak spectral acceleration does not vary with depth for rock, while it increases with depth in sand because of the change in the stiffness of the sand layers, iv) Accelerations, stresses and spectral accelerations are higher in rock than in sand, and the peak spectral accelerations in rock occur at higher frequencies than in sand, v) Shear strains in sand are very much higher than those in rock. The peak strain for the rock is at the rigid base, and near the surface, at about a depth of 100 ft., for sand, and vi) Displacement time histories are similar for rock and sand.

The above results indicate that the stiffness of the medium greatly affects the free field response, and that the accelerations, stresses, spectral accelerations and the frequencies of the peak spectral accelerations are higher; the strains are lower in a medium with a higher shear modulus. Comparisons of time histories of accelerations and stresses in rock and sand indicate that as the damping of the sand is higher than that of rock, stresses and accelerations in rock change their signs more frequently compared to those in sand.

5.3 Containment Geometry

5.3.1 Shape of the Containment

The three shapes in Fig. 4.1 were investigated to compare the shape effects on the response of the soil-structure system. The area of the containment was kept almost constant. The results, presented in

Figs. 4.2 to 4.14, indicate that i) the maximum shear stresses and accelerations in the soil and the spectral accelerations at two locations in the containment for the high horseshoe shape are less than those in the other two shapes, ii) the maximum principal stresses in the high horseshoe are generally 10-20% lower than those in the circular roof-vertical wall containment, iii) the maximum principal stresses in the roof of the flat horseshoe are lower, and those in the walls and the floor are higher than the corresponding values for the high horseshoe, and iv) the soil reaction maxima under the foundation of the high horseshoe containment are about 30% lower than those for the semi-circular roof containment. The conclusion form the above results is that the high horseshoe shape is the best for earthquake excitation, taking into consideration the larger amount of excavation required for the flat horseshoe compared to the high horseshoe. This observation confirms the findings of Refs. 98, 22 and 64 for static and step pulse loadings for the rock medium.

5.3.2 Stiffness of the Containment

As described in sec. 4.3, the thickness of the containment walls and roof was increased from 5 to 10 ft., keeping the floor thickness (10 ft.) unchanged, in order to study the effect of increasing containment thickness on the response of the soil-structure system. The results in Figs. 4.15 to 4.19 show that doubling the thickness of the containment roof and walls, i) reduces the principal stresses in the roof and the walls by about 15-25%, and increases them in the floor by about 20%, ii) increases shear stresses in the soil near the containment walls by about 15%, and above the roof by about 70%, iii) reduces

the accelerations in the soil near the containment by about 8%, and iv) increases the accelerations and the spectral accelerations in the upper half of the containment by about 5%.

The small reduction of the stresses in the containment, and the increase of the stresses in the containment floor and in the soil, imply that the load exerted on the containment is increased by additional thickness. This can be easily interpreted as follows: doubling the thickness increases containment rigidity, and hence reduces its deformation which increases the load exerted by the soil on the structure. So, it seems better to use a flexible structure rather than a rigid one for earthquake resistance.

5.4 Depth of Burial

For the same site, three burial depths were considered; shallow, intermediate and deep with soil cover depths of 70, 150 and 220 ft. (Fig. 4.20). The results in Figs. 4.21 to 4.26 indicate that, compared to the containment at intermediate depth: i) The average increase in the maximum principal stresses in the containment for shallow embedment is about 50% with an increase in the peak value of 33%, and the average stress decrease in deep embedment is 20% with a decrease in the peak value of 33%, ii) The maximum horizontal accelerations in the containment are about 40% higher in the lower half, and almost equal for the upper half for the shallow depth; they are about 25% lower in the upper half and almost equal in the lower half for the deep embedment, iii) The maximum shear stresses in the soil near the containment are 45% higher for the shallow depth, and almost the same for deep embedment. The shear stresses near the ground surface are lower for the shallow embedment

and higher for the deep embedment, and iv) The spectral accelerations at the three locations in the containment (top of the roof, mid-height of the wall, and foundation mid-point) are higher for the shallow embedment and lower for the deep embedment, but the difference is larger in the case of the shallow embedment. The peak spectral acceleration at the top of the roof occurs at lower frequencies for the shallow embedment.

As the accelerations and spectral accelerations in the free field are high near the ground surface, very shallow embedment causes high stresses and accelerations in the containment and the surrounding medium. Taking into account all the factors discussed in Sec. 4.4, a soil cover of a depth of 150-200 ft. above the containment is recommended to i) protect the containment against major earthquakes, conventional weapons and man-caused damage, ii) to provide a static overburden pressure to balance the internal pressure, and iii) to provide additional protection from harmful radiation in the event of a seismic incident or a major accident.

5.5 The Medium Adjacent to the Containment

The medium adjacent to the structure was investigated for two different cases: i) backfill, and ii) isolation of the containment with a soft energy absorbing jacket.

5.5.1 Backfill

As described in Sec. 4.5 and outlined in Figs. 4.27, 4.28 and 4.29, four different materials are considered for the backfill: i) same as the original medium (excavated soil compacted enough to have the same properties as the original medium), ii) loose sand (excavated soil not

compacted enough), iii) stabilized sand (using cement), and iv) reinforced earth. These materials have stiffnesses and densities i) equal to, ii) less than, and iii-iv) higher than those of the medium.

The results in Figs. 4.30 to 4.60 show that, compared to the loose fill, i) The maximum principal stresses in the containment are about 30% higher for the original fill, 20% higher for the stabilized jacket, and about 20% lower for the reinforced earth jacket, ii) The maximum shear stresses in the soil near the containment are about 20% higher for the original fill, 25% higher for the stabilized jacket and 10% lower for reinforced earth at the level of the containment and about 80% higher below the level of the containment foundation, iii) The maximum horizontal accelerations in the soil near the containment are about 8% lower for the original fill, 7% higher for the stabilized jacket, and 10% lower for the reinforced earth jacket, and iv) The spectral accelerations at two points in the containment are about 5% lower for the original fill, 20% lower for the stabilized jacket, and 20-50% higher at low frequencies (0.5-3 Hz) and 20-30% lower at high frequencies (4-20 Hz) for the reinforced earth jacket.

Results for the original fill, the loose fill and the stabilized jacket indicate that, compared to the original fill, the loose fill reduces the stresses in both the containment and the medium; the stabilized jacket increases stresses in the medium and the containment walls and floor, and reduces the stresses in the middle part of the containment roof. This means that a considerable reduction in the maximum stresses in the containment can be achieved by introducing a filling material with a shear modulus less than that of the medium. This is because the deformations of the soft material between the medium and the containment

are larger than those of the medium, and hence part of the energy of the medium is absorbed and the load transmitted to the containment is reduced. The opposite is the case for a stiffer filling material. The conclusion from the above discussion is that the loose fill proved to be better than both the original fill and the stabilized jacket.

The reinforced earth jacket seems to be better than the loose fill as it reduces and redistributes the stresses in the containment, and reduces the maximum stresses and accelerations in the medium near the containment. The interpretation of the above findings is that the reinforcing bars bond the containment with the surrounding medium which allows the containment and a part of the surrounding medium to move as one integrated unit. This reduces the stresses and accelerations in both the containment and the medium. The considerable increase of the spectral accelerations in the containment at low frequencies supports this interpretation.

5.5.2 Effect of the Width of the backfill

The results in Figs. 4.45 to 4.54 indicate that increasing the width of the backfill between the containment and the surrounding medium from 10 to 70 ft., i) increases the soil and containment stresses by about 10% for loose fill, and 20% for the stabilized jacket, ii) reduces the accelerations in the soil at the containment level, and increases them near the ground surface for both the loose fill and the stabilized jacket, and iii) increases the spectral accelerations in the containment at low frequencies and reduces them at high frequencies for the stabilized jacket, while no significant variations are obtained for the case of the loose fill. In the case of the stabilized jacket, the increase

in the containment and medium stresses is due to the effect of the thin stabilized jacket described in Sec. 5.5.1. For the case of the loose fill, the increase in the medium and containment stresses is due to the existence of a considerably large region of loose material between the medium and the containment, which acts as an additional load on both the medium and the containment thereby increasing the stresses. The conclusion form the above discussion is that a relatively thin side cover of the filling material seems to be better than a thick one.

5.5.3 Isolation Jackets

Two types of crushable energy absorbing materials (polyurethane foam and foamed concrete) are used to isolate the containment in the sand medium (Fig. 4.61). The results in Figs. 4.62 to 4.73 indicate that, compared to the case of the loose fill (no isolation), i) Containment stresses are 65% lower for the polyurethane foam jacket, and 10% higher for the foamed concrete jacket, ii) Soil stresses at the containment level are 40% lower for the polyurethane foam jacket, and 15% higher for the foamed concrete jacket, iii) Soil accelerations at the containment level are lower by 15% for the polyurethane foam jacket, and 7% for the foamed concrete jacket, and iv) For the polyurethane foam jacket, the containment accelerations are 20% lower and 10% higher in the upper and lower containment halves respectively. The containment spectral accelerations are lower for the high frequencies while there are no significant differences in the accelerations or the spectral accelerations for the foamed concrete jacket.

The considerable reduction in the containment and medium stresses when using the polyurethane foam jacket, and the stress increase for the

case of the foamed concrete jacket are due to the same reason as that discussed in Section 5.5.1. As the stiffness of the polyurethane foam is very small compared to that of the medium, and the stiffness of the foamed concrete is relatively higher, the deformations of the polyurethane foam are considerably greater than those of the adjacent medium; those for the foamed concrete will be less than those of the medium which reduces the load transmitted to the containment for the polyurethane foam lining and increases it for the foamed concrete.

As described in Sec. 4.7, the containment in the rock medium was isolated by a jacket of foamed concrete. The pattern of stresses in the medium near the foamed concrete-lined containment in the rock medium is the same as that for the polyurethane foam-lined containment in the sand medium. This implies that the role of the foamed concrete jacket in the rock medium is similar to that for the polyurethane foam in the sand medium. As the stiffness of the foamed concrete is higher than that of the sand medium, and lower than that of the rock medium, the containment and medium stresses increased for the sand medium, and reduced in the rock medium for foamed concrete jackets.

5.5.4 General Conclusion

The materials used as backfill and isolating jackets are: i) loose fill (E = 150,000 to 240,000 psi and w = 95 pcf), ii) stabilized fill ($E = 1.5 \times 10^6$ psi and w = 145 pcf), iii) polyurethane foam (E = 319 psi and w = 1.5 pcf), and iv) foamed concrete (E = 375,000 psi and w = 50 pcf). The conclusions from the discussion of the results in Sec. 5.5.1 to 5.5.3 indicate that the relative stiffness of the filling material and the medium has a very significant effect on the stresses

in the containment and the medium. If the stiffness of the filling material is less than that of the medium, stresses in both the containment and medium will be reduced and vice versa. The lower the modulus of elasticity of the filling material, the greater is the reduction in the stresses. A reduction in the containment stresses, as much as 65%, can be achieved using a polyurethane foam jacket for the sand medium. Considerable reduction in containment stresses could be achieved in rock siting using a foamed concrete jacket. Using a reinforced earth jacket in a sand medium reduces containment stresses by 20%. Relatively thin jackets are better than thick ones.

5.6 Structure-Medium Interaction

5.6.1 Soil-Structure Interaction

The selected results of the typical case, described in Sec. 3.5.3 and outlined in Fig. 4.27(i), are used to study the degree of interaction of the soil-structure system. Figs. 3.35 to 3.39 show the interaction effects on response values at various depths in the soil profile, and Figs. 3.40 and 3.41 on the soil accelerations and stresses at vertical planes near the containment. As indicated in Figs. 3.35 to 3.41, the maximum soil accelerations, shear stresses and acceleration response spectra are considerably affected by the interaction specially near the structure. The presence of the containment reduces the free field soil stresses and accelerations. Comparison of the results of the underground siting presented herein and similar results for aboveground siting, presented in Ref. 47, indicate the interaction effect in the aboveground siting to be larger than that for underground siting. As a) the spectral and the maximum accelerations at the ground surface are consid-

erably larger than those below the ground surface, and b) the aboveground structure represents an additional mass and stiffness to the soil, while the underground structure substitutes the mass and stiffness of the excavated soil, the disturbance in the medium caused by the existence of the aboveground structure is greater than that caused by the underground one.

5.6.2 Rock Structure Interaction

The results, presented in Figs. 4.86 to 4.91 for a containment isolated by a foamed concrete jacket in a rock medium, indicate that in a sand medium the containment is subjected to higher stresses and lower accelerations compared to that in a rock medium. This means that, as the rock stiffness is higher than that of sand, a containment in a sand medium will be subjected to a higher dynamic loading.

5.7 Examination of Accuracy of Results

The accuracy of the free field response was checked by comparing the computed response obtained by LUSH (finite element) and SHAKE (wave propagation). As shown in Figs. 3.6 and 4.76 for sand and rock media respectively, there is good agreement between responses obtained by the finite element and wave propagation solutions.

The accuracy of the results of the soil-structure response, for each case studied, was checked by comparing the computed response at an ample distance away from the containment with the free field response obtained from the one-dimensional column studies. This also provides a check on the adequacy of the extent of the finite element mesh. As described in section 3.5, good agreement between the response values near the boundaries of the two-dimensional finite element model and the

one-dimensional column studies was obtained in each case.

5.8 Conclusions

The following conclusions are drawn from this study:

1. The response values of the medium near the containment are considerably affected by the interaction. Stresses, accelerations and spectral accelerations in the medium near the containment are lower than those in the free field.

2. The interaction affect in aboveground siting is larger than that for underground siting.

3. The dynamic load exerted by the medium on the containment in sand is larger than that for rock, but the containment accelerations are lower.

4. The shape of the containment affects the response of the containment and the medium. The horseshoe shape proves to be better than the one with a semi-circular roof and vertical walls - a reduction in the containment stresses of 10-20%. The high horseshoe containment (rise-to-span ratio of 1/2) is better than the flat horseshoe (rise-to-span ratio of 1/4) taking into consideration that the latter needs a larger amount of excavation due to the need for a wider pit.

5. Dynamic loading of the medium on the containment increases by a rise in the containment stiffness. So, it seems better to use a flexible containment rather than a rigid one.

6. The containment stresses and accelerations can be significantly reduced if the containment is placed in deeper locations. Successive reductions in containment stresses to 67% of the initial values are associated with each additional 70 ft. embedment depth.

7. The relative stiffness of the filling material and the medium has a significant effect on the containment and medium responses. Material with stiffness lower than that of the medium reduces the stresses in both the medium and the containment and vice versa. A filling material, with stiffness 30% lower than that of the medium, reduces the stresses by about 30% in the containment and about 20% in the medium.

8. A considerable reduction in the containment stresses can be achieved by isolating the containment from the surrounding medium by a jacket of energy absorbing material. The stiffness of the jacket material should be very small compared to that of the medium. This can be achieved by using a jacket of polyurethane foam in a sand medium, and foamed concrete or polyurethane foam jacket in a rock medium.

9. A reduction of 65% in the containment stresses and 40% in the medium stresses was accomplished using a polyurethane foam jacket in a sand medium.

10. Introducing a system of steel bars or nets around the containment to form a reinforced earth jacket reduces the stresses in the containment by about 20%.

11. Increasing the width of the side cover of the filling material form 10 ft. to 70 ft., increases the stresses in the medium and the containment by about 10-20% for both stiffer and softer filling material. So, it seems better to provide a relatively small side cover width.

12. Vertical element size affects the response of the finite element model. Elements with larger vertical element size are unable to transmit shear waves with short wave lenghts (high frequencies).

5.9 Contributions

1. Development of a finite element model for soil-structure interaction analysis of a full-scale cut-and-cover type underground nuclear reactor containment subjected to earthquake excitation.

2. Study of soil structure interaction taking into account soil non-linear behaviour and variable damping in each element.

3. Application of LUSH for underground analysis.

4. A study of the effect of the following parameters on the dynamic response and earthquake resistance:

a) containment shape,

b) depth of burial,

c) relative stiffness of the containment and the medium,

d) relative stiffness of the filling material and the medium, and

e) isolation of the containment.

5. Evaluation of the effectiveness of a reinforced earth jacket around the containment to reduce its stresses.

6. Indication that the relative stiffness of the filling material has the most significant effect on the containment stresses (Ref. 64 did not make a clear conclusion of this nature).

7. Comparison of the response and the degree of interaction:

a) in rock and sand siting and b) for aboveground and underground siting in sand.

8. Study of the effect of the vertical element size on the free field response.

5.10 Summary

A finite element model has been established to study the response

of a 1100-MWe cut-and-cover type underground nuclear reactor containment to earthquake excitation. The analyses have been carried out using two available computer programmes, LUSH and SHAKE, taking into account the strong non-linear effects which occur in soil masses subjected to strong earthquake motions. All the parameters needed for the analysis, including the details of the finite element model, have been investigated and carefully chosen. The extensive care taken to minimize the computation time enabled a considerable saving in the cost of the analysis.

Parametric studies have been carried out for the shape, stiffness and burial depth of the containment, and the relative stiffness of the filling material and the medium, including isolating jackets.

Comparative studies are presented for rock vs. sand siting and aboveground vs. underground siting.

The accuracies of the response for the free field and structure-medium interaction have been verified.

5.11 Recommendations for Further Research

1. Analysis of multi-structure-soil interaction by considering the actual configuration of the underground power plants (reactor containment, turbine generator building ... etc.).

2. Increased complexity of structural detail in the reactor structure (variable thickness, layout of steel reinforcement, configuration of prestressing cables ... etc.).

3. The analysis of the crushable materials used in the isolation jackets by eliminating the cracked and crushed elements from the system.

4. More exact non-linear analysis to account for the actual soil stress-strain characteristics. (This study considered the non-linear

soil behaviour in an approximate manner i.e. the equivalent linear method).

5. Inclusion of a capability for node separation due to the poor tensile strength of soil, or separation of the reactor structure from the surrounding medium.

6. Study of the effect of liquefacation of saturated sand layers during strong earthquakes.

7. Study of the feasibility of introducing new artificial absorbing boundaries with elements of considerably high damping and low stiffness (possibly using the variable damping analysis provided in LUSH).

8. Application of three-dimensional finite element analysis.

TABLES AND FIGURES

Table 1. Summary of Underground Nuclear Power Plant Feasibility Studies [97].

Study By	Concept	Criteria and Features	Conclusions	Unresolved Issues
(1) Ref. 8 (1958)	General underground	To evaluate both advantages and disadvantages	(a) 3 to 7% more costly; (b) Effective concontainment; (c) Extensive site investigation; (d) Limited expansion capabilities	----------
(2) Ref. 70 (1966)	Annular space around structure filled with water or mud	To withstand differential ground displacement	(a) Further studies required to assess feasibility; (b) No cost comparison with surface sites; (c) No safety conclusions	(a) Tilting and rotations caused by earthquakes; (b) additional engineering systems and requirements
(3) Ref. 67 (1969)	Within a hillside (horizontal access)	(a) Good quality rock; (b) 500 Mw BWR and/or AGR	(a) Feasible; (b) Construction costs less than 3% more for underground; (c) Safe	(a) Seismic effects; (b) Use of rock as containment; (c) Ground water contamination
(4) Ref. 77 (1971)	450 feet below ground level	(a) Good quality rock; (b) 2,000 Mw EWR in 2 units	(a) Feasible; (b) Additional $6 to $10 per kw on construction costs; (c) Added safety; (d) Incentive for urban siting	(a) Possible elimination of primary containment; (b) Use of ultimate flooding system in worst emergency

Table 1 (continued)

Study By	Concept	Criteria and Features	Conclusions	Unresolved Issues
(5) Ref. 96 (1971/72)	Deep rock cavity below grade	(a) Good quality rock; (b) 1,000 Mw PWR	(a) Feasible; (b) Construction costs 5 to 20% more for underground	(a) Geotechnical and seismic design criteria
(6) Ref. 89 (1971)	2 alternatives: (a) Totally underground; (b) Near surface reactor only underground	(a) Good quality rock for totally underground option, wider variety of rock quality for near surface option; (b) 1,000 to 1,500 Mw BWR	(a) Feasible; (b) Safe, increased protection from surface hazards	(a) Possible reduction in earthquake design force
(7) Ref. 98 (1972)	Deep rock cavity	(a) Good quality rock; (b) 1,000 Mw BWR	(a) Feasible; (b) Underground cost penalty about 5% of total cost; (c) Safe, should allow reduction in population distance	(a) Seismic response; (b) Population-distance criteria (c) Contianment criteria
(8) Ref. 87 (1972)	Underground generally	(a) LMFBR demonstration plant, Oakridge, Tennessee	(a) Distinct advantage with underground concept because of consequences of LMFBR accident	----------

Table 1 (continued)

Study By	Concept	Criteria and Features	Conclusions	Unresolved Issues
(9) Ref. 15 (1973)	General Underground concepts	----------	----------	(a) Proof of fault inactivity; (b) Lack of measurements or studies on the frequency characteristics of strong earthquake motion at depth
(10) Ref.21 (1973)	Above grade construction with crushed rock and earth cover to a minimum of 50'	----------	(a) Improved safety, less susceptible to surface phenomena and sabotage, minor radioactivity releases are made less severe	----------
(11) Ref.43 (1973)	General study, variety of underground and aboveground concepts. Underground types include deep rock cavity & "cut and cover" concepts.	Deep Rock Cavity (a) Good quality rock, no faults. Cut and Cover (a) Variety of rock and soil conditions allowable. Possibly allow for faulted rocks. (c) All studies based on 1,000 Mw LWR.	(a) Few sites available in California for deep rock cavities; (b) Generally more sites available inland for surface plants; (c) All options technically feasible; (d) Improved safety compared with surface plants	(a) Lack of seismic field data regarding possibility of reducing seismic loadings underground

Table 1 (continued)

Study By	Concept	Criteria and Features	Conclusions	Unresolved Issues
(12) Ref.3 (1973)	Cut and cover selected back-fill material	(a) Variety of ground conditions; (b) 1,100 Mw reactor, no limitations on type	(a) Feasible; (b) Additional costs of undergrounding are negligible; (c) Harmful radiation from worst possible accident can be confined	----------

General conclusions of the above studies regarding the underground siting of nuclear power plants can be summarized as follows [97]

(a) Placing nuclear power plants underground is technically feasible without an excessive economic penalty compared with surface plants.

(b) There are potential safety advantages which may permit such plants to be sited closer to population (and load) centers.

(c) There is a potential for a reduction in the design seismic loads on various components of the plant. However, at present there is a lack of field data to substantiate the design approach of reducing seismic loads.

(d) Conventional excavation methods would be satisfactory for caverns of the sizes required.

Table 2. Assessment of underground siting [53]

Potential advantages	Potential disadvantages
1. Additional confinement of radioactive materials with leakproof sealing of containment penetrations-possibilities for controlling hypothetical accidents and thus reducing the distance from densely populated areas required for safety 2. Elimination of the load cases 'airplane crash', 'pressure wave', 'extreme effects of weather'-possible protection from attack with weapons 3. Additional protection from direct radiation 4. Protection from leaking combustible liquids 5. Better response in the event of an earthquake when the surrounding soil is sufficiently compact 6. Better protection from the possibilities and effects of serious sabotage-greater assurance of supply in times of war as the result of underground siting of the entire plant 7. Better adaptability to future requirements by increasing the earth fill 8. Additional freedom in designing and site selection, including lower land acquisition costs 9. Defined surrounding conditions 10. Simplification of the problems resulting on termination of reactor operation	1. Limitation of the height of the structure (rock caverns) 2. Ground water problems-particularly during construction 3. Higher costs and longer construction periods with indefinite data as to their extent 4. Less flexibility within the plant for later changes and technical innovations 5. Insufficient experience with commercial nuclear power plants 6. Less accessibility-extension of supply lines might be necessary <u>Unclarified aspects</u> 1. Effect on public opinion and licensing procedure 2. Questions of landscape preservation and aesthetics 3. Effects of soil and water pressure 4. Possibilities for subsequent use of the containment for storing radioactive materials

Table 3. Summary of Assessment of Soil-structure Interaction Techniques [1]

Approach	Advantages	Disadvantages
Closed form solution	Valuable for indicating trends regarding the effects of various parameters on soil-structure interaction under earthquake loading. Some three-dimensional problems have been solved.	Solutions limited to simplified representations of structure geometry, soil material properties, and loading conditions.
Finite difference techniques	Attractive approach for studying soil-structure interaction. Can accommodate complicated boundaries, partial loading, nonlinear material properties, and layered sites. Satisfactory model of soil mass and stiffness is provided. Quiet boundary adaptations currently being developed.	Displacements, stresses defined by interpolation except at finite number of points. Increased computer run time and associated technical effort required for analysis. Many refined finite difference codes, although widely used in nuclear weapons effects problems, have never been applied to earthquake problems. At present, practical use in dynamic problems is limited to two-dimensional idealizations.
Finite element techniques	Same advantages as indicated above for finite difference technique. Generally, wider application to earthquake response calculations than many finite difference techniques.	Unless quiet boundary techniques are available, radiation damping not accounted for. Except for some non-linear codes, internal damping simulated by approximate viscous damping mechanism. Increased computer run time and associated technical effort required for analysis. Relatively few studies of convergence of solution. At present practical use in dynamic problems is limited to two-dimensional idealizations.

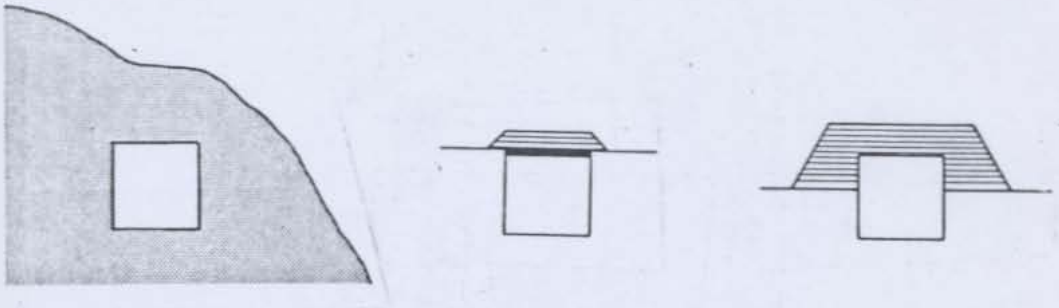

FIG. 2.1 VARIATIONS OF UNDERGROUND SITING [53]

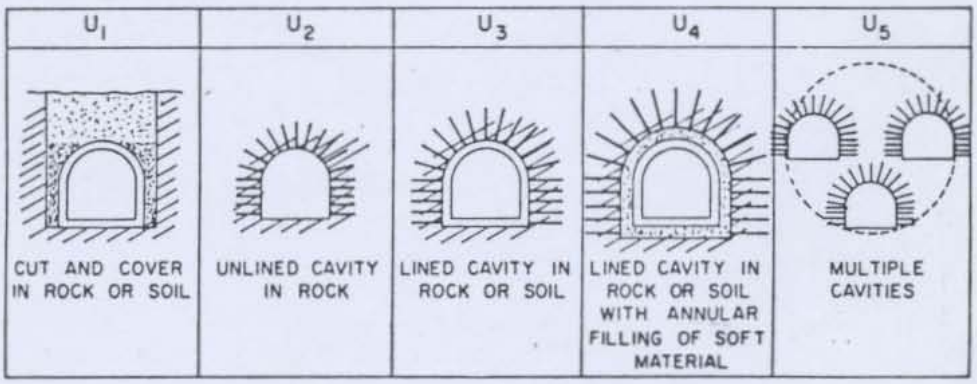

FIG. 2.2 UNDERGROUNED CAVITIES (SHOWING ROCK BOLTING) [75]

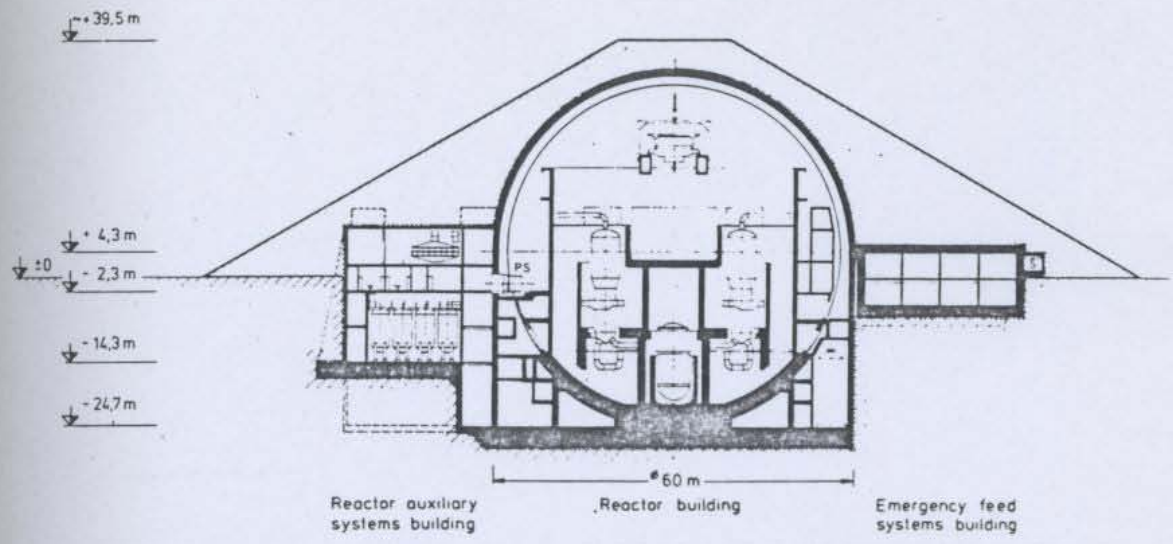

i- Semi-Embedded PWR Plant

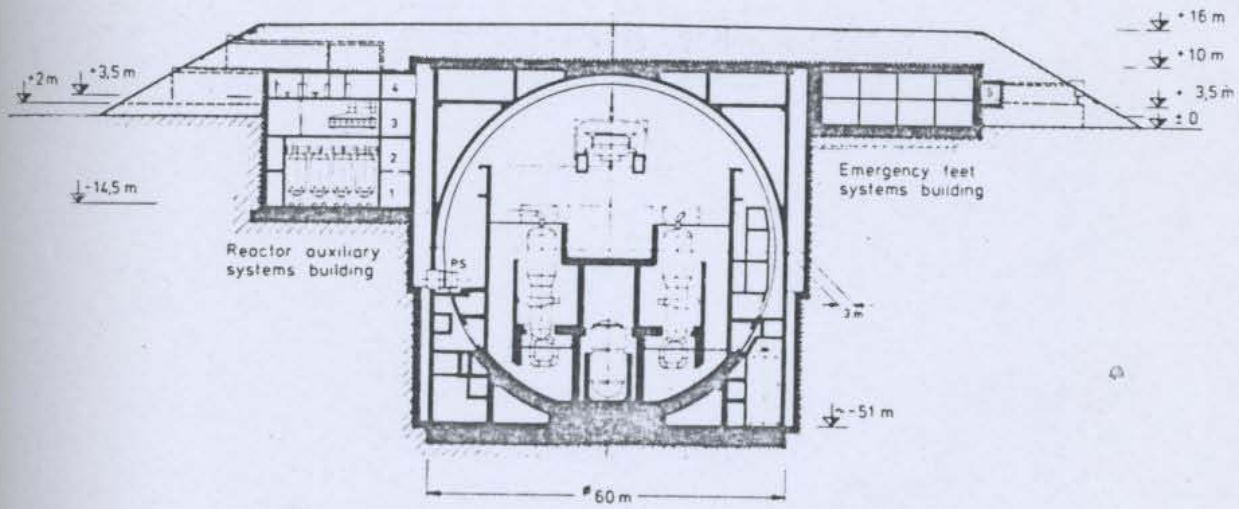

ii- Totally Embedded PWR plant

FIG. 2.3 SEMI AND TOTAL EMBEDMENTS FOR 'CUT-AND-COVER' TYPE NUCLEAR REACTOR CONTAINMENTS [53]

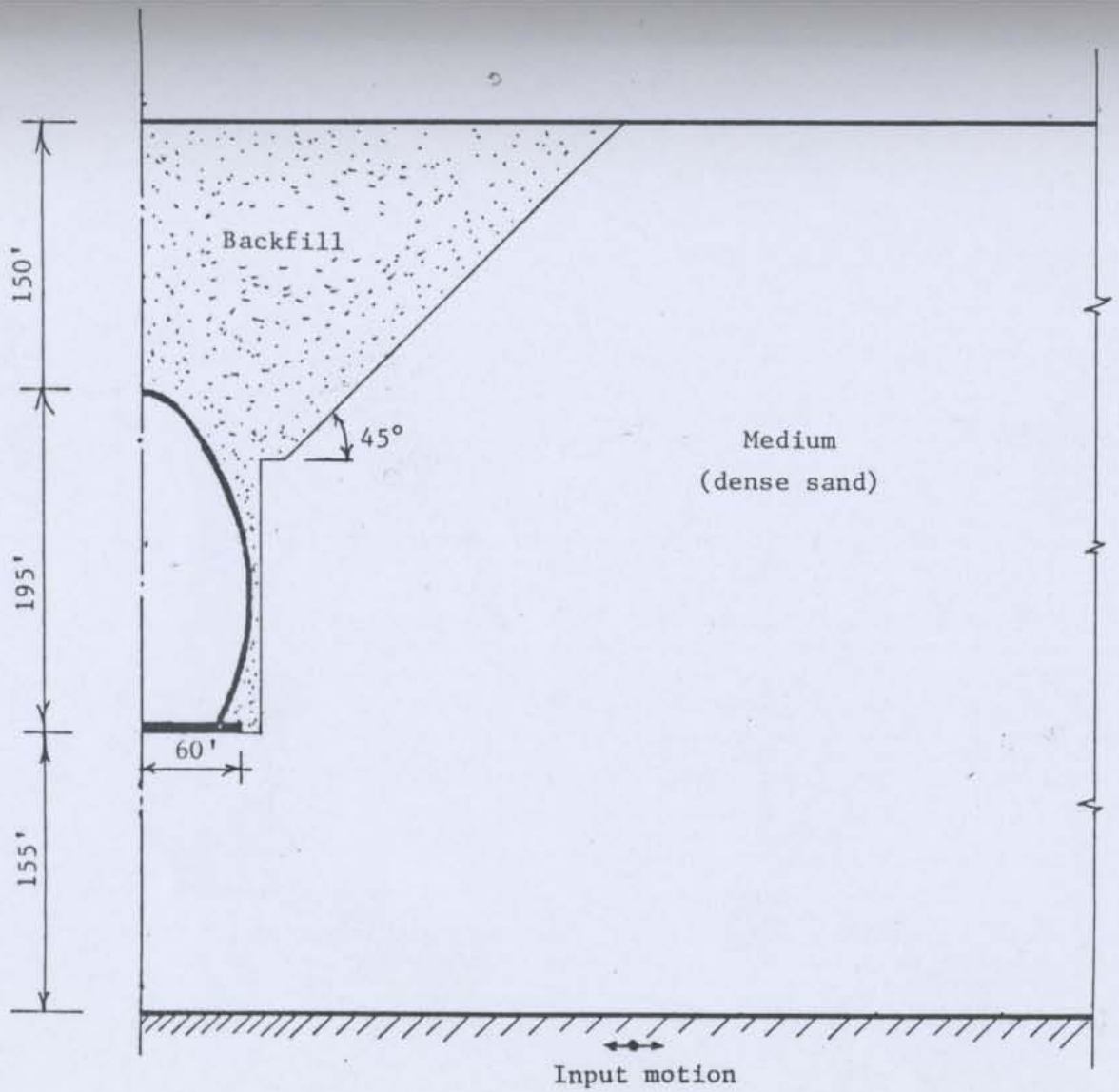

FIG. 3.1A CONTAINMENT, MEDIUM AND BACKFILL FOR A TYPICAL CASE

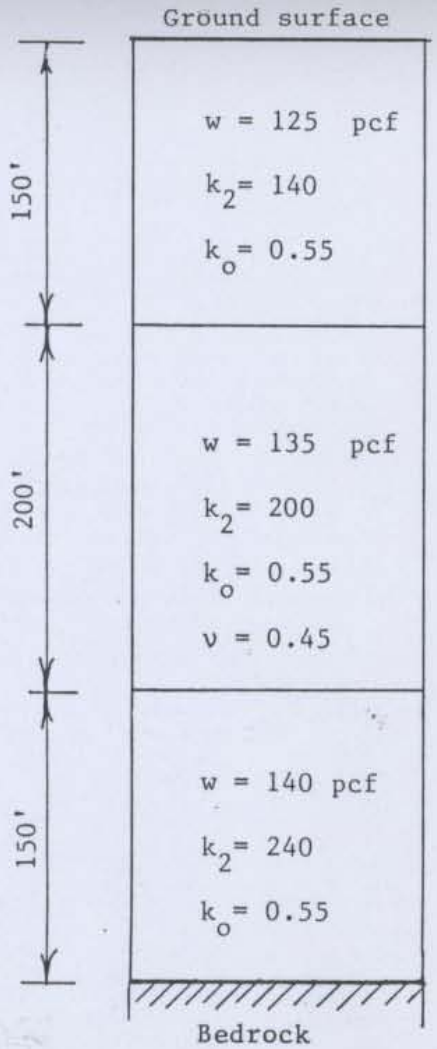

FIG. 3.1B SOIL PROFILE AND PROPERTIES

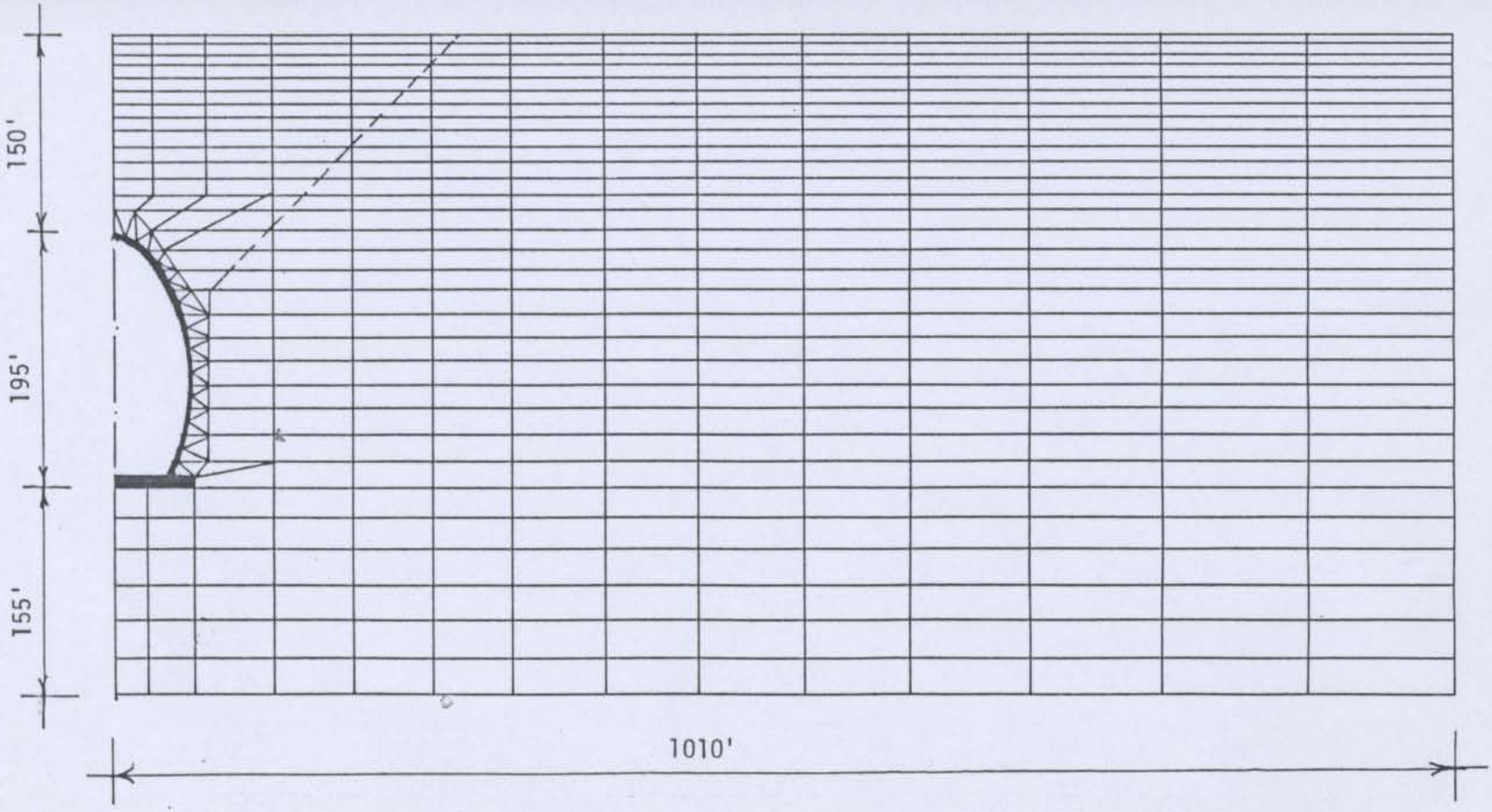

FIG. 3.2 FINITE ELEMENT DISCRETIZATION OF THE SOIL-STRUCTURE SYSTEM

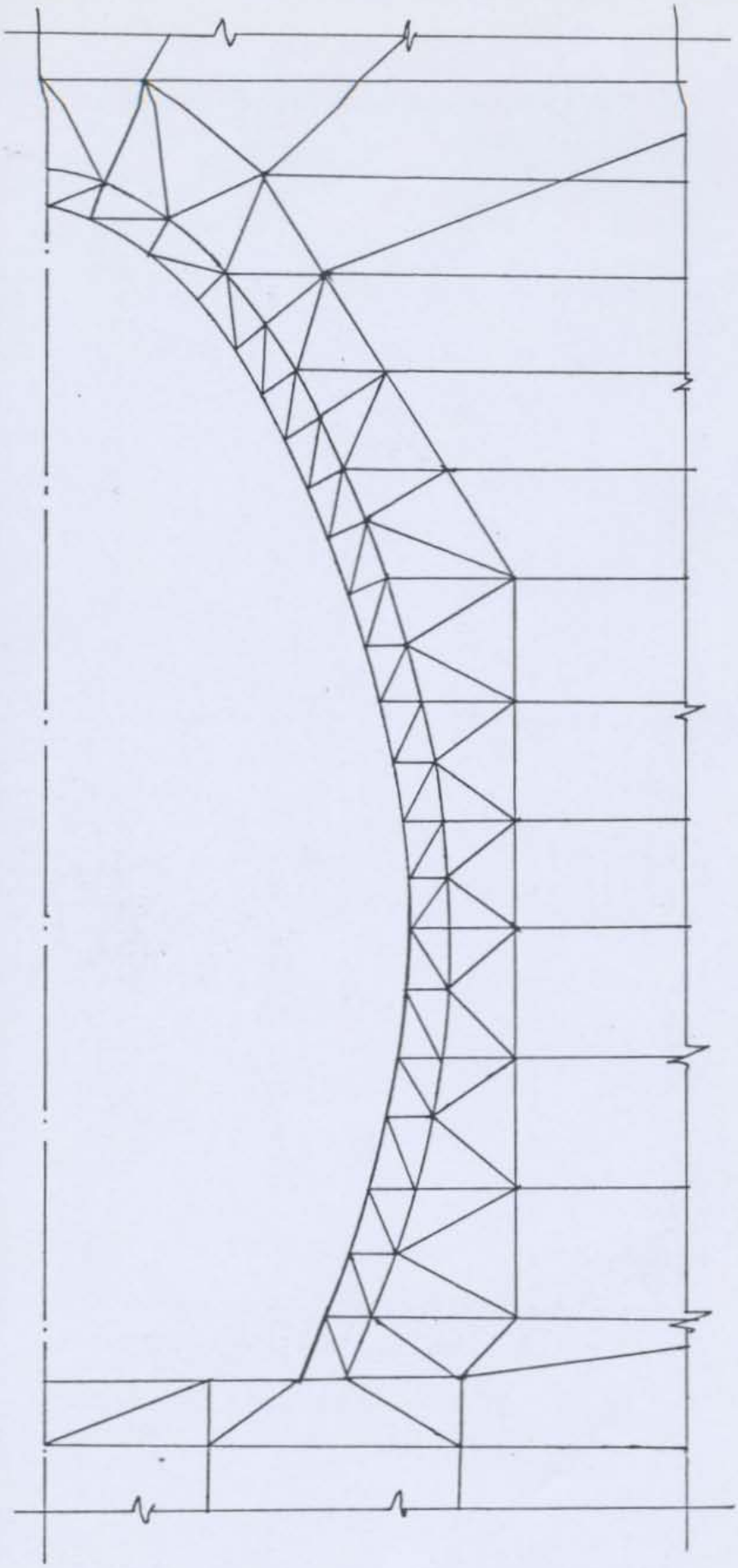

FIG. 3.3 FINITE ELEMENT MESH FOR THE STRUCTURE AND PART OF THE ADJACENT MEDIUM

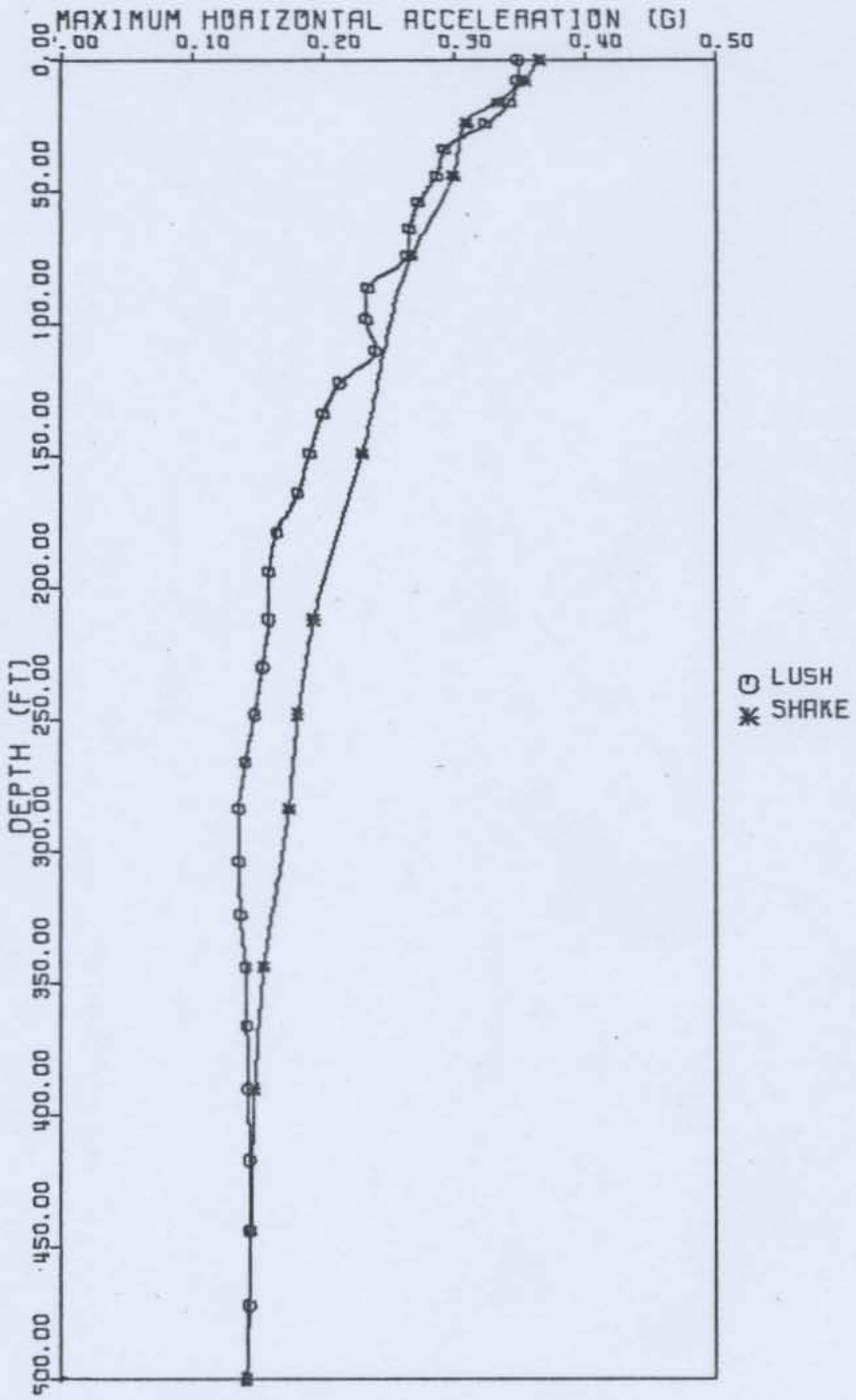

FIG. 3.4 MAXIMUM FREE FIELD HORIZONTAL ACCELERATION IN SAND - COMPUTED FROM LUSH AND SHAKE

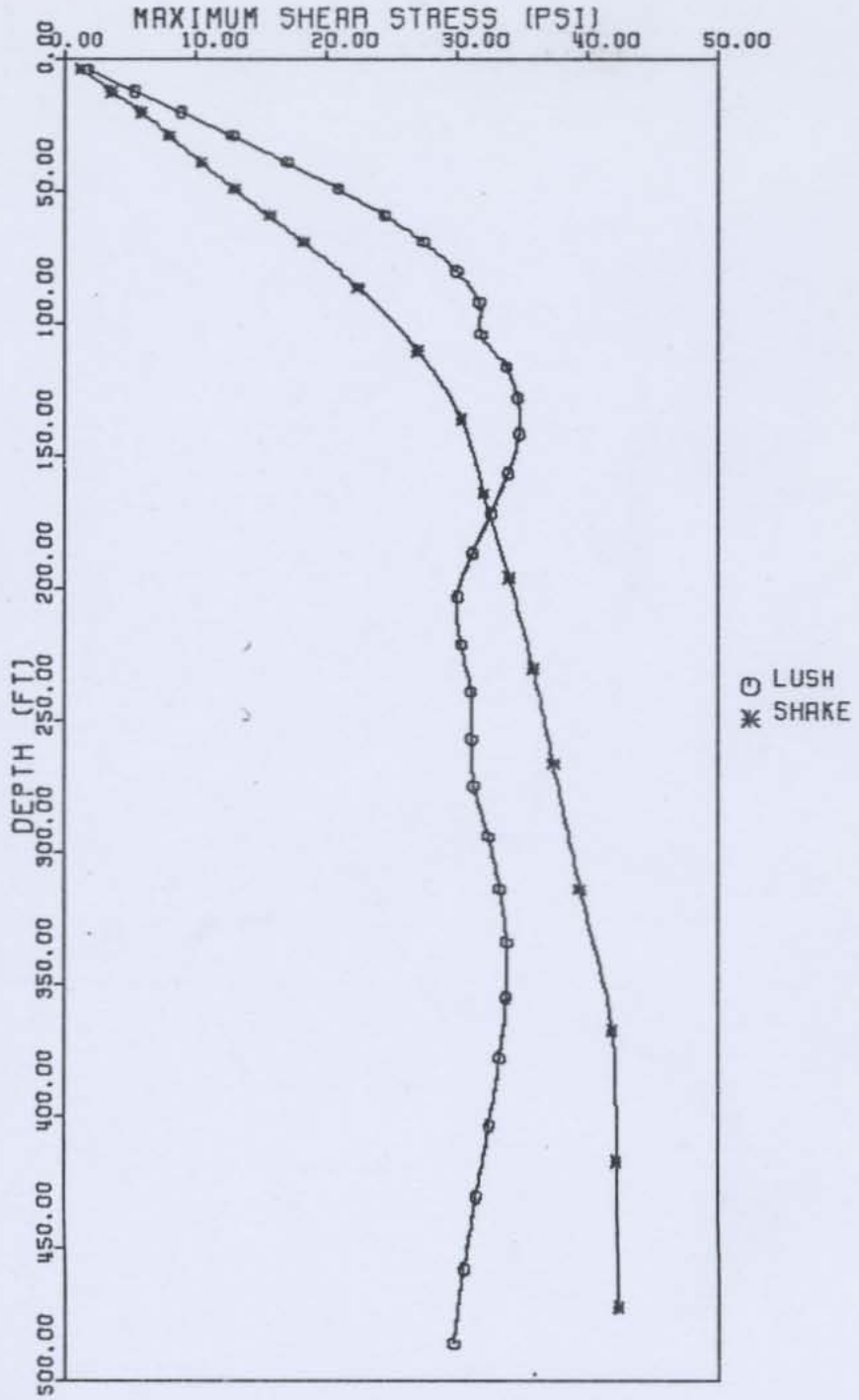

FIG. 3.5 MAXIMUM FREE FIELD SHEAR STRESSES IN SAND COMPUTED FROM LUSH AND SHAKE

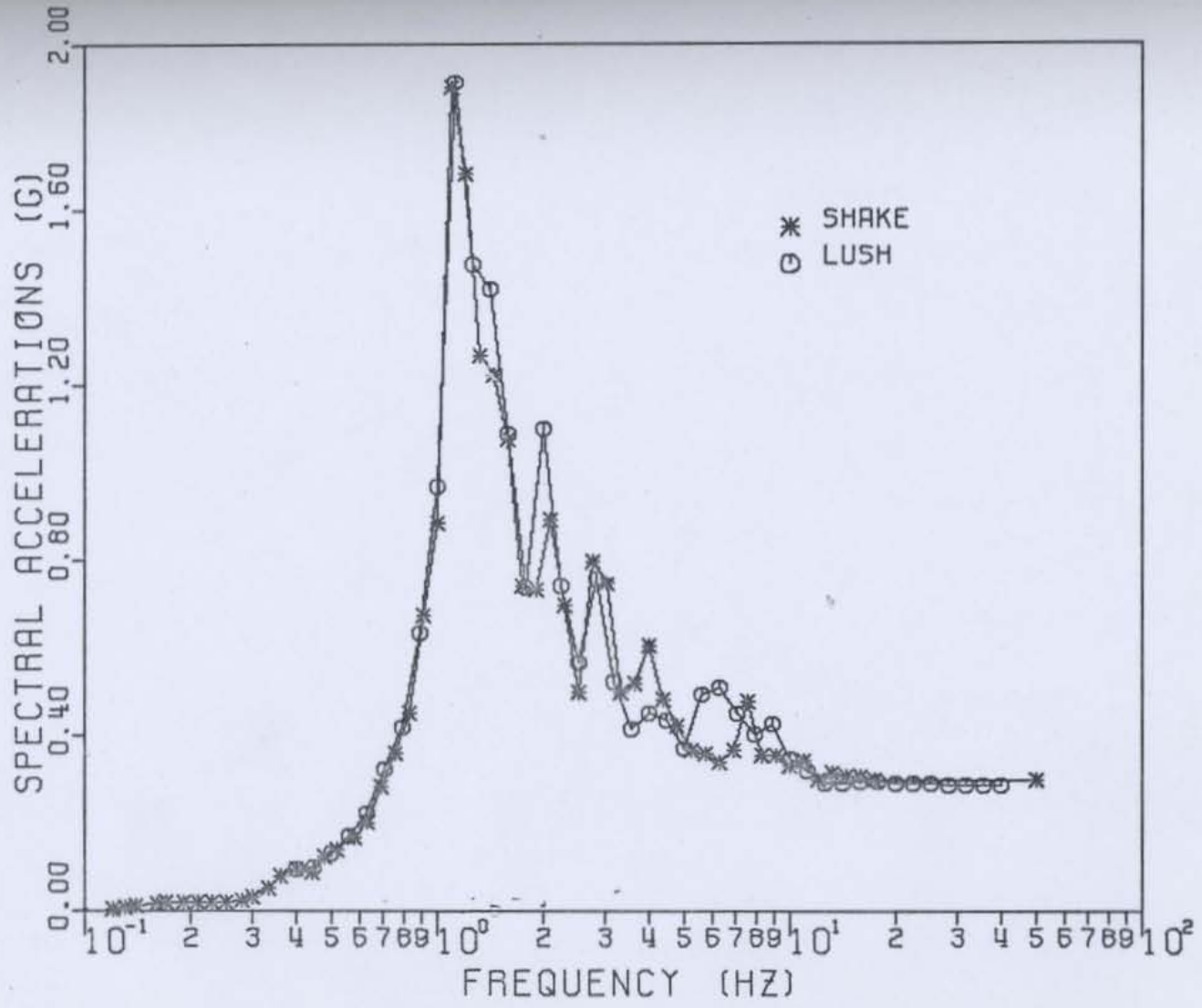

FIG. 3.6 FREE FIELD ACCELERATION SPECTRA AT A DEPTH OF 44 FT - COMPUTED FROM LUSH AND SHAKE - SAND MEDIUM (SPECTRAL DAMPING=2%)

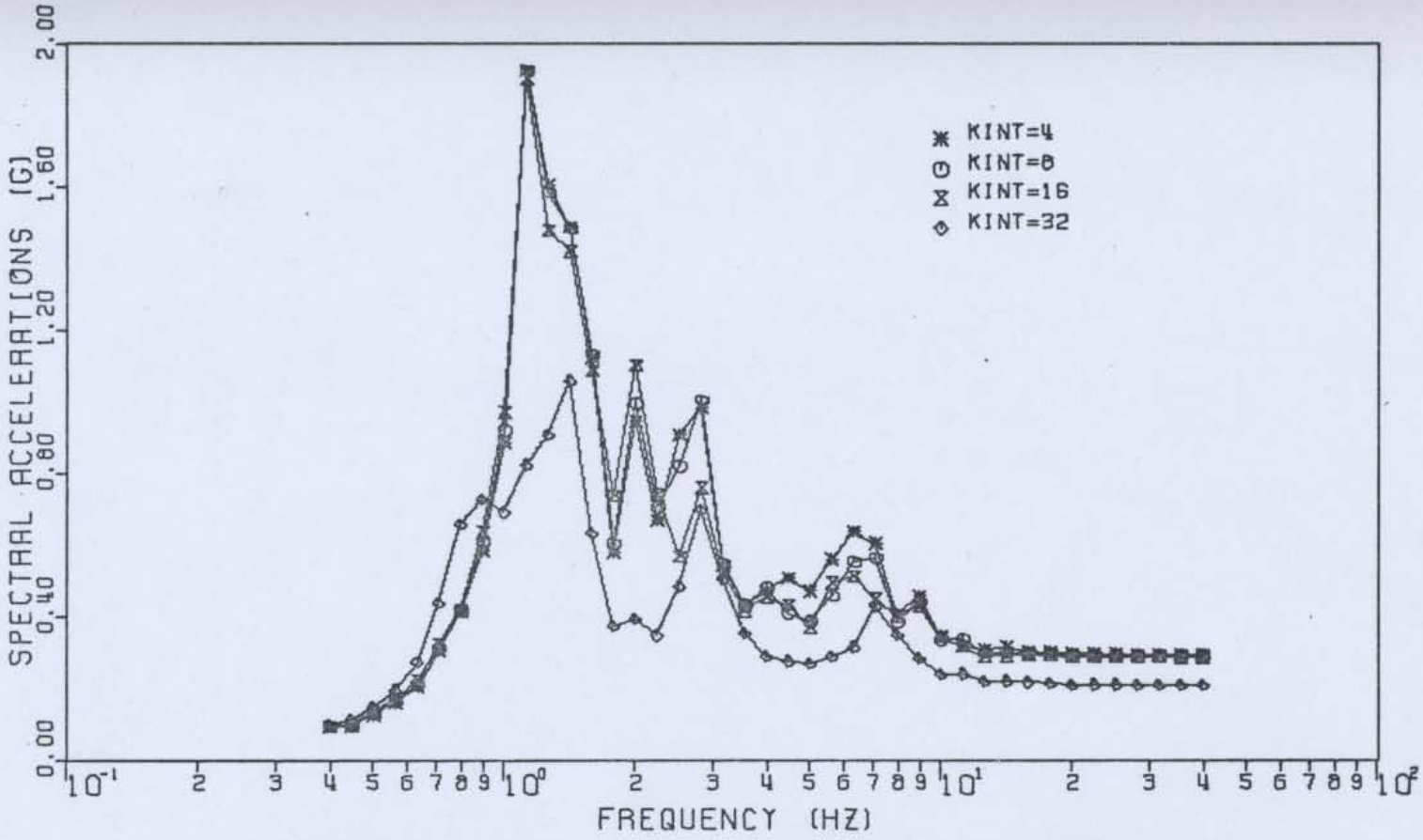

FIG. 3.7 FREE FIELD ACCELERATION RESPONSE SPECTRA AT A DEPTH OF 40 FT FOR DIFFERENT VALUES OF THE INTERPOLATION COEFFICIENT (KINT) (SPECTRAL DAMPING = 2%)

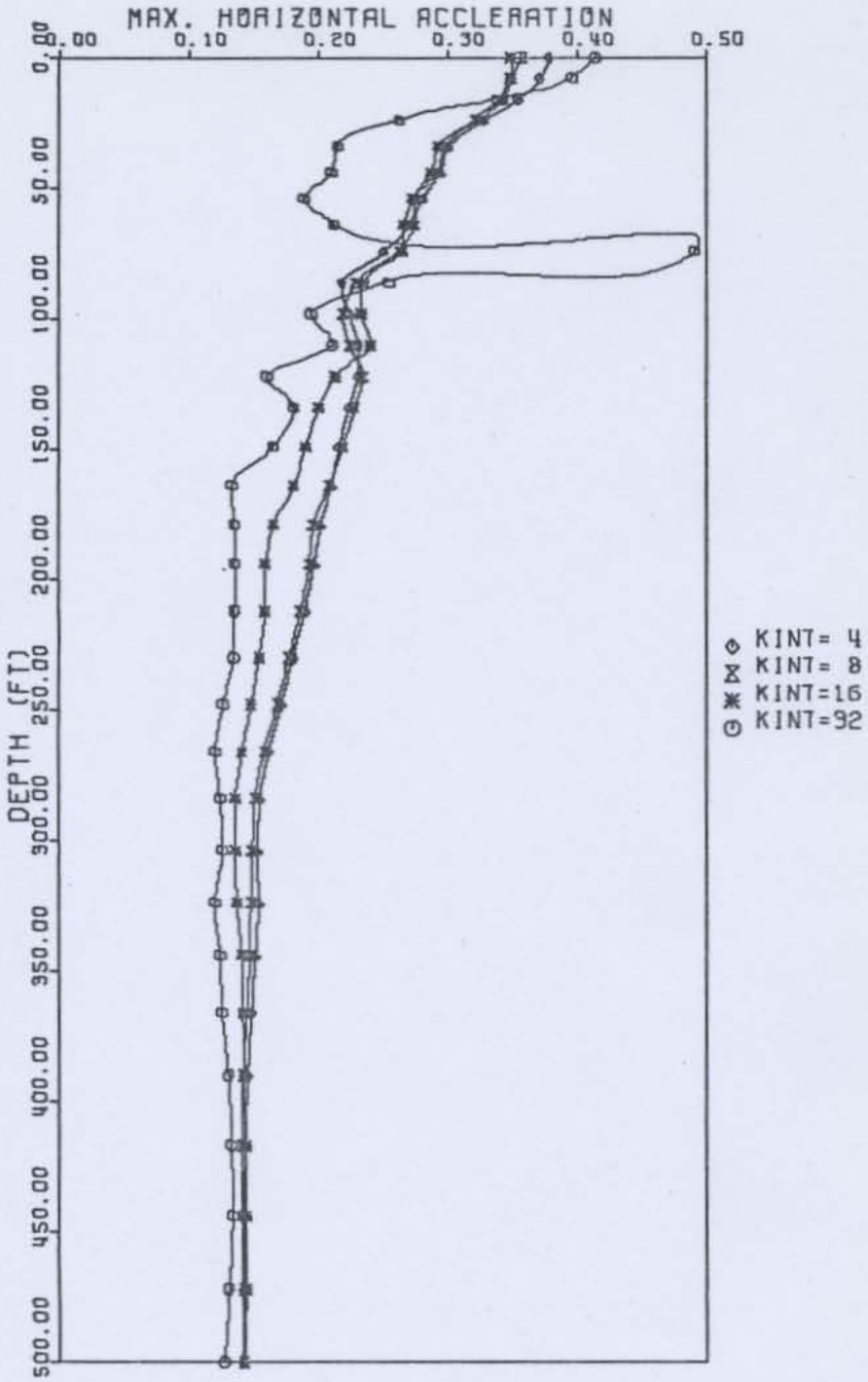

FIG. 3.8 MAXIMUM FREE FIELD HORIZONTAL ACCELERATION IN SAND FOR DIFFERENT VALUES OF THE INTERPOLATION COEFFICIENT (KINT)

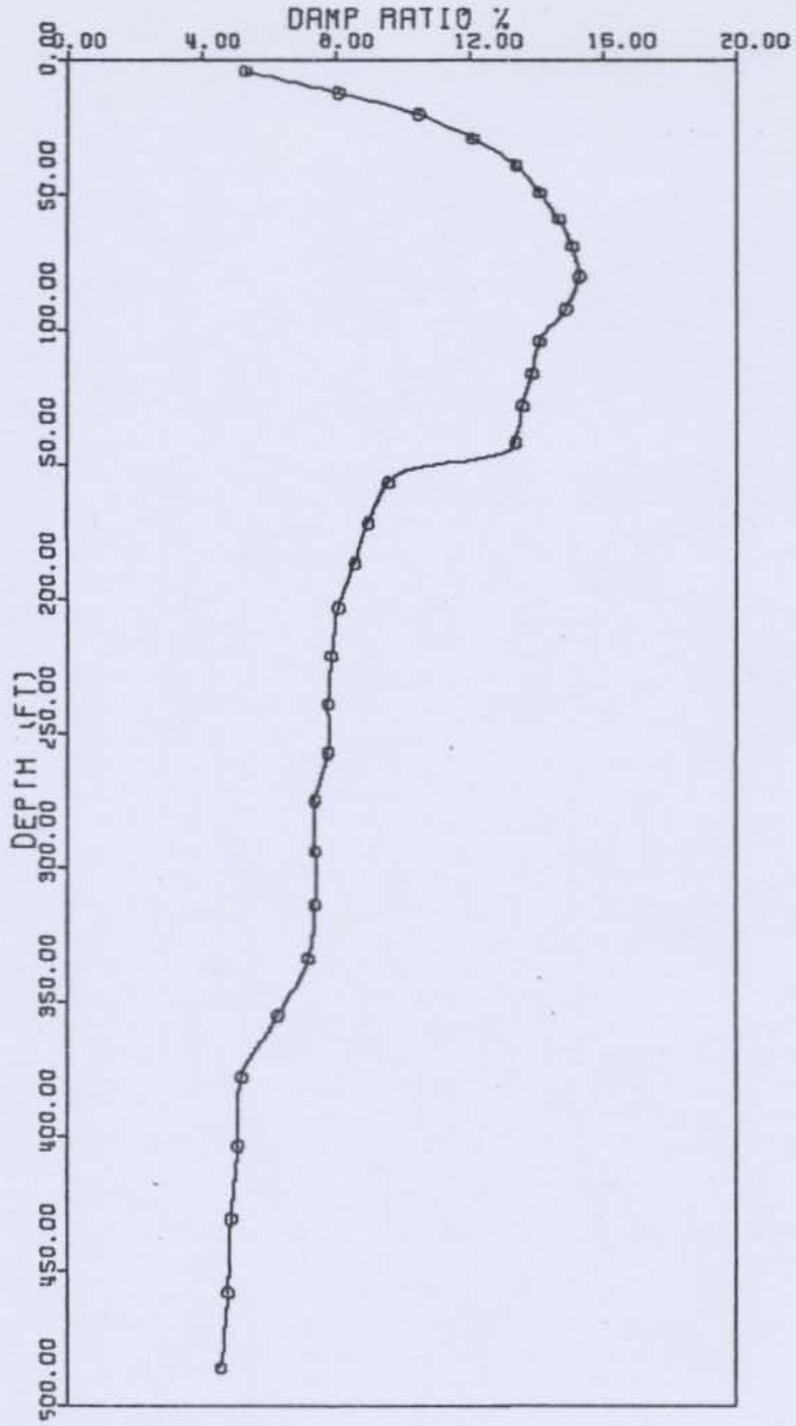

FIG. 3.9(A) STRAIN-COMPATIBLE DAMPING RATIO - SAND

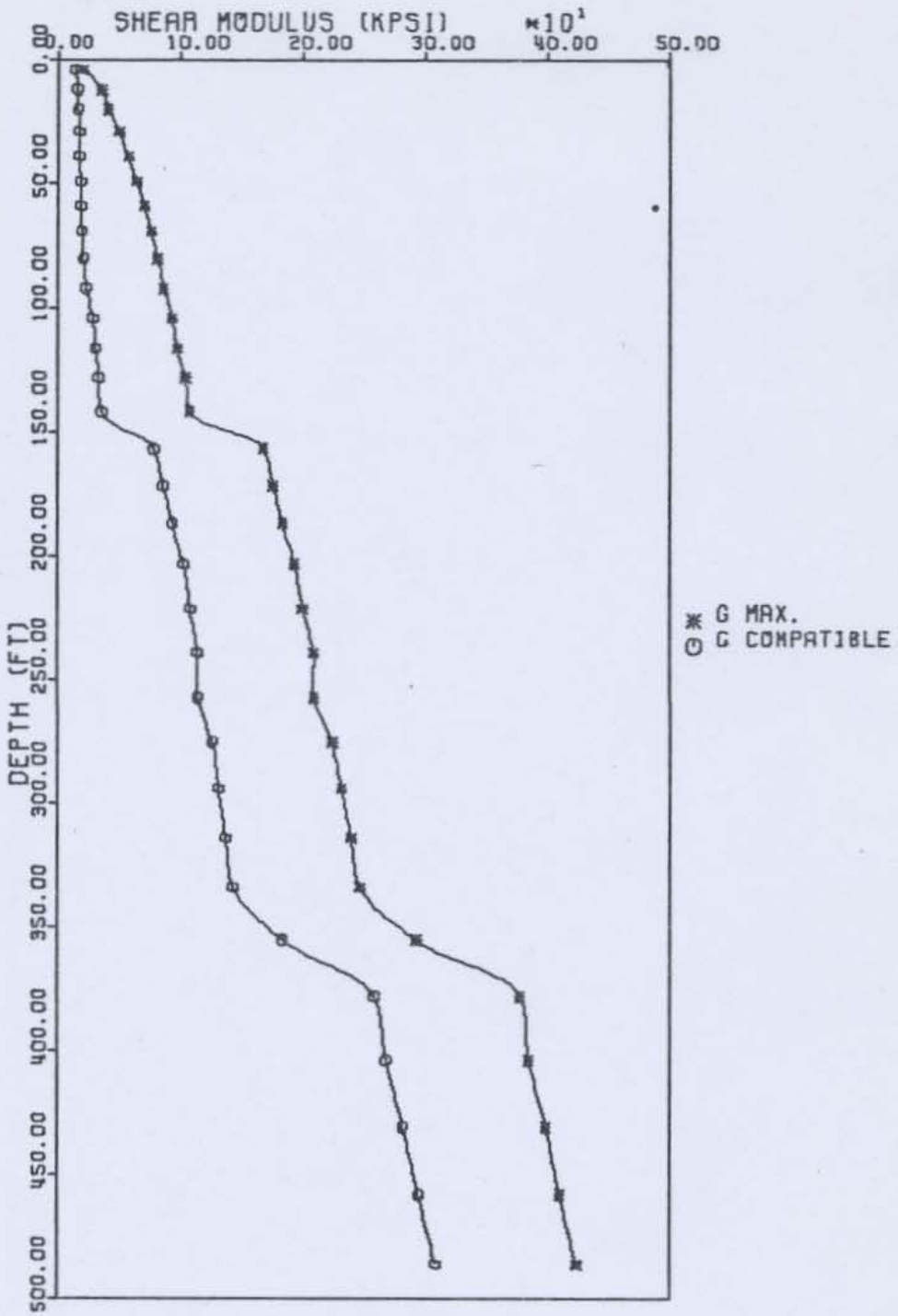

FIG. 3.9(B) MAXIMUM AND STRAIN-COMPATIBLE FREE FIELD SHEAR MODULI FOR SAND

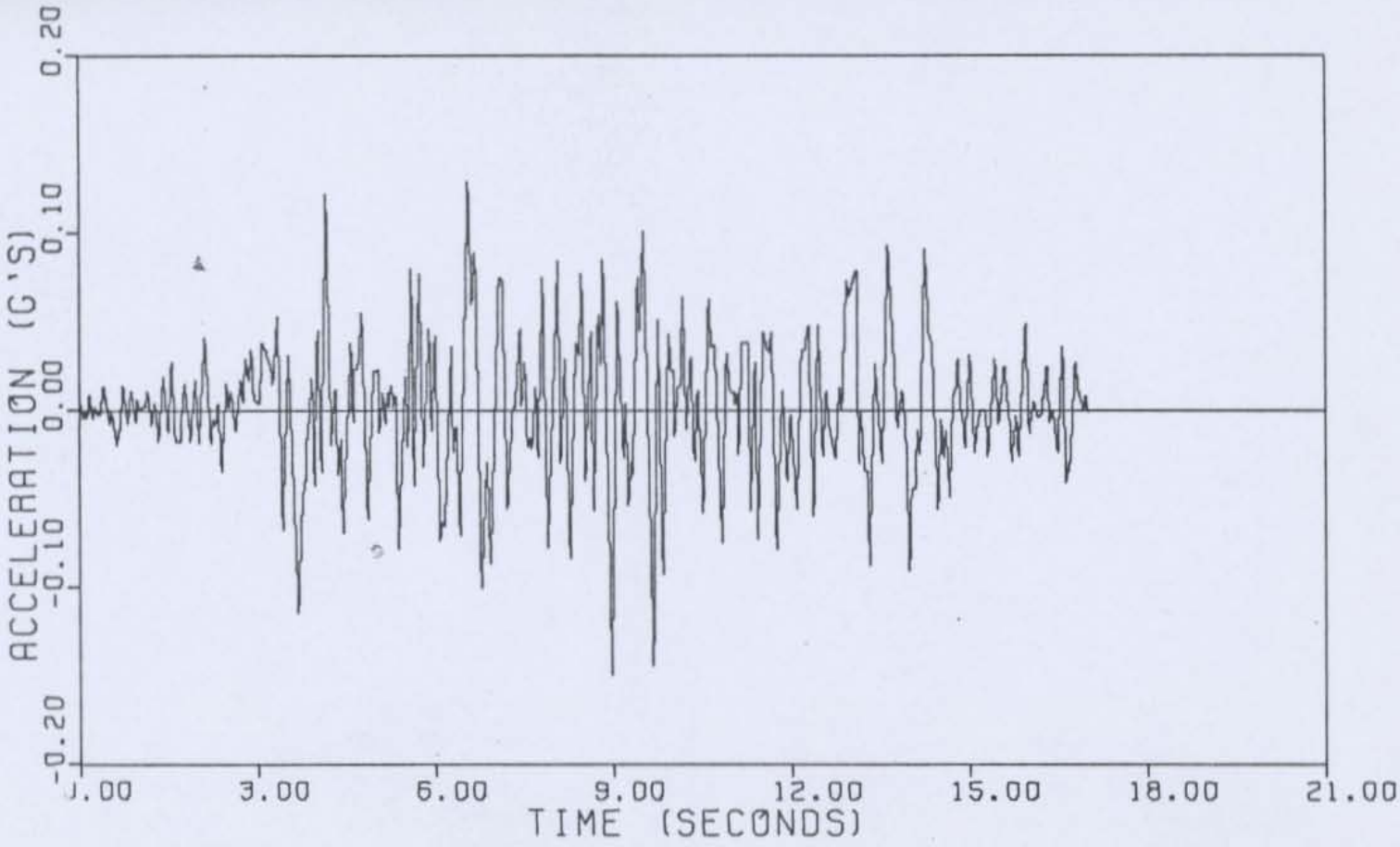

FIG. 3.10 INPUT MOTION FOR TAFT EARTHQUAKE

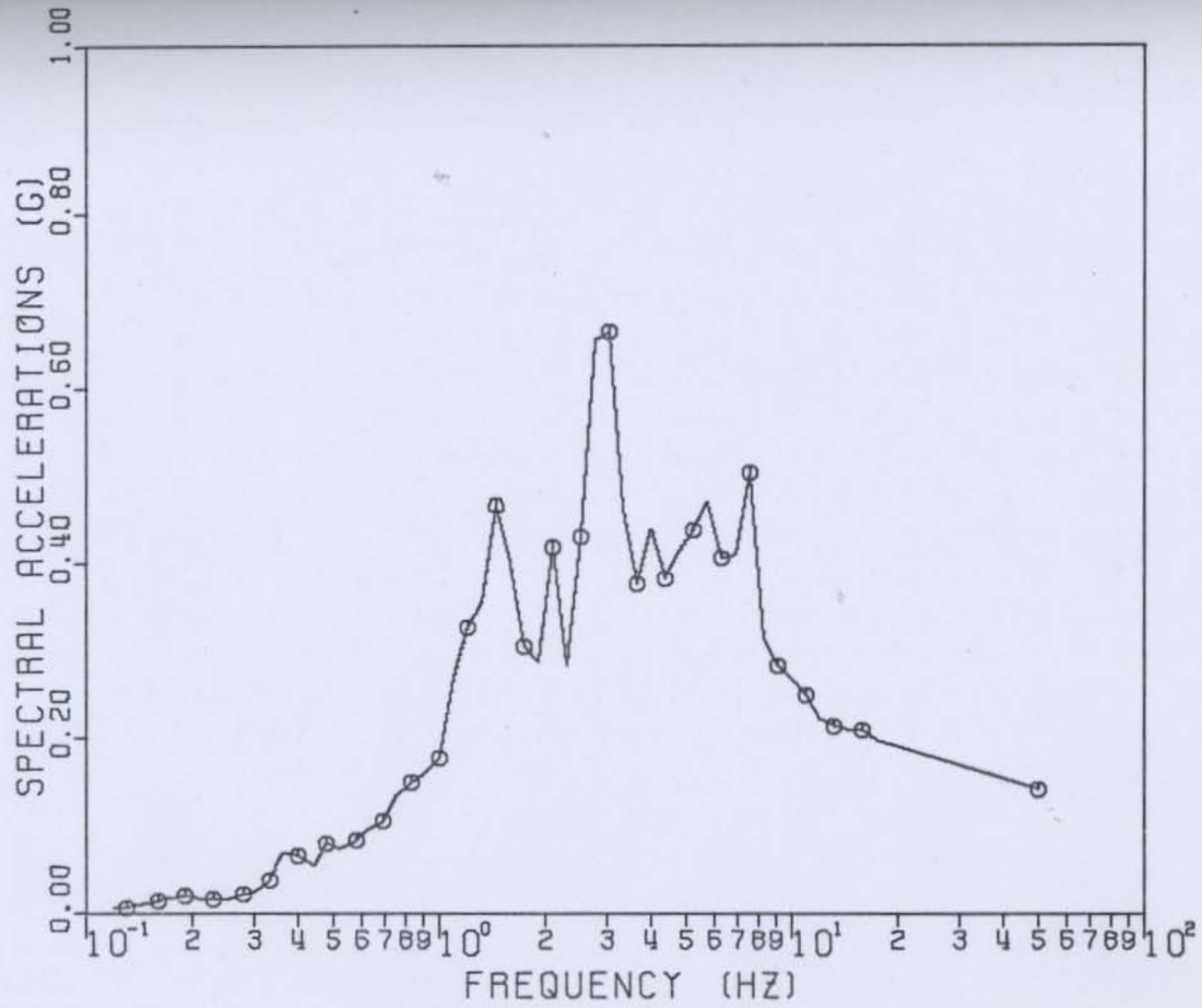

FIG. 3.11 COMPUTED ACCELERATION SPECTR OF THE TAFT INPUT MOTION. (SPECTRAL DAMPING=2%)

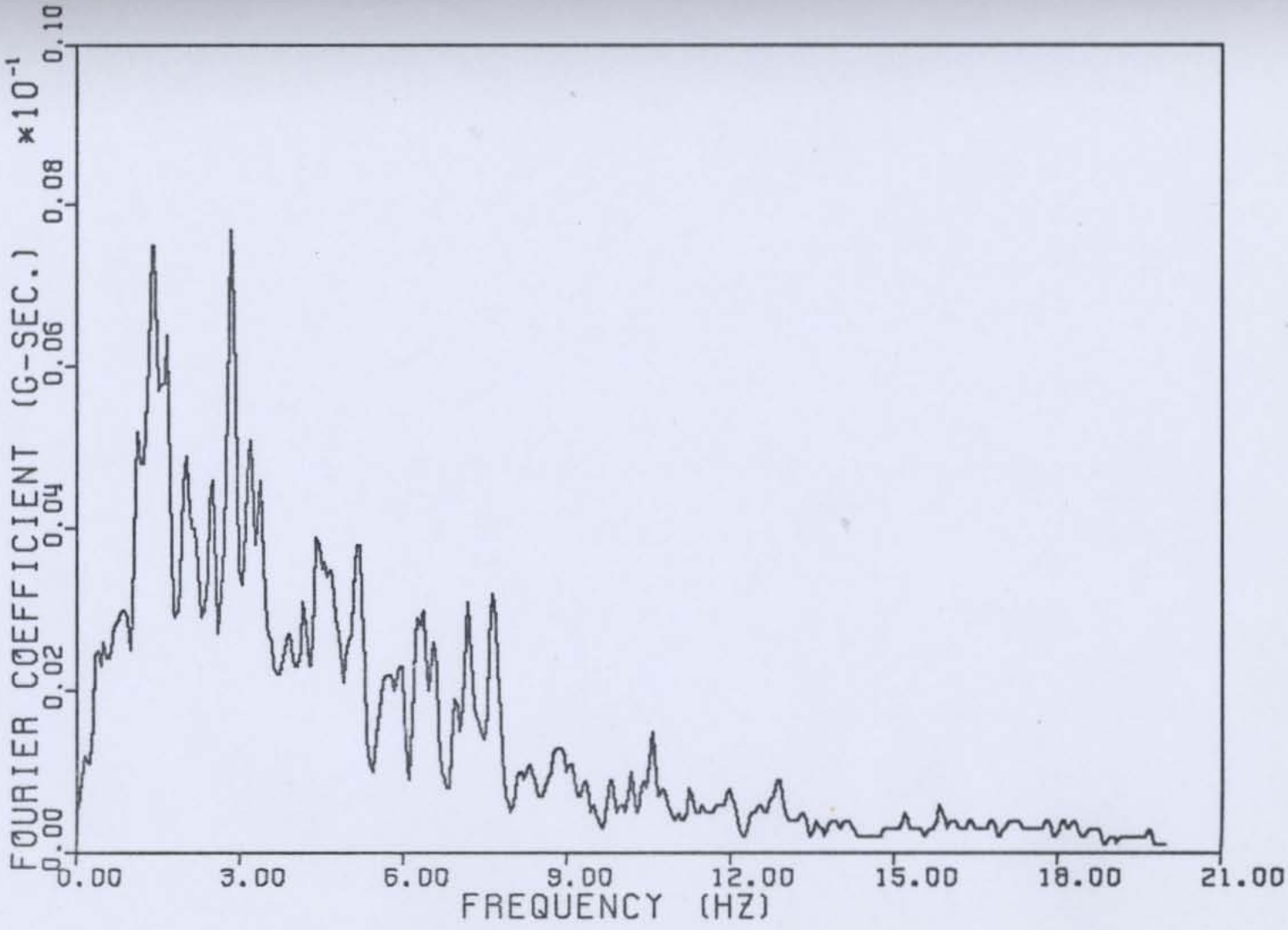

FIG. 3.12 FOURIER SPECTRA OF THE TAFT INPUT MOTION

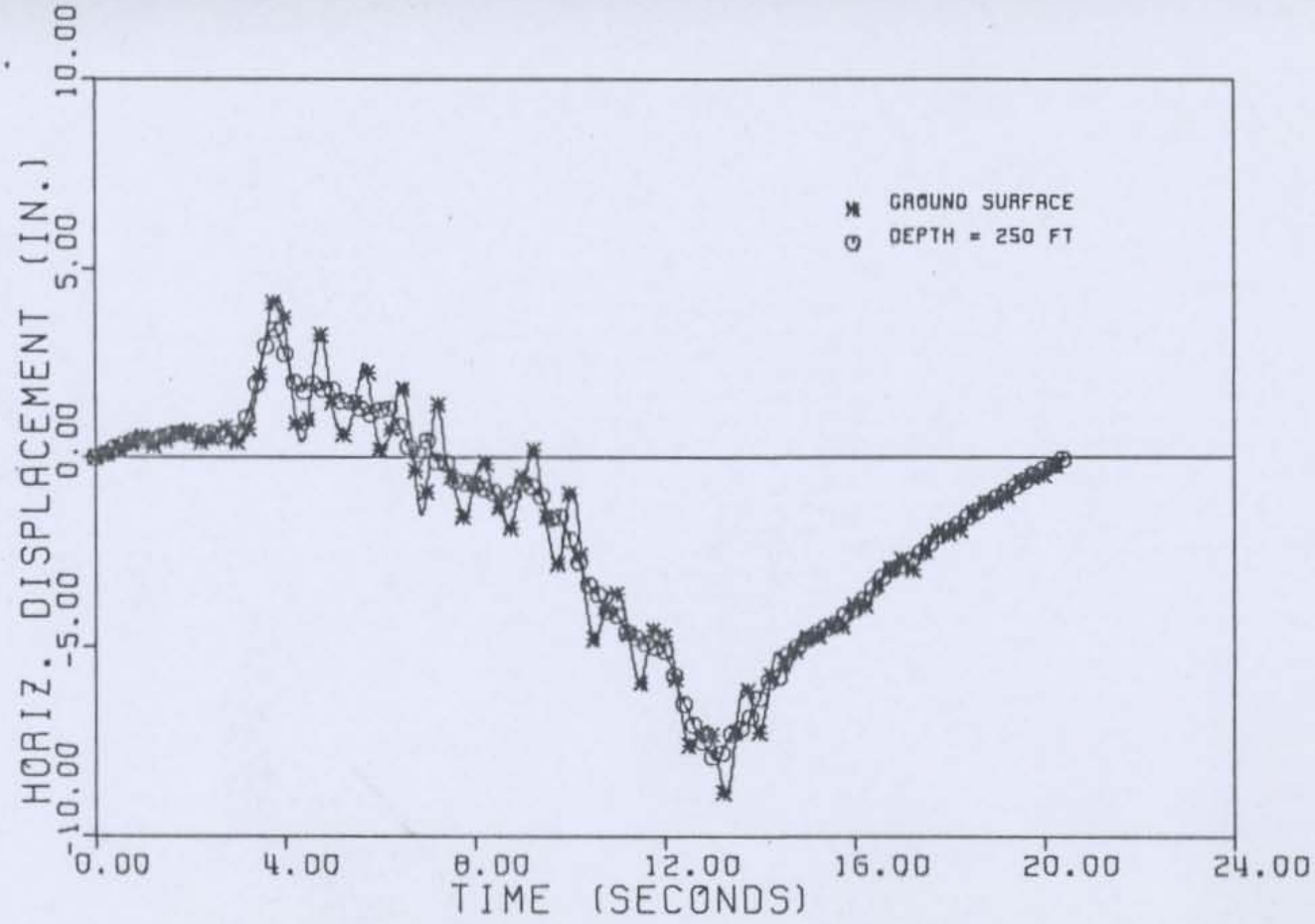

FIG. 3.13 FREE FIELD DISPLACEMENT AT GROUND SURFACE AND AT A DEPTH OF 250 FT

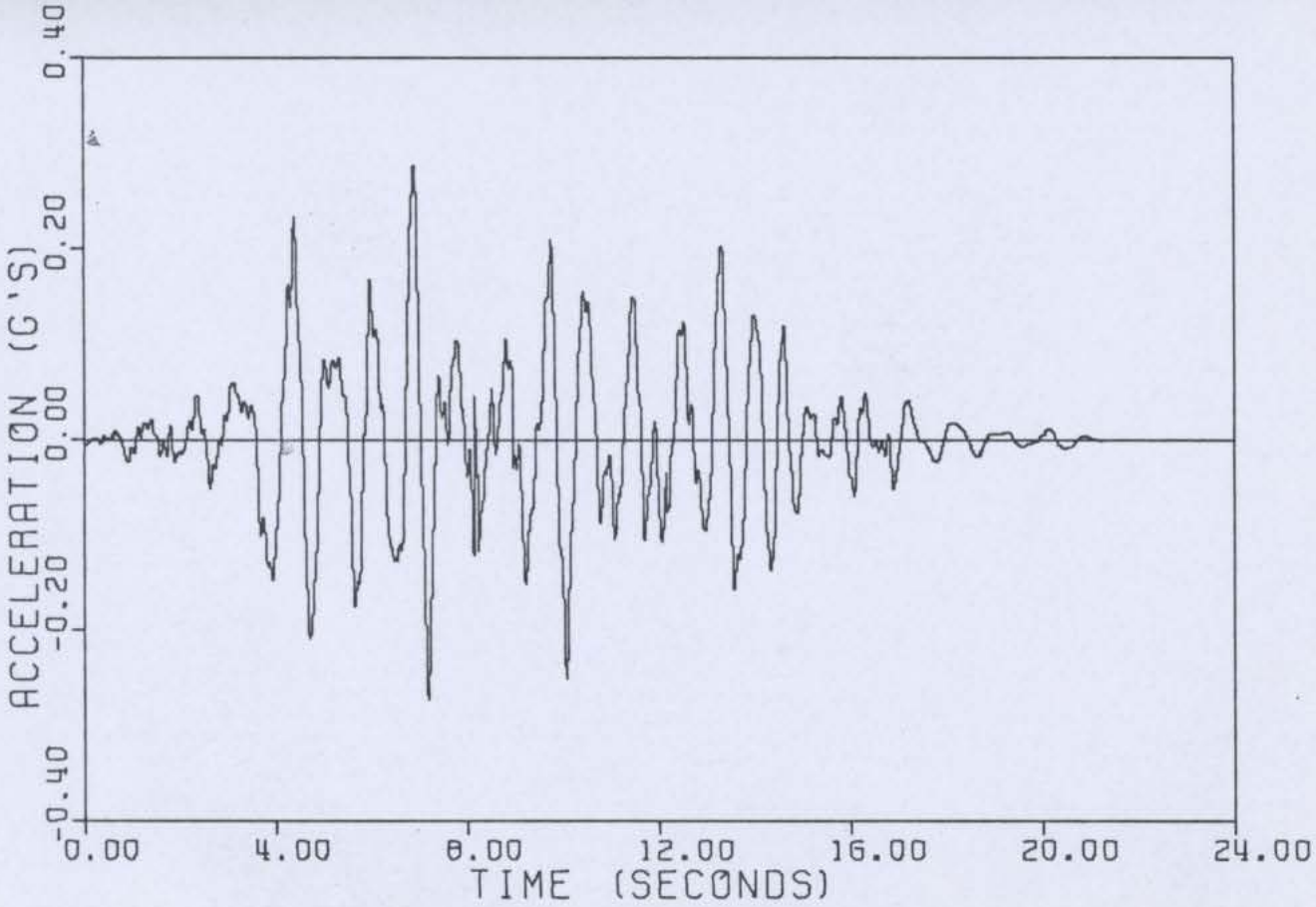

FIG. 3.14 OUTPUT FREE FIELD ACCELERATION AT A DEPTH OF 44 FT IN SAND

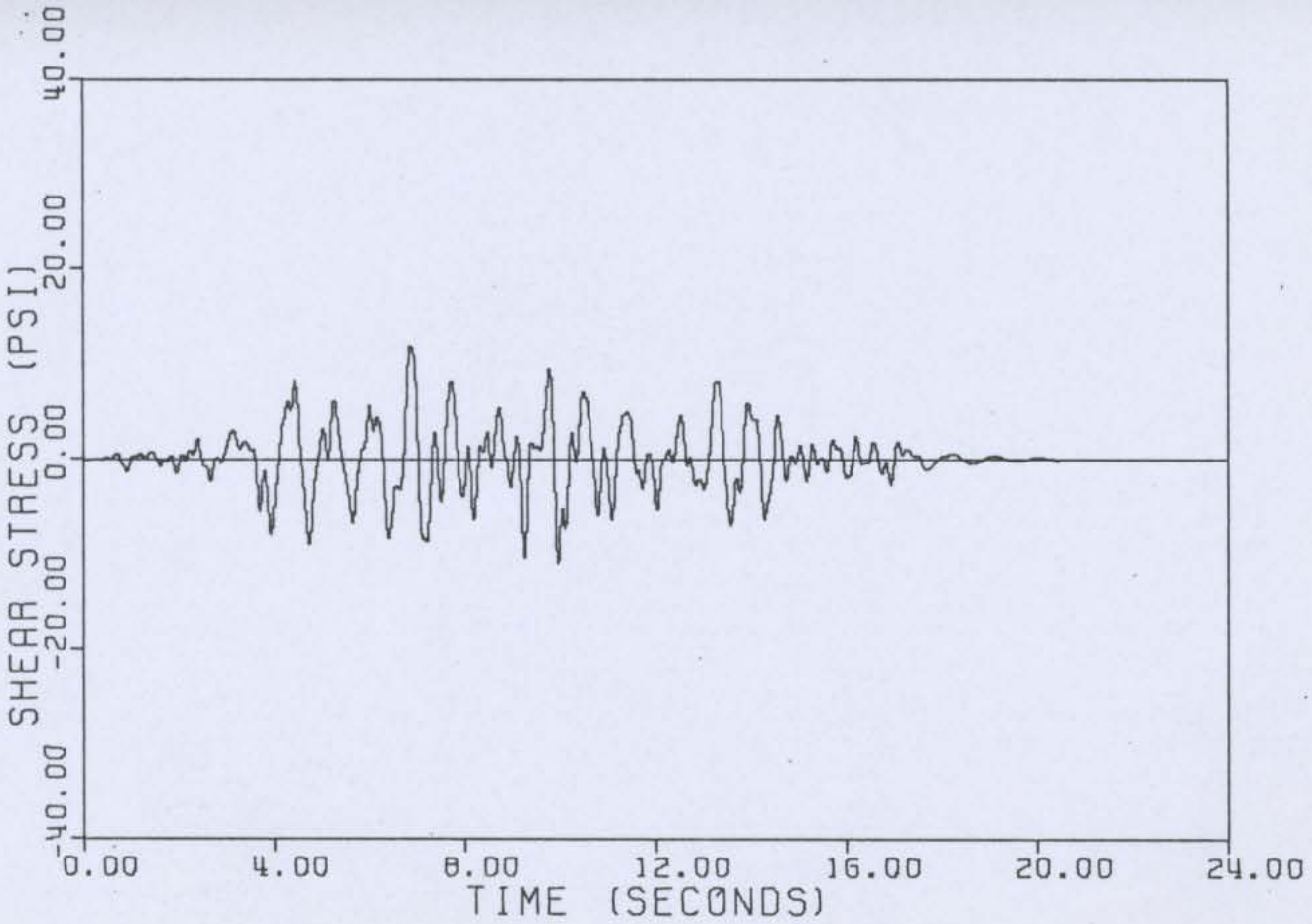

FIG. 3.15 FREE FIELD SHEAR STRESS TIME HISTORY AT A DEPTH OF 44 FT IN SAND

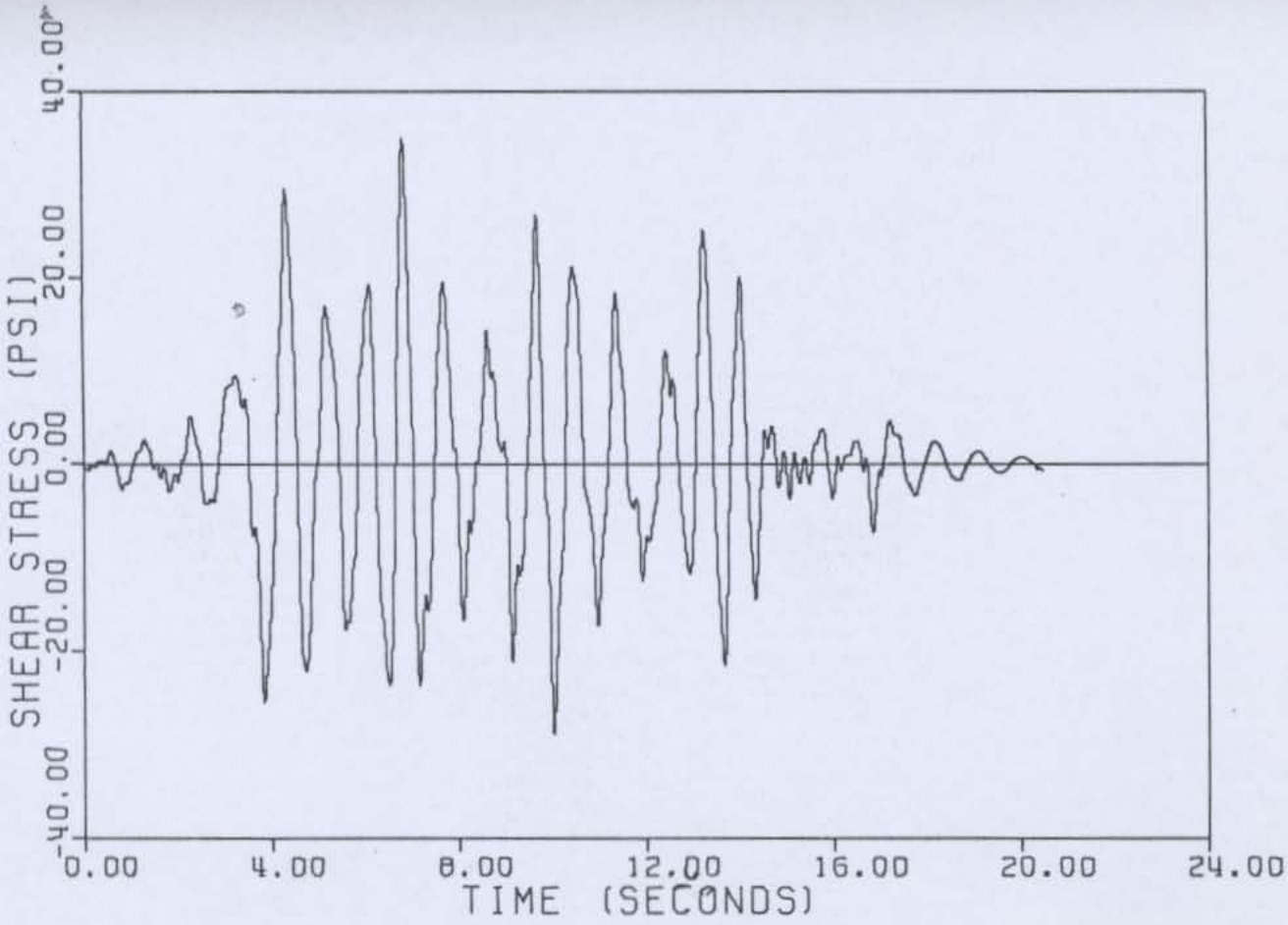

FIG. 3.16 FREE FIELD SHEAR STRESS TIME HISTORY
AT A DEPTH OF 212 FT IN SAND

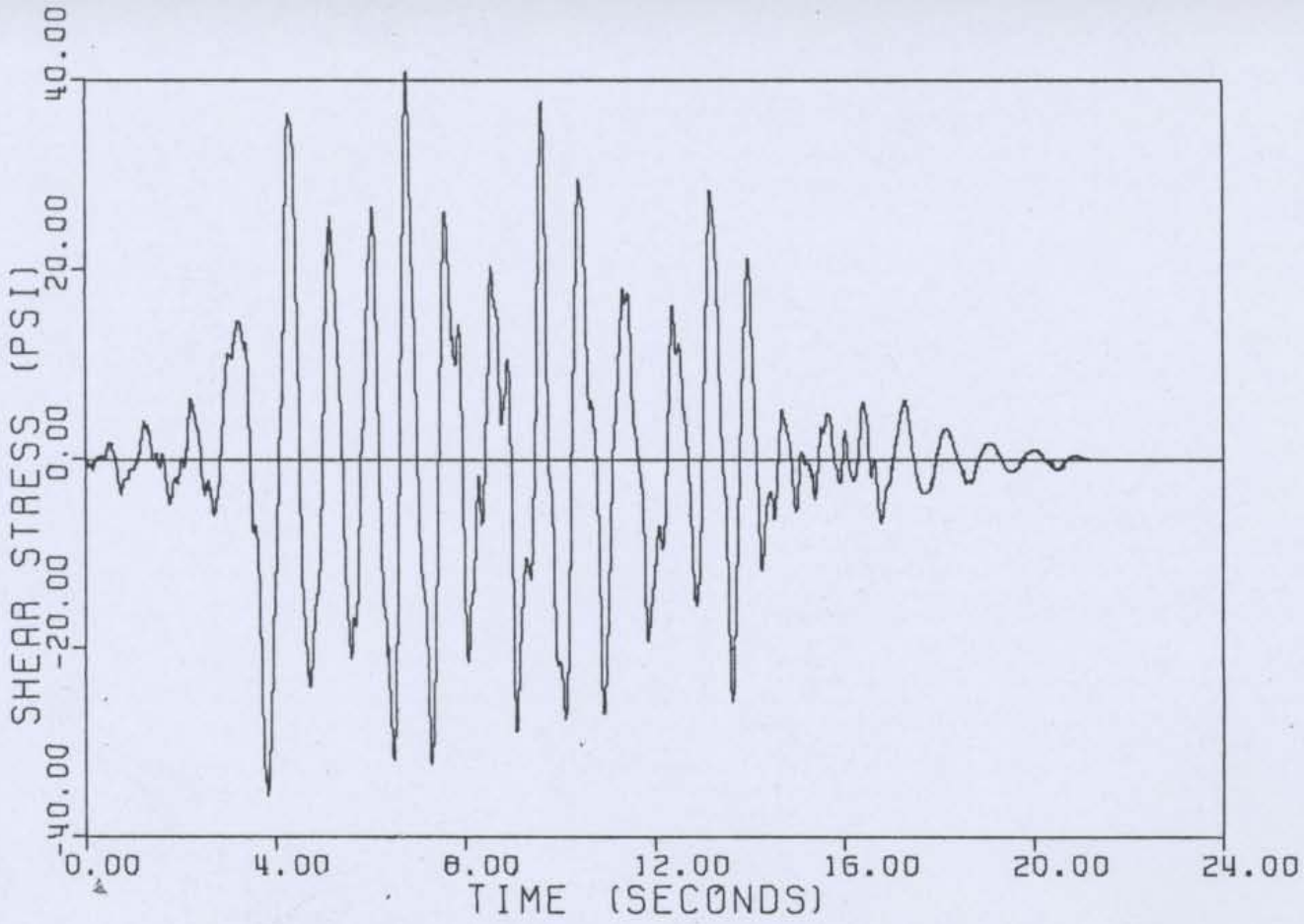

FIG. 3.17 FREE FIELD SHEAR STRESS TIME HISTORY
AT A DEPTH OF 344 FT IN SAND

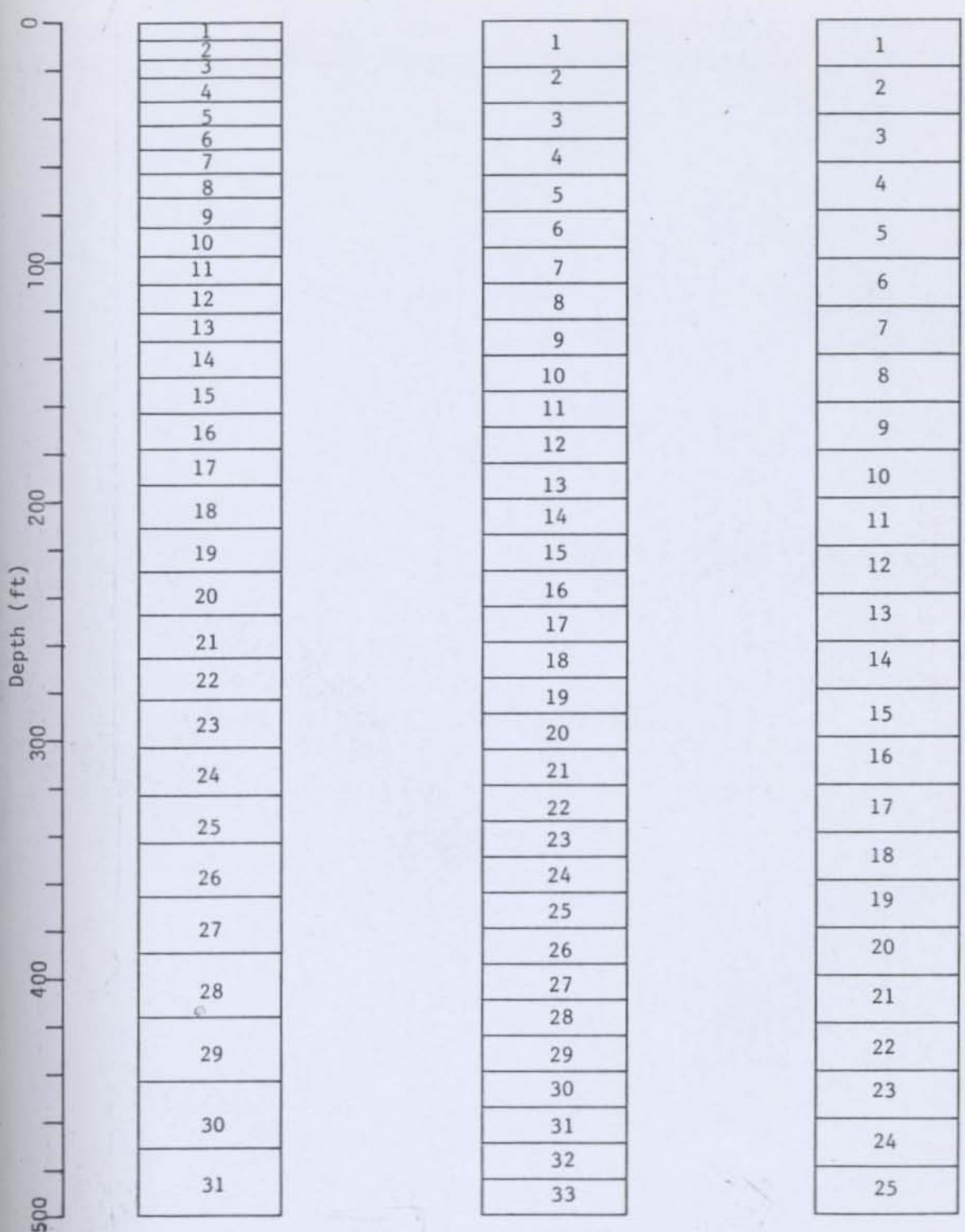

I) MESH NO. 1 II) MESH NO. 2 III) MESH NO. 3

FIG. 3.18 THREE MESHES USED TO STUDY THE EFFECT OF ELEMENT SIZE ON THE FREE FIELD RESPONSE

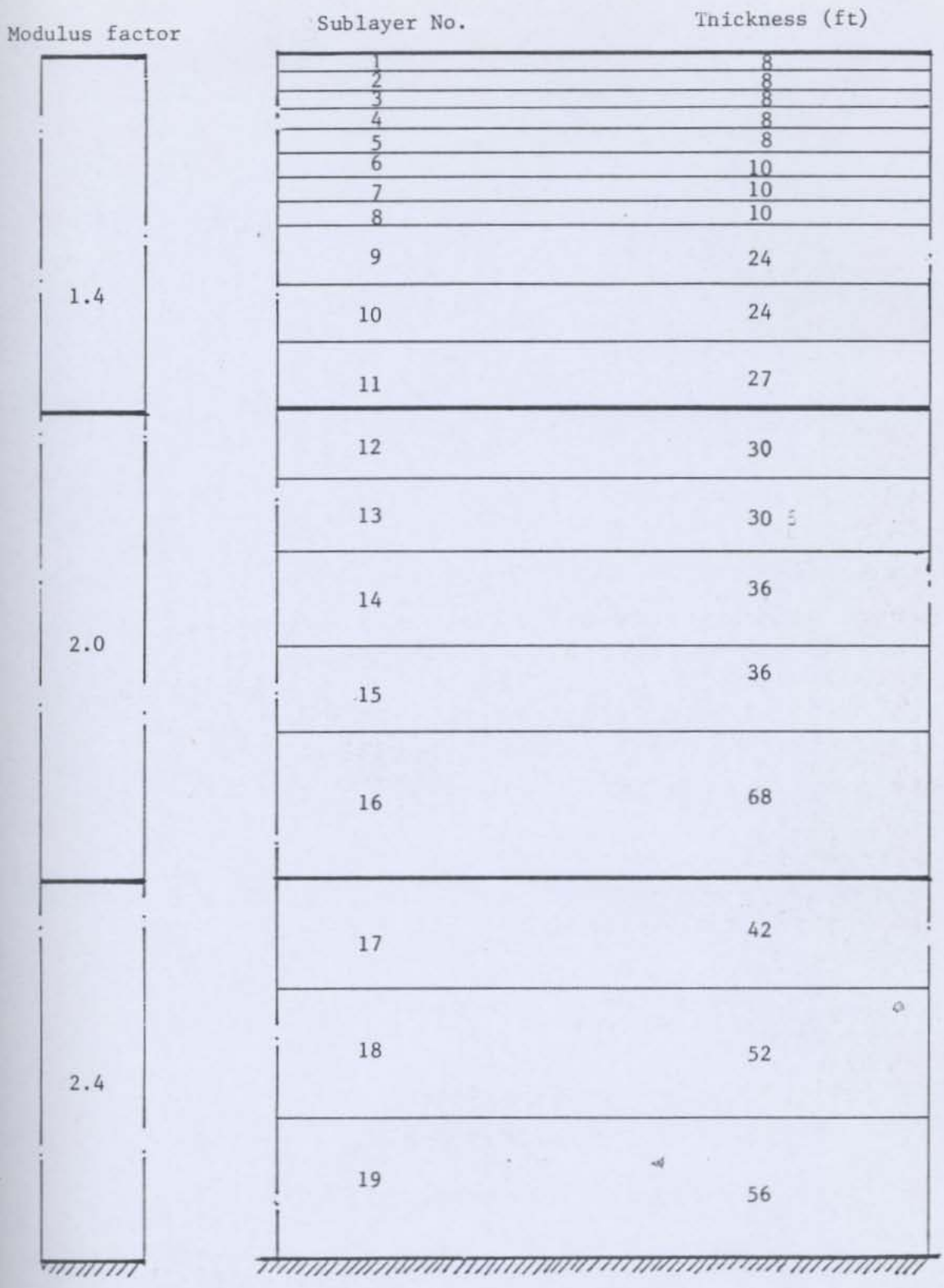

FIG. 3.19 SUBLAYER SYSTEM USED IN SHAKE ANALYSIS

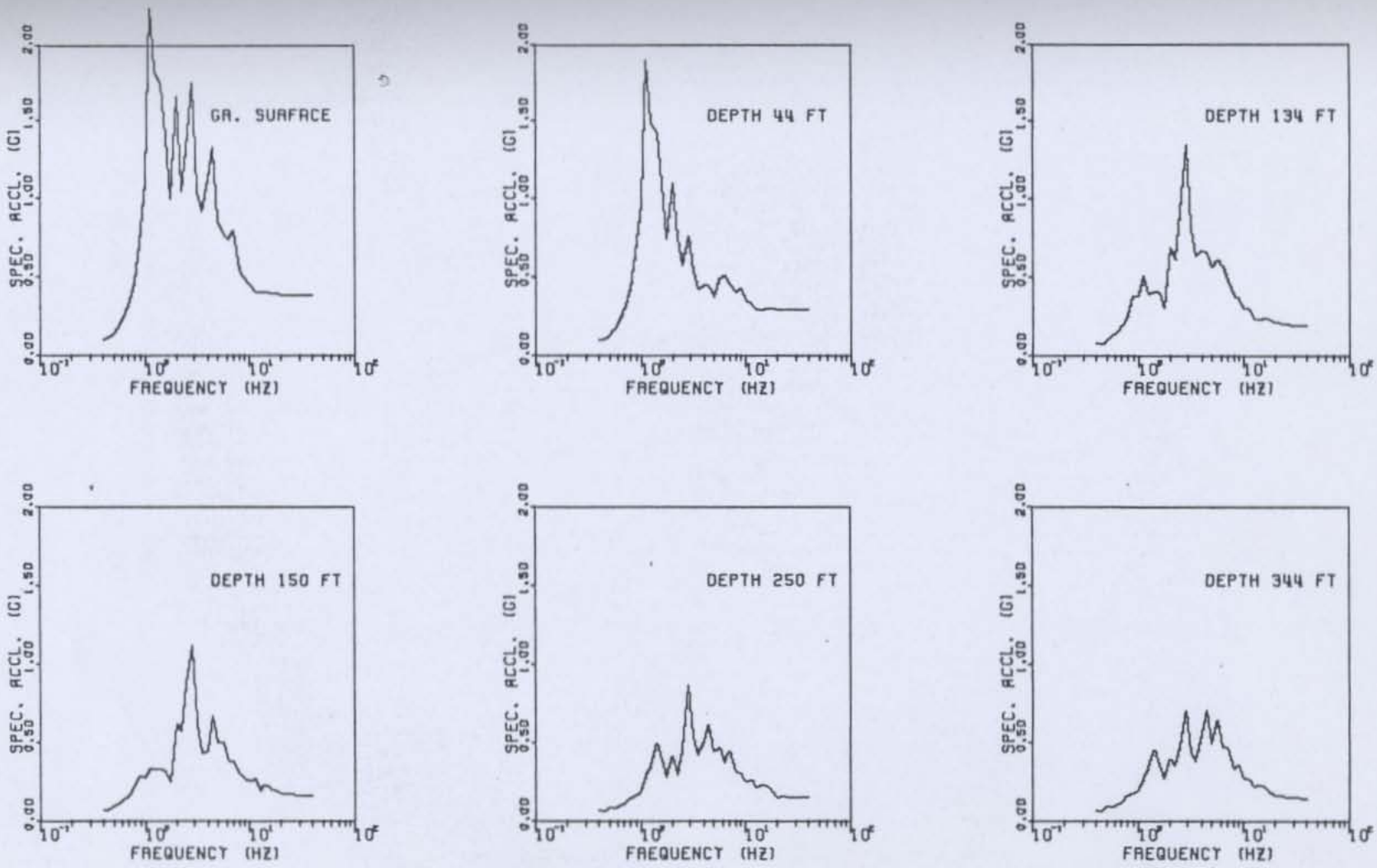

FIG. 3.20 FREE FIELD ACCELERATION RESPONSE SPECTRA AT DIFFERENT DEPTHS IN SAND

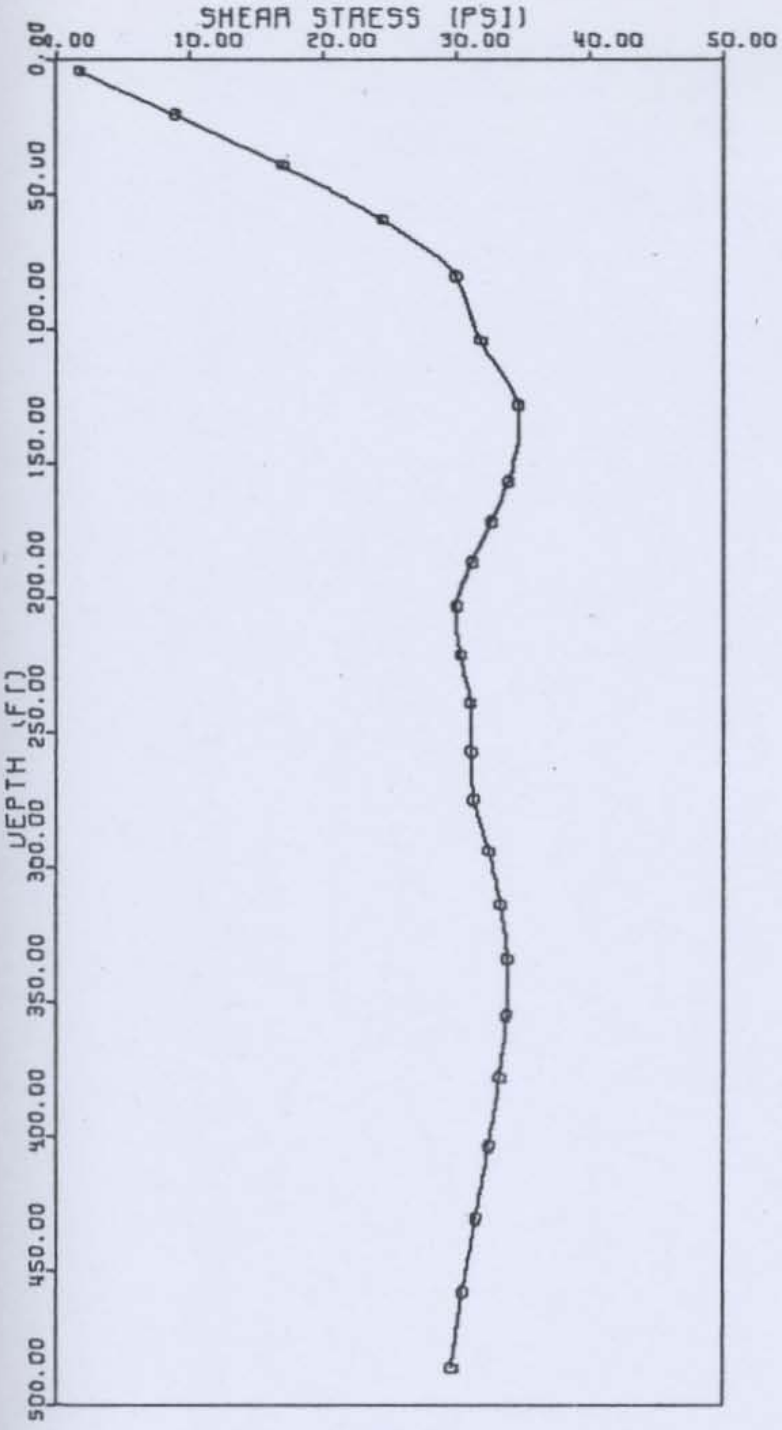

FIG. 3.21 FREE FIELD SHEAR STRESS DISTRIBUTION IN SAND

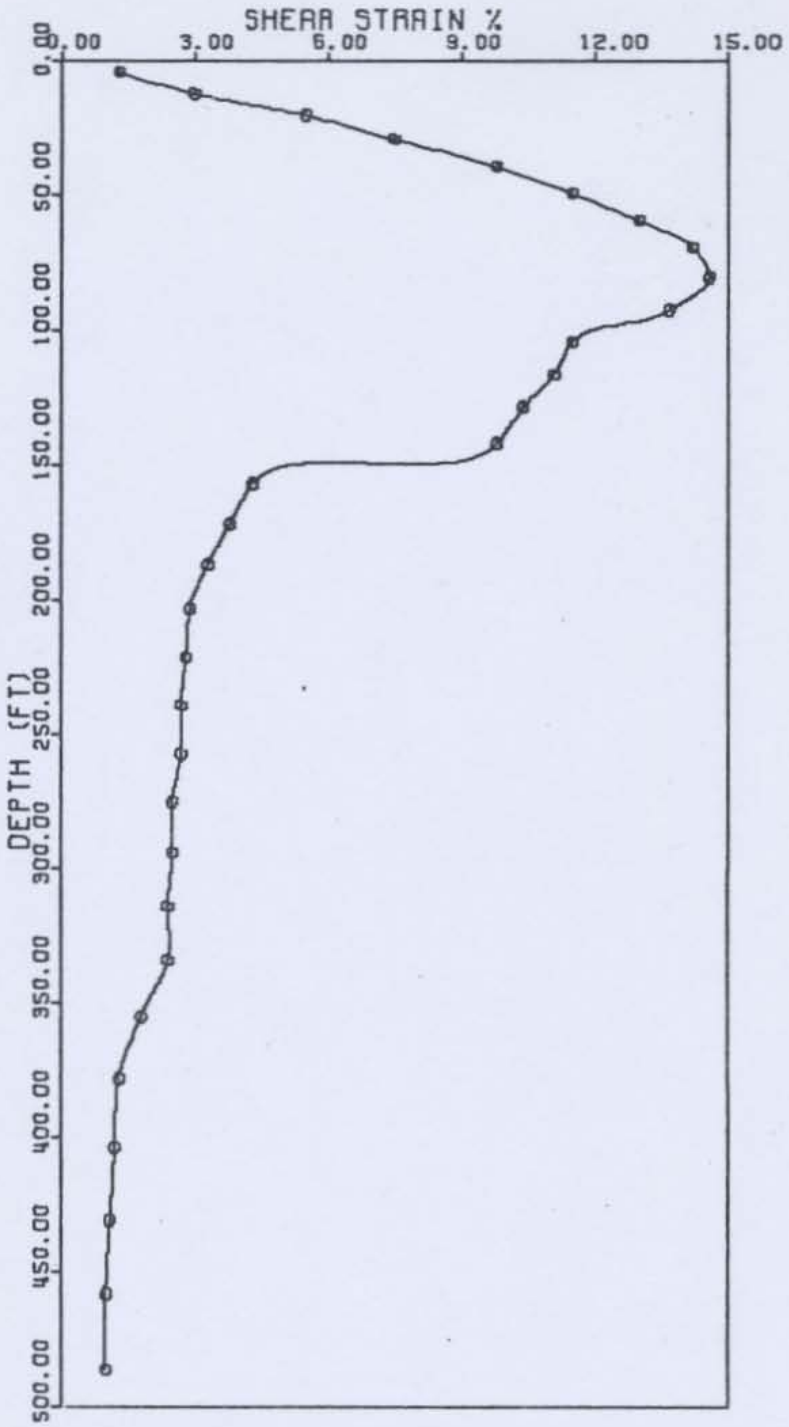

FIG. 3.22 MAXIMUM FREE FIELD SHEAR STRAIN IN SAND

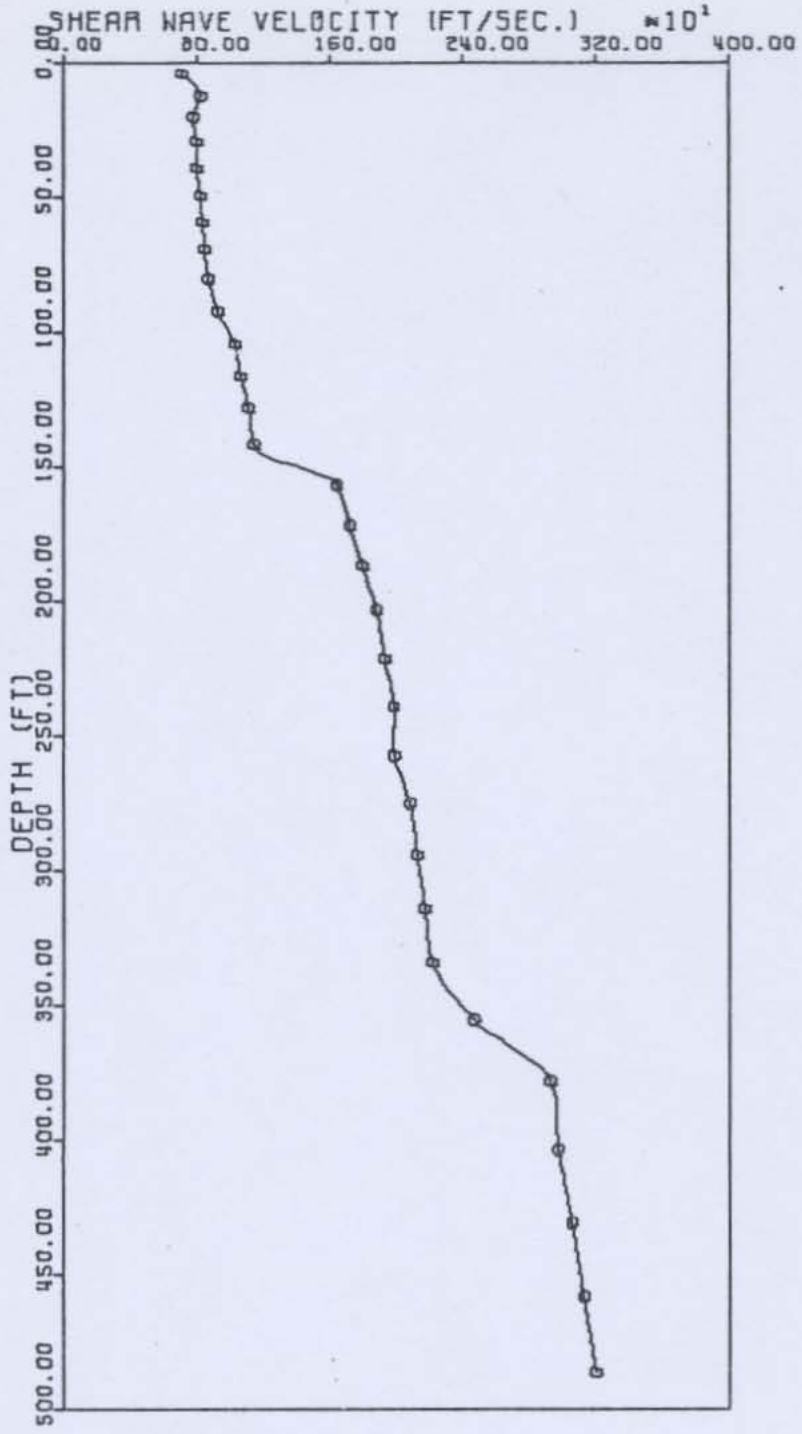

FIG. 3.23 FREE FIELD SHEAR WAVE VELOCITY IN SAND

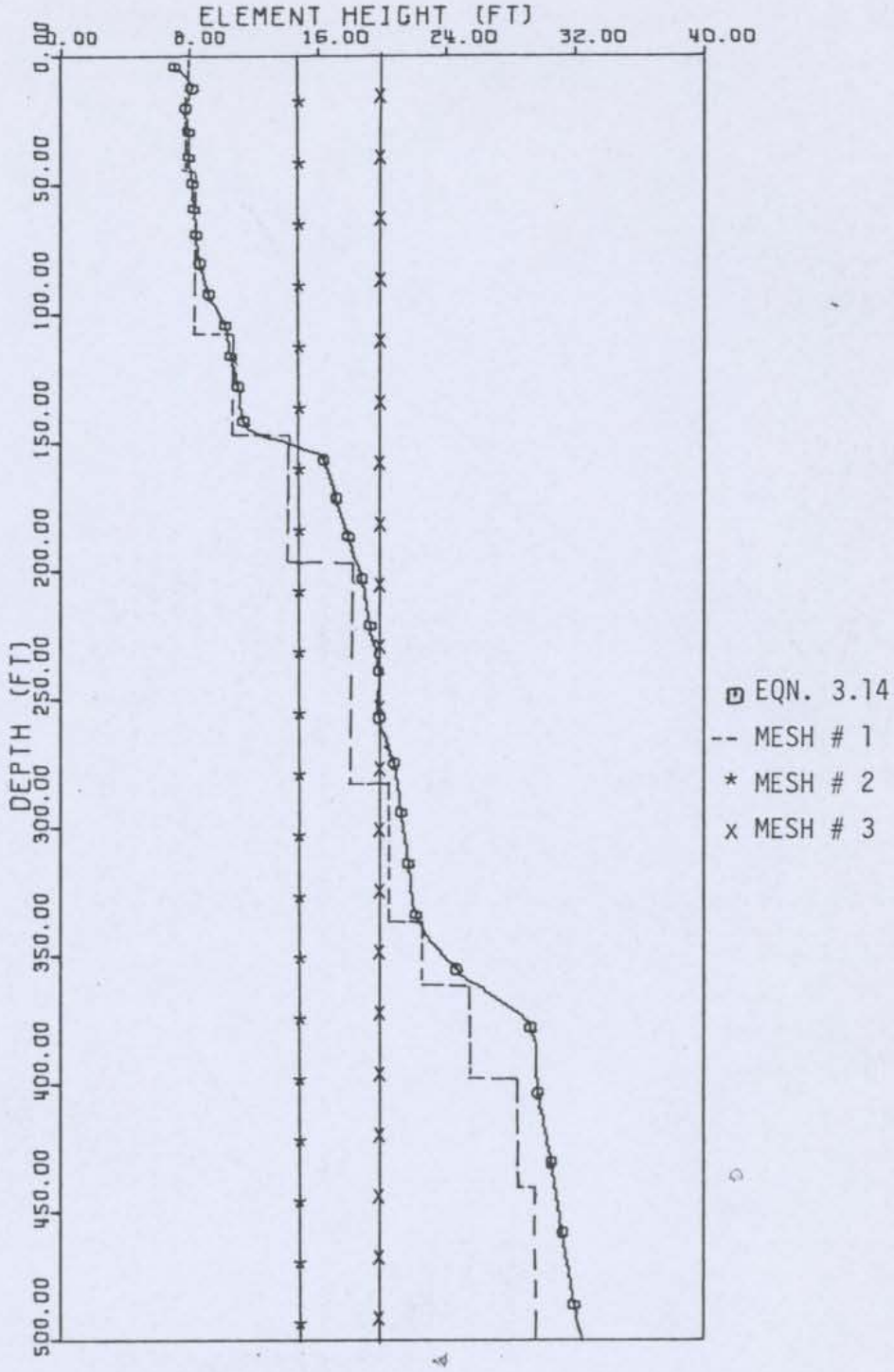

FIG. 3.24 MAXIMUM ELEMENT HEIGHTS COMPUTED FROM EQN.3.14 AND THE ELEMENT HEIGHTS CHOSEN FOR THREE MESHES USED IN THE ONE-DIMENSIONAL COLUMN STUDY - SAND MEDIUM

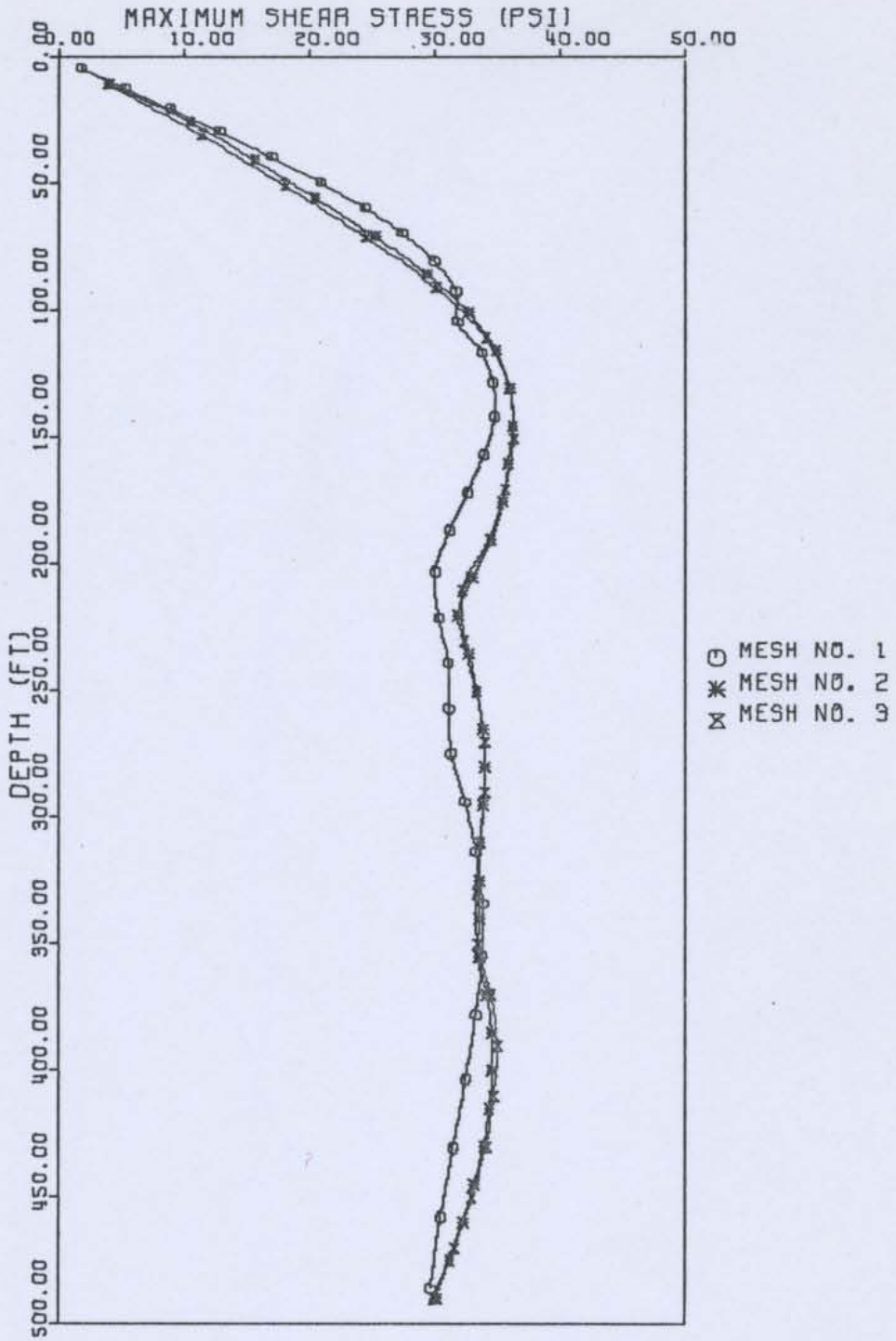

FIG. 3.25 EFFECT OF THE VERTICAL ELEMENT SIZE ON THE MAXIMUM FREE FIELD SHEAR STRESSES IN SAND

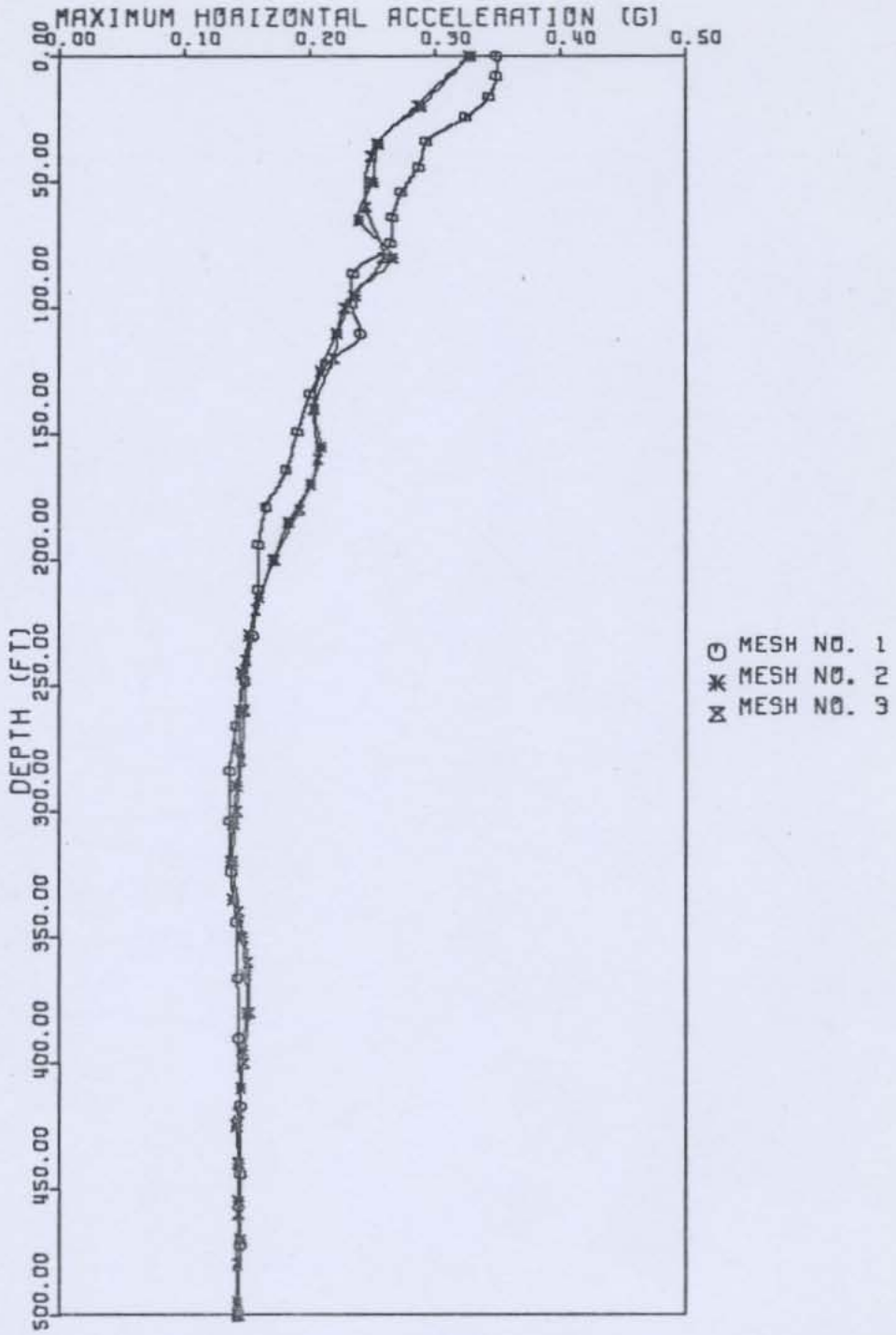

FIG. 3.26 EFFECT OF THE VERTICAL ELEMENT SIZE ON THE MAXIMUM FREE FIELD HORIZONTAL ACCELERATION IN SAND

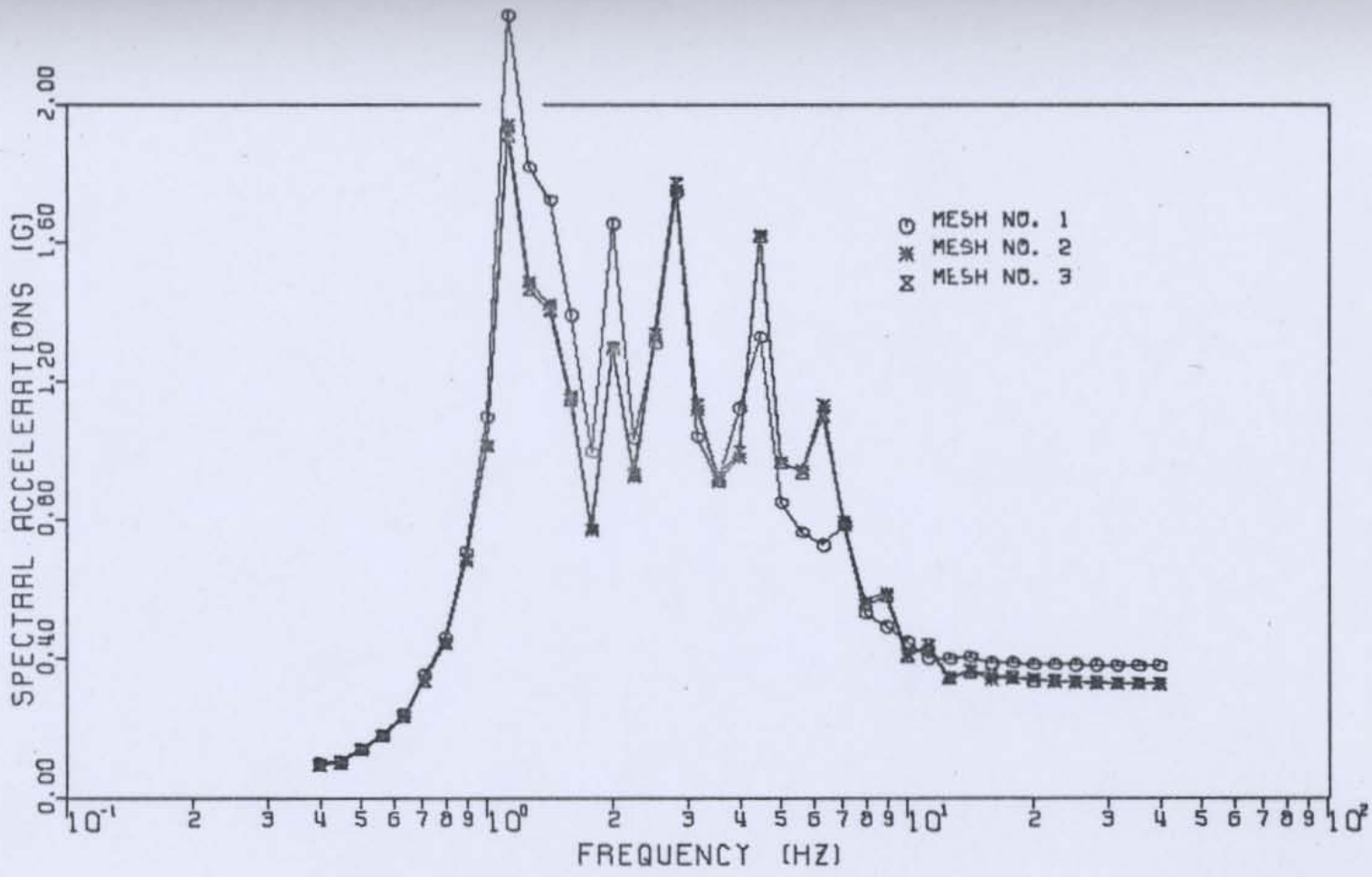

FIG. 3.27 EFFECT OF THE VERTICAL ELEMENT SIZE ON THE FREE FIELD ACCELERATION RESPONSE SPECTRA AT THE GROUND SURFACE IN SAND
(SPECTRAL DAMPING = 2%)

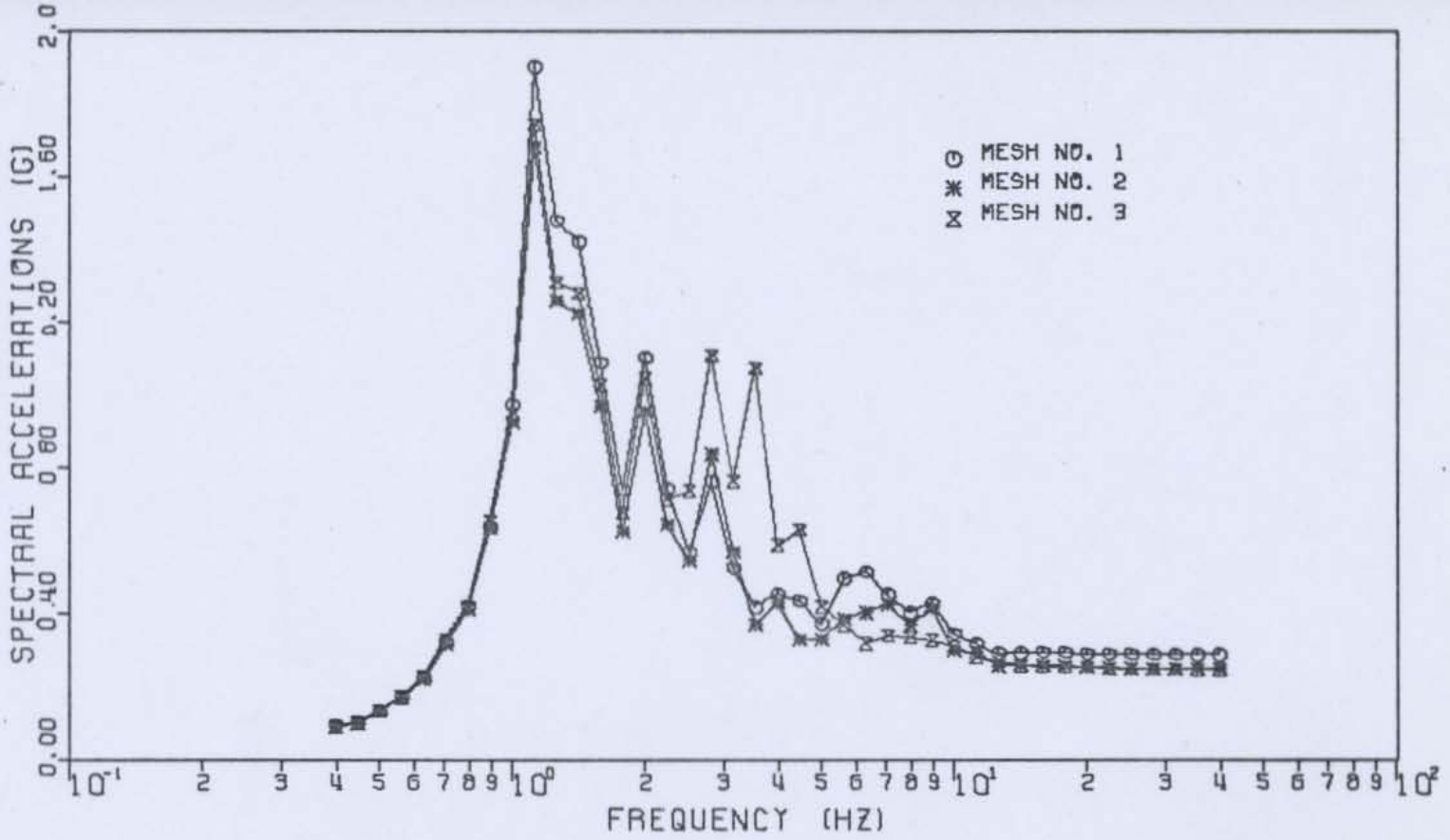

FIG. 3.28 EFFECT OF THE VERTICAL ELEMENT SIZE ON THE FREE FIELD ACCELERATION RESPONSE SPECTRA AT A DEPTH OF 40 FT IN SAND
(SPECTRAL DAMPING = 2%)

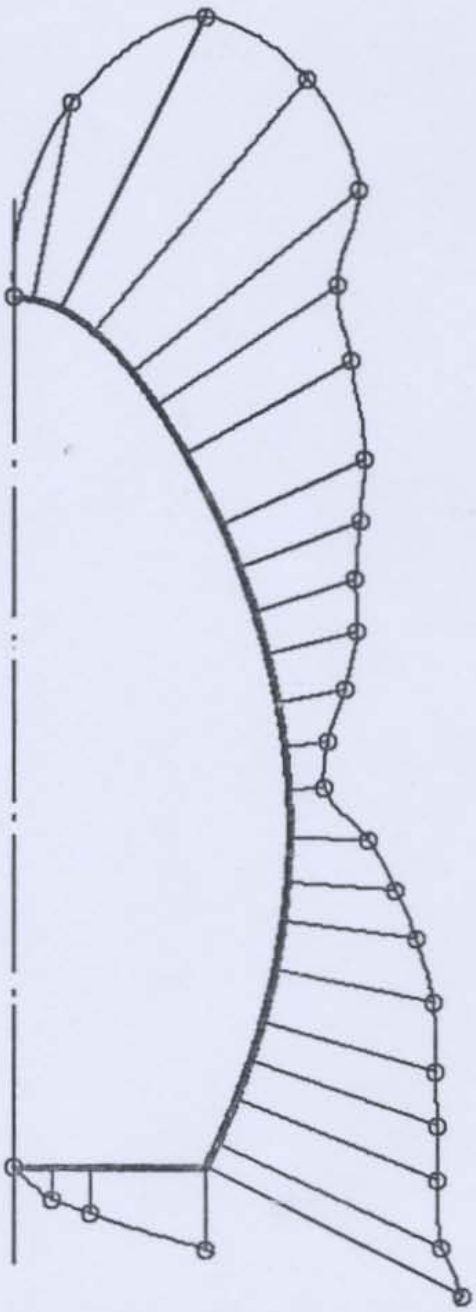

FIG. 3.29 MAXIMUM PRINCIPAL STRESS DIAGRAM FOR A HIGH HORSESHOE CONTAINMENT - LOOSE FILL (SCALE: 1 INCH = 400 P.S.I.)

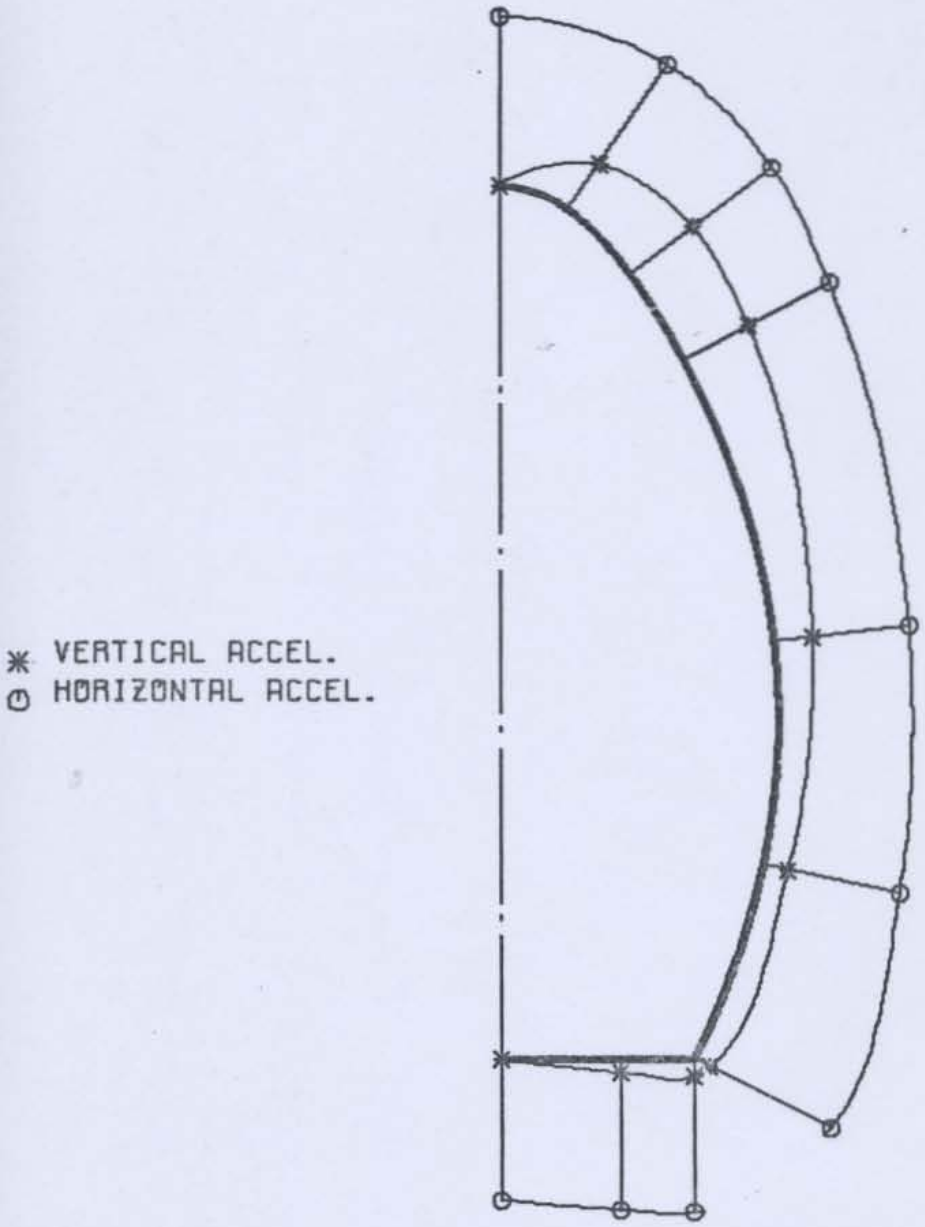

FIG. 3.30 MAXIMUM HORIZONTAL AND VERTICAL ACCELERATIONS IN THE HIGH HORSESHOE-LOOSE FILL (SCALE: 1 INCH=0.2G)

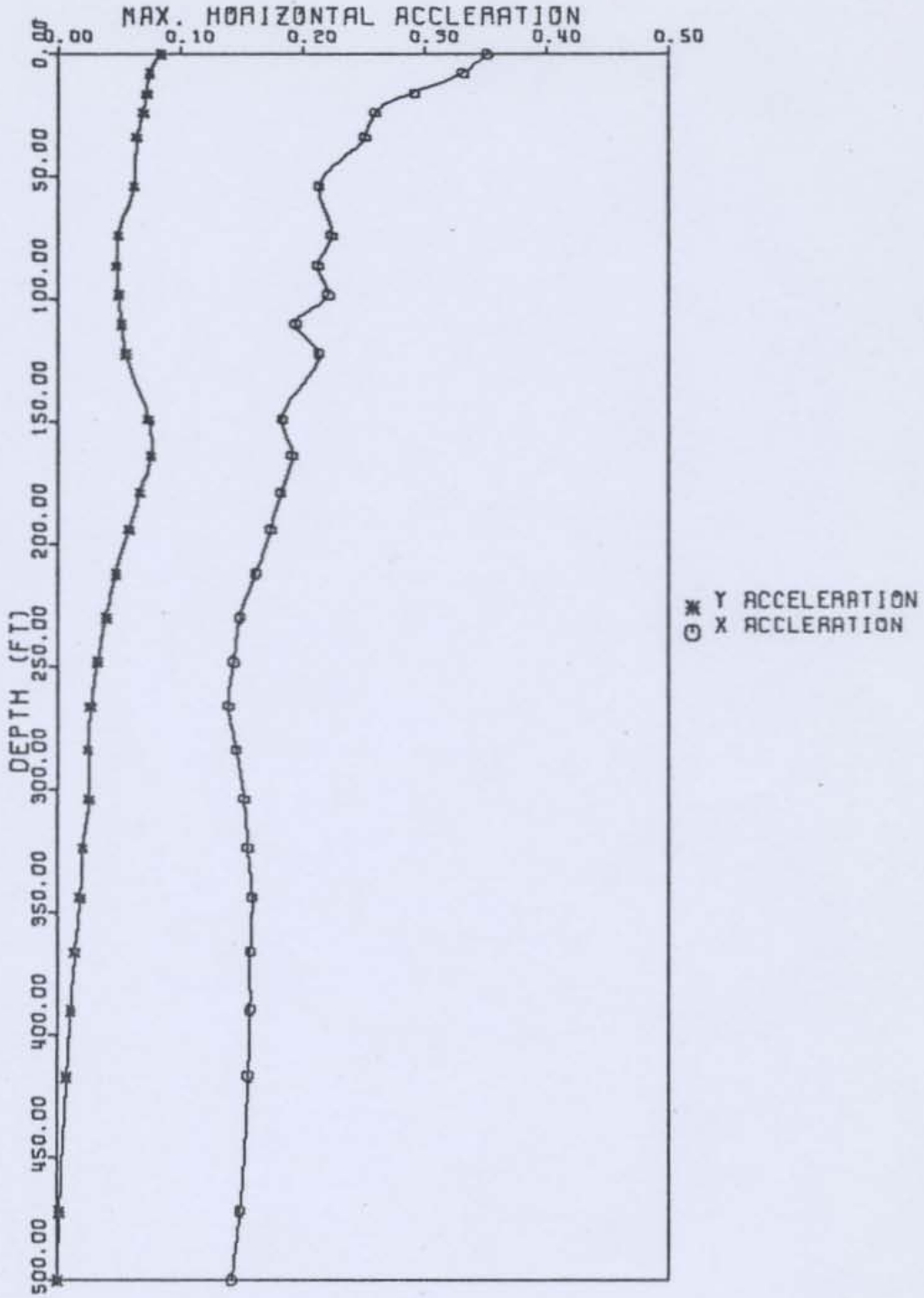

FIG. 3.31 MAXIMUM HORIZONTAL AND VERTICAL ACCELERATIONS AT A VERTICAL PLANE 10 FT AWAY FROM THE HIGH HORSESHOE CONTAINMENT - THIN LOOSE FILL

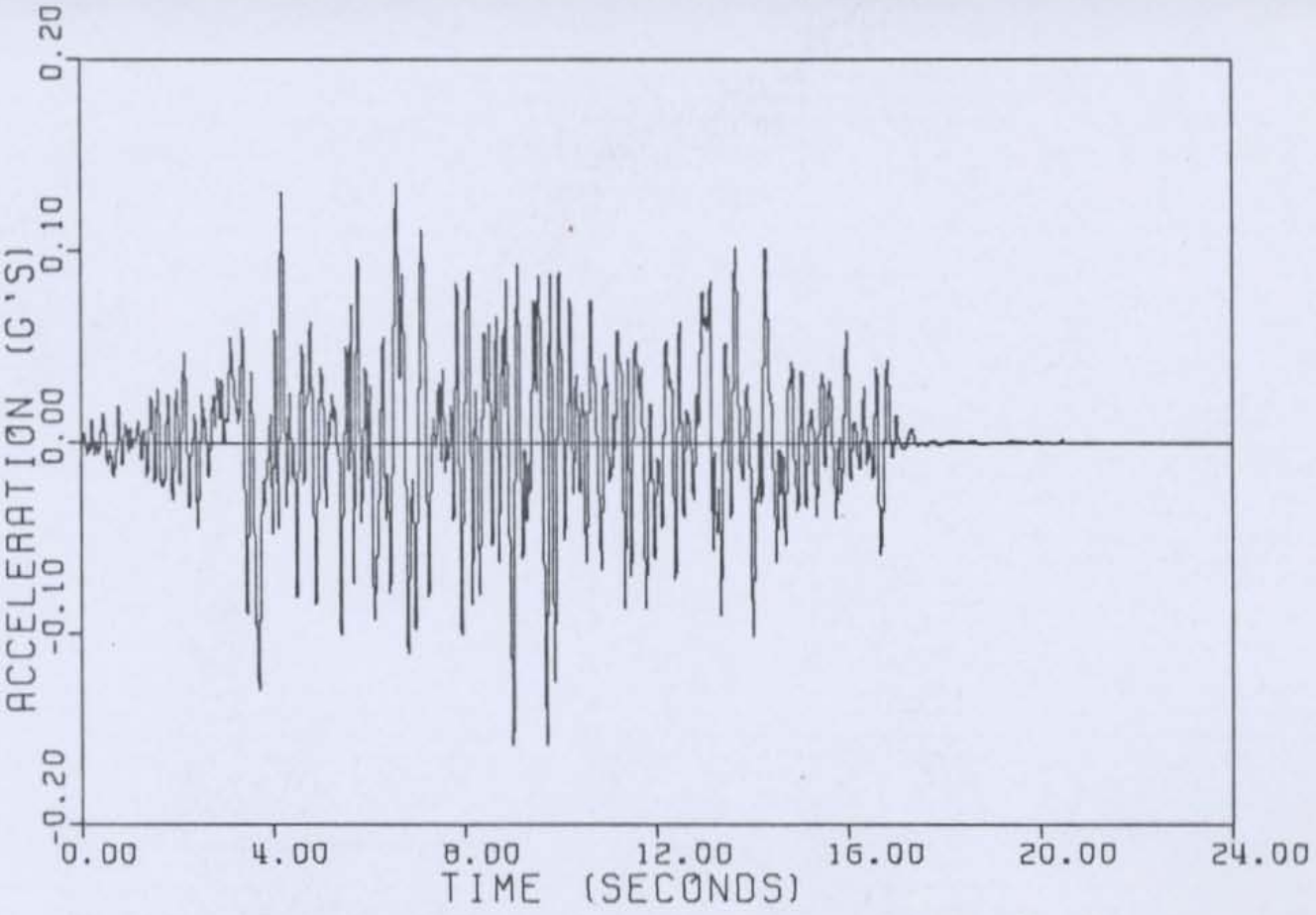

FIG. 3.32 TIME HISTORY OF THE ACCELERATION AT THE CONTAINMENT FOUNDATION MID-POINT

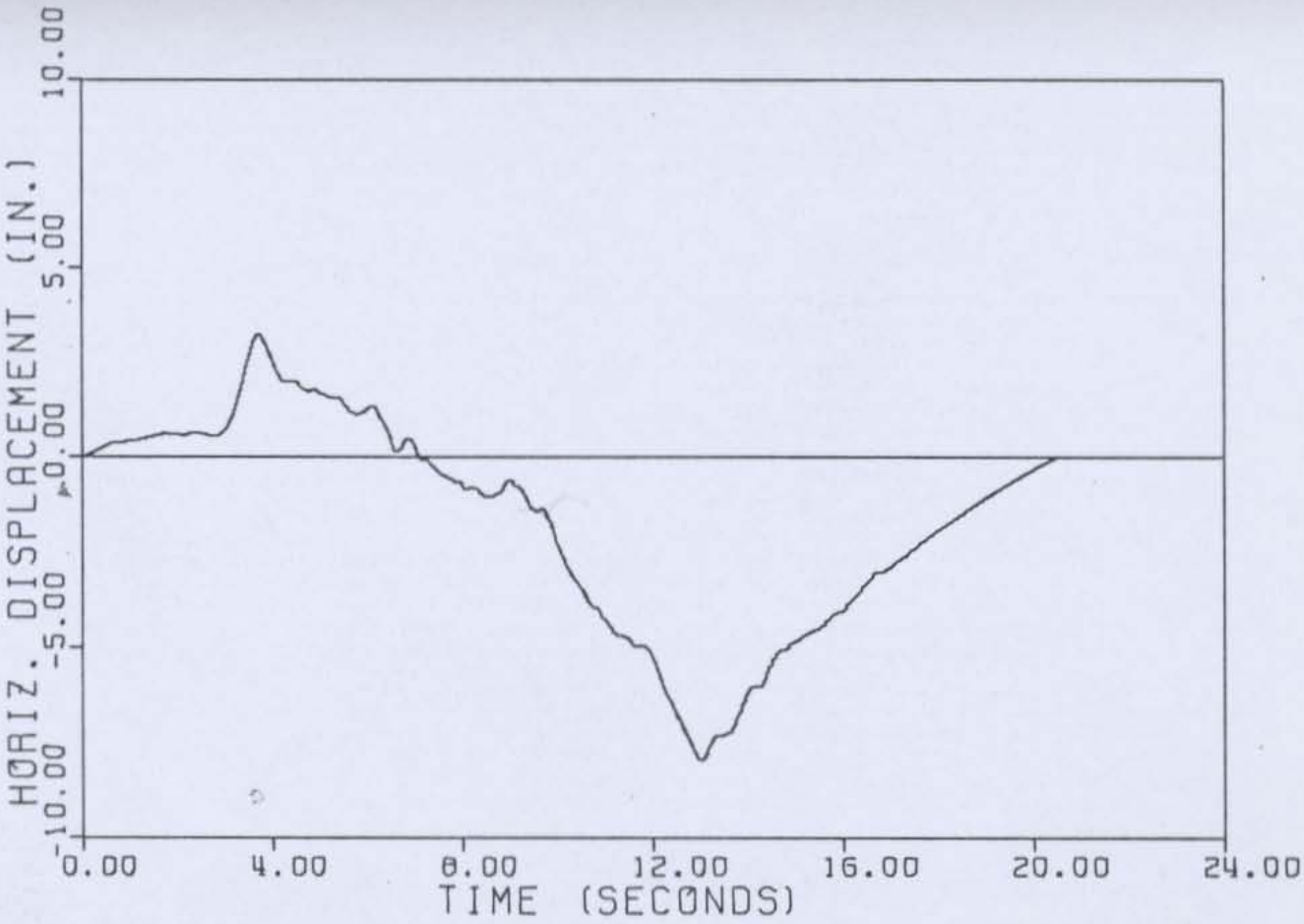

FIG. 3.33 HORIZONTAL DISPLACEMENT AT THE CONTAINMENT FOUNDATION MID-POINT

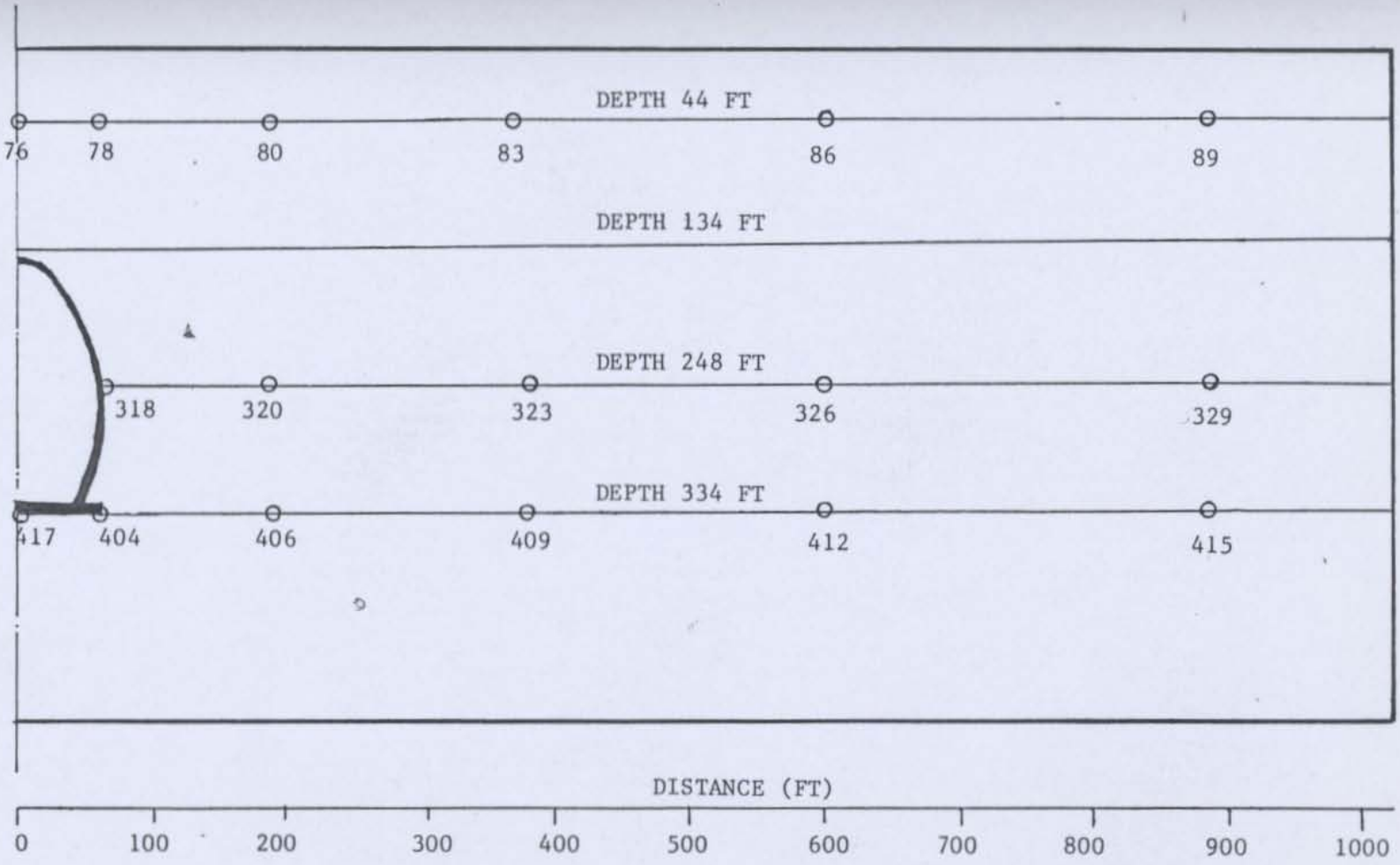

FIG. 3.34 LOCATIONS OF THE LEVELS AND NODAL POINTS AT WHICH THE RESULTS ARE PRESENTED

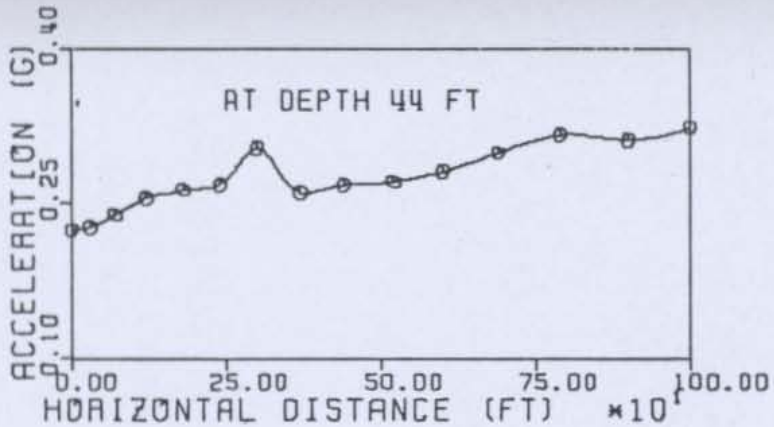

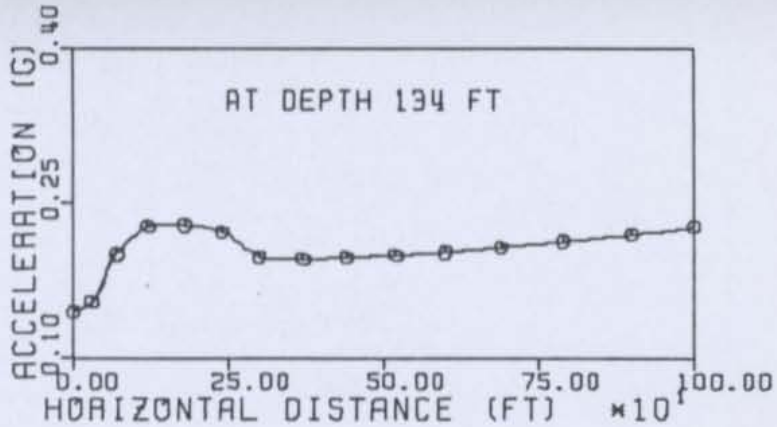

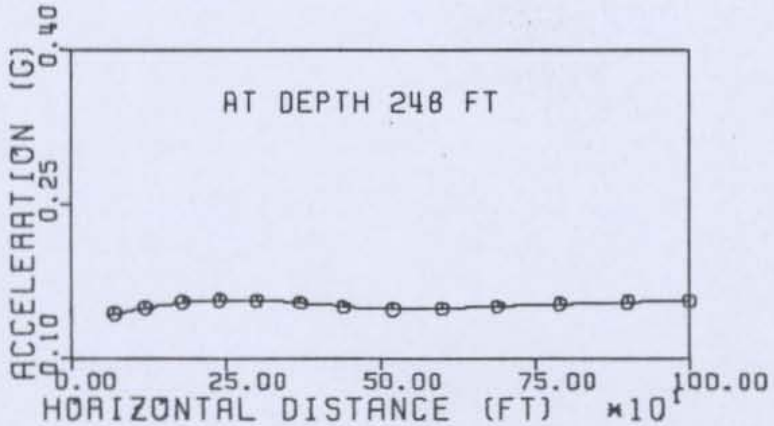

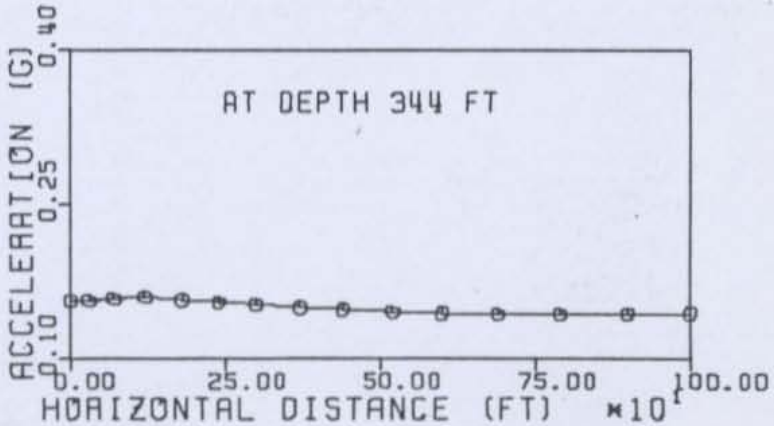

FIG. 3.35 VARIATION OF MAXIMUM HORIZONTAL ACCELERATION ALONG HORIZONTAL PLANES AT DEPTHS 44,134,248, AND 344 FT FOR A TYPICAL SOIL STRUCTURE MODEL - LOOSE FILL

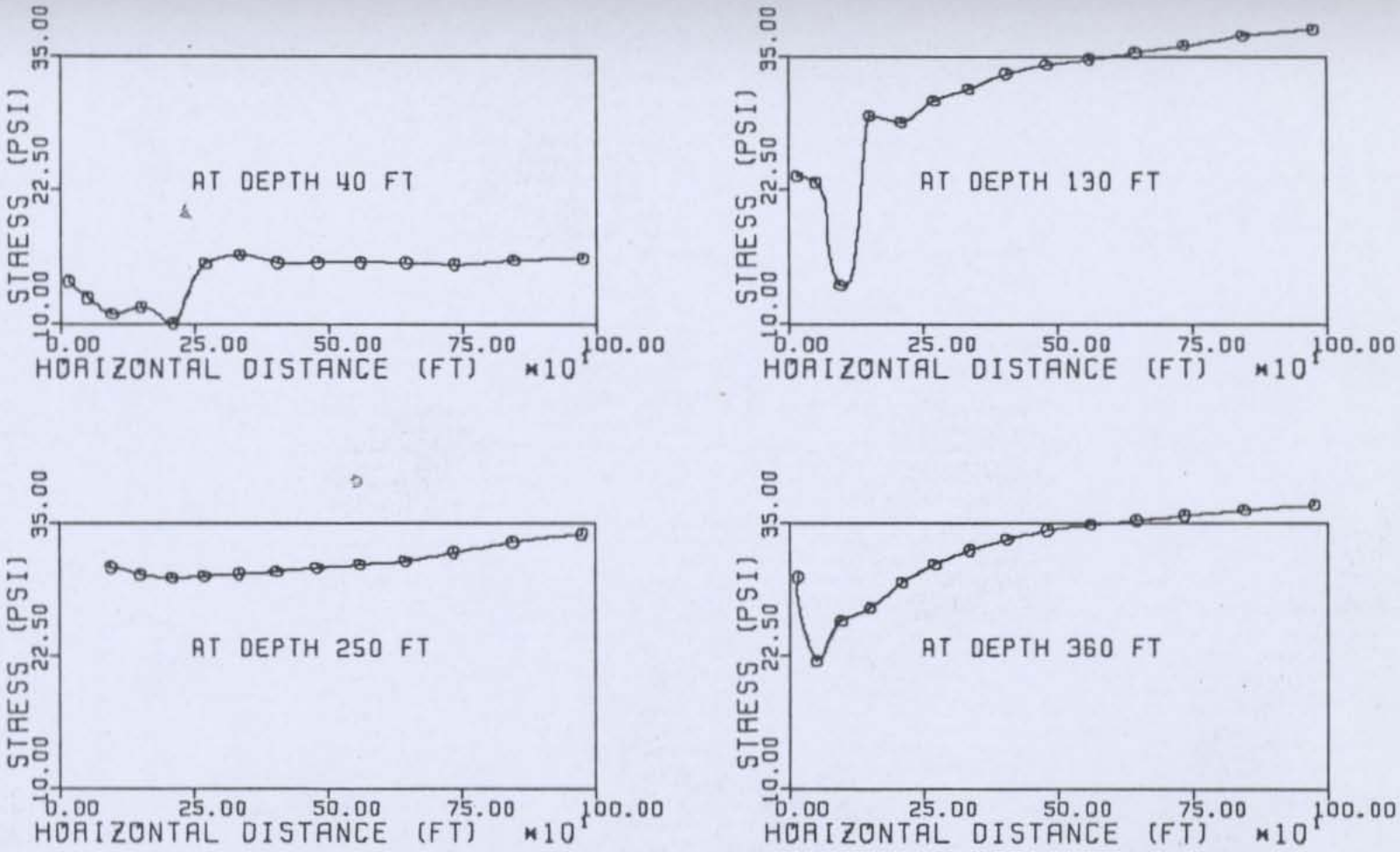

FIG. 3.36 VARIATION OF MAXIMUM SHEAR STRESSES ALONG HORIZONTAL PLANES AT DEPTHS 40, 130, 250 AND 360 FT FOR A TYPICAL SOIL-STRUCTURE MODEL - LOOSE FILL

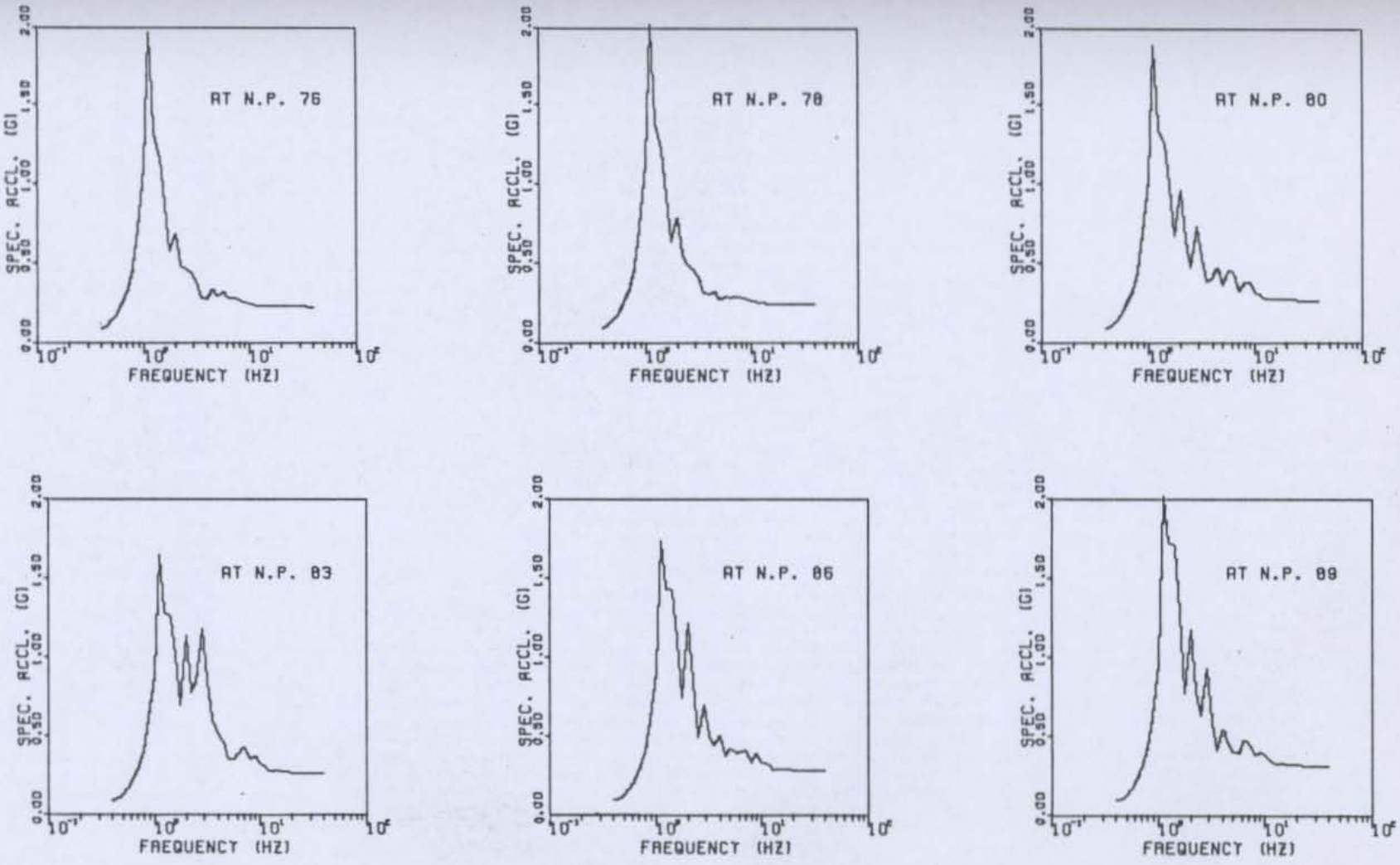

FIG. 3.37 ACCELERATION RESPONSE SPECTRA AT DIFFERENT LOCATIONS - DEPTH 44 FT IN A TYPICAL SOIL STRUCTURE MODEL - LOOSE FILL

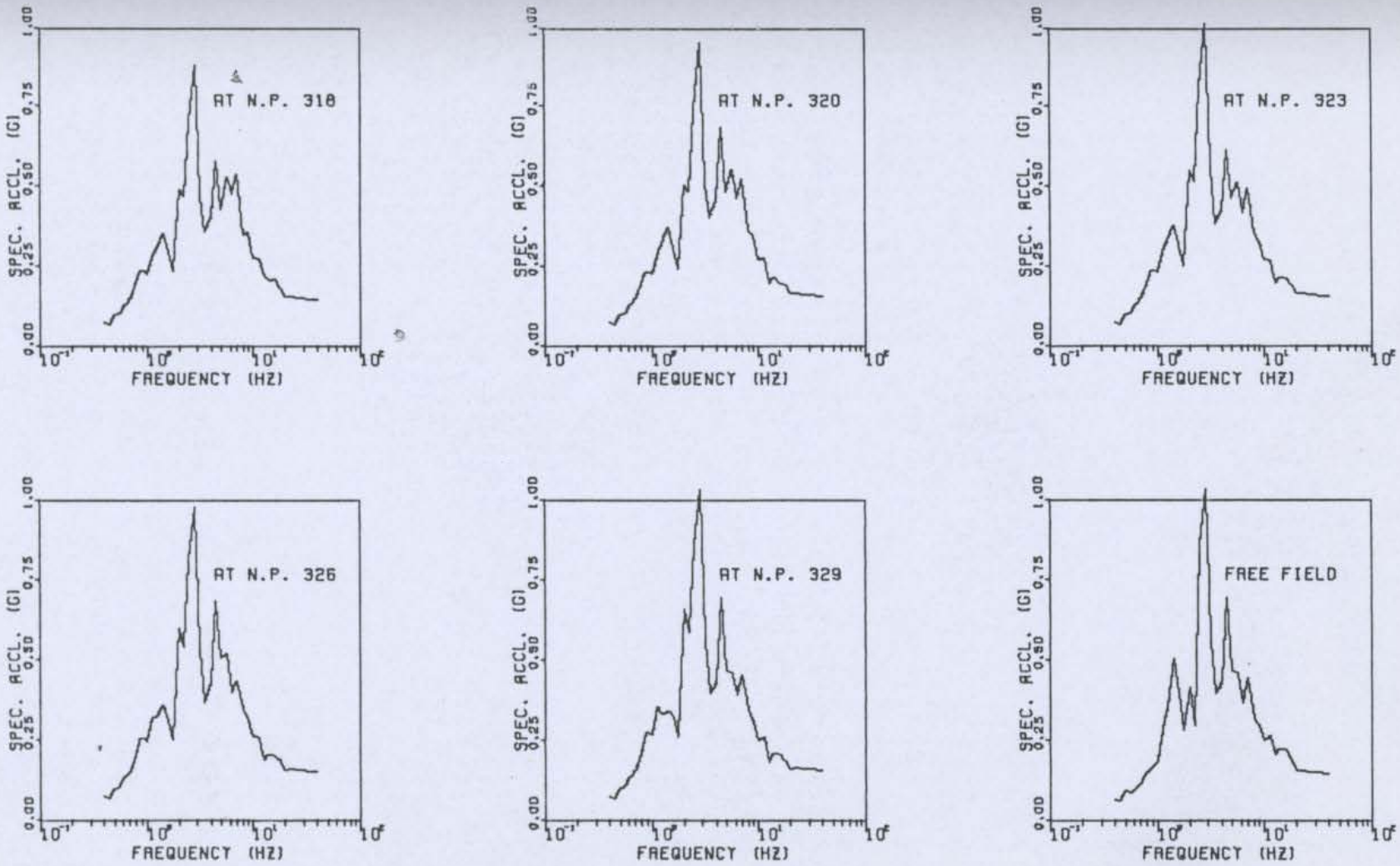

FIG. 3.38 ACCELERATION RESPONSE SPECTRA AT DIFFERENT LOCATIONS - DEPTH 250 FT IN A TYPICAL SOIL STRUCTURE MODEL - LOOSE FILL

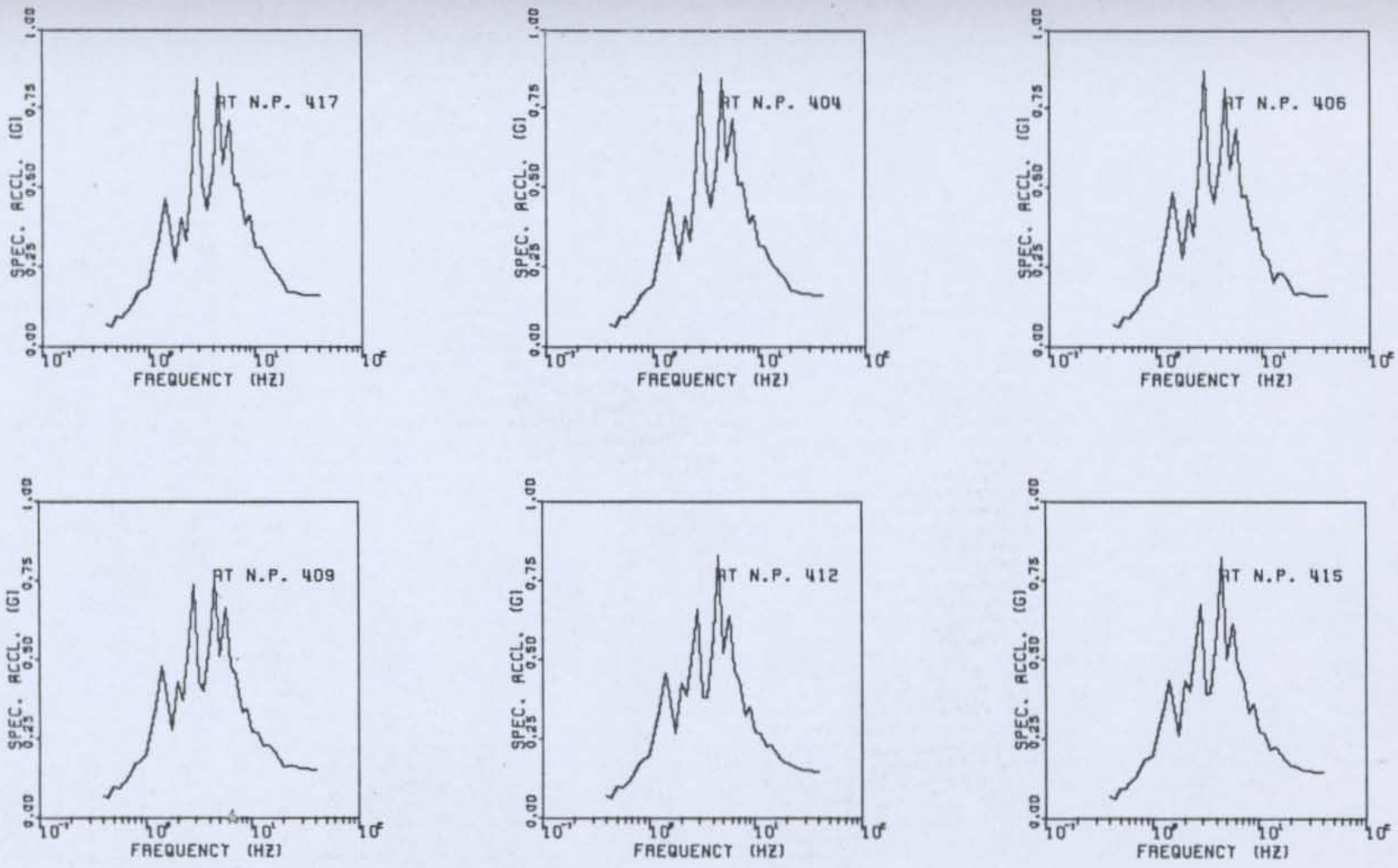

FIG. 3.39 ACCELERATION RESPONSE SPECTRA AT DIFFERENT LOCATIONS - DEPTH 344 FT IN A TYPICAL SOIL STRUCTURE MODEL - LOOSE FILL

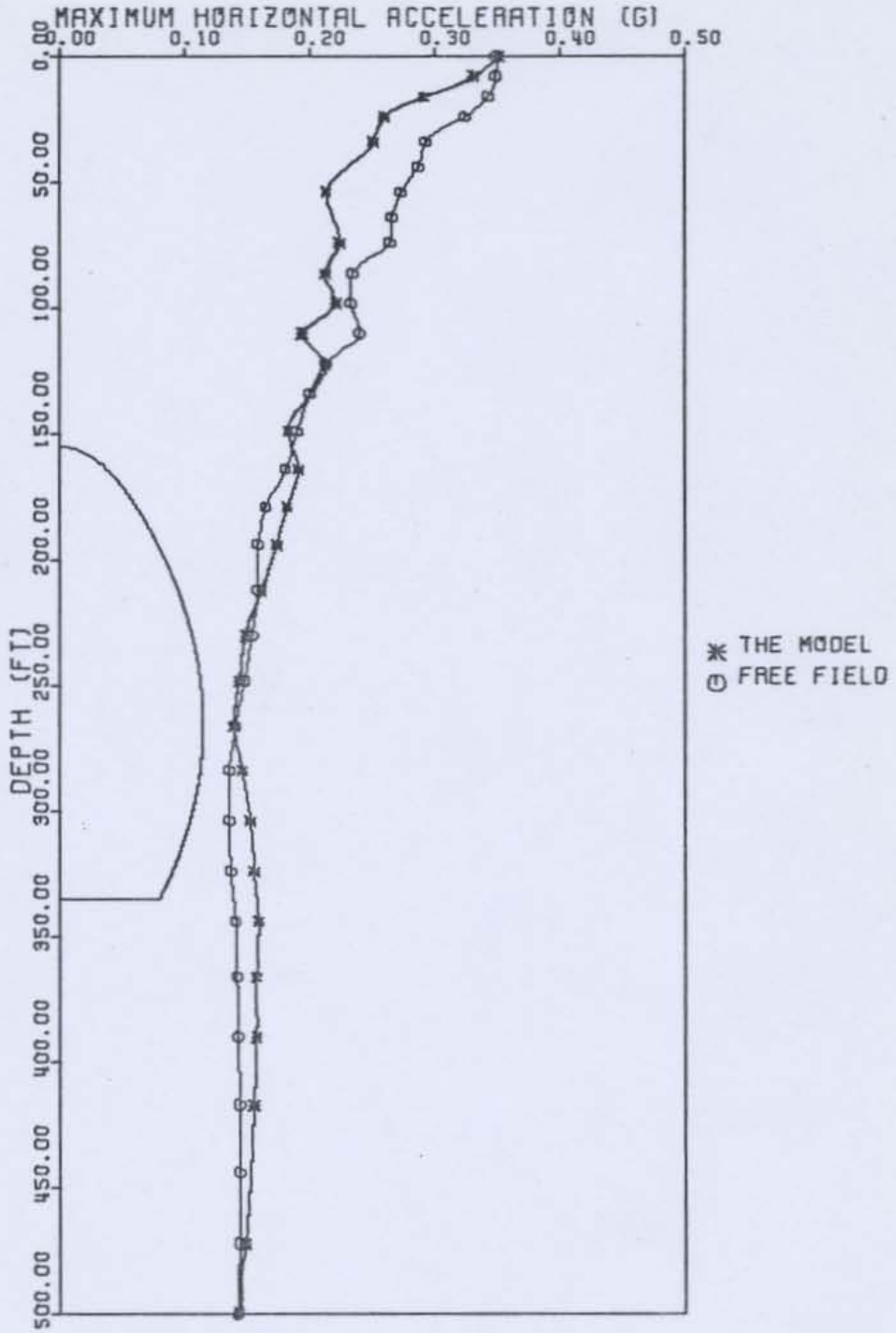

FIG. 3.40 MAXIMUM HORIZONTAL ACCELERATIONS IN SAND 10 FT AWAY FROM THE STRUCTURE AND IN THE FREE FIELD

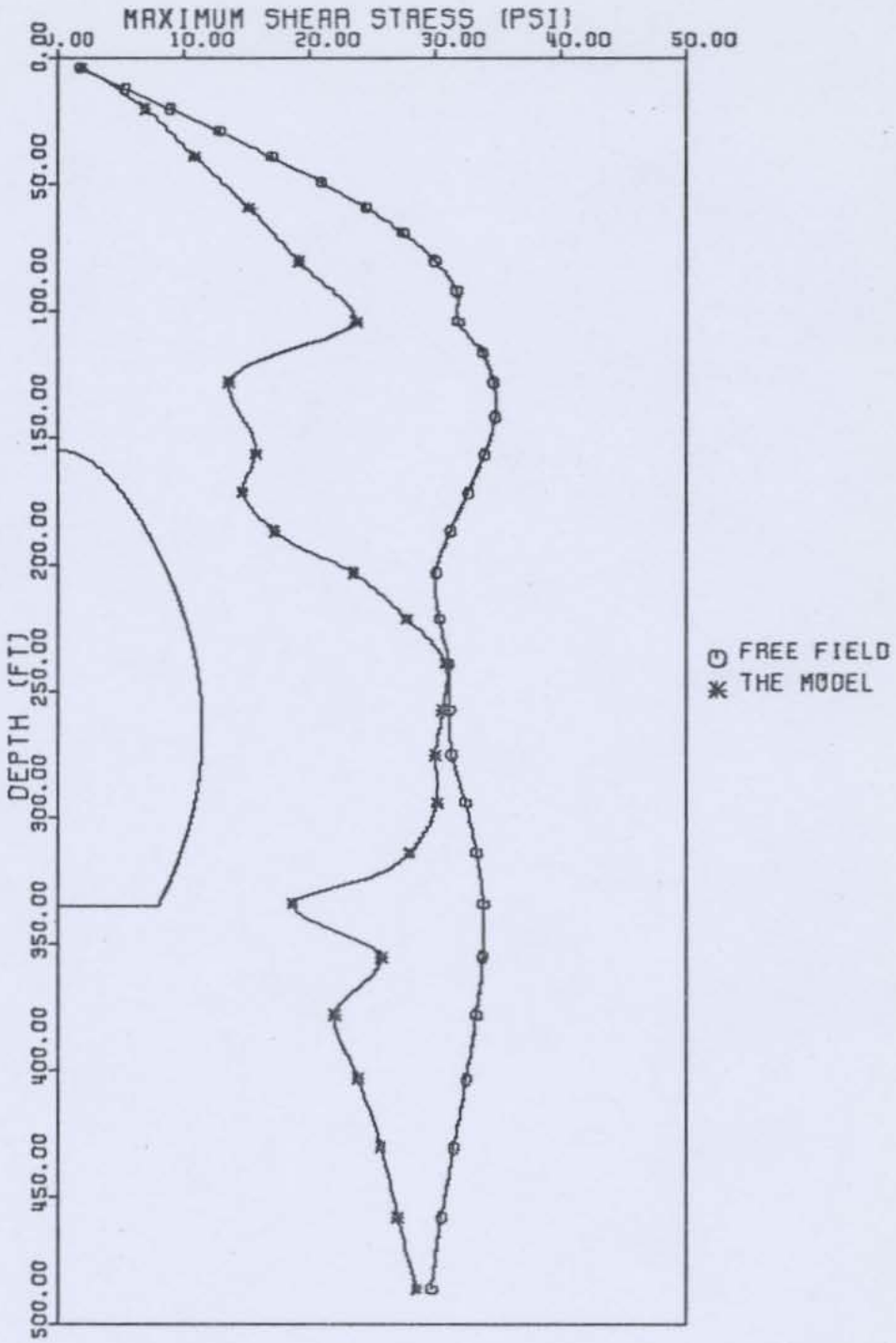

FIG. 3.41 MAXIMUM SHEAR STRESSES IN SAND - 70 FT AWAY FROM THE STRUCTURE AND IN THE FREE FIELD

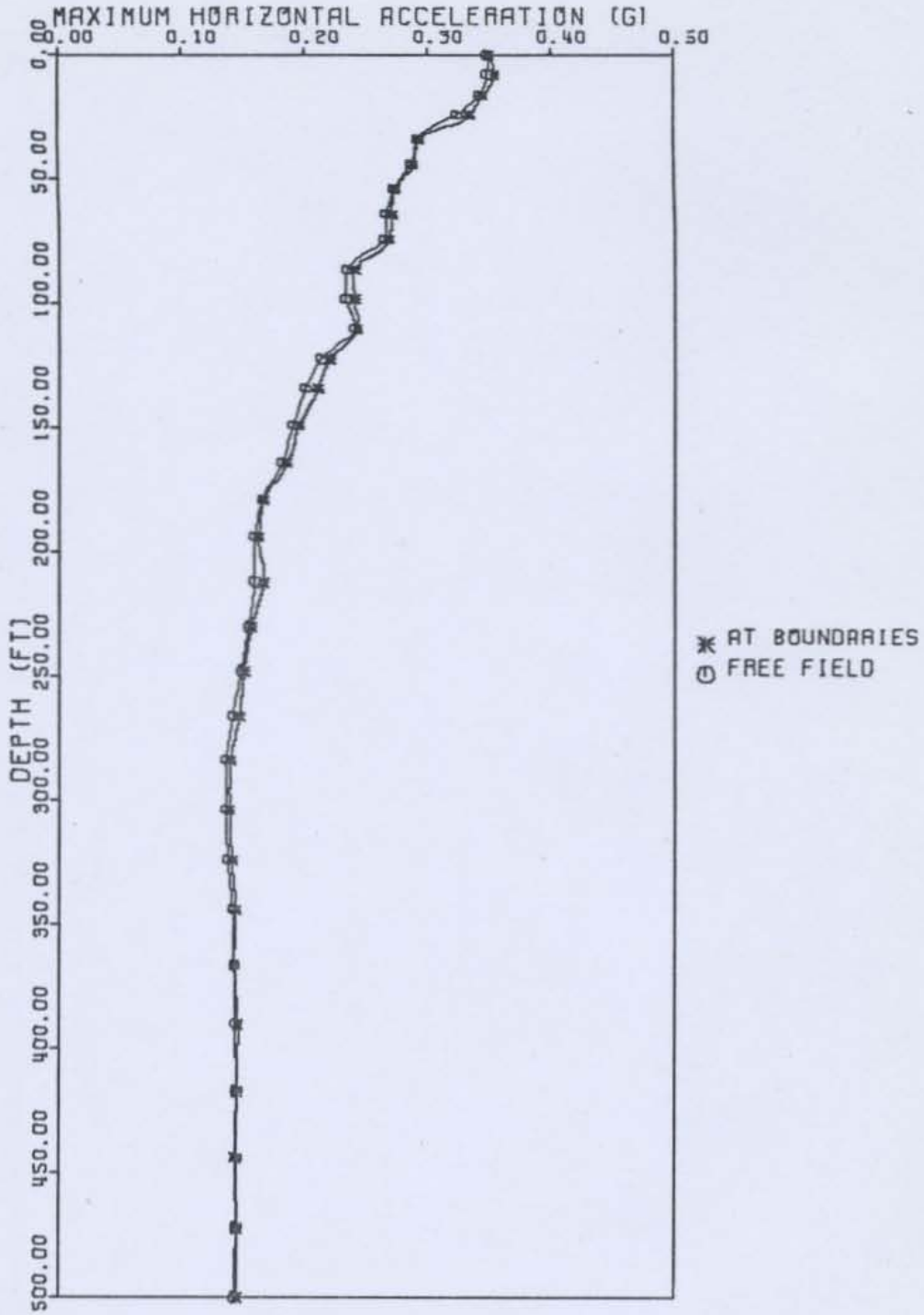

FIG. 3.42 MAXIMUM HORIZONTAL ACCELERATIONS IN SAND AT BOUNDARIES OF THE MODEL AND IN THE FREE FIELD

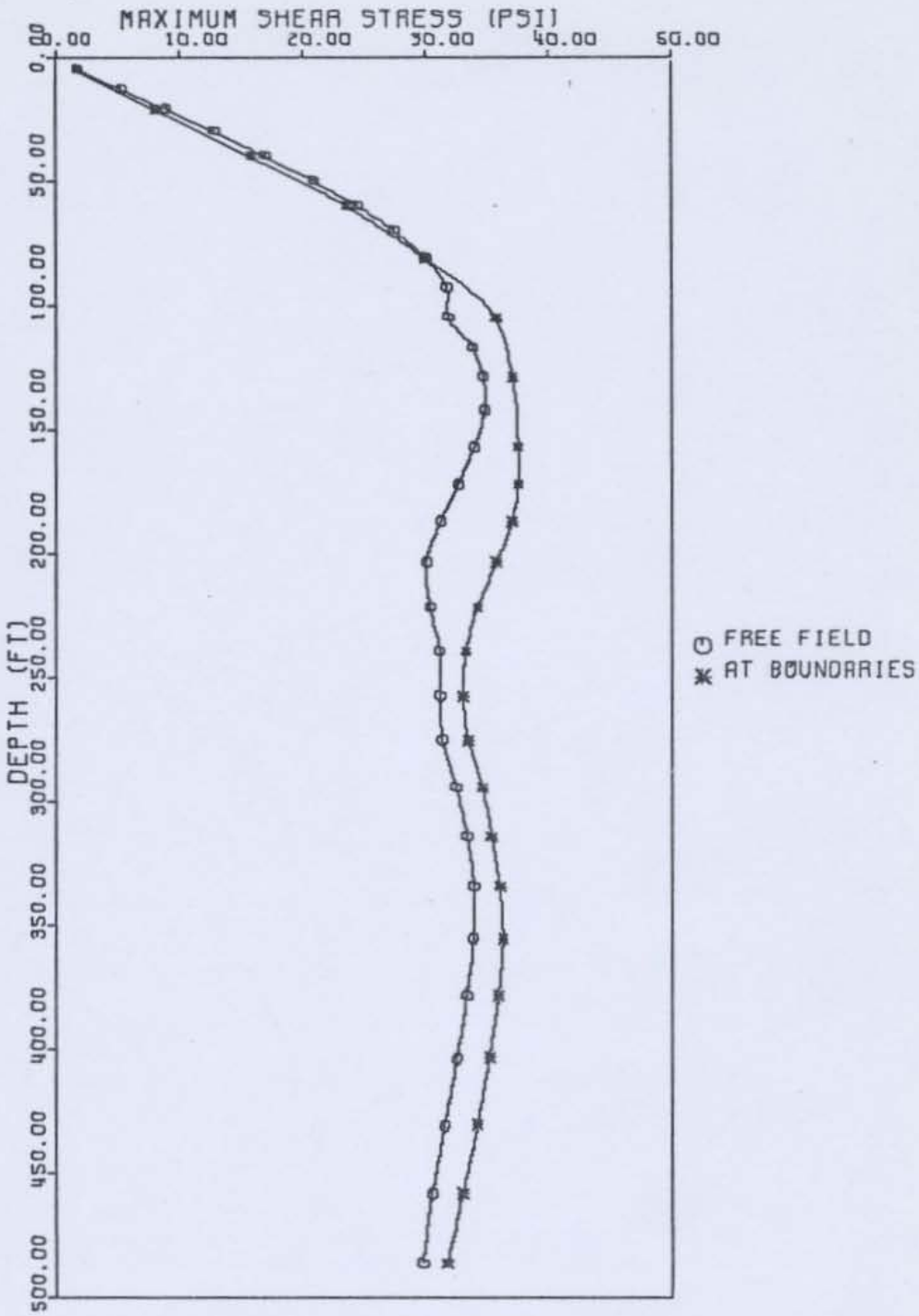

FIG. 3.43 MAXIMUM SHEAR STRESSES IN SAND AT BOUNDARIES OF THE MODEL AND IN THE FREE FIELD

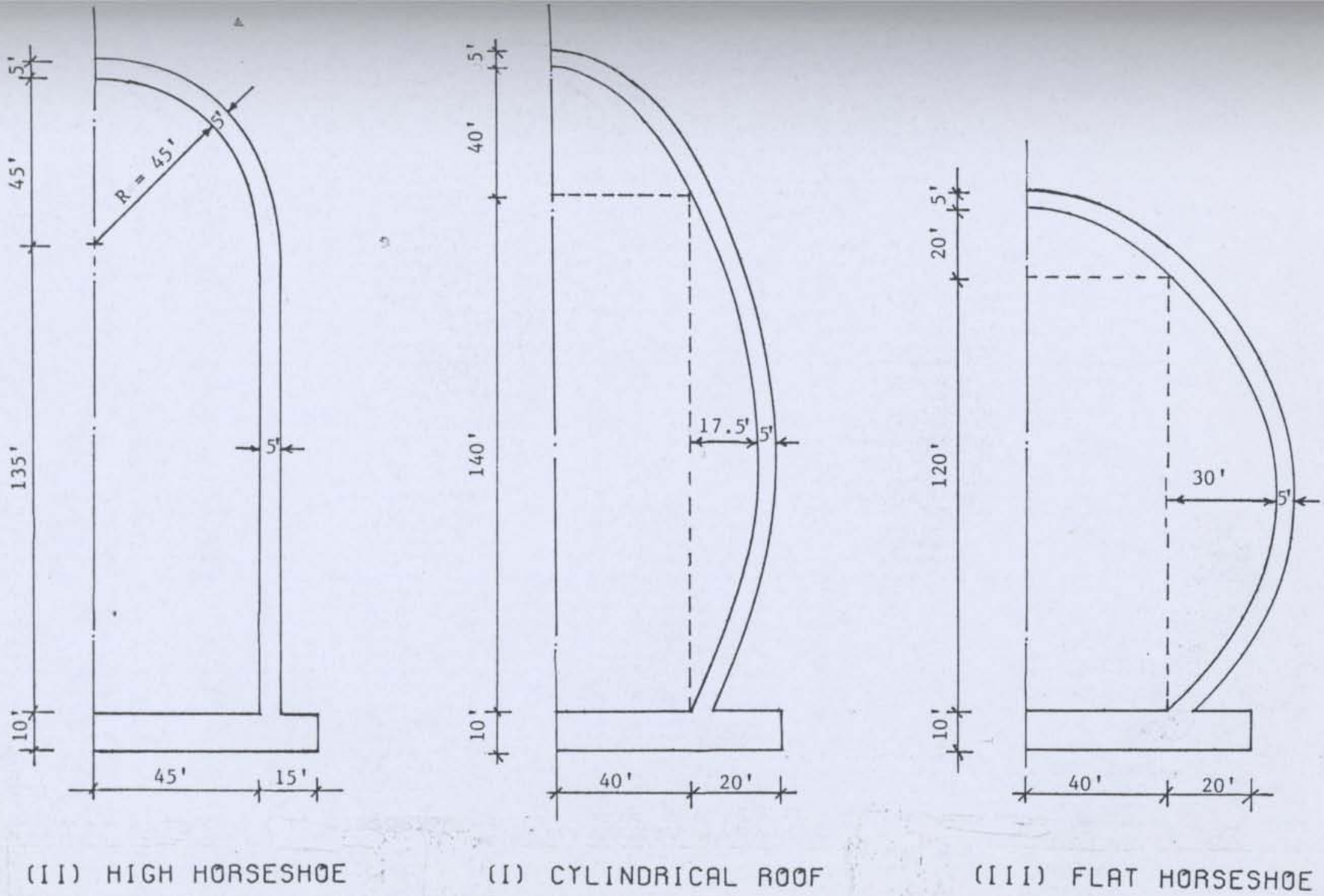

FIG.4.1 THREE CONTAINMENT SHAPES CONSIDERED IN THE ANALYSIS

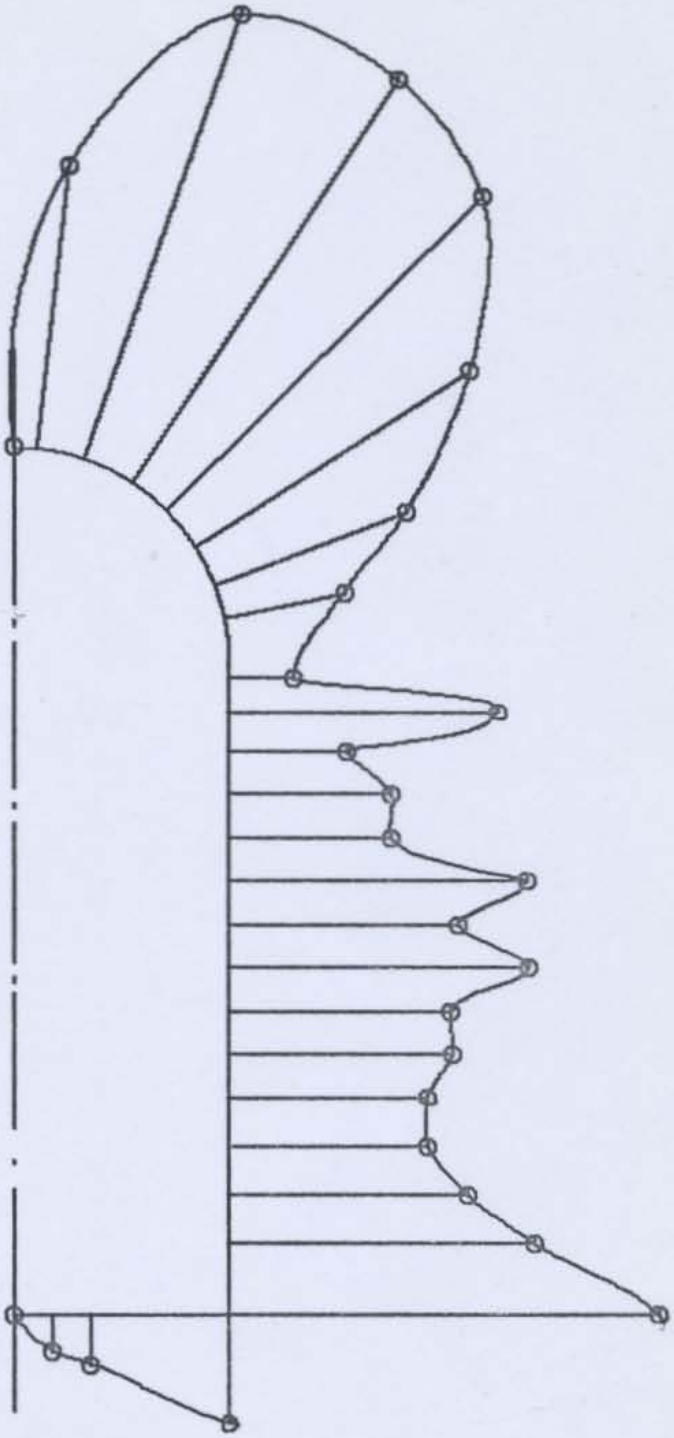

FIG. 4.2 MAXIMUM PRINCIPAL STRESS DIAGRAM FOR A CONTAINMENT WITH CYLINDRICAL ROOF AND VERTICAL WALLS - ORIGINAL FILL
(SCALE: 1 INCH = 400 P.S.I.)

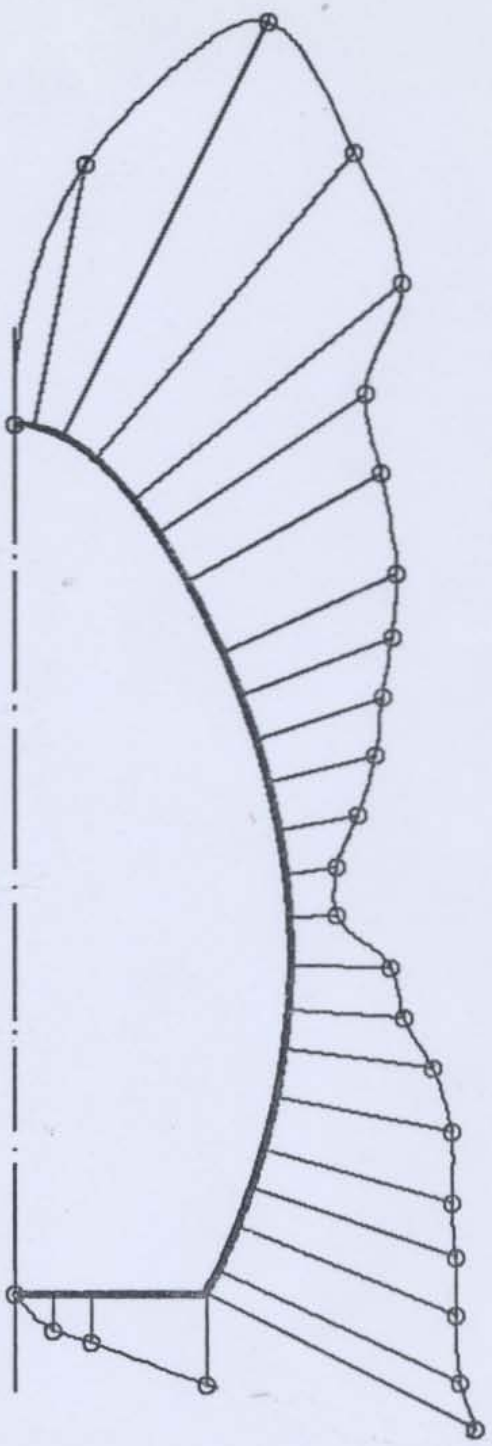

FIG. 4.3 MAXIMUM PRINCIPAL STRESS DIAGRAM FOR THE HIGH HORSESHOE CONTAINMENT- ORIGINAL FILL
(SCALE: 1 INCH = 400 P.S.I.)

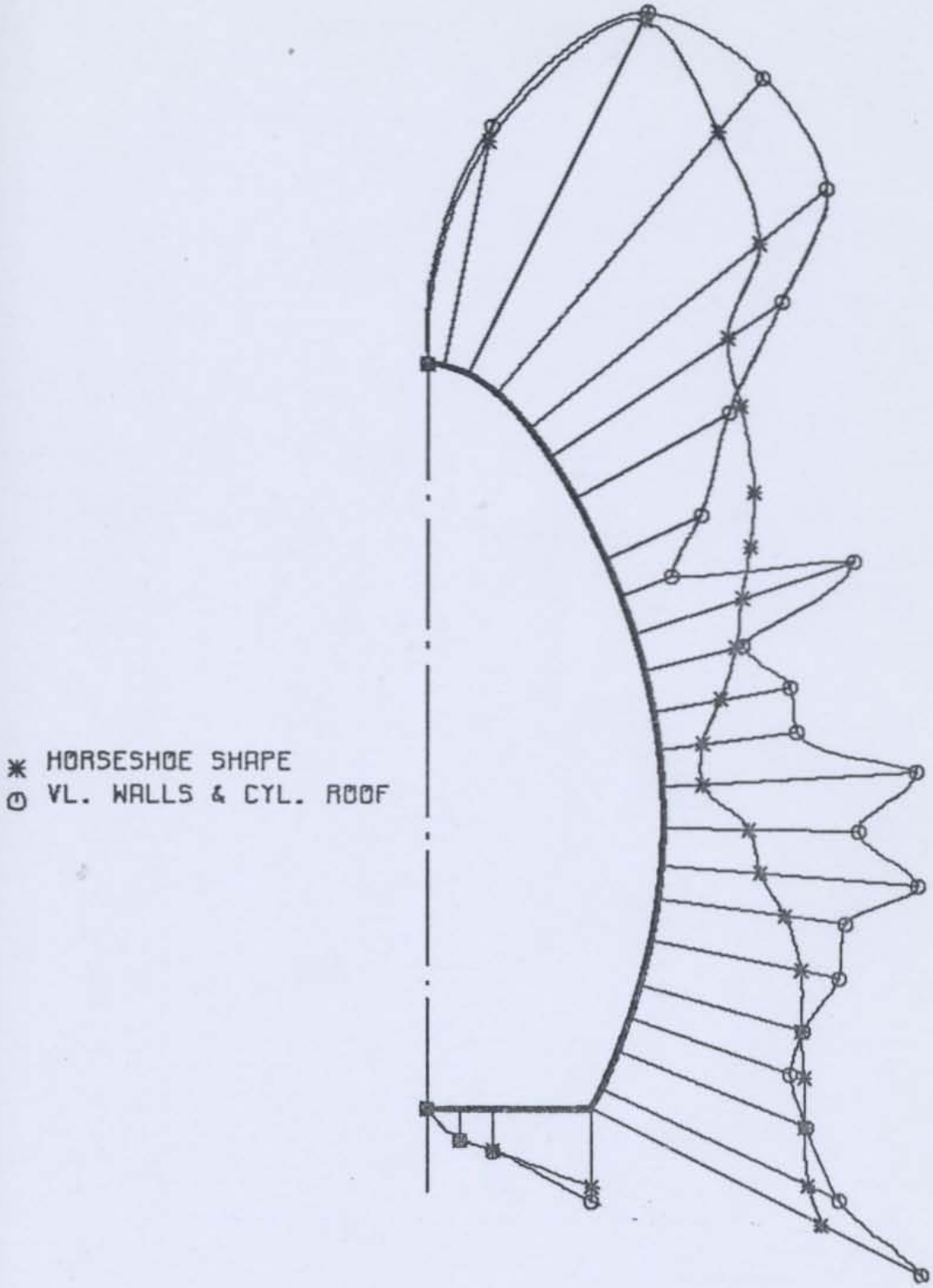

FIG. 4.4 MAXIMUM PRINCIPAL STRESS DIAGRAMS FOR HIGH HORSESHOE AND VERTICAL WALL-CYLINDRICAL ROOF CONTAINMENTS - ORIGINAL FILL
(SCALE: 1 INCH = 400 P.S.I.)

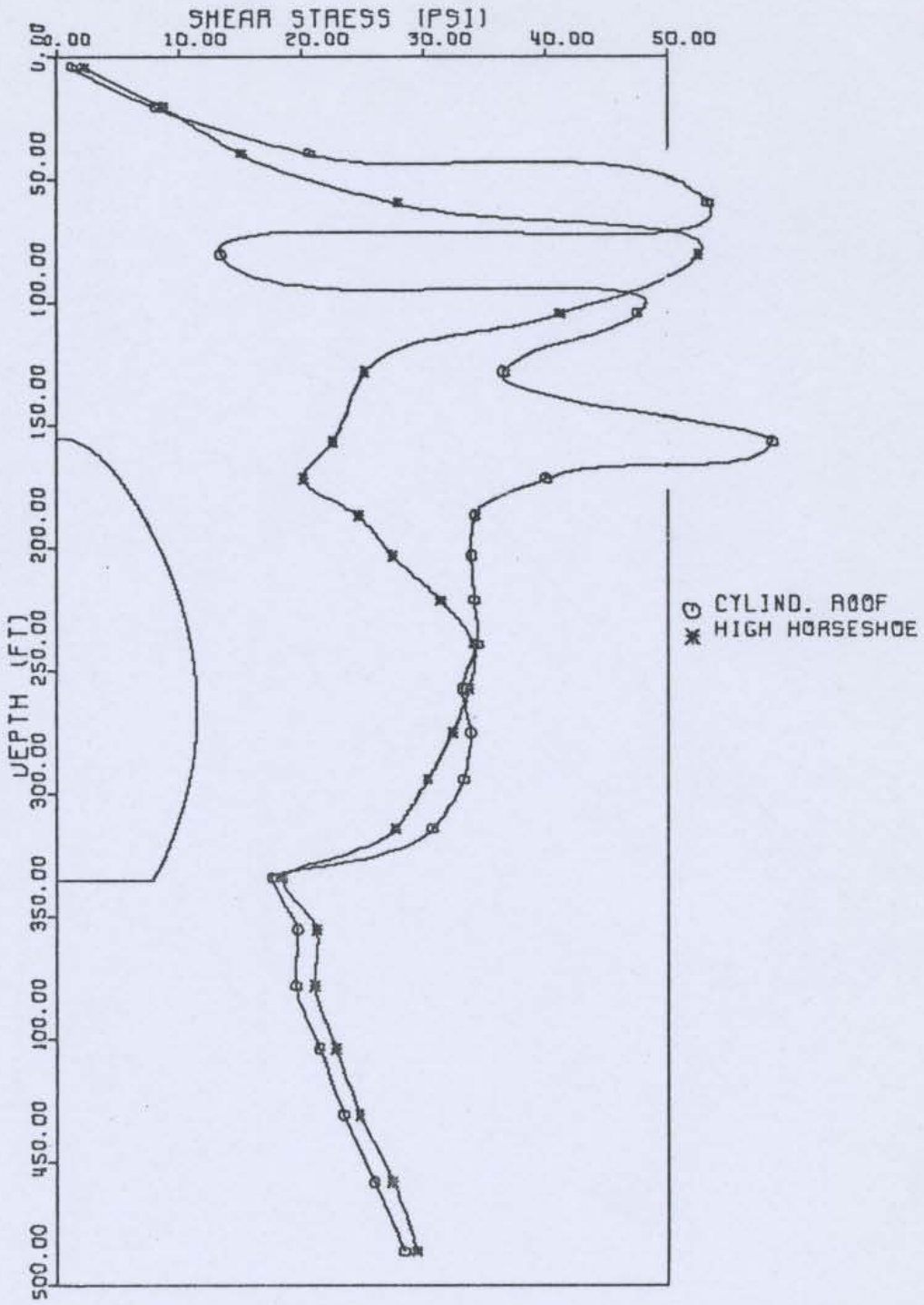

FIG. 4.5 MAXIMUM SHEAR STRESSES IN THE SOIL AT A VERTICAL PLANE 40 FT AWAY FROM THE CONTAINMENT FOR THE HIGH HORSESHOE AND THE CYLINDRICAL ROOF-VERTICAL WALL SHAPES

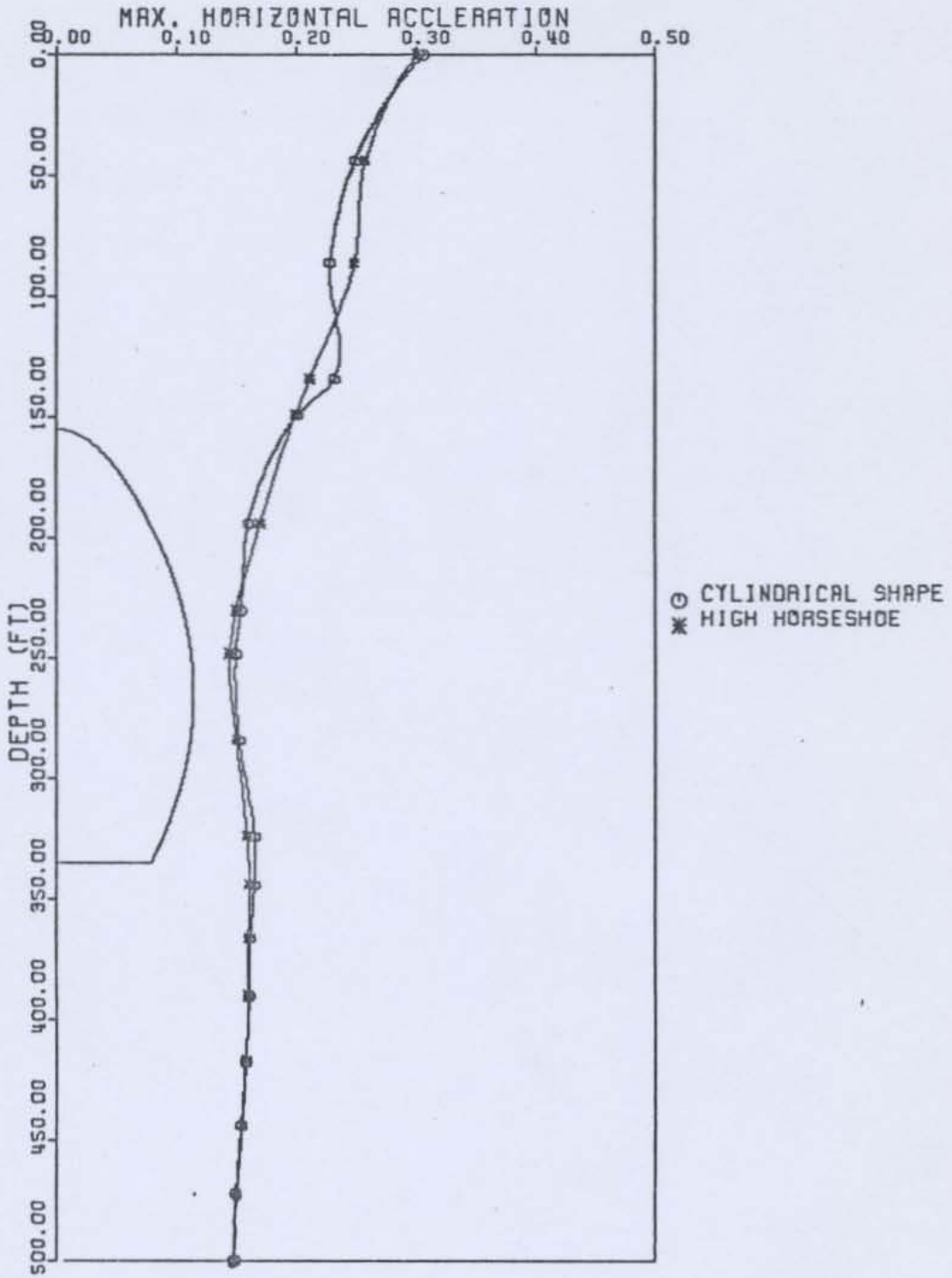

FIG. 4.6 MAXIMUM HORIZONTAL ACCELERATIONS IN THE SOIL AT A VERTICAL PLANE 70 FT AWAY FROM THE CONTAINMENT - HIGH HORSESHOE AND CYLINDRICAL ROOF CONTAINMENTS

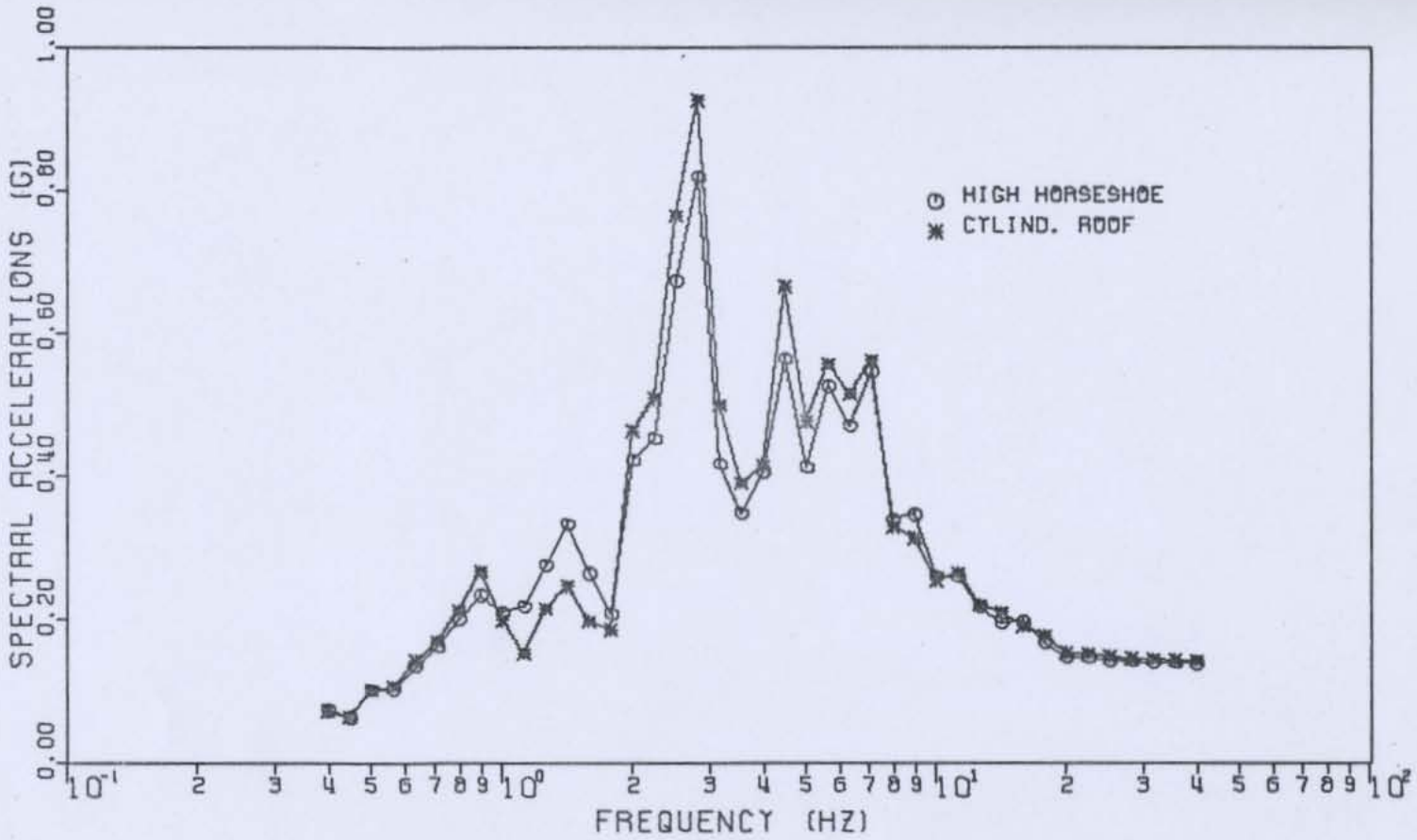

FIG. 4.7 ACCELERATION RESPONSE SPECTRA AT MID-HEIGHT OF THE CONTAINMENT WALL FOR THE HIGH HORSESHOE AND THE CYLINDRICAL ARCH ROOF CONTAINMENTS - ORIGINAL FILL. (SPECTRAL DAMPING = 2%)

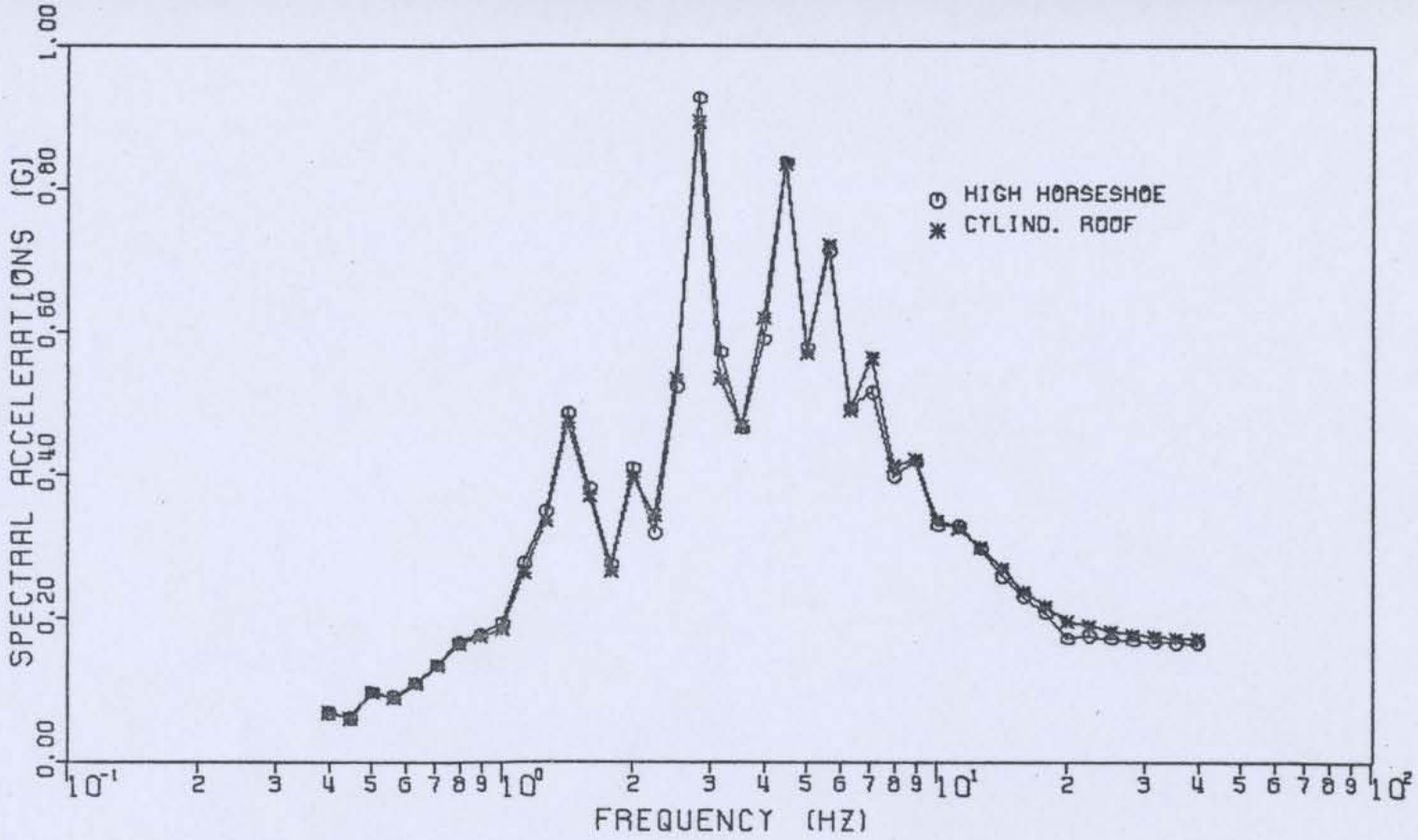

FIG. 4.8 ACCELERATION RESPONSE SPECTRA AT THE CONTAINMENT FOUNDATION MID-POINT FOR THE HIGH HORSESHOE AND THE CYLINDRICAL ARCH ROOF CONTAINMENTS - ORIGINAL FILL. (SPECTRAL DAMPING = 2%)

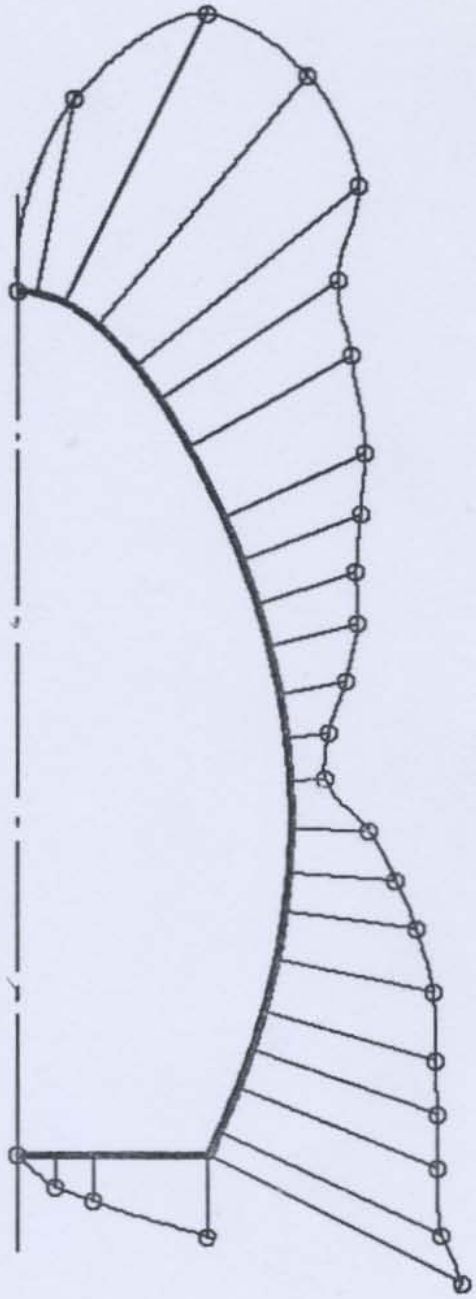

FIG. 4.9 MAXIMUM PRINCIPAL STRESS DIAGRAM FOR A HIGH HORSESHOE CONTAINMENT - LOOSE FILL
(SCALE: 1 INCH = 400 P.S.I.)

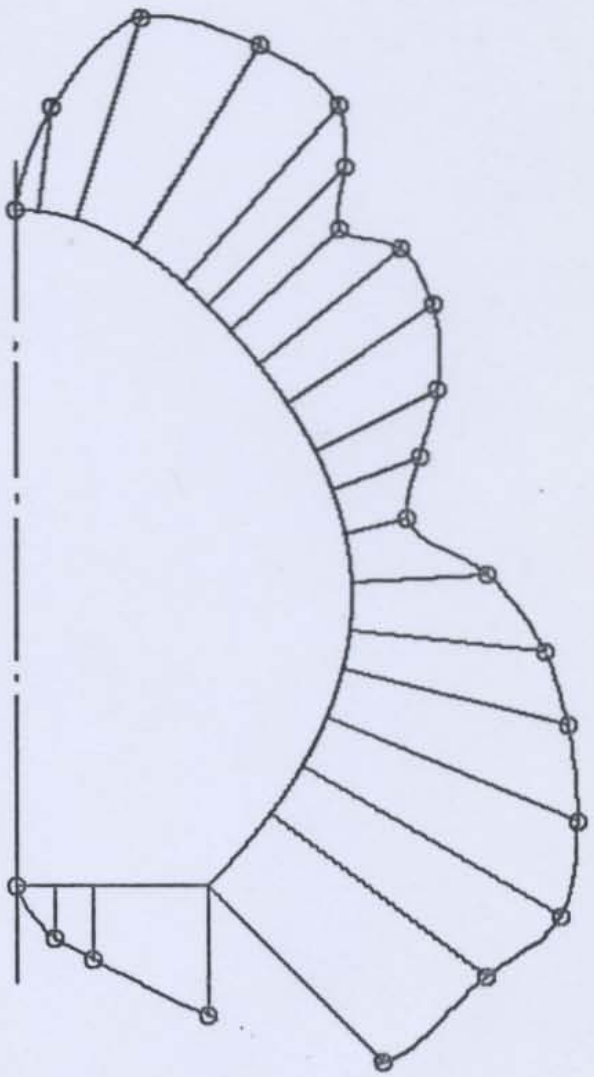

FIG. 4.10 MAXIMUM PRINCIPAL STRESS DIAGRAM FOR THE FLAT HORSESHOE CONTAINMENT - LOOSE FILL
(SCALE: 1 INCH = 400 P.S.I.)

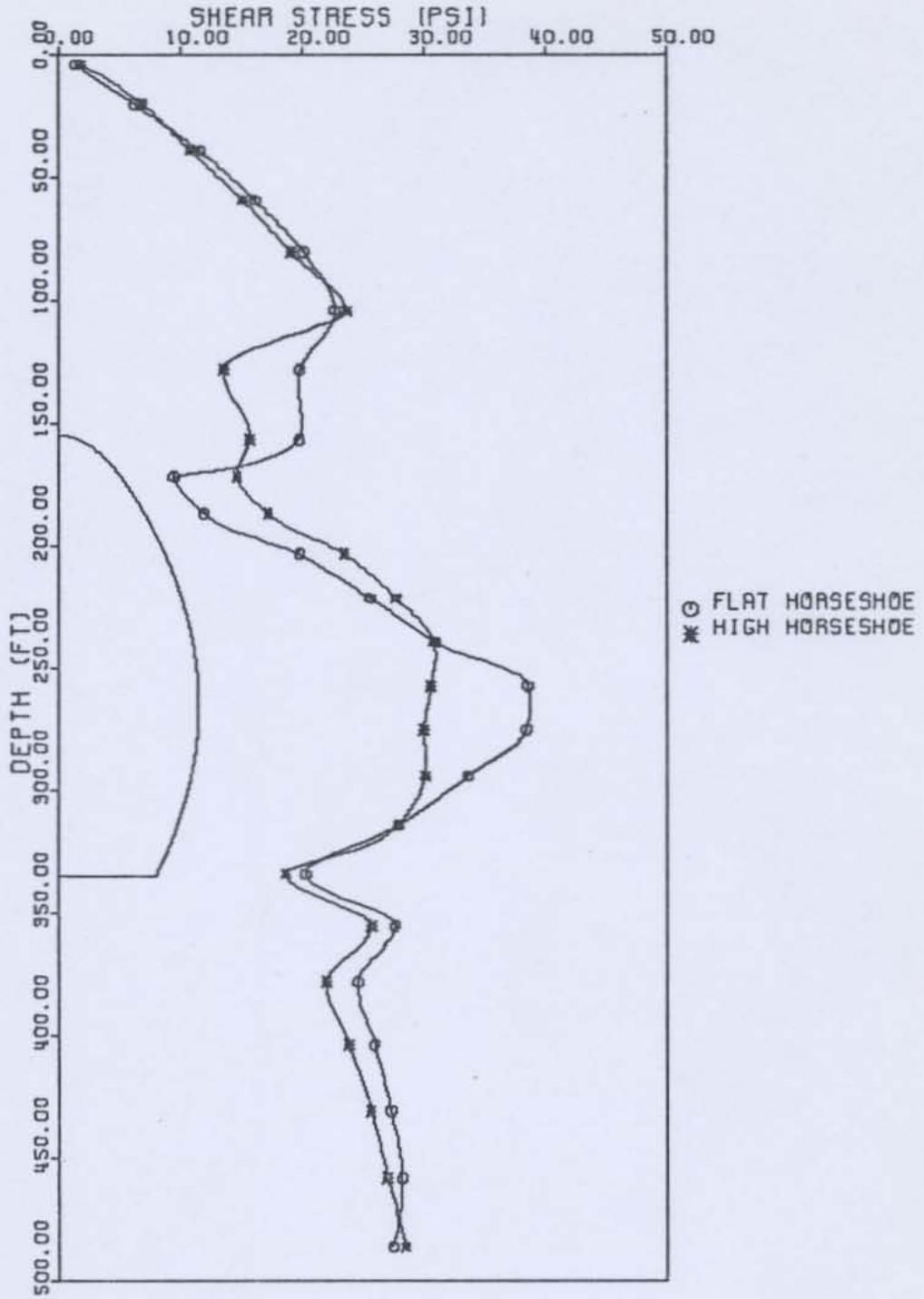

FIG. 4.11 MAXIMUM SHEAR STRESSES IN THE SOIL AT A VERTICAL PLANE 40 FT AWAY FROM THE CONTAINMENT - FLAT AND HIGH HORSESHOE CONTAINMENTS

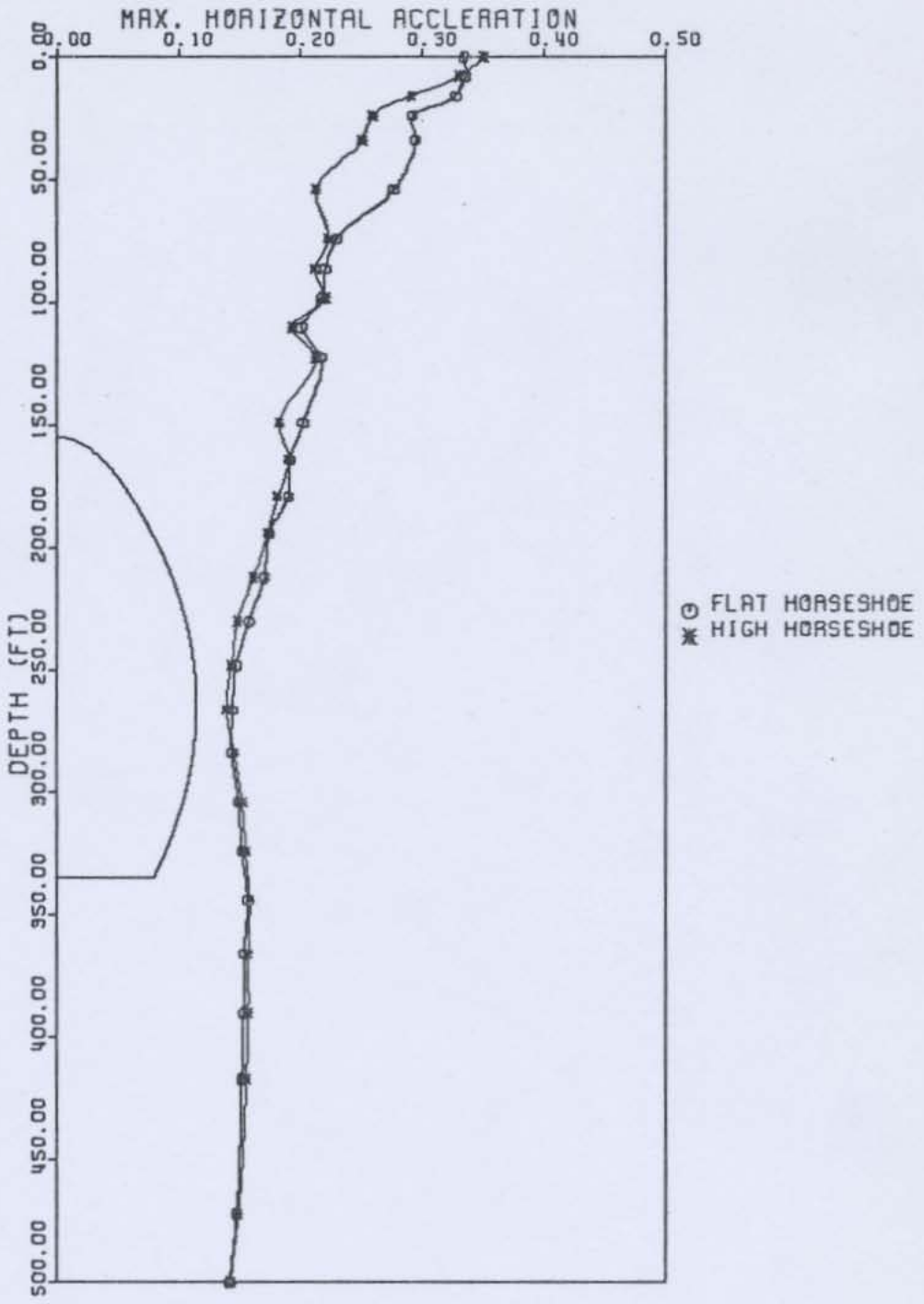

FIG. 4.12 MAXIMUM HORIZONTAL ACCELERATIONS IN THE SOIL AT A VERTICAL PLANE 10 FEET AWAY FROM THE CONTAINMENT - FLAT AND HIGH HORSESHOE CONTAINMENTS

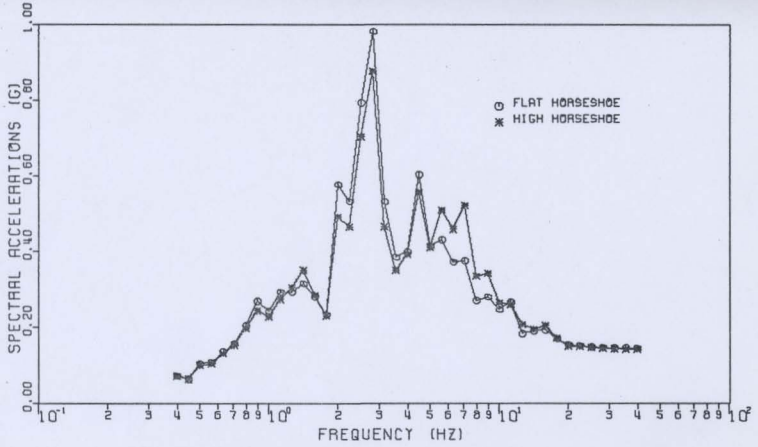

FIG. 4.13 ACCELERATION RESPONSE SPECTRA AT MID-HEIGHT OF THE CONTAINMENT WALL FOR THE HIGH AND FLAT HORSESHOE CONTAINMENTS - LOOSE FILL
(SPECTRAL DAMPING = 2%)

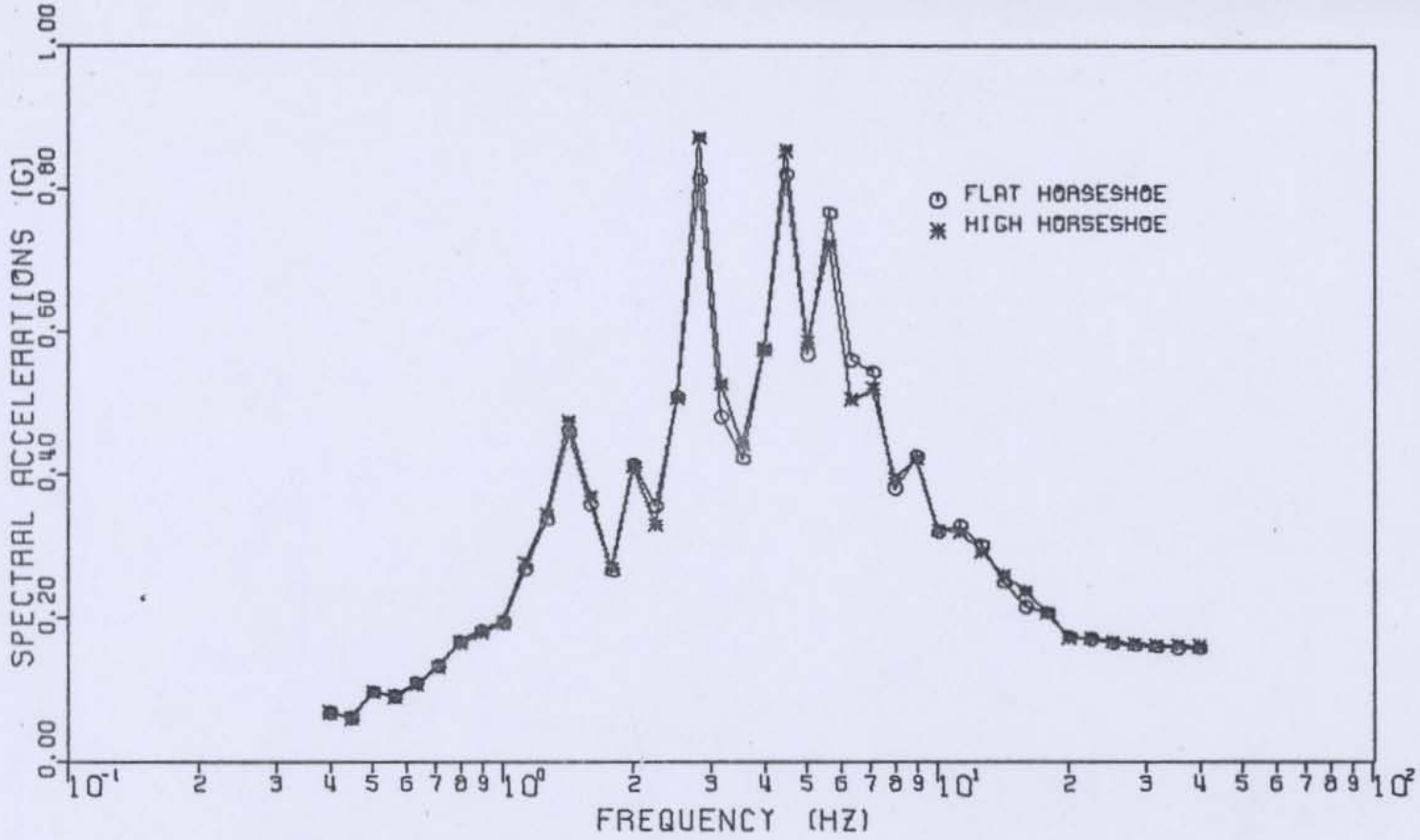

FIG. 4.14 ACCELERATION RESPONSE SPECTRA AT THE CONTAINMENT FOUNDATION MID-POINT FOR THE HIGH AND FLAT HORSESHOE CONTAINMENTS - LOOSE FILL
(SPECTRAL DAMPING = 2%)

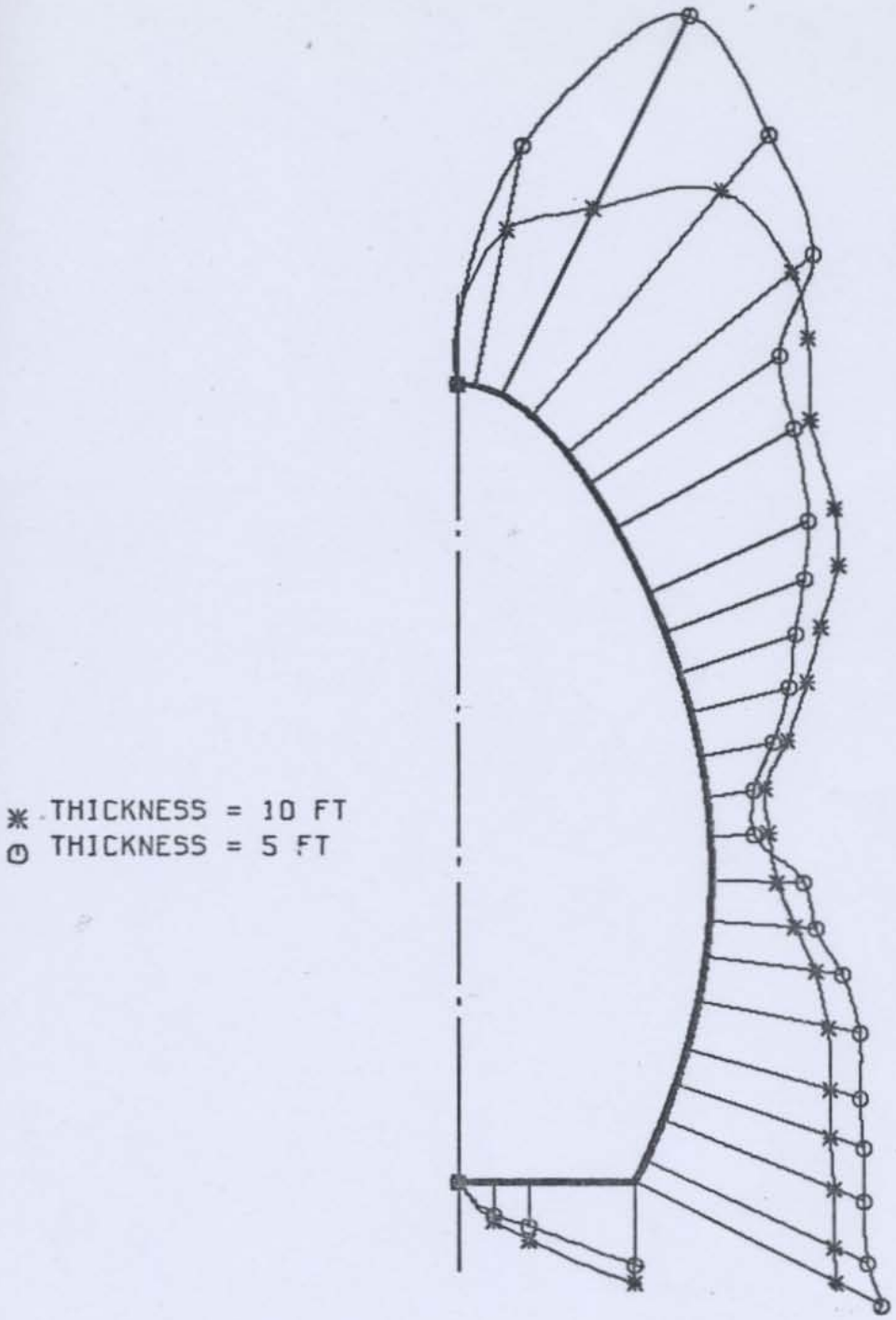

FIG. 4.15 EFFECT OF CONTAINMENT THICKNESS ON MAXIMUM PRINCIPAL STRESSES IN THE CONTAINMENT (SCALE: 1 INCH = 400 P.S.I.)

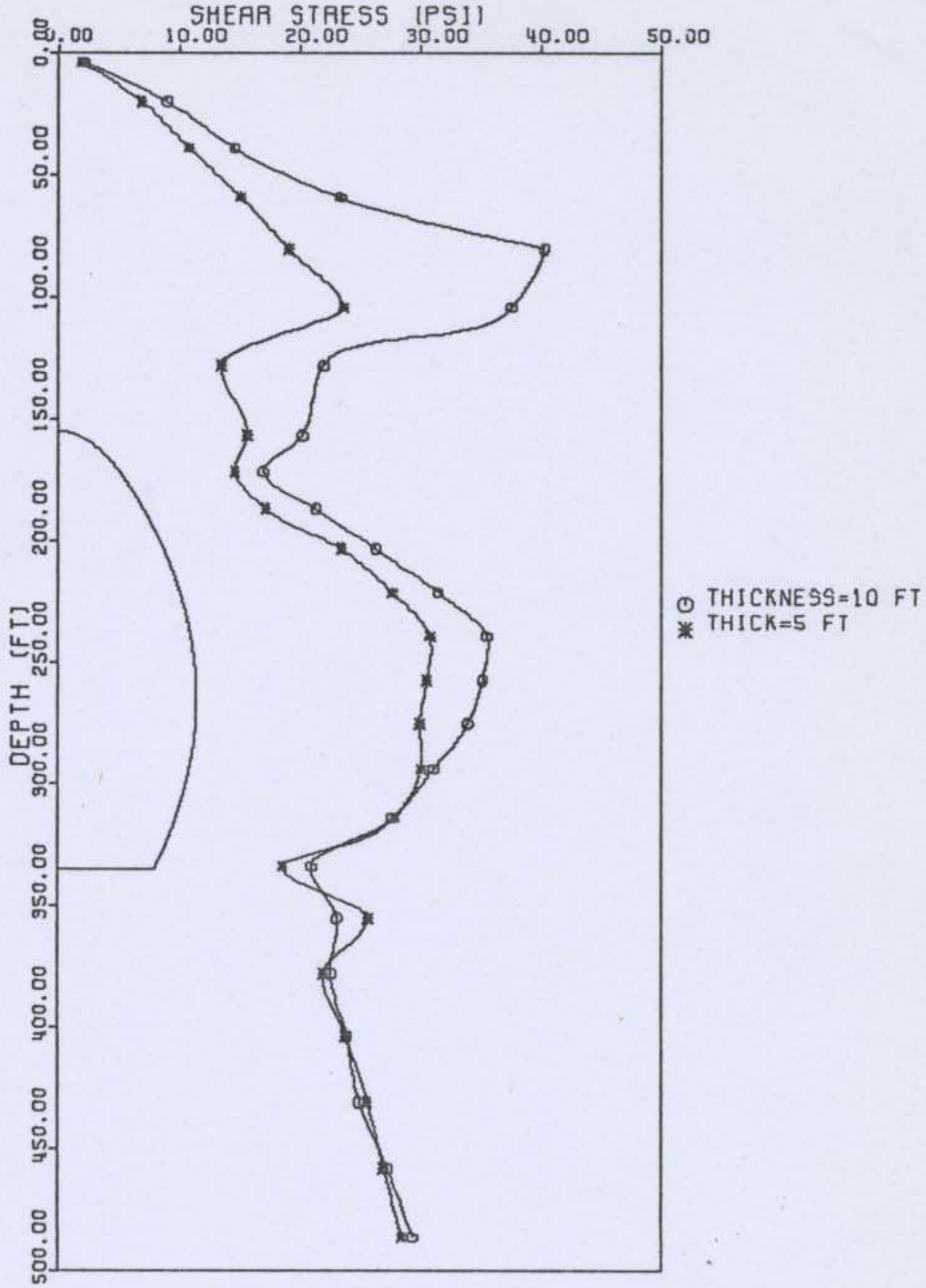

FIG. 4.16 MAXIMUM SHEAR STRESSES IN THE SOIL AT A VERTICAL PLANE 40 FT AWAY FROM THE CONTAINMENT - THIN (5') AND THICK (10') HIGH HORSESHOE CONTAINMENTS

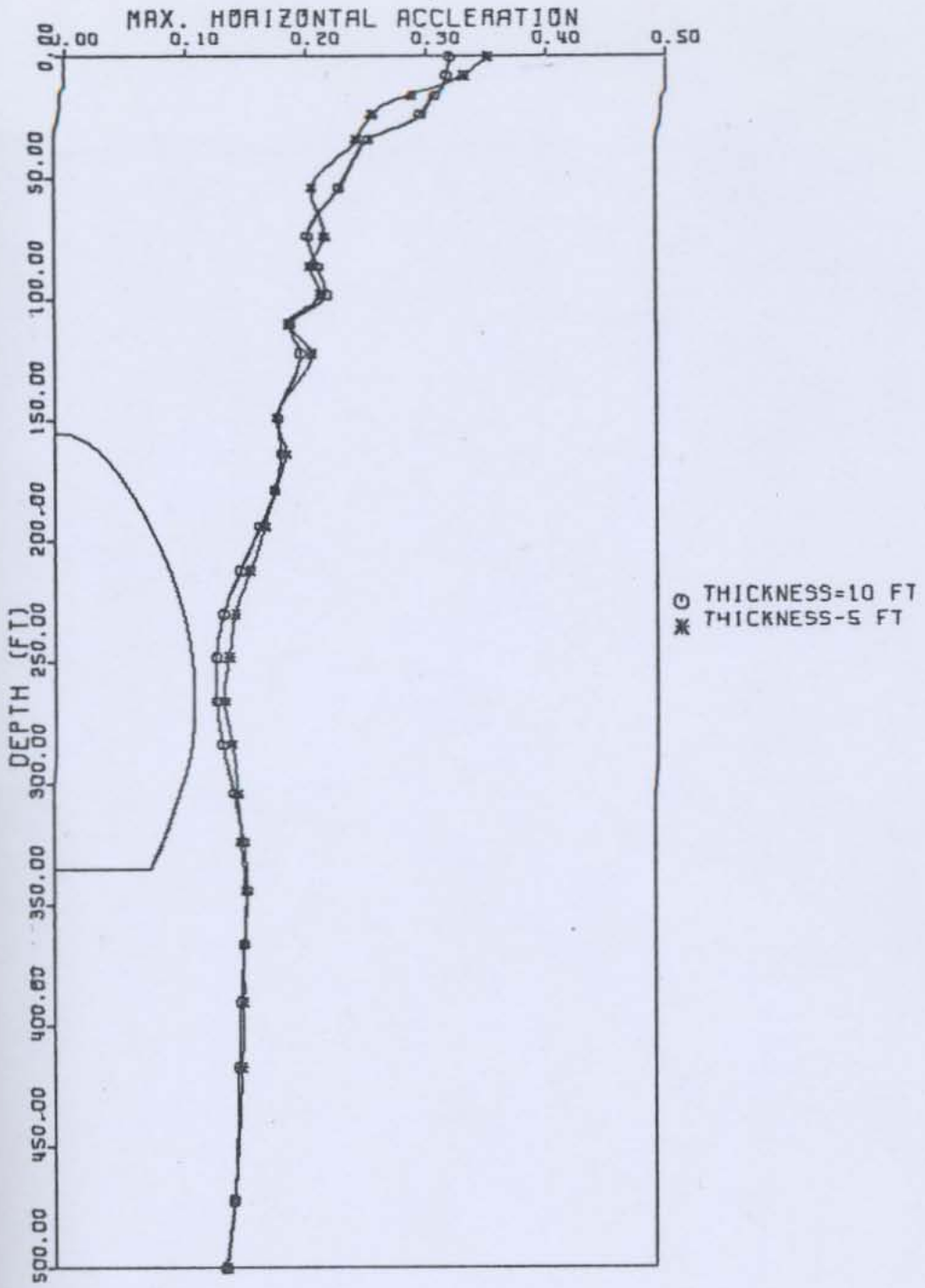

FIG. 4.17 MAXIMUM HORIZONTAL ACCELERATIONS IN THE SOIL AT A VERTICAL PLANE 10 FEET AWAY FROM THE CONTAINMENT - THIN AND THICK HORSESHOE CONTAINMENTS

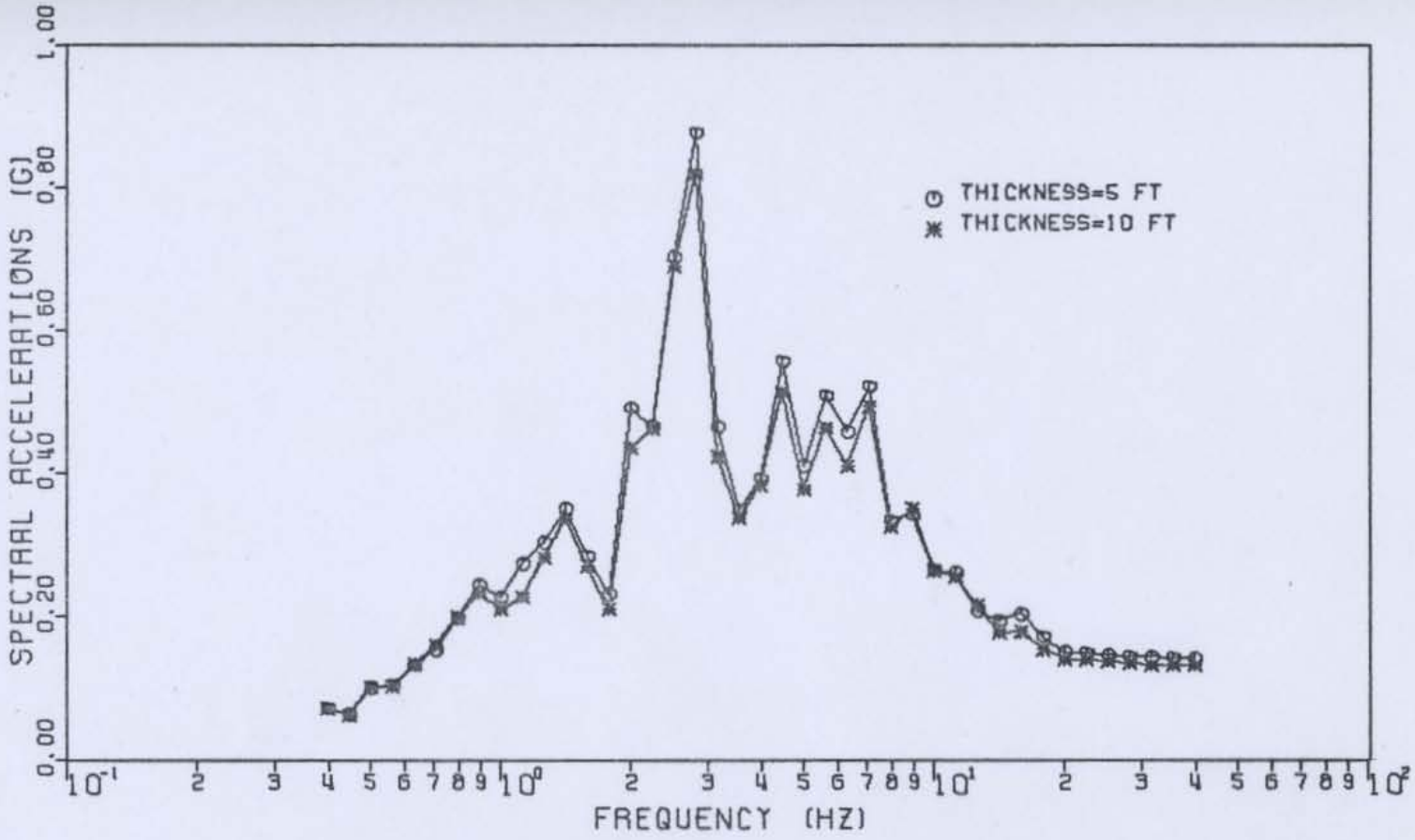

FIG. 4.18 ACCELERATION RESPONSE SPECTRA AT MID-HEIGHT OF THE CONTAINMENT WALL FOR THE THIN (5') AND THICK (10') CONTAINMENTS - LOOSE FILL
(SPECTRAL DAMPING = 2%)

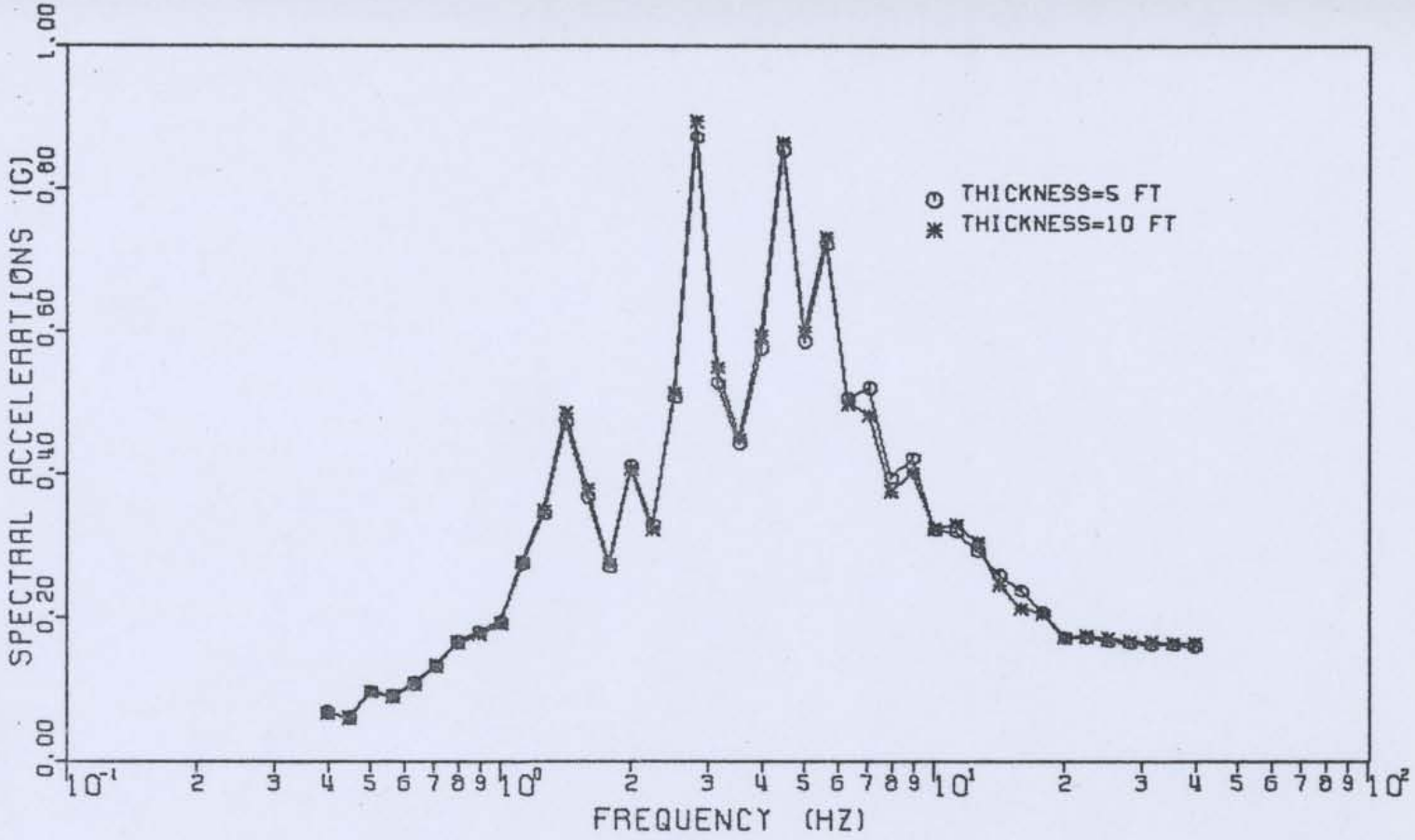

FIG. 4.19 ACCELERATION RESPONSE SPECTRA AT THE CONTAINMENT FOUNDATION MID-POINT FOR THE THIN (5') AND THICK (10') CONTAINMENTS - LOOSE FILL
(SPECTRAL DAMPING = 2%)

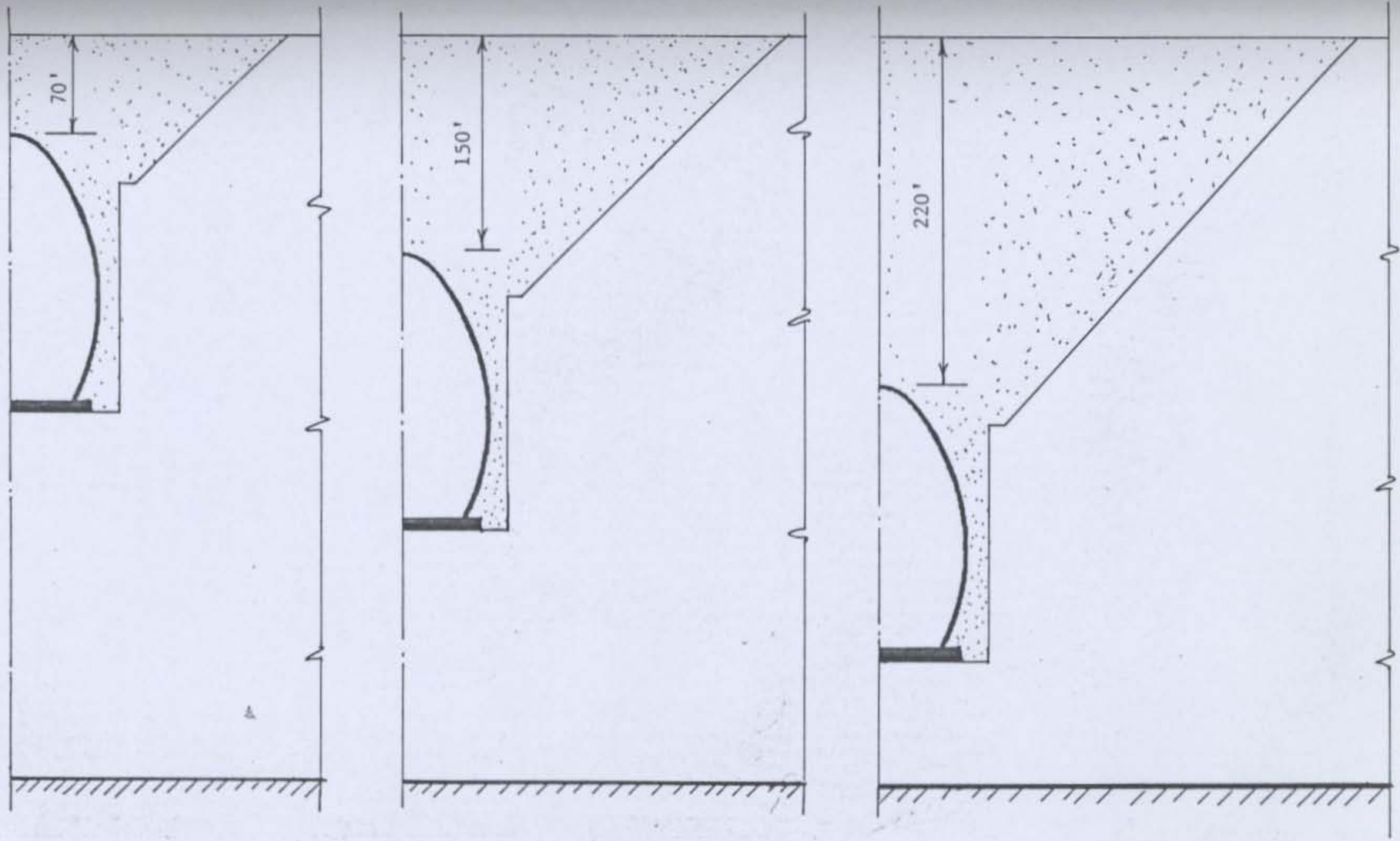

FIG. 4.20 BURIAL DEPTHS

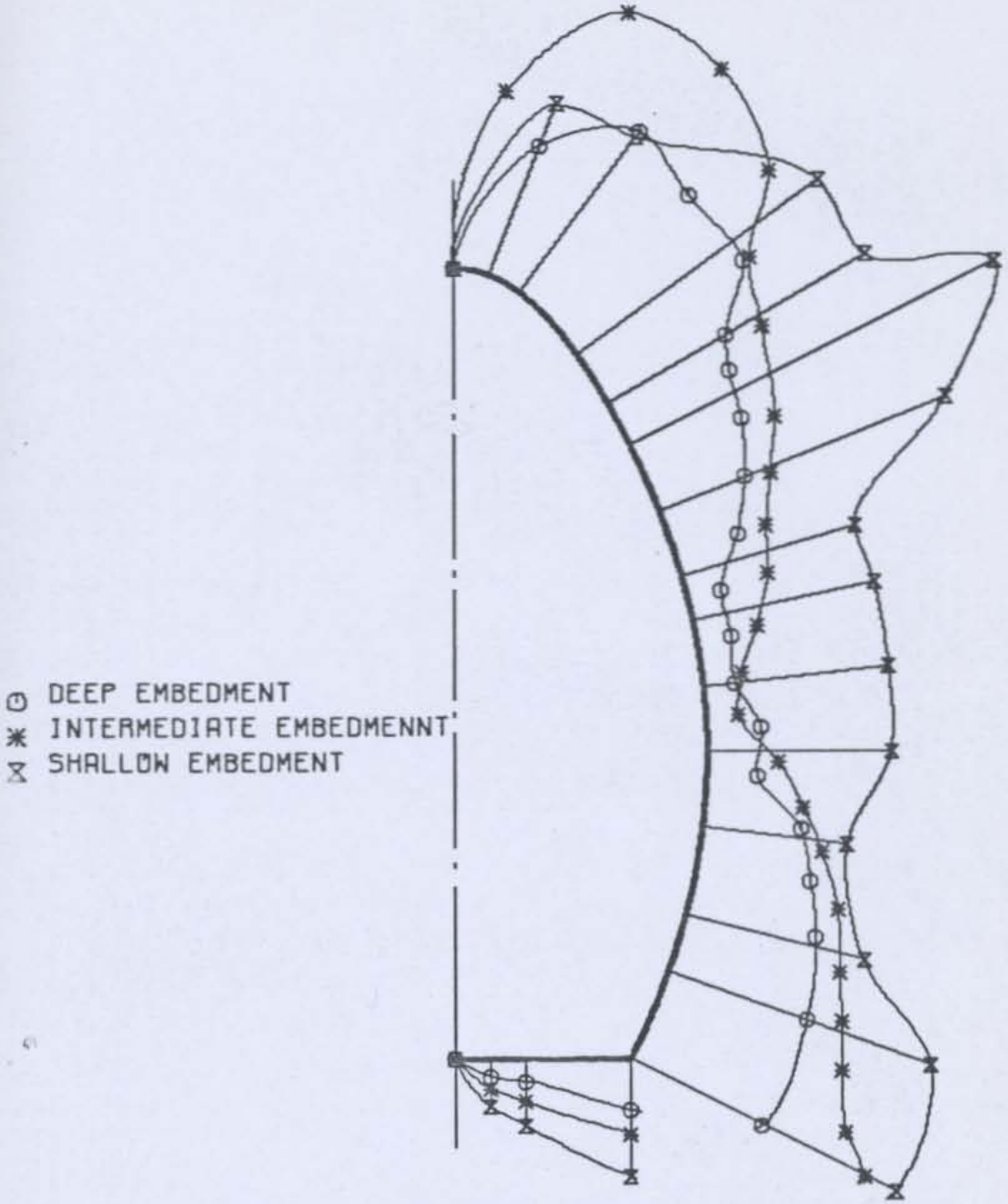

FIG. 4.21 MAXIMUM PRINCIPAL STRESS DIAGRAMS FOR CONTAINMENTS AT SHALLOW, INTERMEDIATE AND DEEP EMBEDMENTS
(SCALE: 1 INCH ≐ 400 P.S.I.)

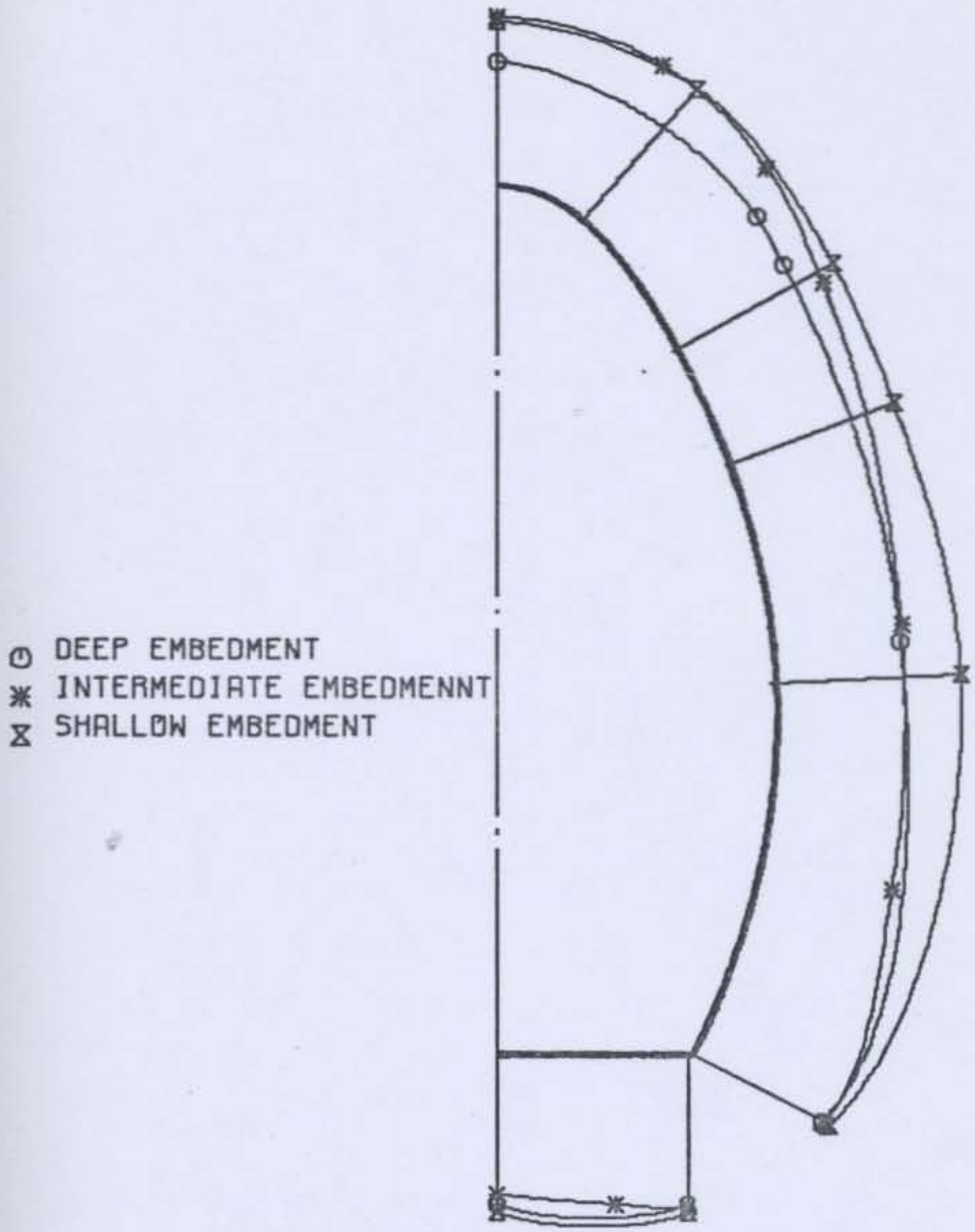

FIG. 4.22A MAXIMUM HORIZONTAL ACCELERATIONS OF CONTAINMENTS FOR THREE EMBEDMENT DEPTHS (SCALE: 1 INCH = 0.2G)

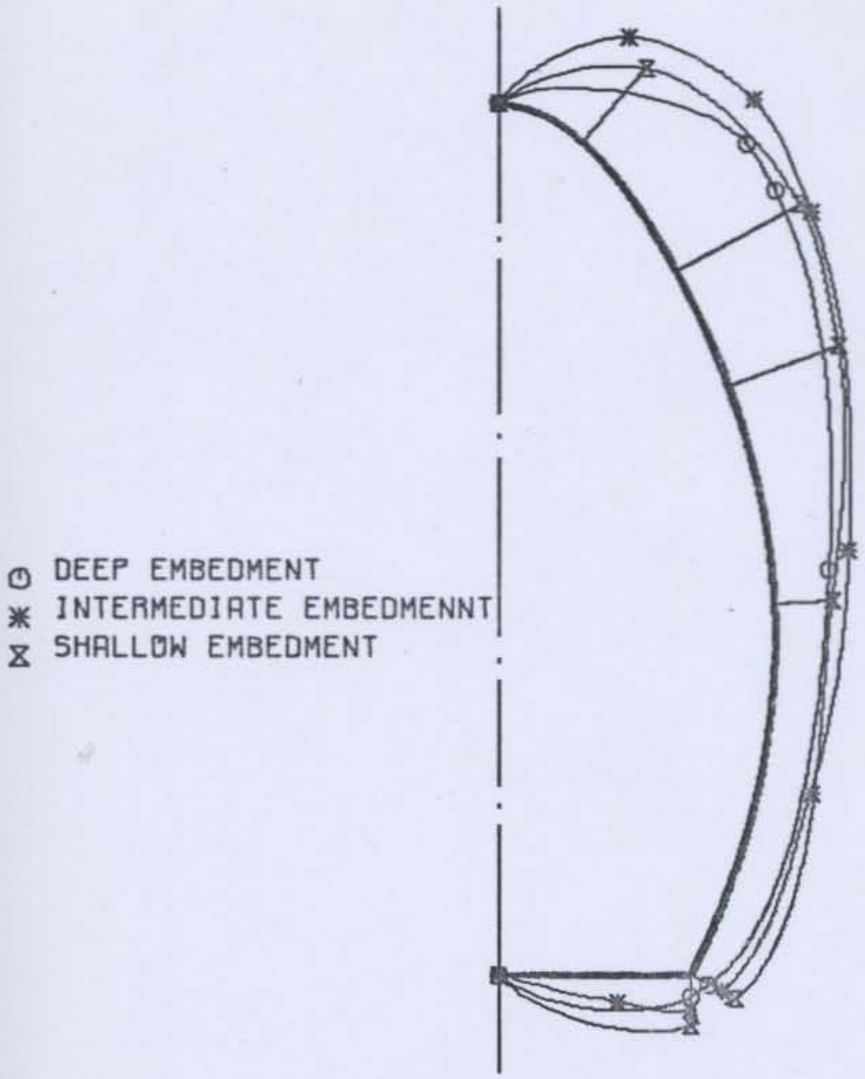

FIG. 4.22B MAXIMUM VERTICAL ACCELERATIONS OF CONTAINMENTS FOR THREE EMBEDMENT DEPTHS (SCALE: 1 INCH = 0.1G)

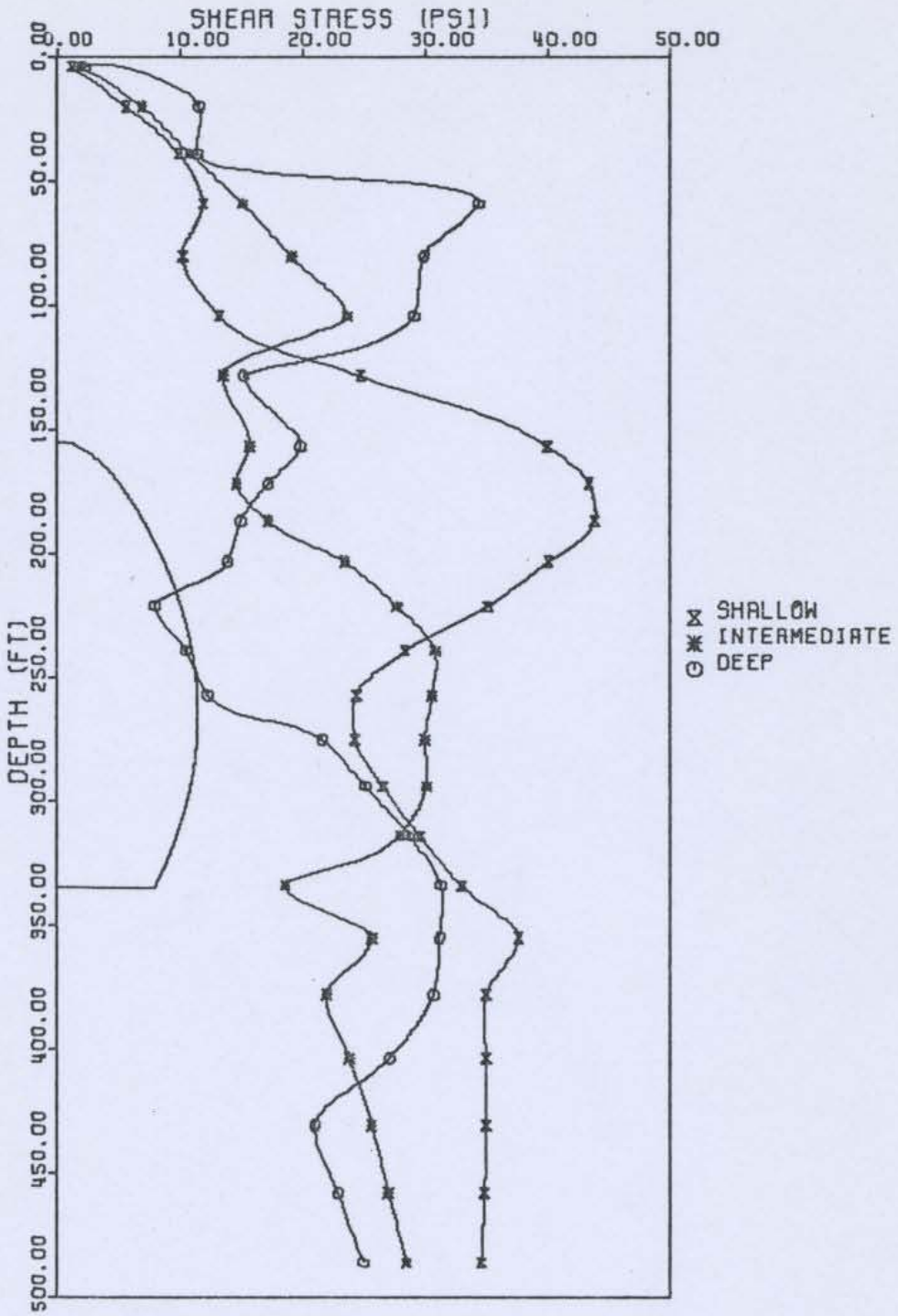

FIG. 4.23 MAXIMUM SHEAR STRESSES IN THE SOIL AT A VERTICAL PLANE 40 FT AWAY FROM THE CONTAINMENT FOR SHALLOW. INTERMEDIATE AND DEEP EMBEDMENTS

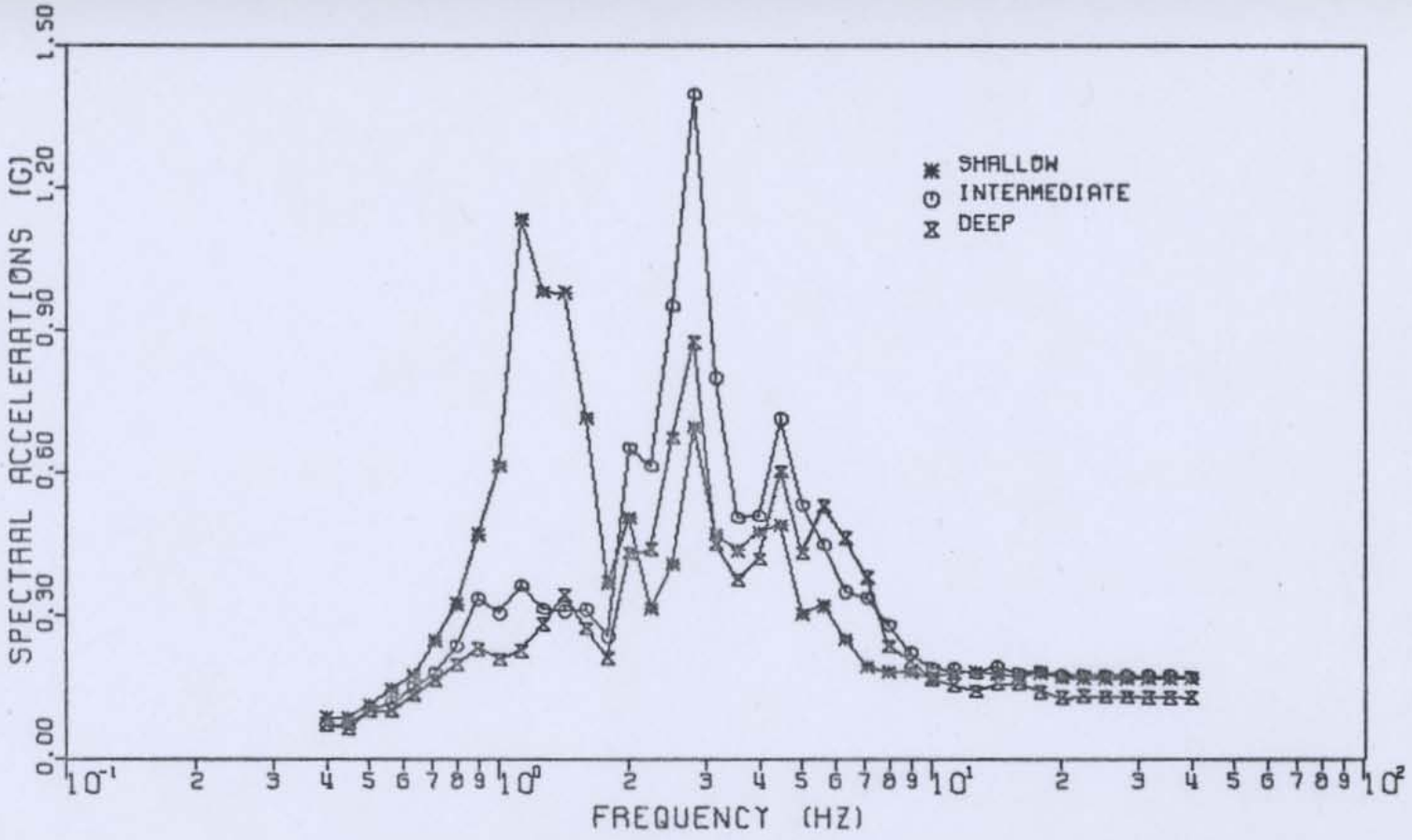

FIG. 4.24 ACCELERATION RESPONSE SPECTRA AT THE CROWN OF THE CONTAINMENT FOR SHALLOW, INTERMEDIATE AND DEEP EMBEDMENTS - LOOSE FILL
(SPECTRAL DAMPING = 2%)

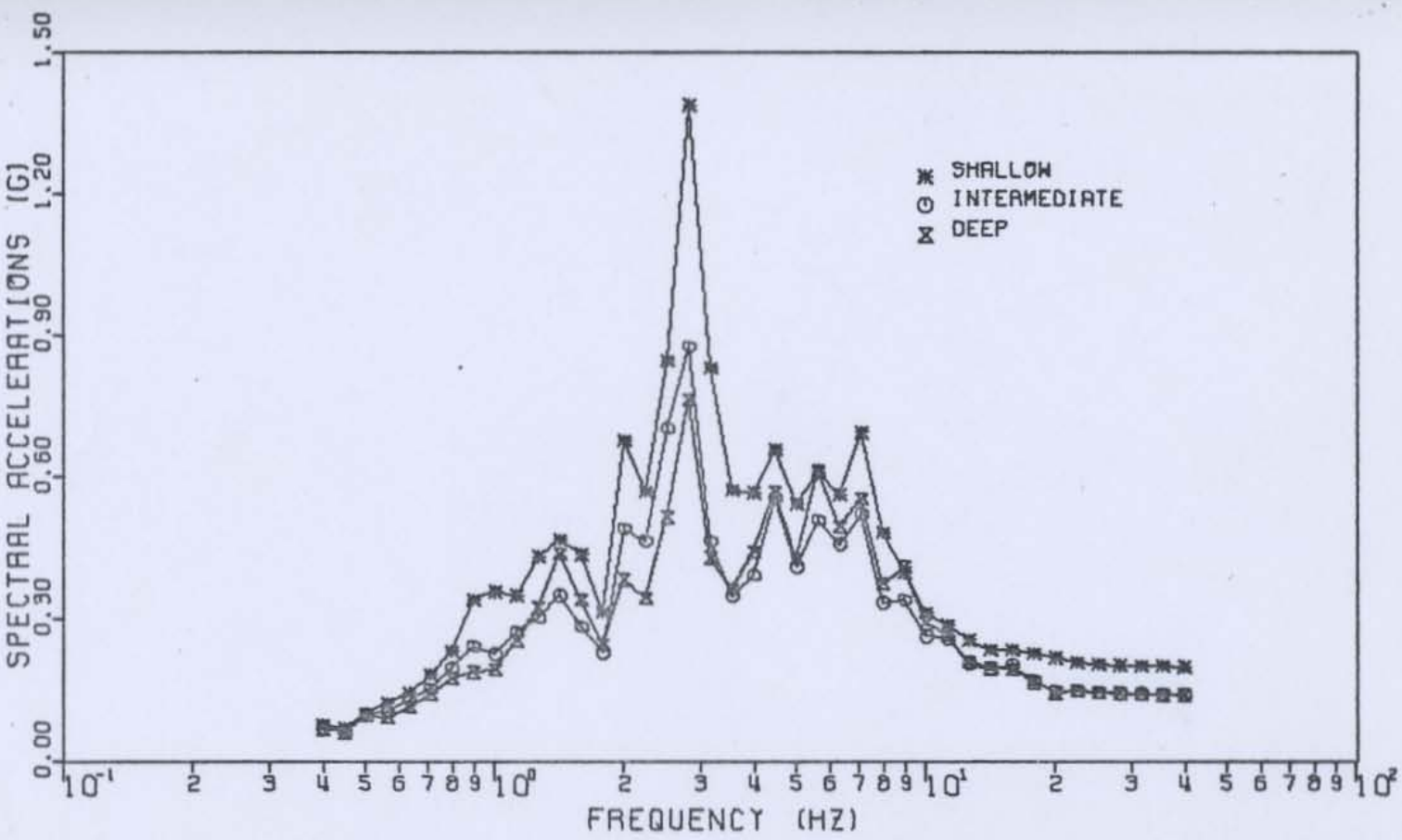

FIG. 4.25 ACCELERATION RESPONSE SPECTRA AT MID-HEIGHT OF THE CONTAINMENT WALL FOR SHALLOW, INTERMEDIATE, AND DEEP EMBEDMENTS - LOOSE FILL
(SPECTRAL DAMPING = 2%)

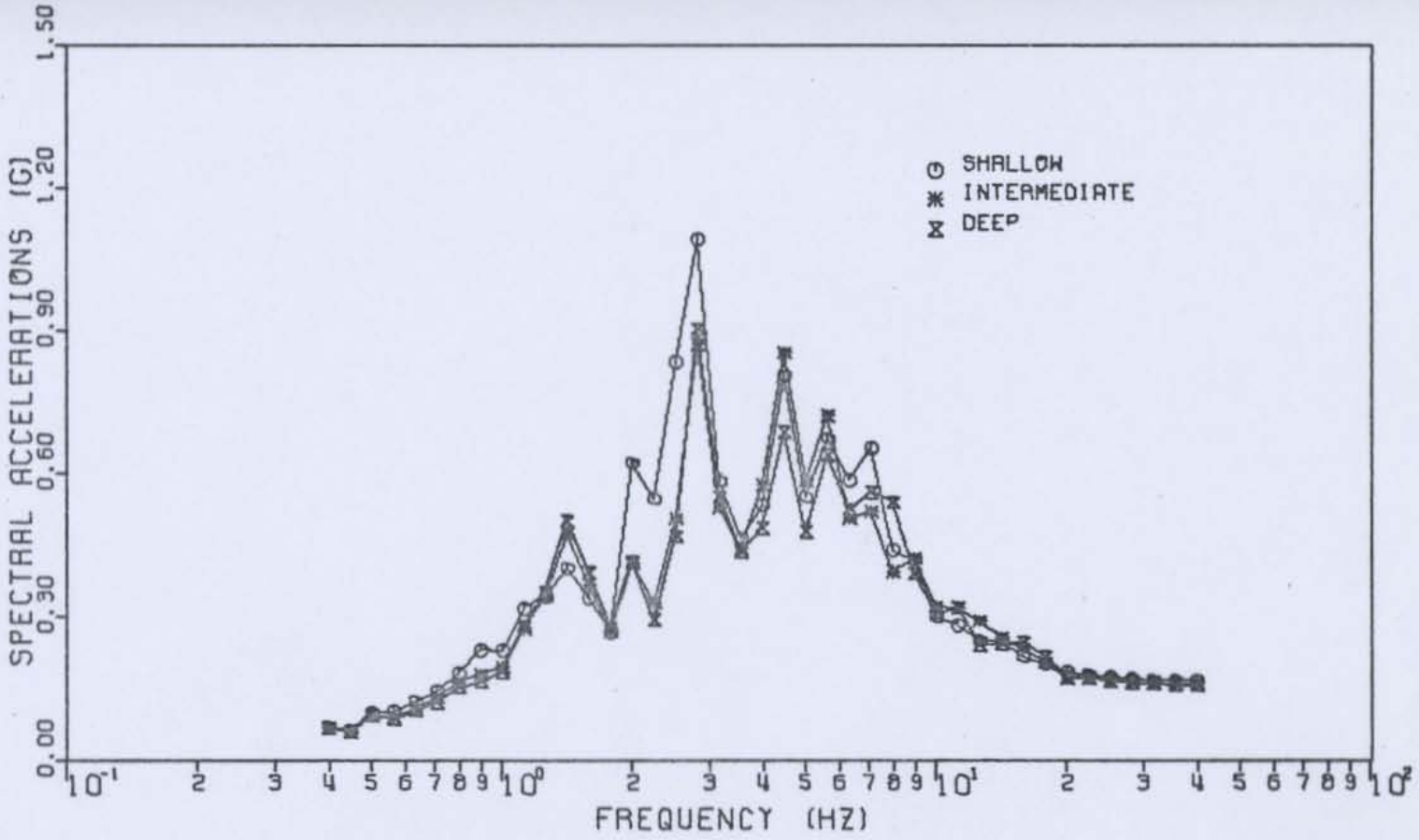

FIG. 4.26 ACCELERATION RESPONSE SPECTRA AT THE CONTAINMENT FOUNDATION MID-POINT FOR SHALLOW, INTERMEDIATE AND DEEP EMBEDMENTS - LOOSE FILL
(SPECTRAL DAMPING = 2%)

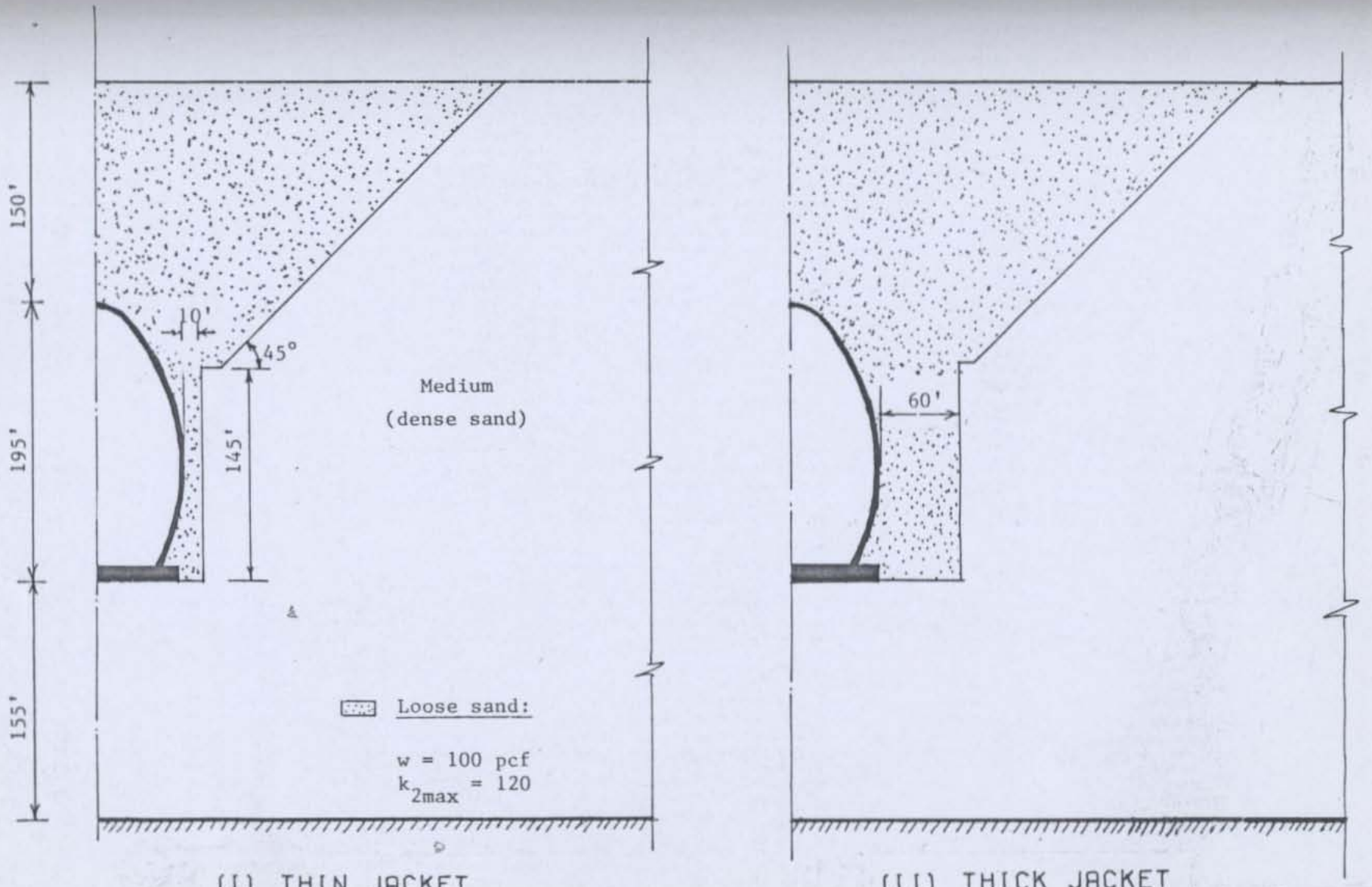

FIG. 4.27 CONFIGURATION AND PROPERTIES OF LOOSE SAND BACKFILL

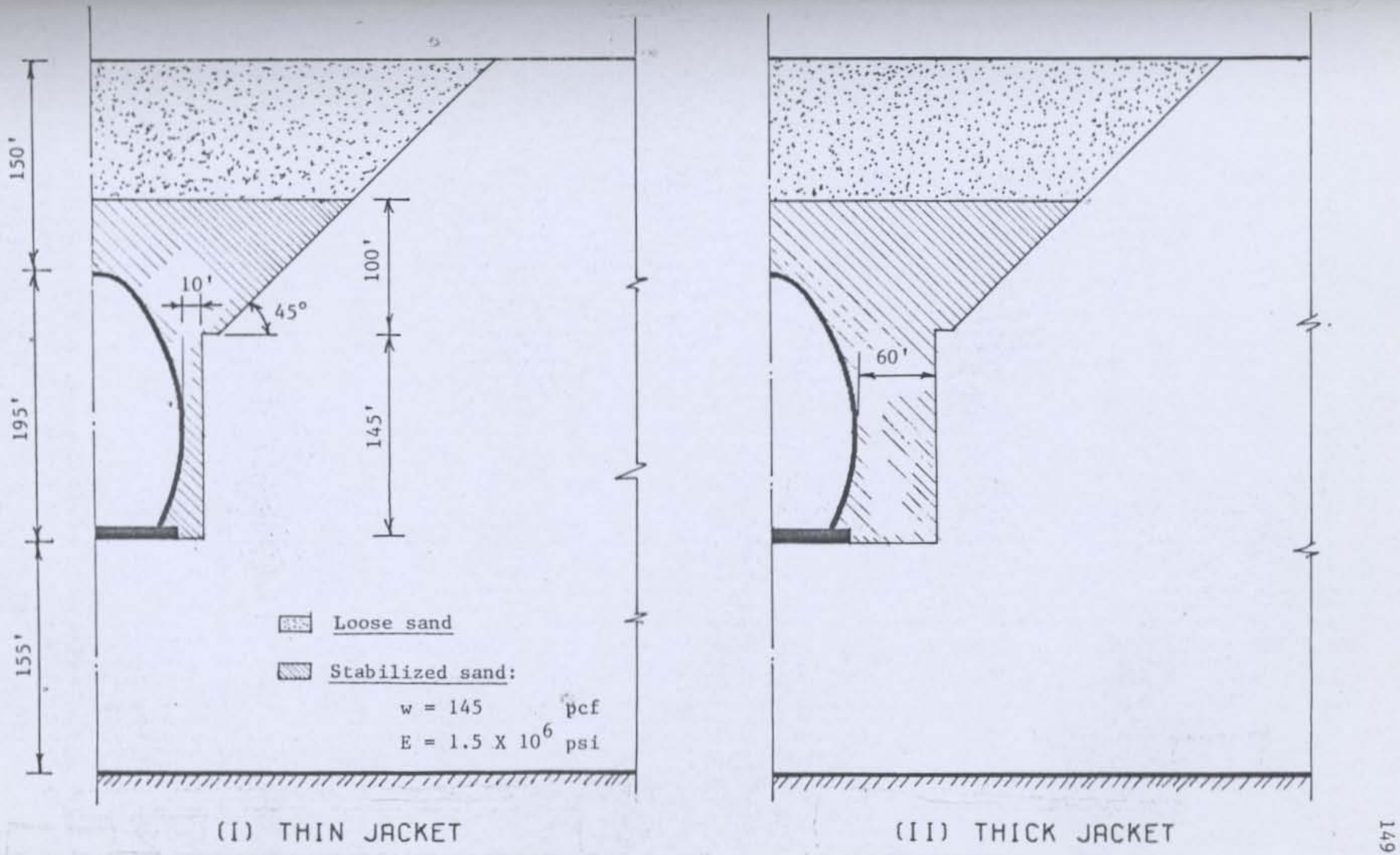

FIG. 4.28 CONFIGURATION AND PROPERTIES OF THE STABILIZED SAND JACKETS

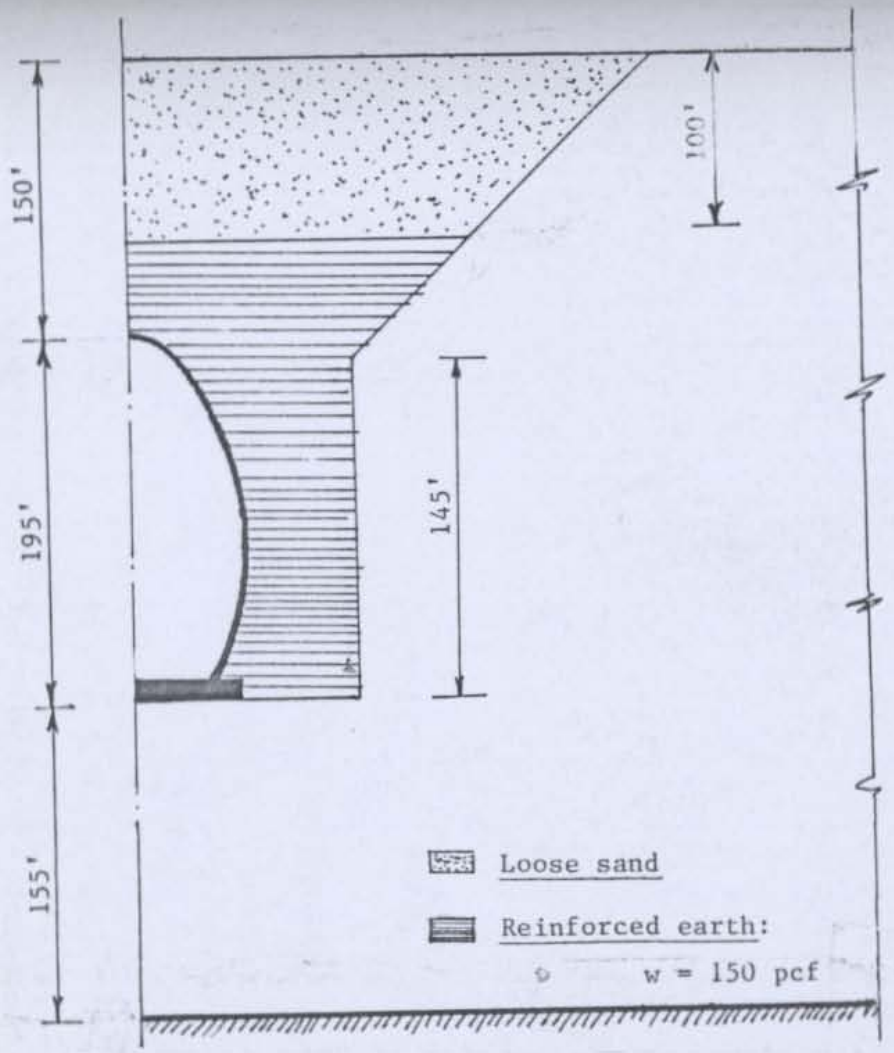

(I) REINFORCED EARTH JACKET

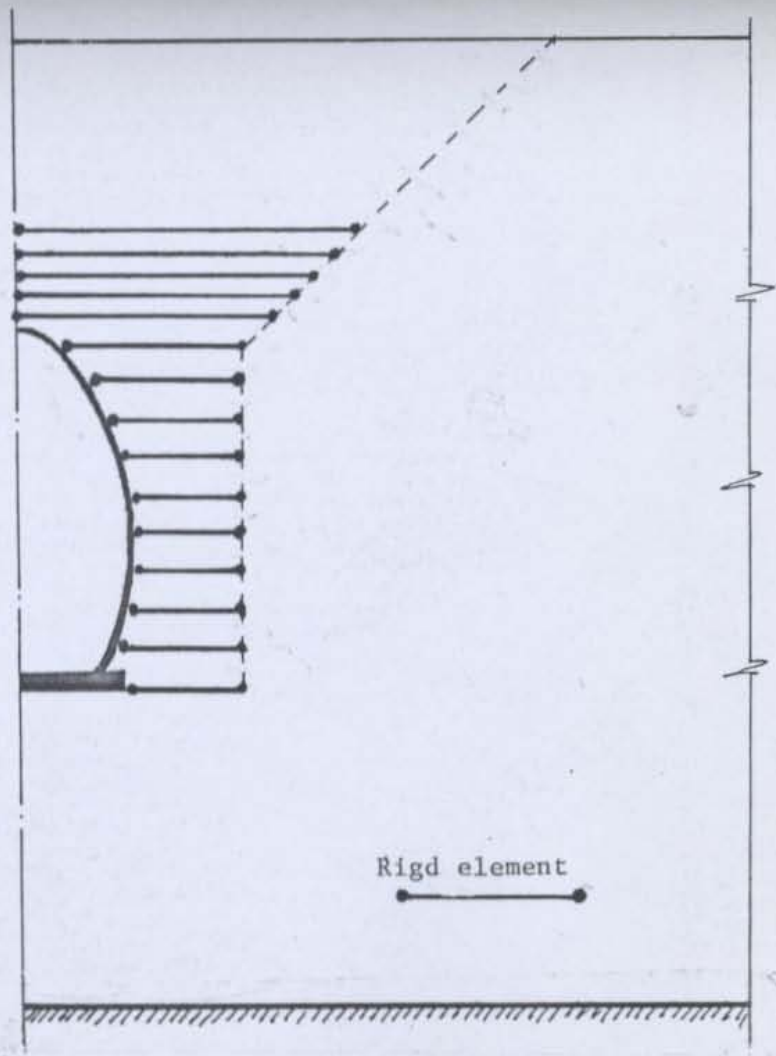

(II) RIGID ELEMENTS TO SIMULATE THE REINFORCING BARS

FIG. 4.29 CONFIGURATION OF THE REINFORCED EARTH JACKET

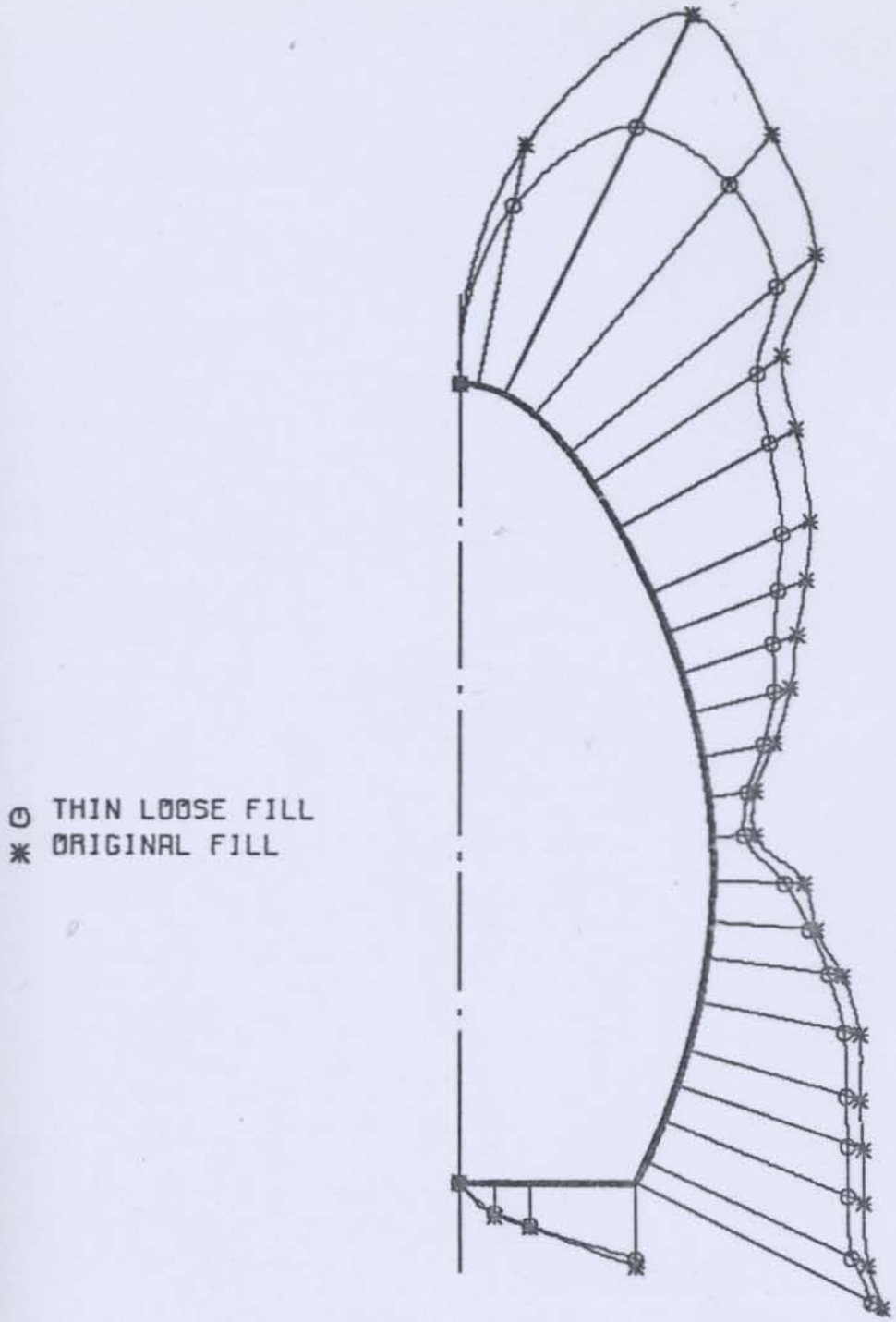

FIG. 4.30 MAXIMUM PRINCIPAL STRESSES IN THE CONTAINMENT FOR ORIGINAL AND THIN LOOSE FILL (SCALE: 1 INCH = 400 P.S.I.)

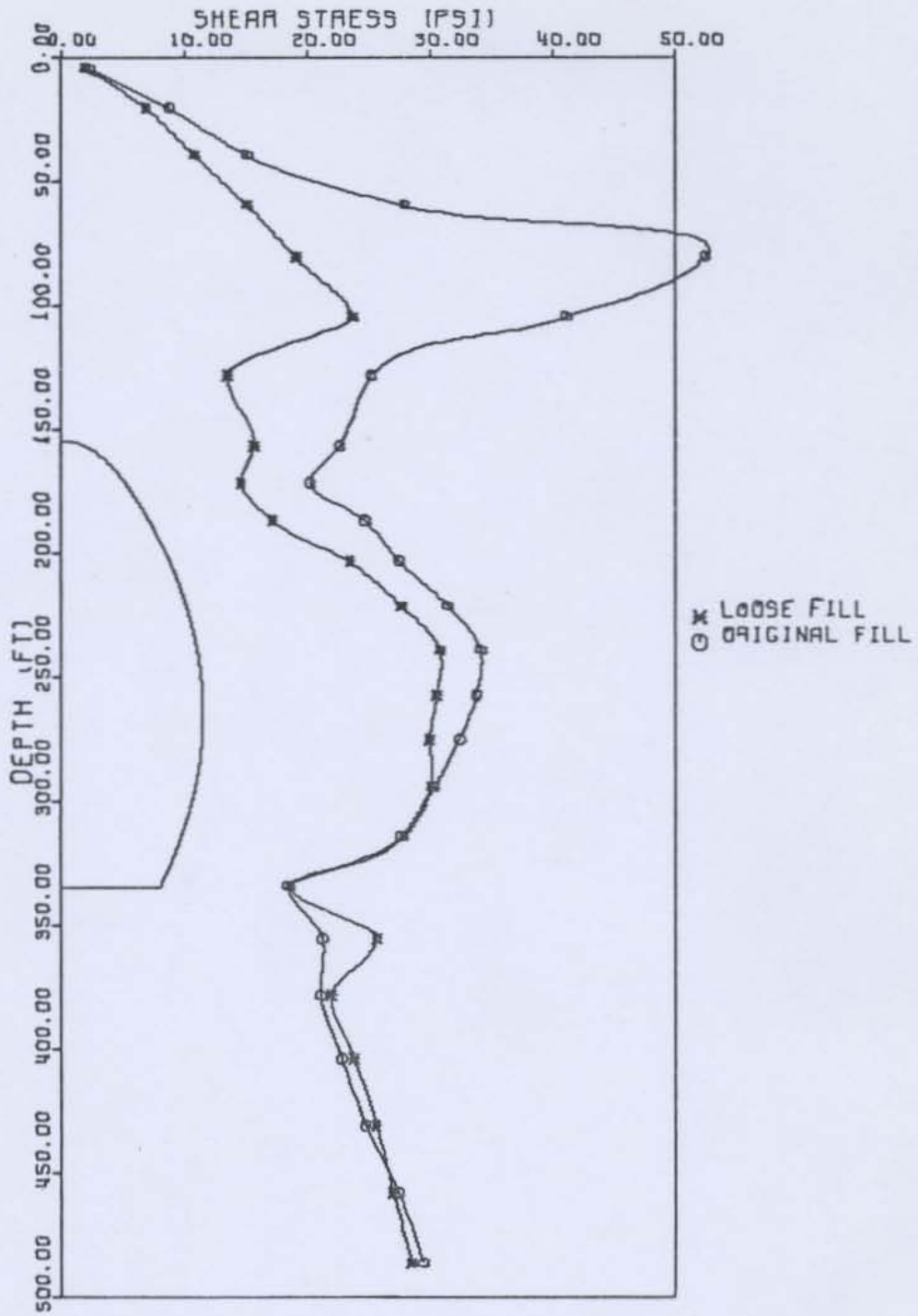

FIG. 4.31 MAXIMUM SHEAR STRESSES IN THE SOIL AT A VERTICAL PLANE 40 FT AWAY FROM THE CONTAINMENT - ORIGINAL AND THIN LOOSE FILL

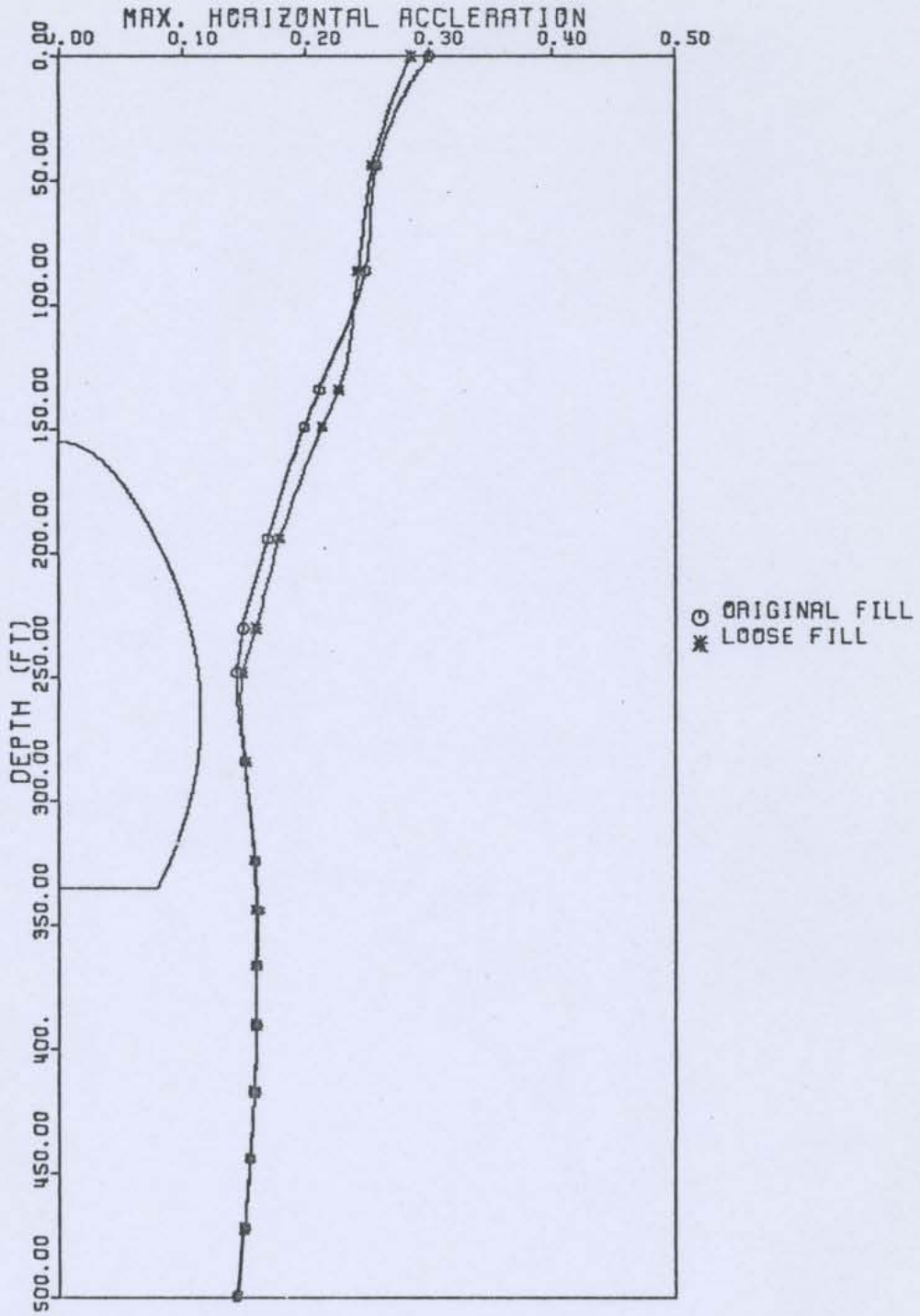

FIG. 4.32 MAXIMUM HORIZONTAL ACCELERATIONS IN THE SOIL AT A VERTICAL PLANE 70 FT AWAY FROM THE CONTAINMENT - LOOSE AND ORIGINAL FILL

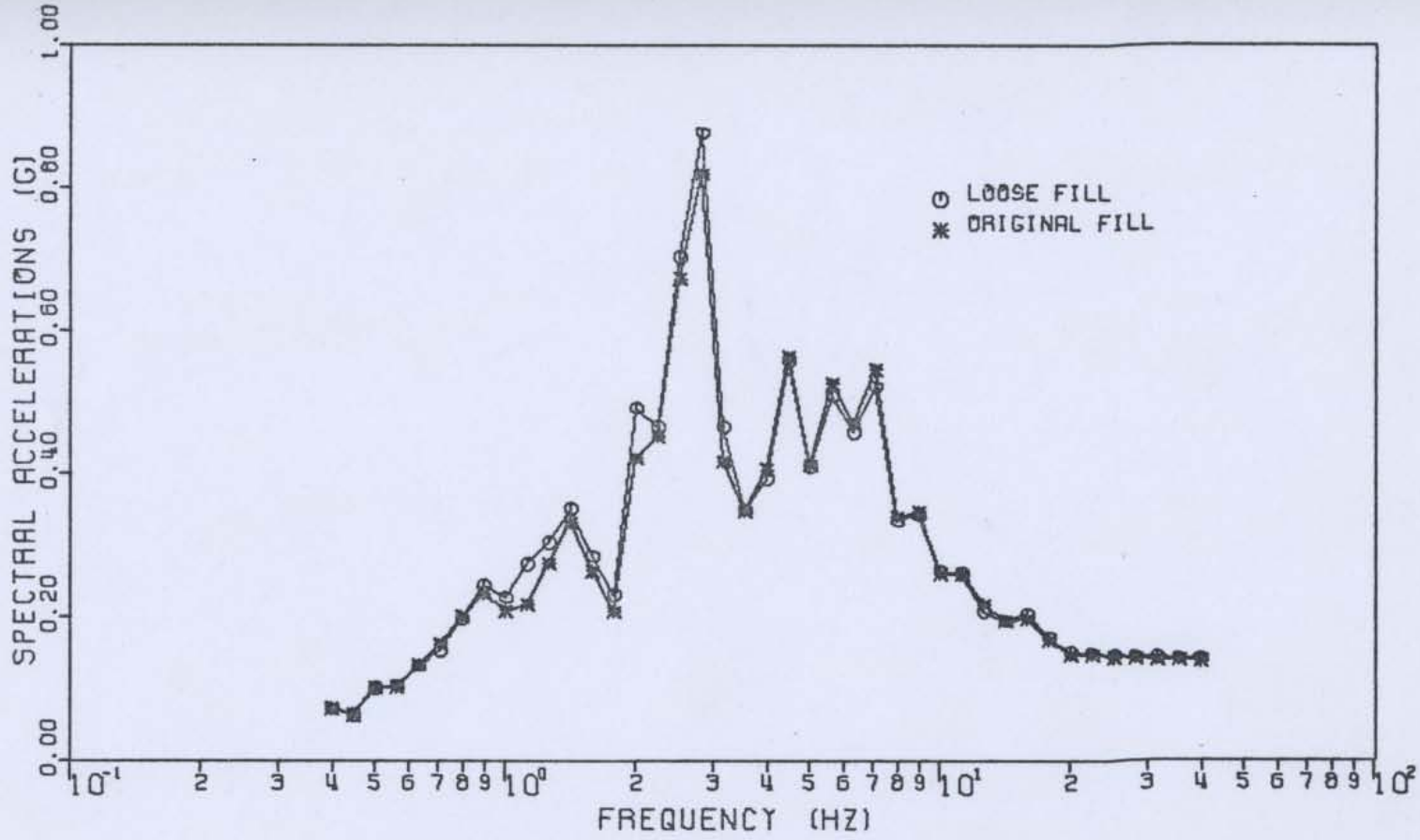

FIG. 4.33 ACCELERATION RESPONSE SPECTRA AT MID-HEIGHT OF THE CONTAINMENT WALL - ORIGINAL AND LOOSE FILL (SPECTRAL DAMPING = 2%)

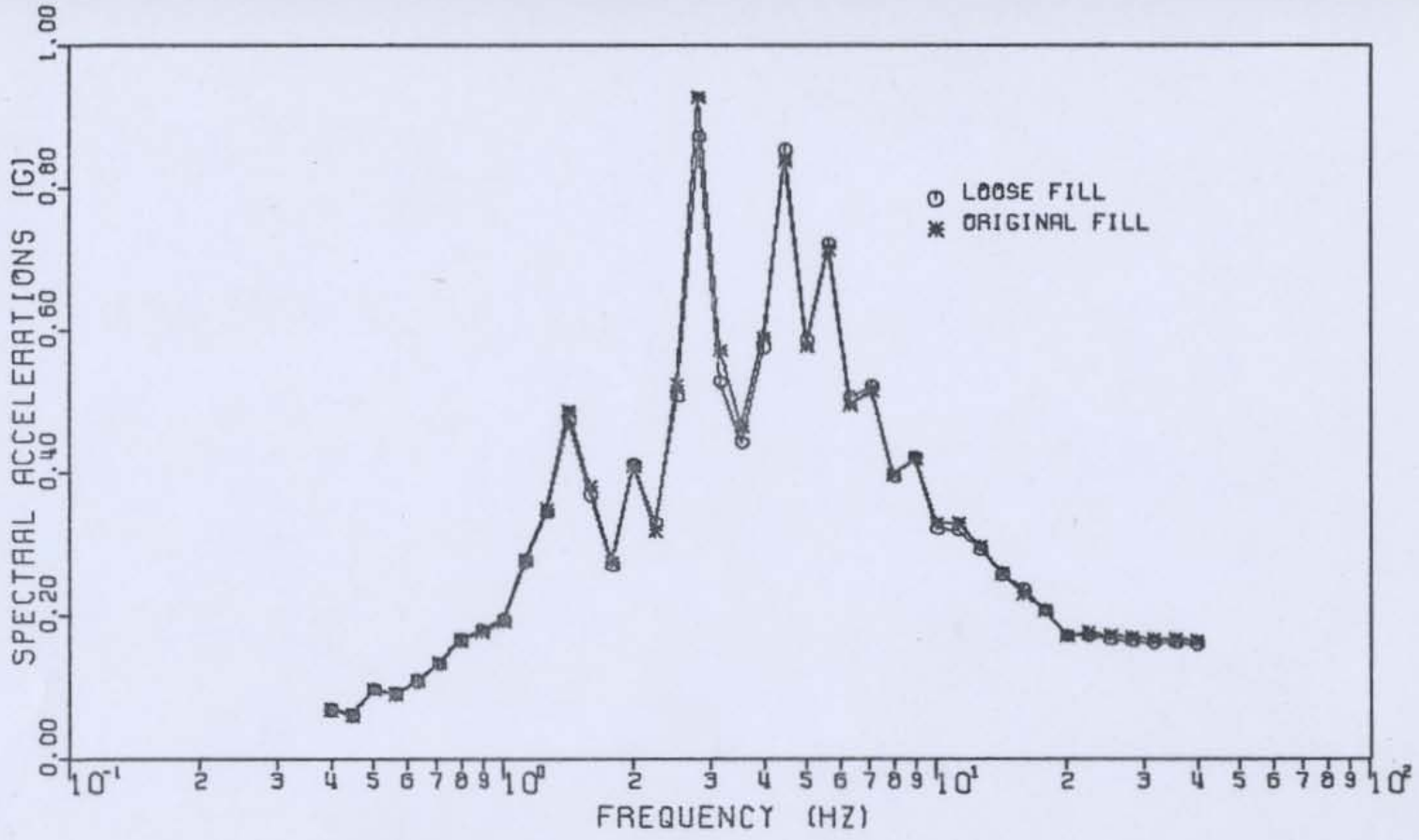

FIG. 4.34 ACCELERATION RESPONSE SPECTRA AT THE CONTAINMENT FOUNDATION MID-POINT - ORIGINAL AND LOOSE FILL (SPECTRAL DAMPING = 2%)

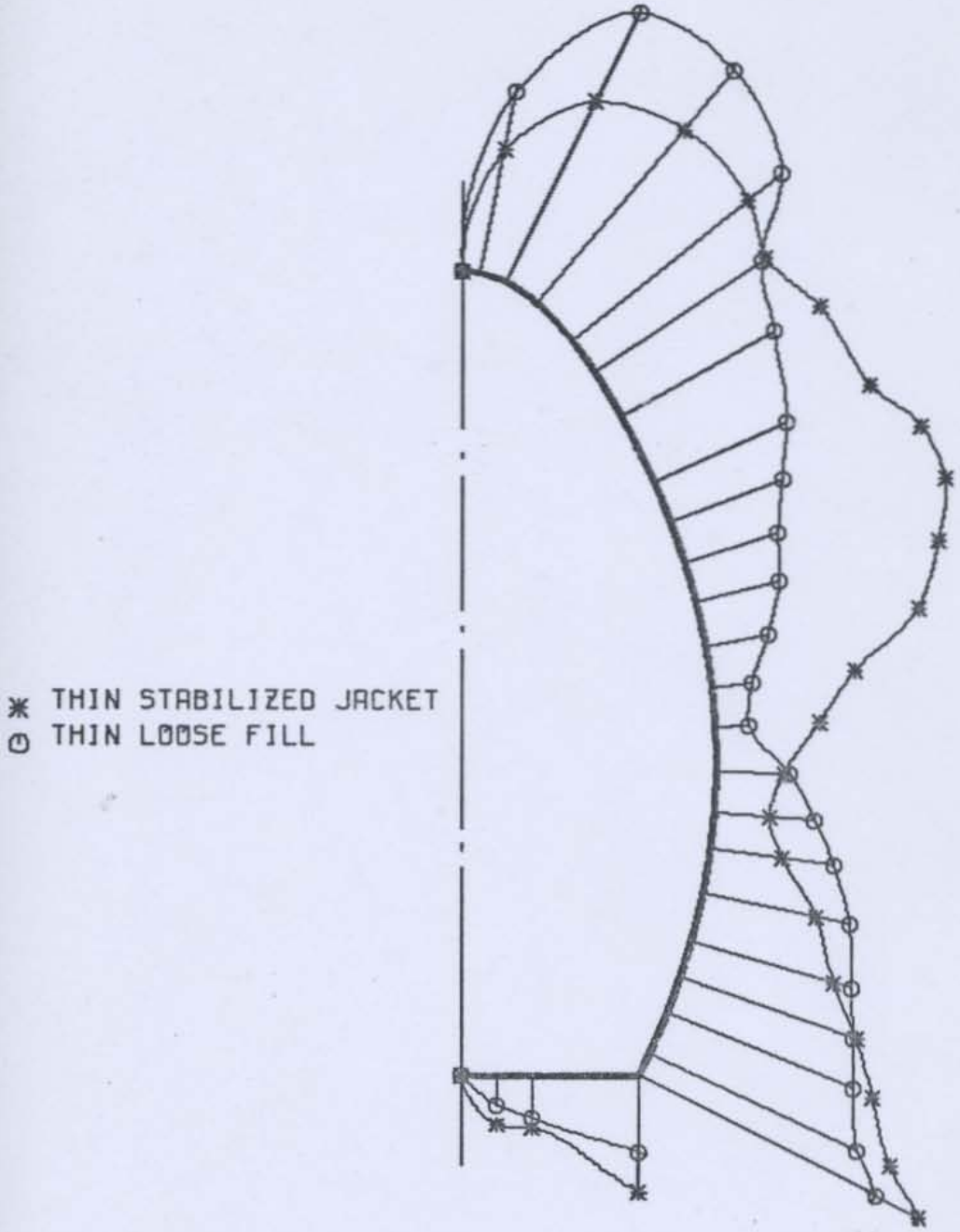

FIG. 4.35 MAXIMUM PRINCIPAL STRESSES IN THE CONTAINMENT FOR THIN STABILIZED JACKET AND THIN LOOSE FILL
(SCALE: 1 INCH = 400 P.S.I.)

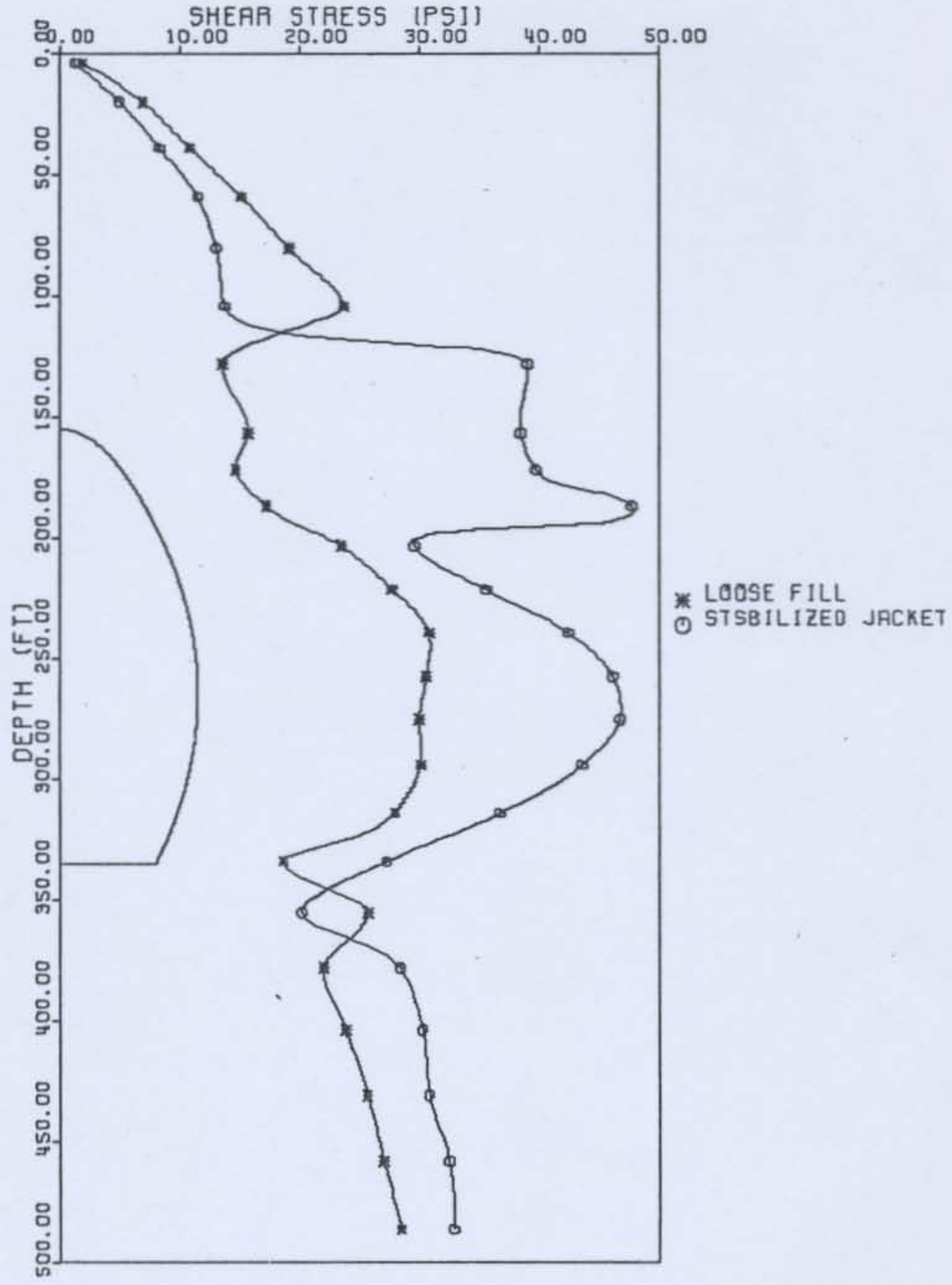

FIG. 4.36 MAXIMUM SHEAR STRESSES IN THE SOIL AT A VERTICAL PLANE 40 FT AWAY FROM THE CONTAINMENT - THIN STABILIZED JACKET AND THIN LOOSE FILL

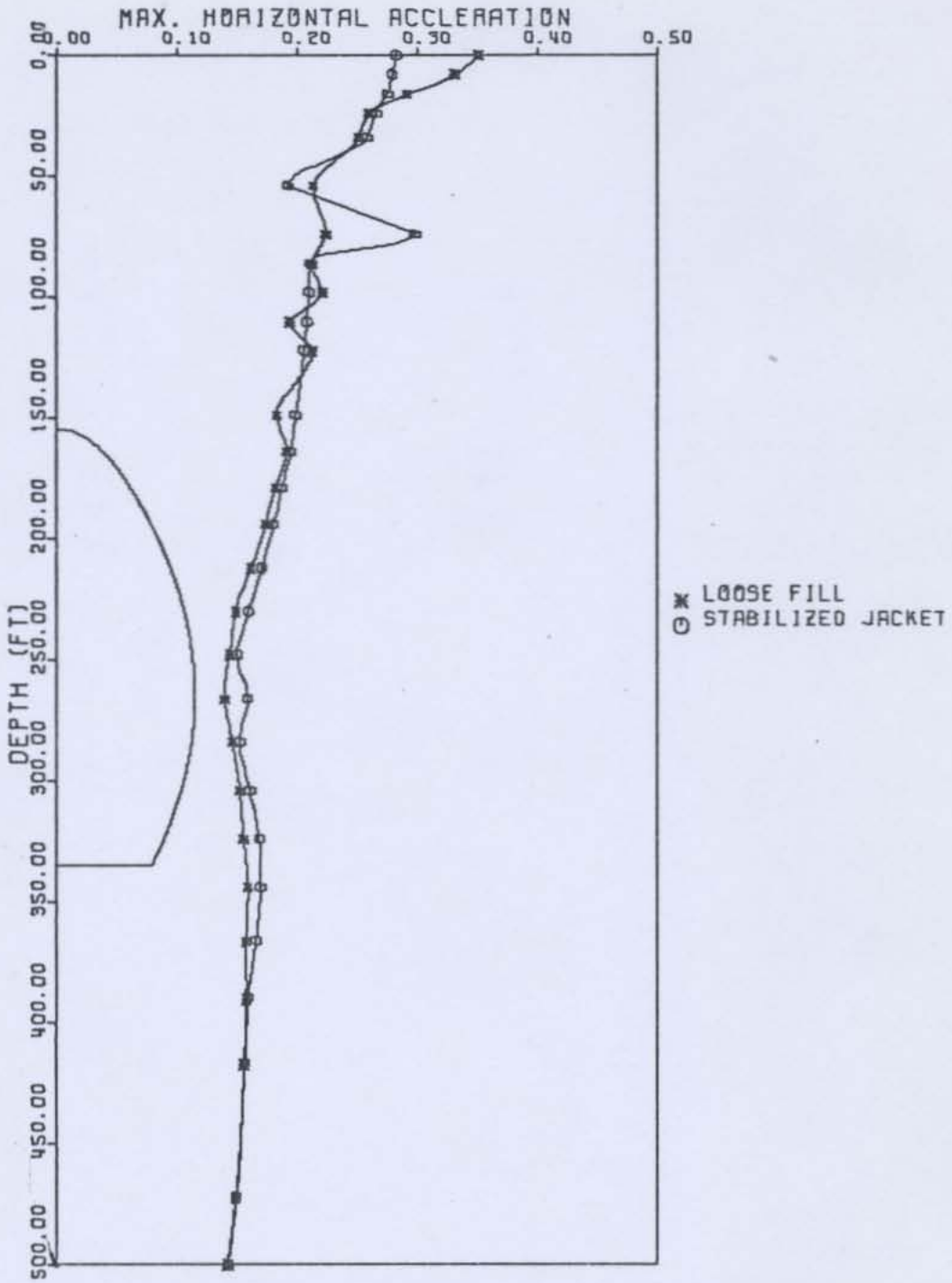

FIG. 4.37 MAXIMUM HORIZONTAL ACCELERATIONS IN THE SOIL AT A VERTICAL PLANE 10 FEET AWAY FROM THE CONTAINMENT - THIN LOOSE FILL AND THIN STABILIZED JACKET

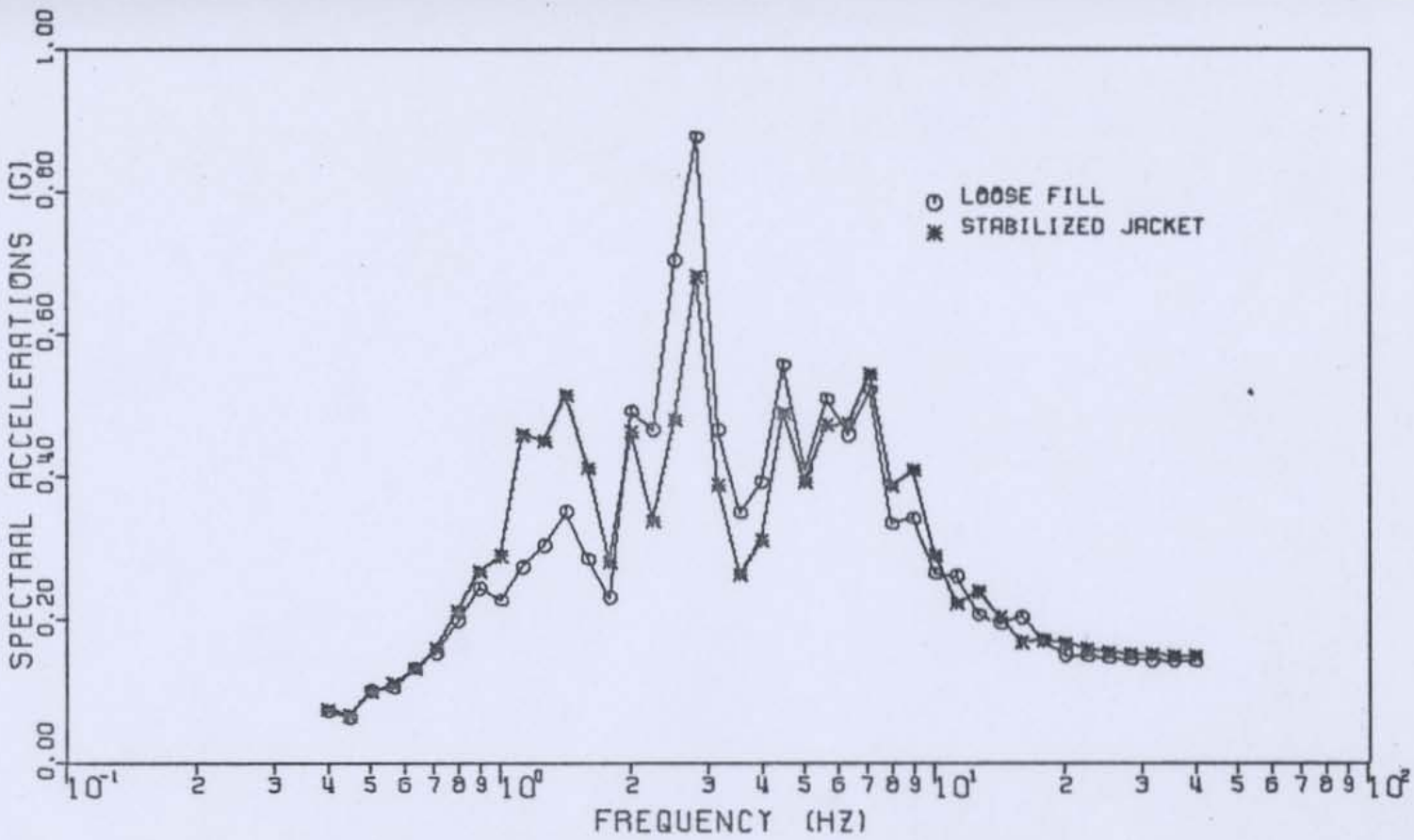

FIG. 4.38 ACCELERATION RESPONSE SPECTRA AT MID-HEIGHT OF THE CONTAINMENT WALL - THIN LOOSE FILL AND THIN STABILIZED SAND JACKET
(SPECTRAL DAMPING = 2%)

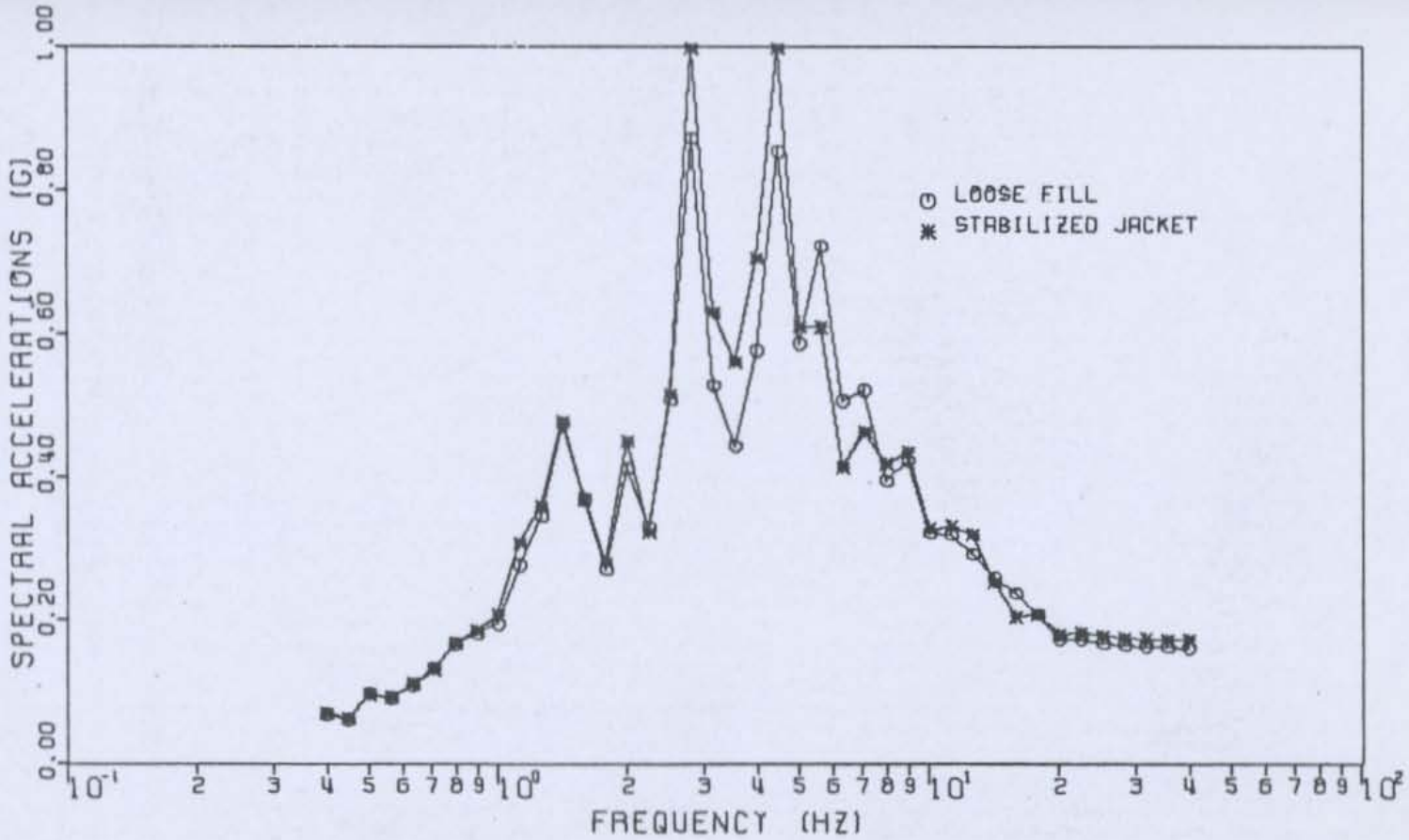

FIG. 4.39 ACCELERATION RESPONSE SPECTRA AT THE CONTAINMENT FOUNDATION MID-POINT - THIN LOOSE FILL AND THIN STABILIZED SAND JACKET
(SPECTRAL DAMPING = 2%)

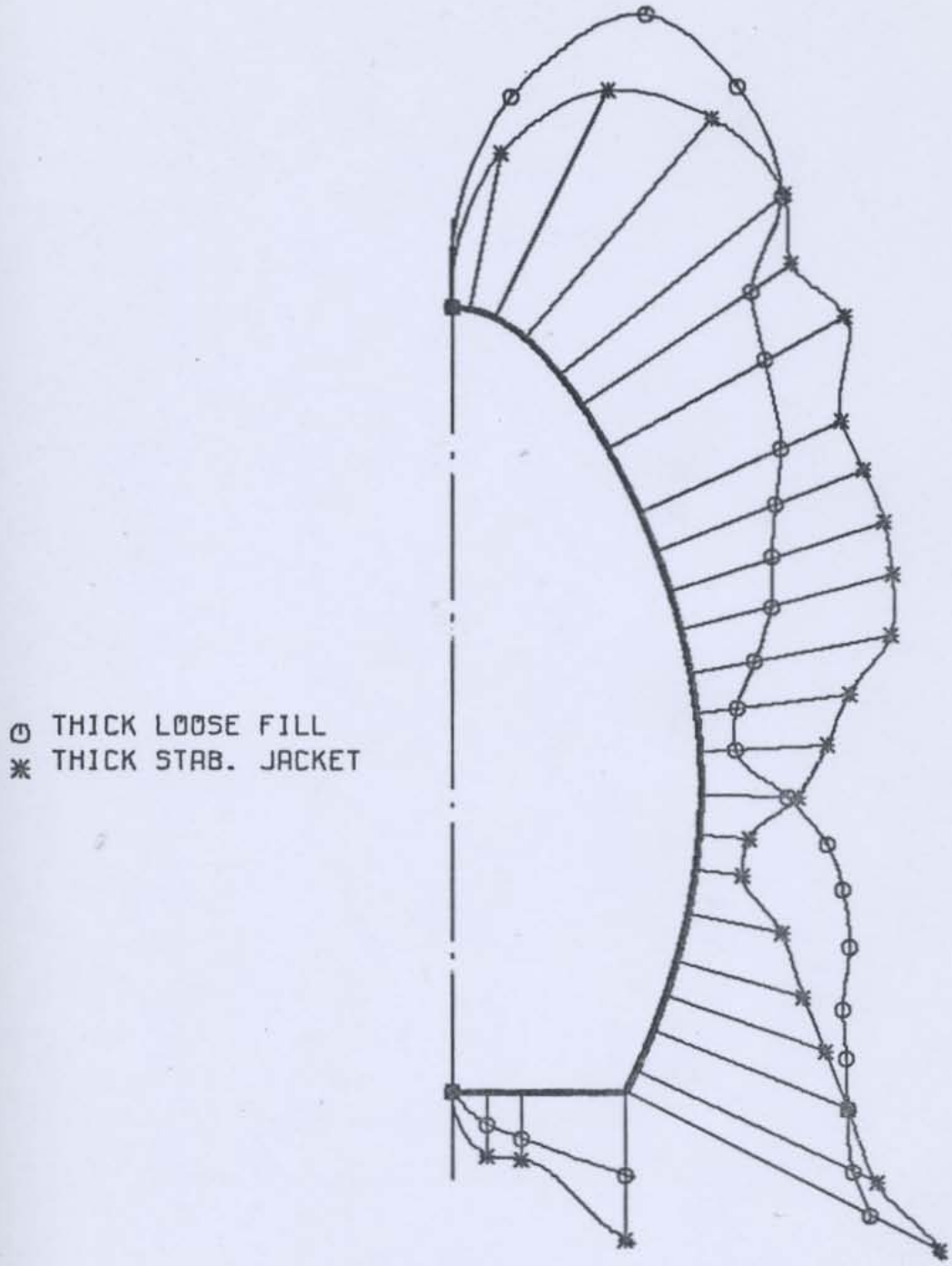

FIG. 4.40 MAXIMUM PRINCIPAL STRESSES IN THE CONTAINMENT FOR THICK STABILIZED SAND JACKET AND THICK LOOSE FILL
(SCALE: 1 INCH = 400 P.S.I.)

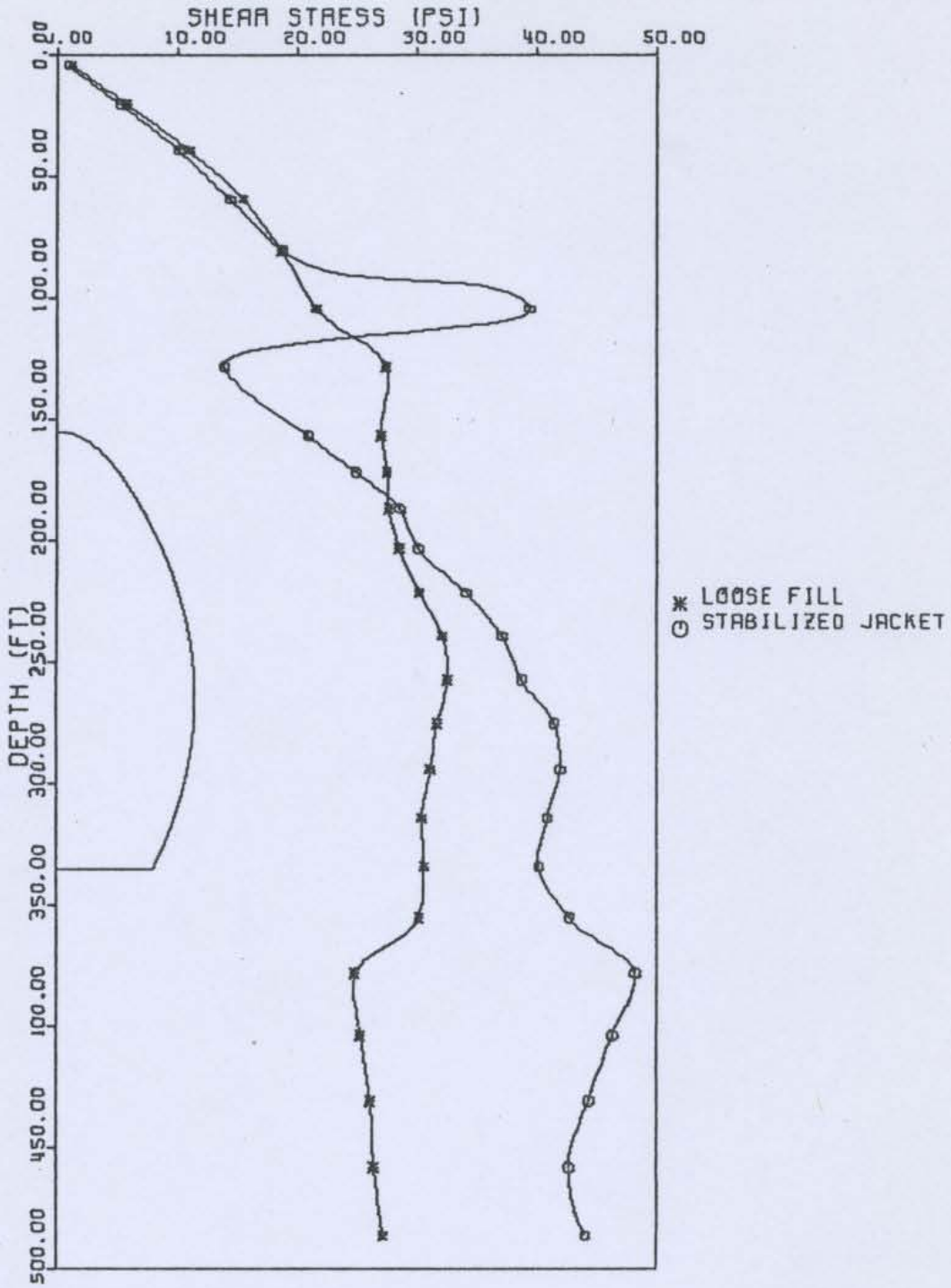

FIG. 4.41 MAXIMUM SHEAR STRESSES IN THE SOIL AT A VERTICAL PLANE 100 FT AWAY FROM THE CONTAINMENT - THICK LOOSE FILL AND THICK STABILIZED JACKET

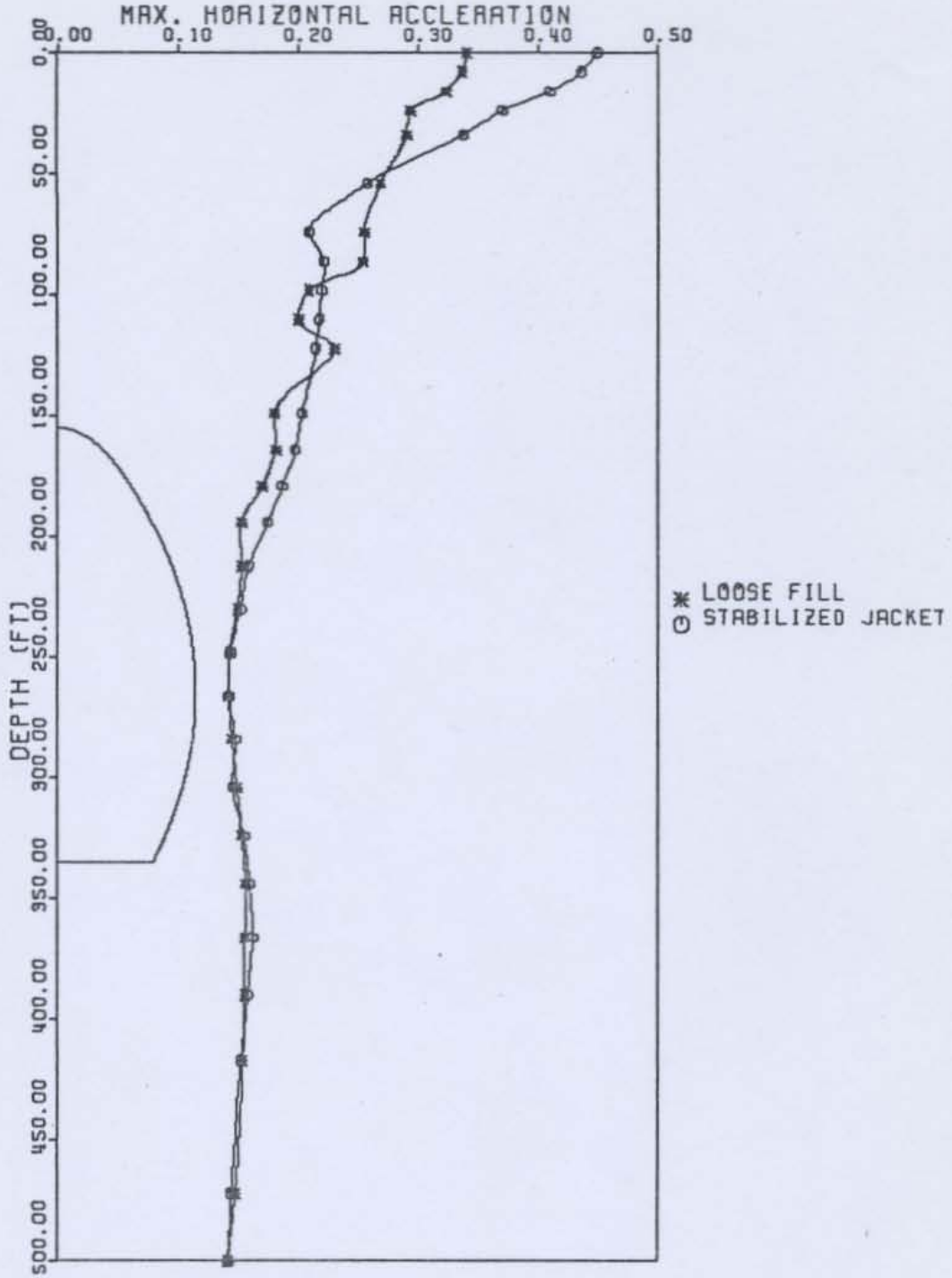

FIG. 4.42 MAXIMUM HORIZONTAL ACCELERATIONS IN THE SOIL AT A VERTICAL PLANE 10 FEET AWAY FROM THE CONTAINMENT - THICK LOOSE FILL AND THICK STABILIZED JACKET

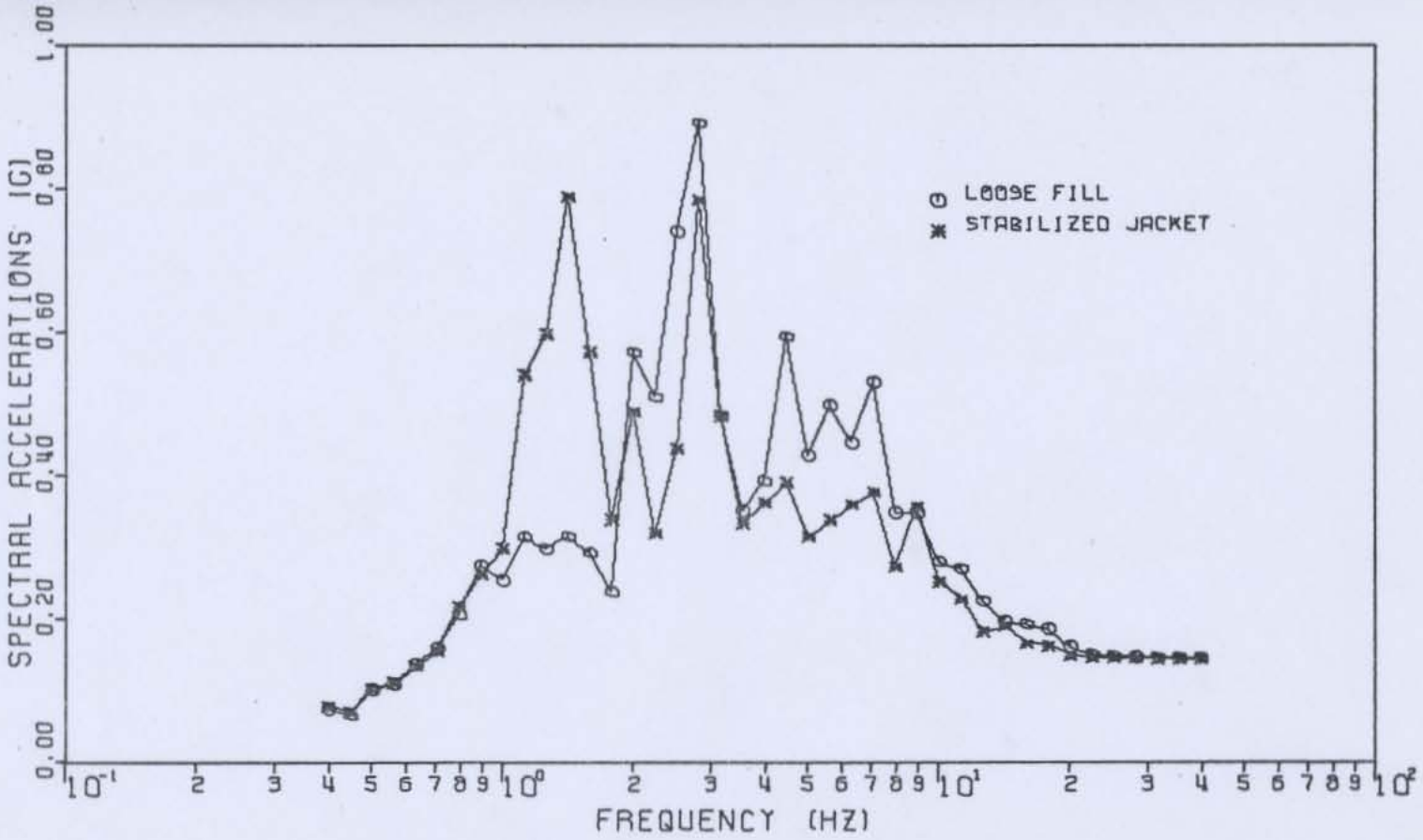

FIG. 4.43 ACCELERATION RESPONSE SPECTRA AT MID-HEIGHT OF THE CONTAINMENT WALL - THICK LOOSE FILL AND THICK STABILIZED SAND JACKET
(SPECTRAL DAMPING = 2%)

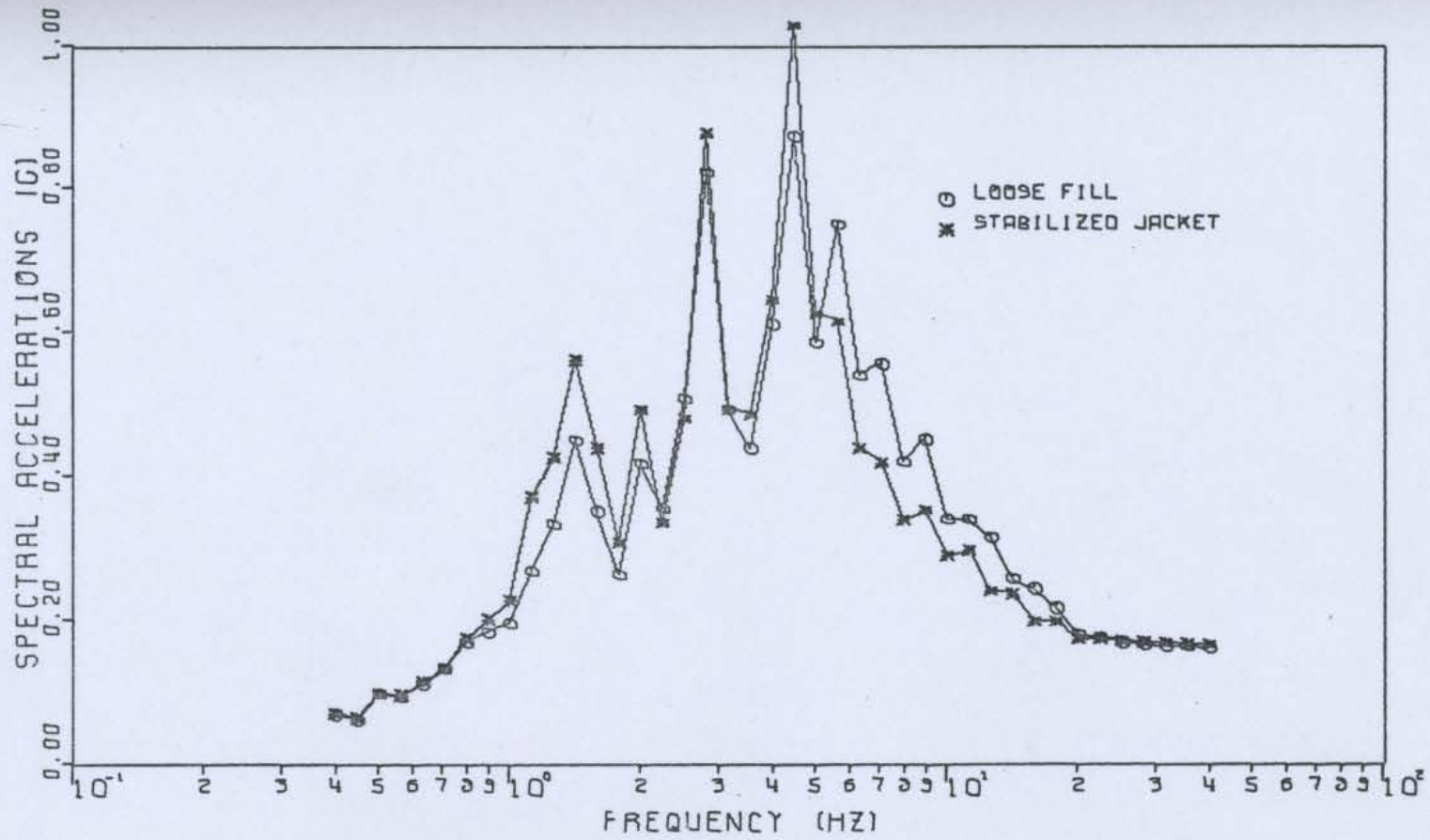

FIG. 4.44 ACCELERATION RESPONSE SPECTRA AT THE CONTAINMENT FOUNDATION MID-POINT - THICK LOOSE FILL AND THICK STABILIZED SAND JACKET
(SPECTRAL DAMPING = 2%)

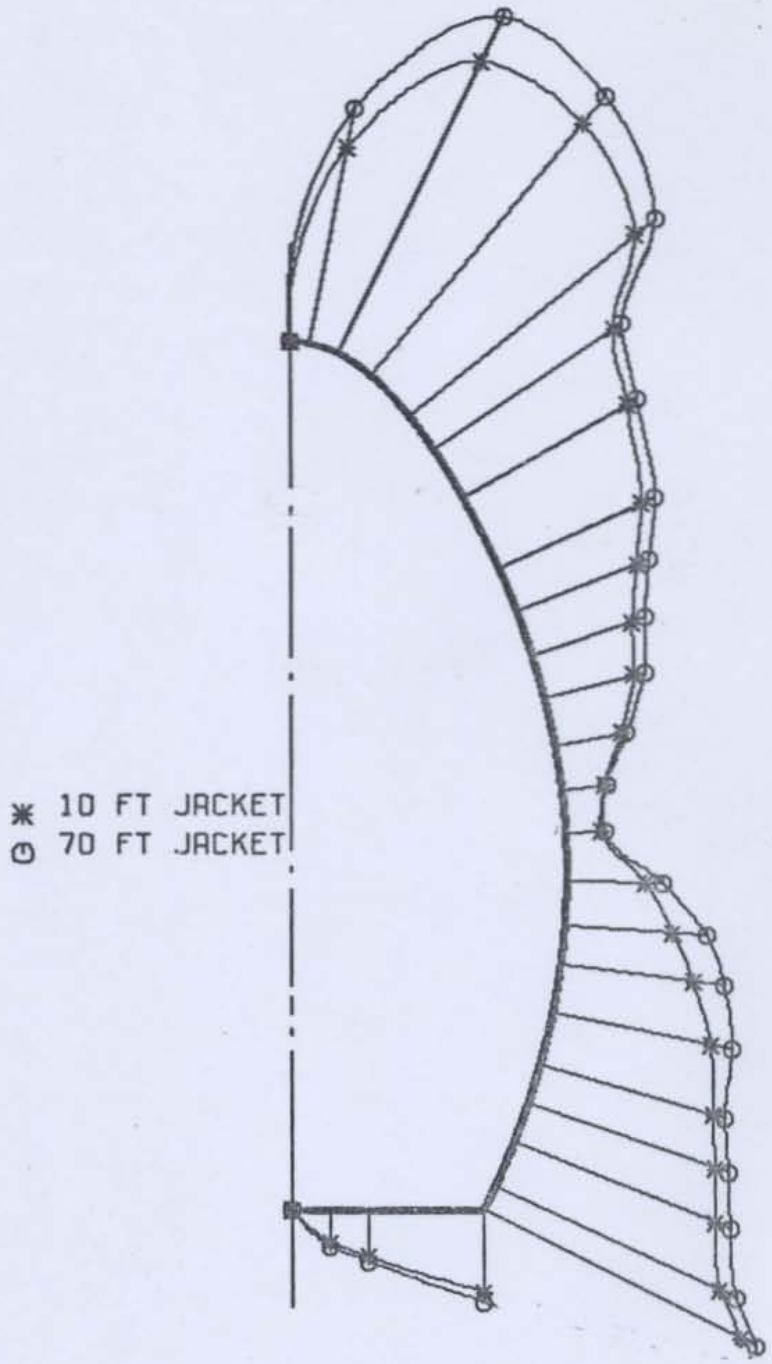

FIG. 4.45 EFFECT OF THE THICKNESS OF THE LOOSE FILL JACKET ON THE MAXIMUM PRINCIPAL STRESSES IN THE CONTAINMENT (SCALE: 1 INCH = 400 P.S.I.)

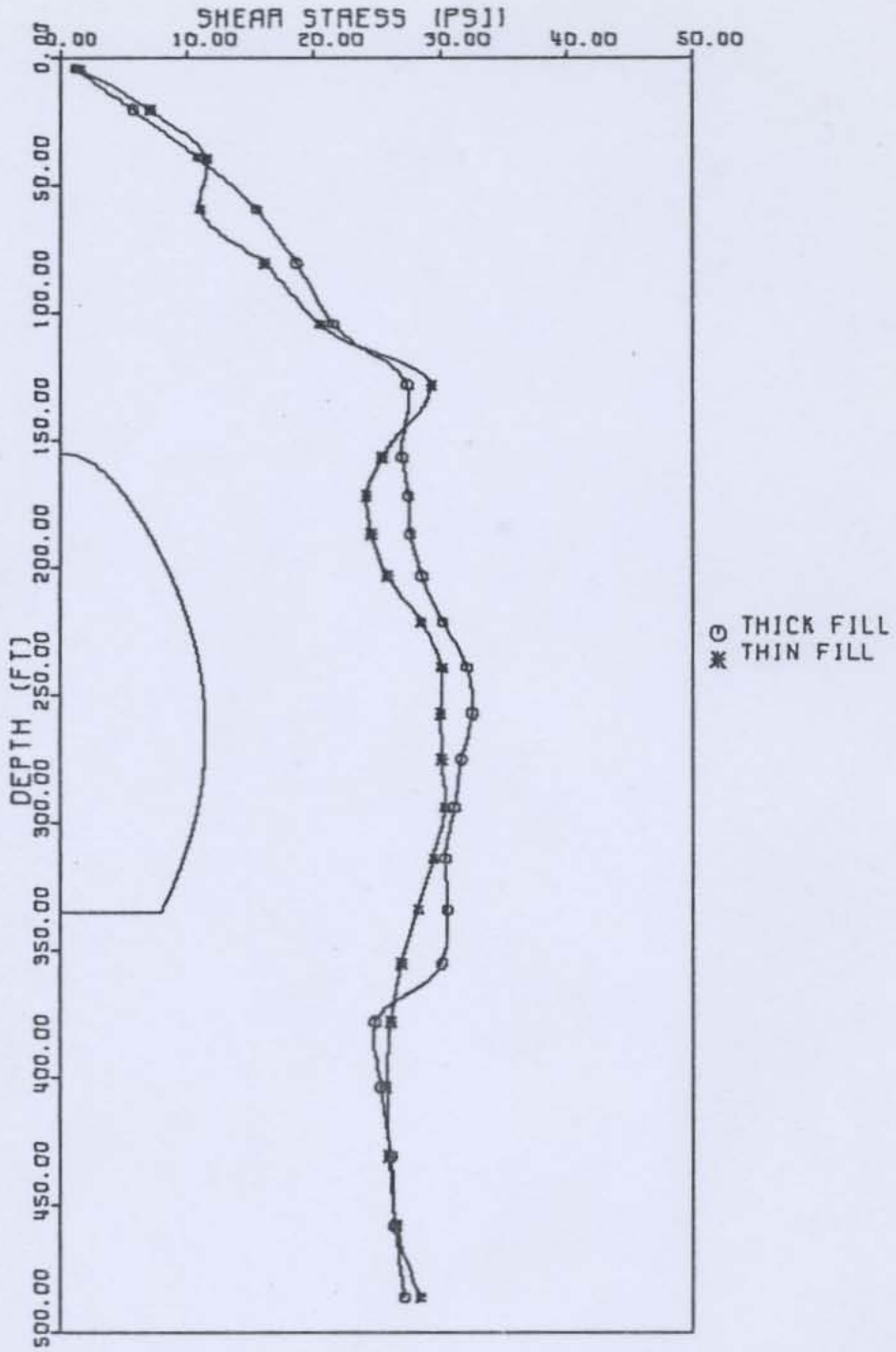

FIG. 4.46 MAXIMUM SHEAR STRESSES IN THE SOIL AT A VERTICAL PLANE 100 FT AWAY FROM THE CONTAINMENT - THICK AND THIN LOOSE FILL

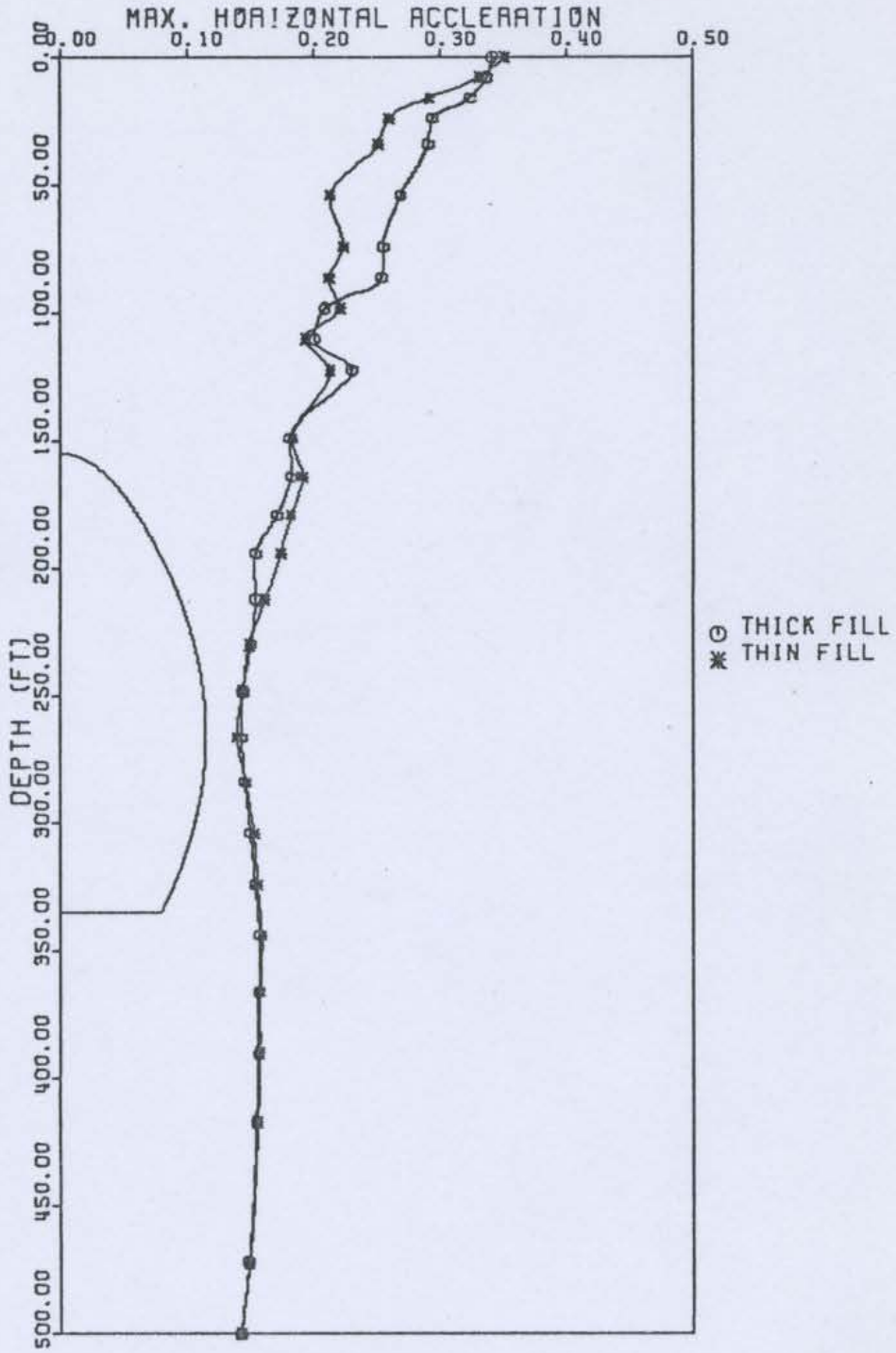

FIG. 4.47 MAXIMUM HORIZONTAL ACCELERATIONS IN THE SOIL AT A VERTICAL PLANE 10 FEET AWAY FROM THE CONTAINMENT - THIN AND THICK LOOSE FILL

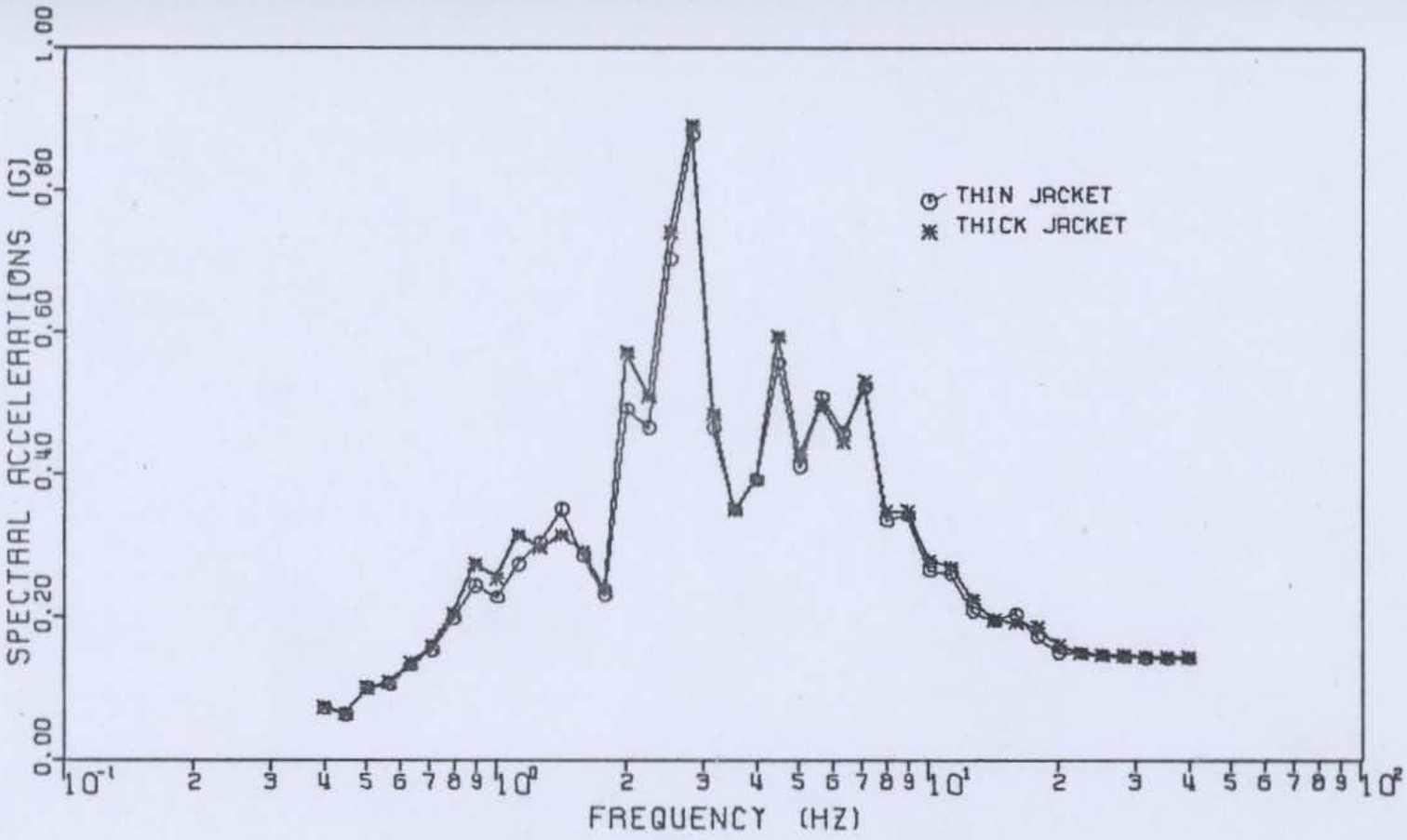

FIG. 4.48 ACCELERATION RESPONSE SPECTRA AT MID-HEIGHT OF THE CONTAINMENT WALL- THIN AND THICK LOOSE FILL (SPECTRAL DAMPING = 2%)

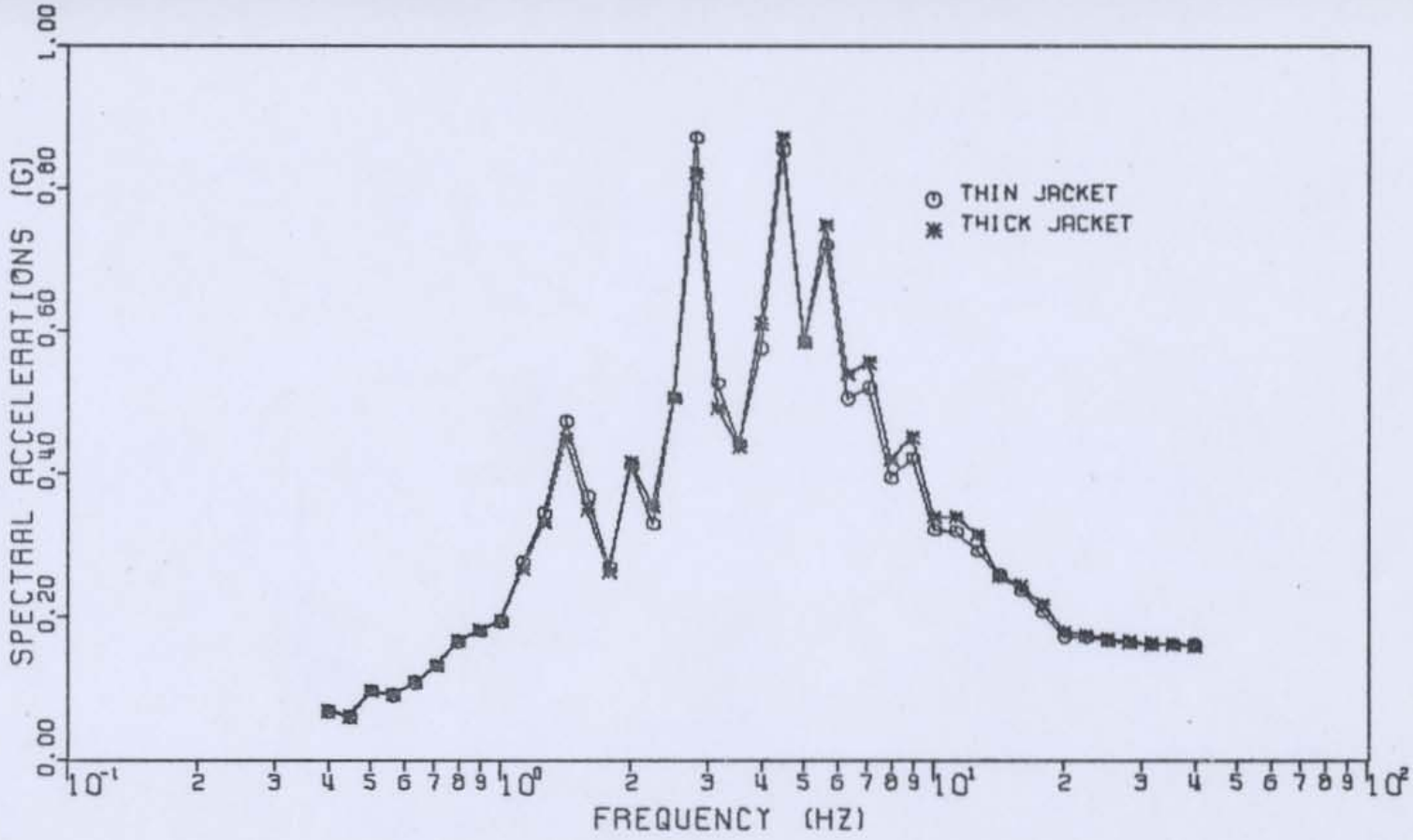

FIG. 4.49 ACCELERATION RESPONSE SPECTRA AT THE CONTAINMENT FOUNDATION MID-POINT - THIN AND THICK LOOSE FILL
(SPECTRAL DAMPING = 2%)

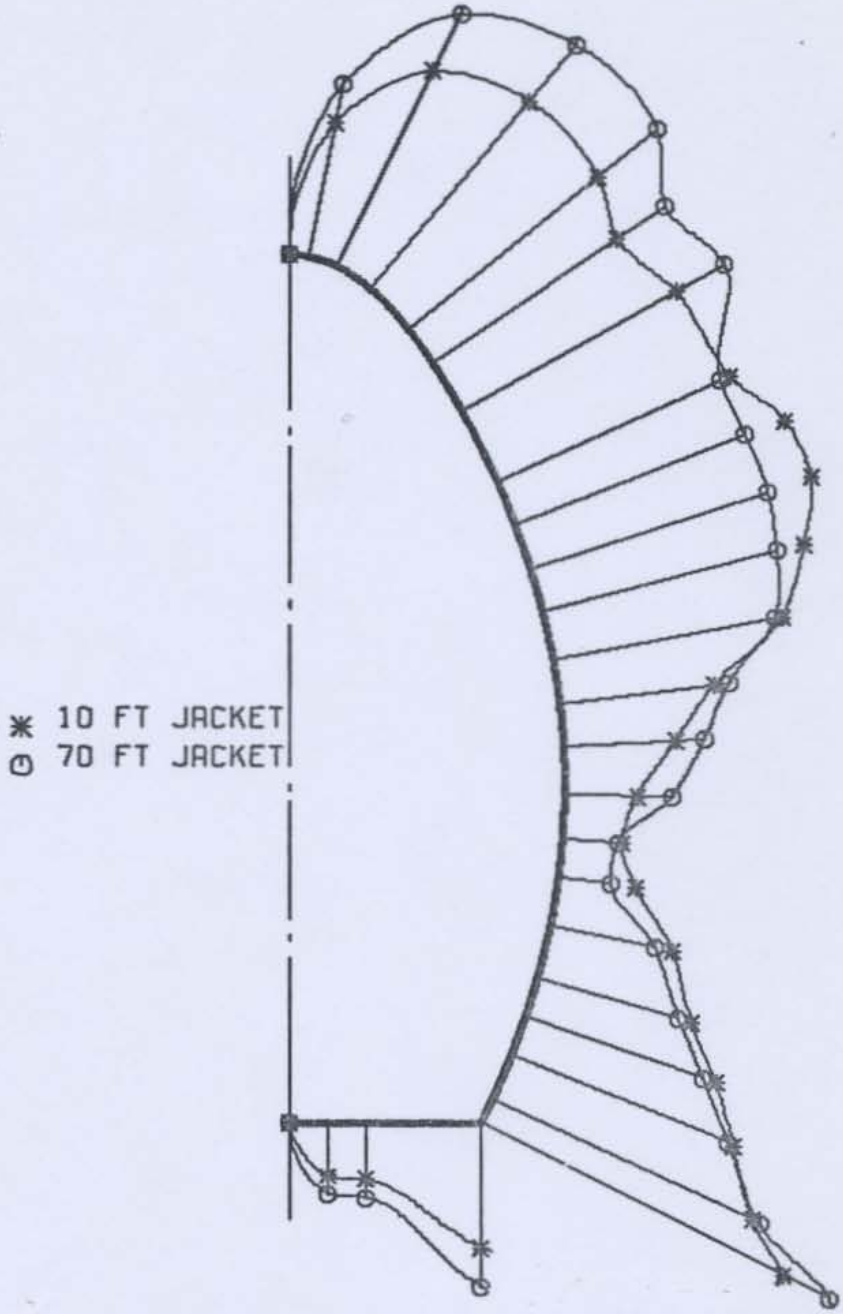

FIG. 4.50 EFFECT OF THE THICKNESS OF THE STABILIZED SAND JACKET ON THE MAXIMUM PRINCIPAL STRESSES IN THE CONTAINMENT
(SCALE: 1 INCH = 400 P.S.I.)

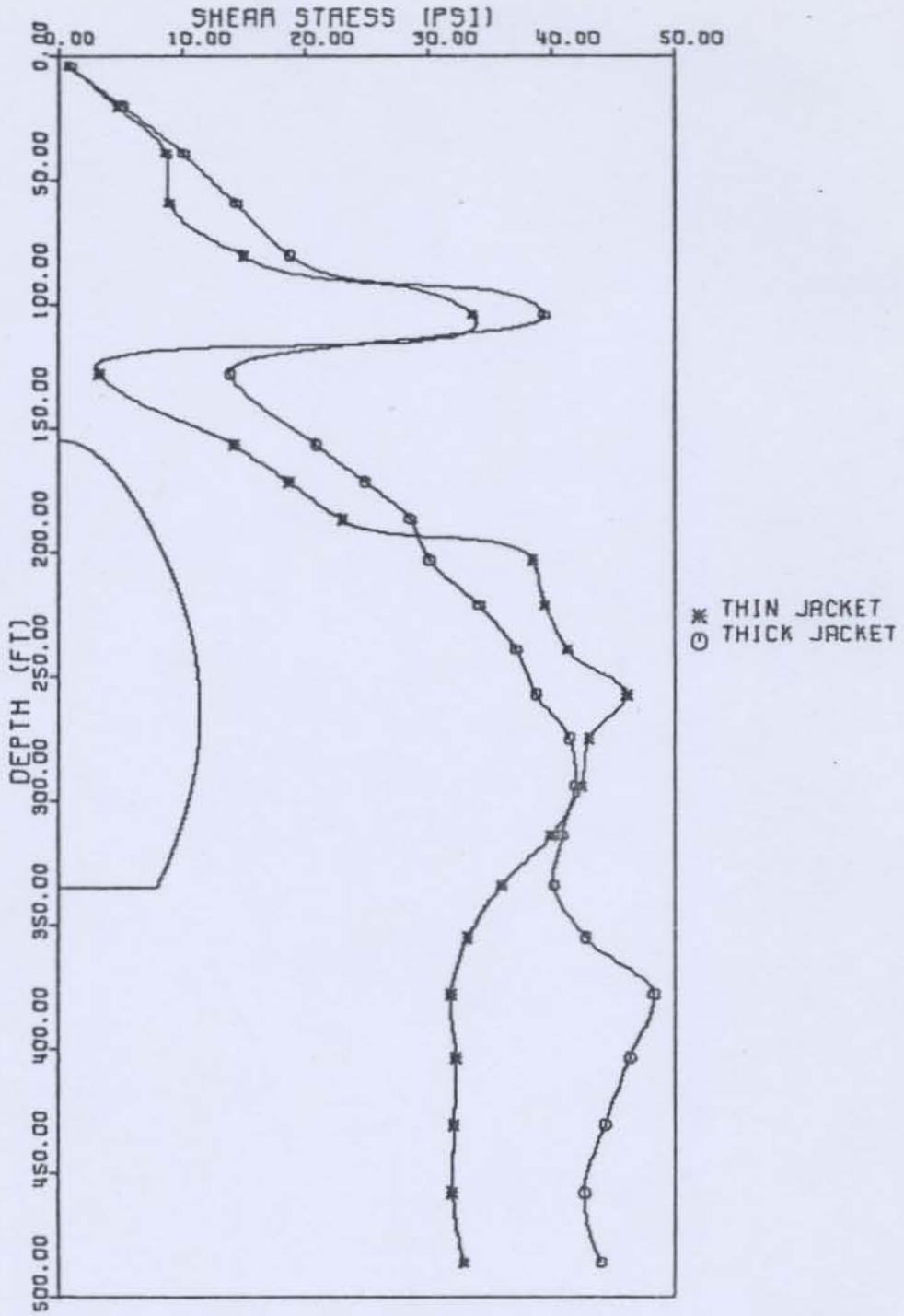

FIG. 4.51 MAXIMUM SHEAR STRESSES IN THE SOIL AT A VERTICAL PLANE 100 FT AWAY FROM THE CONTAINMENT - THIN AND THICK STABILIZED JACKETS

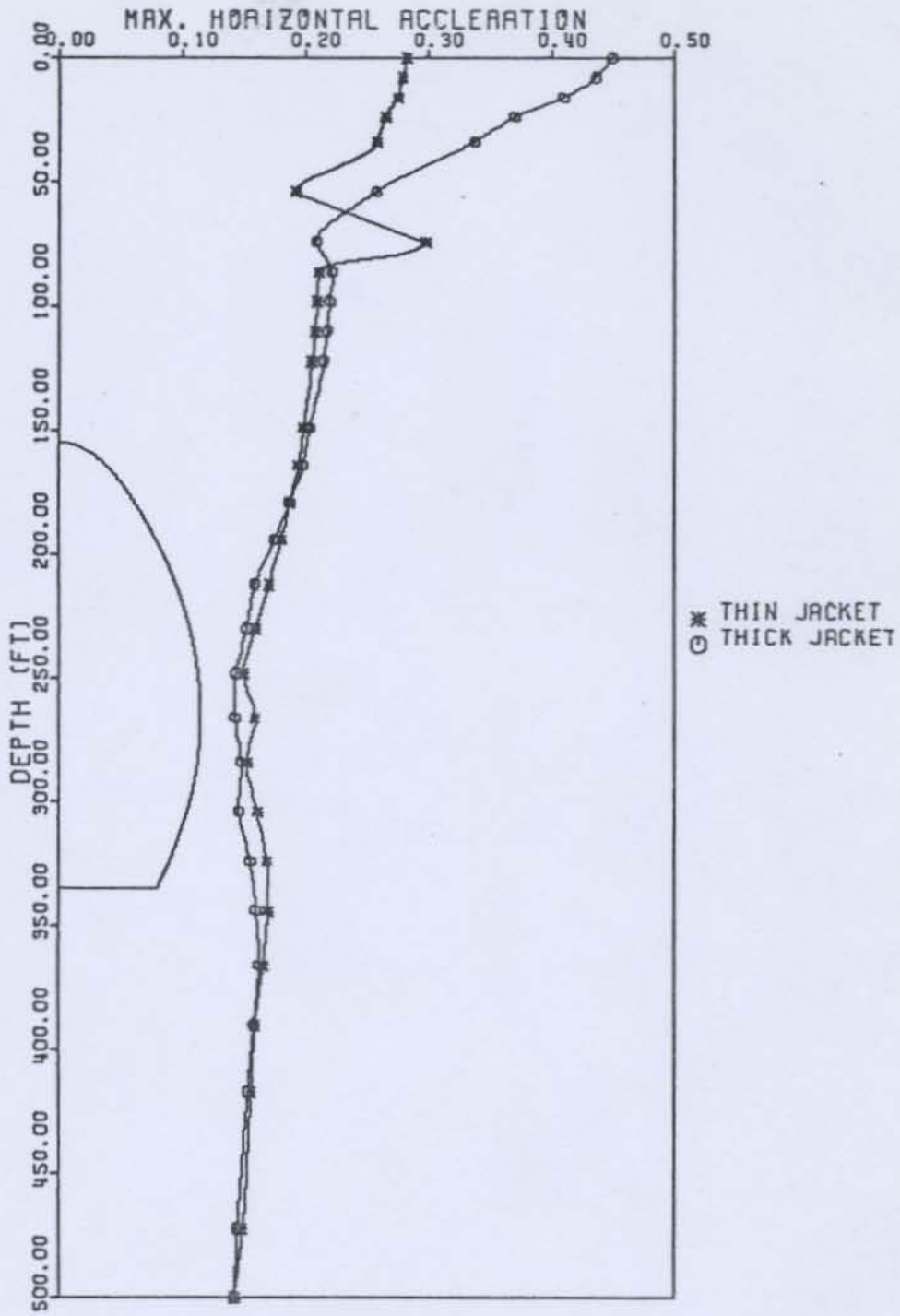

FIG. 4.52 MAXIMUM HORIZONTAL ACCELERATIONS IN THE SOIL AT A VERTICAL PLANE 10 FEET AWAY FROM THE CONTAINMENT - THIN AND THICK STABILIZED JACKETS

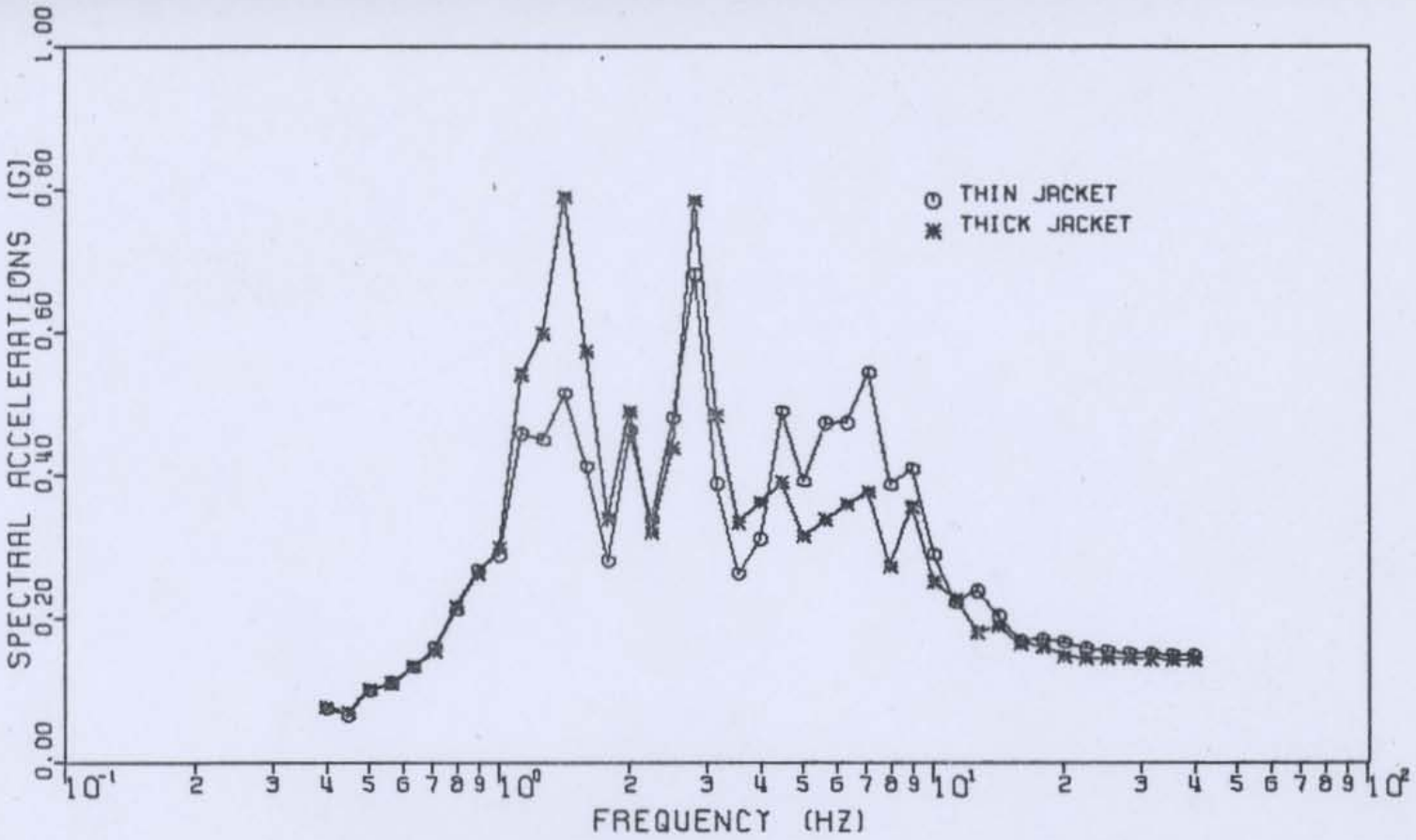

FIG. 4.53 ACCELERATION RESPONSE SPECTRA AT MID-HEIGHT OF THE CONTAINMENT WALL - THIN AND THICK STABILIZED SAND JACKETS (SPECTRAL DAMPING = 2%)

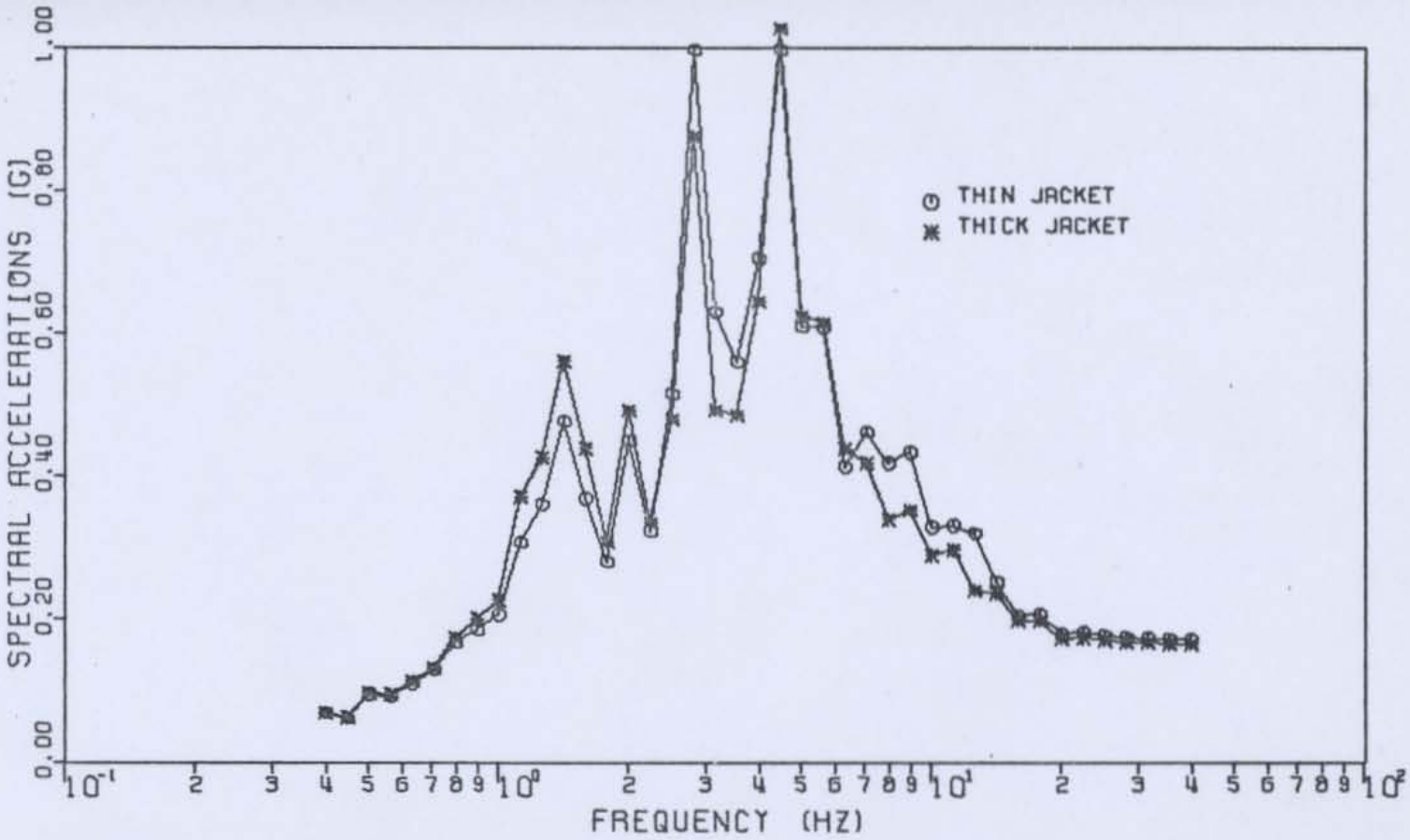

FIG. 4.54 ACCELERATION RESPONSE SPECTRA AT THE CONTAINMENT FOUNDATION MID-POINT - THIN AND THICK STABILIZED SAND JACKETS . (SPECTRAL DAMPING = 2%)

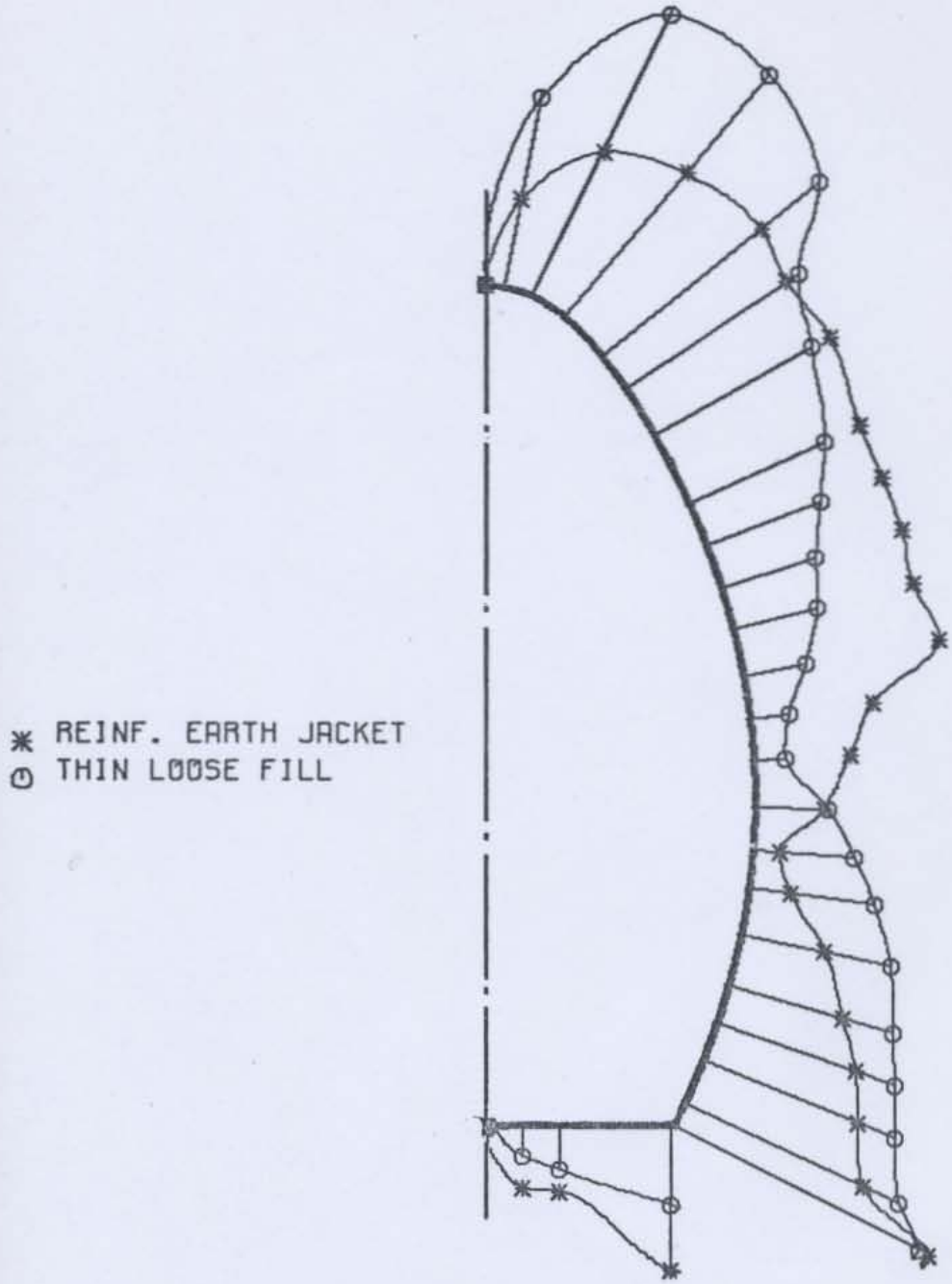

FIG. 4.55 MAXIMUM PRINCIPAL STRESSES IN THE CONTAINMENT FOR REINFORCED EARTH JACKET AND THIN LOOSE FILL
(SCALE: 1 INCH = 400 P.S.I.)

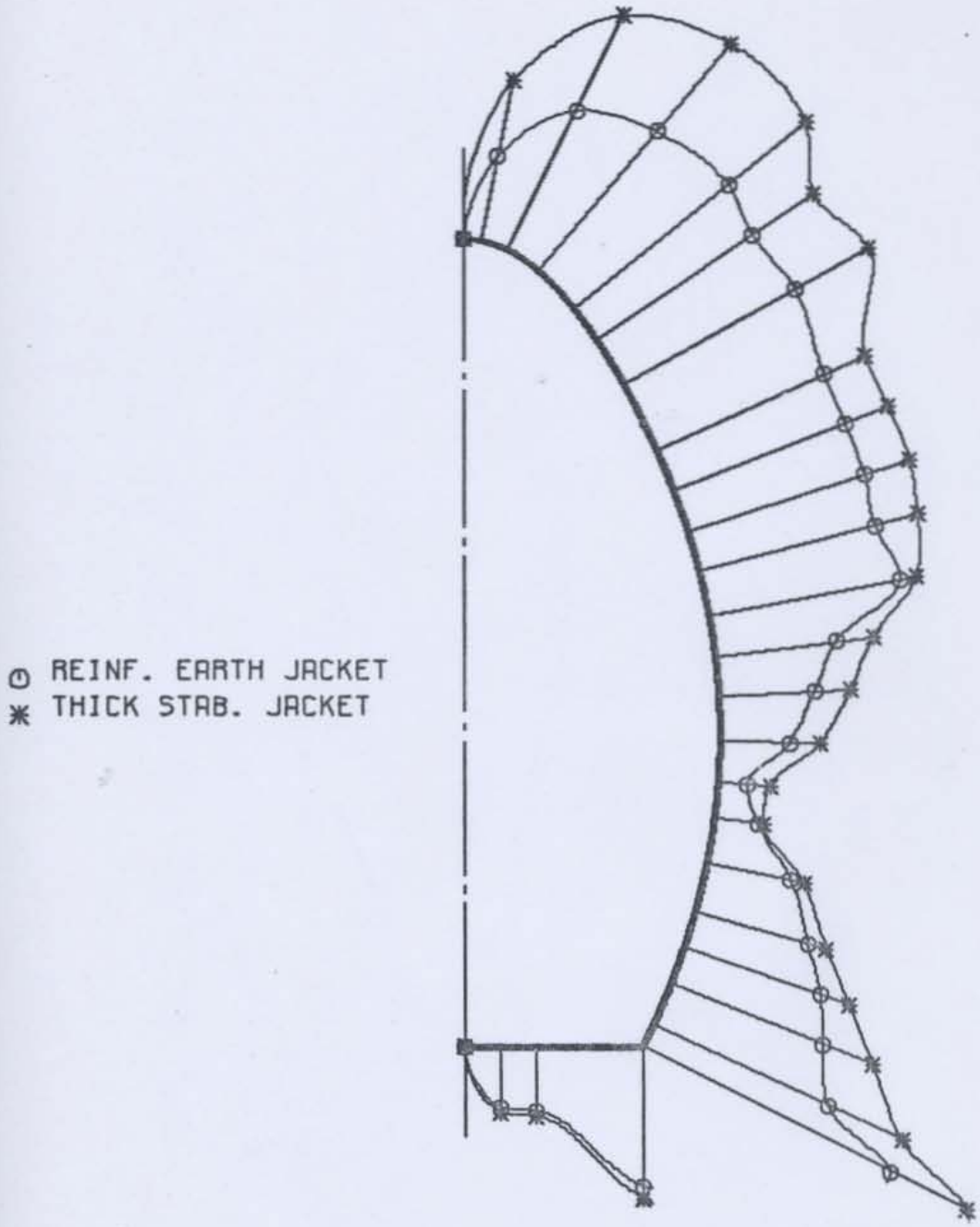

FIG. 4.56 MAXIMUM PRINCIPAL STRESSES IN THE CONTAINMENT FOR REINFORCED EARTH AND STABILIZED SAND JACKETS
(SCALE: 1 INCH = 400 P.S.I.)

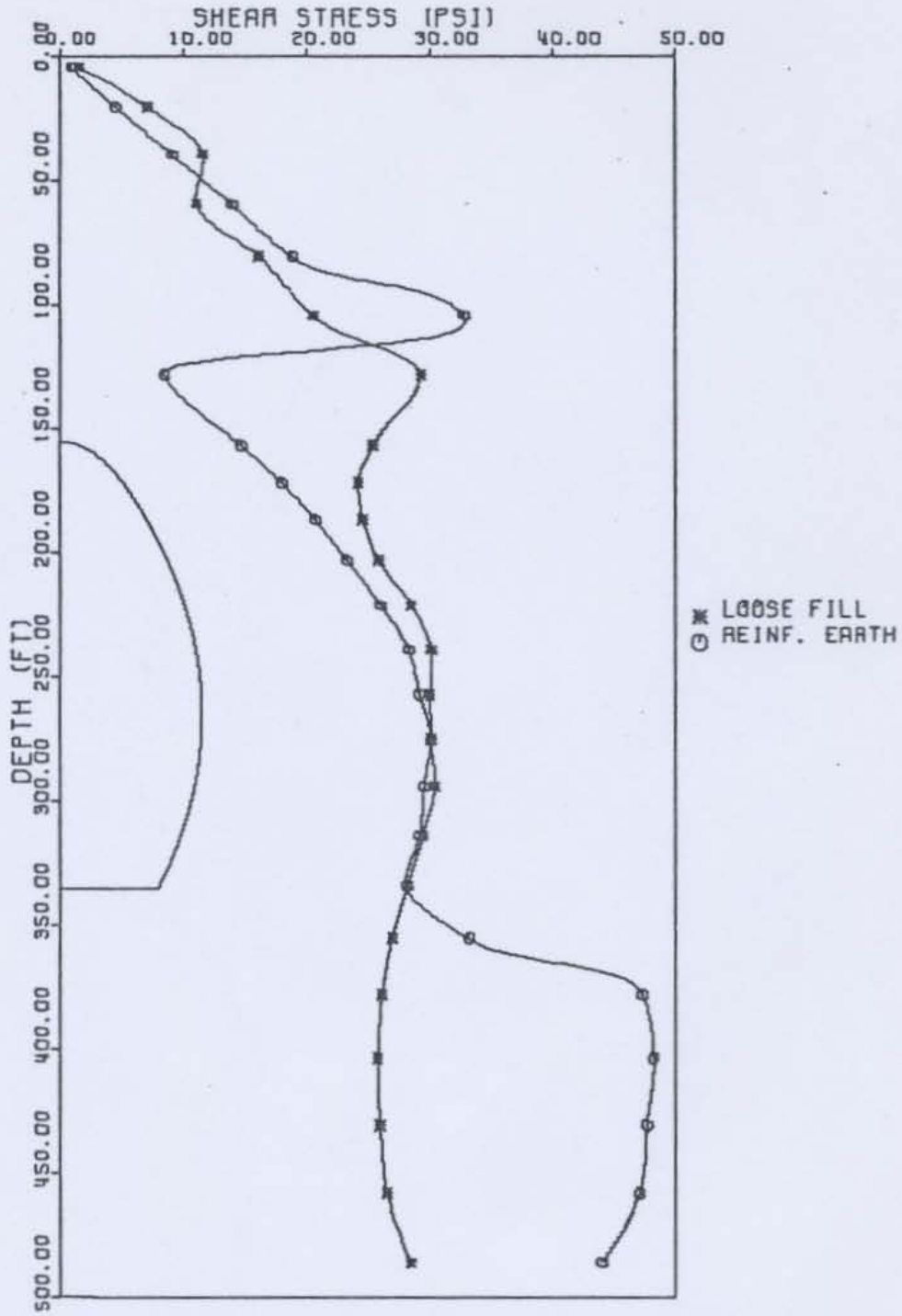

FIG. 4.57 MAXIMUM SHEAR STRESSES IN THE SOIL AT A VERTICAL PLANE 100 FT AWAY FROM THE CONTAINMENT - LOOSE FILL AND REINFORCED EARTH JACKET

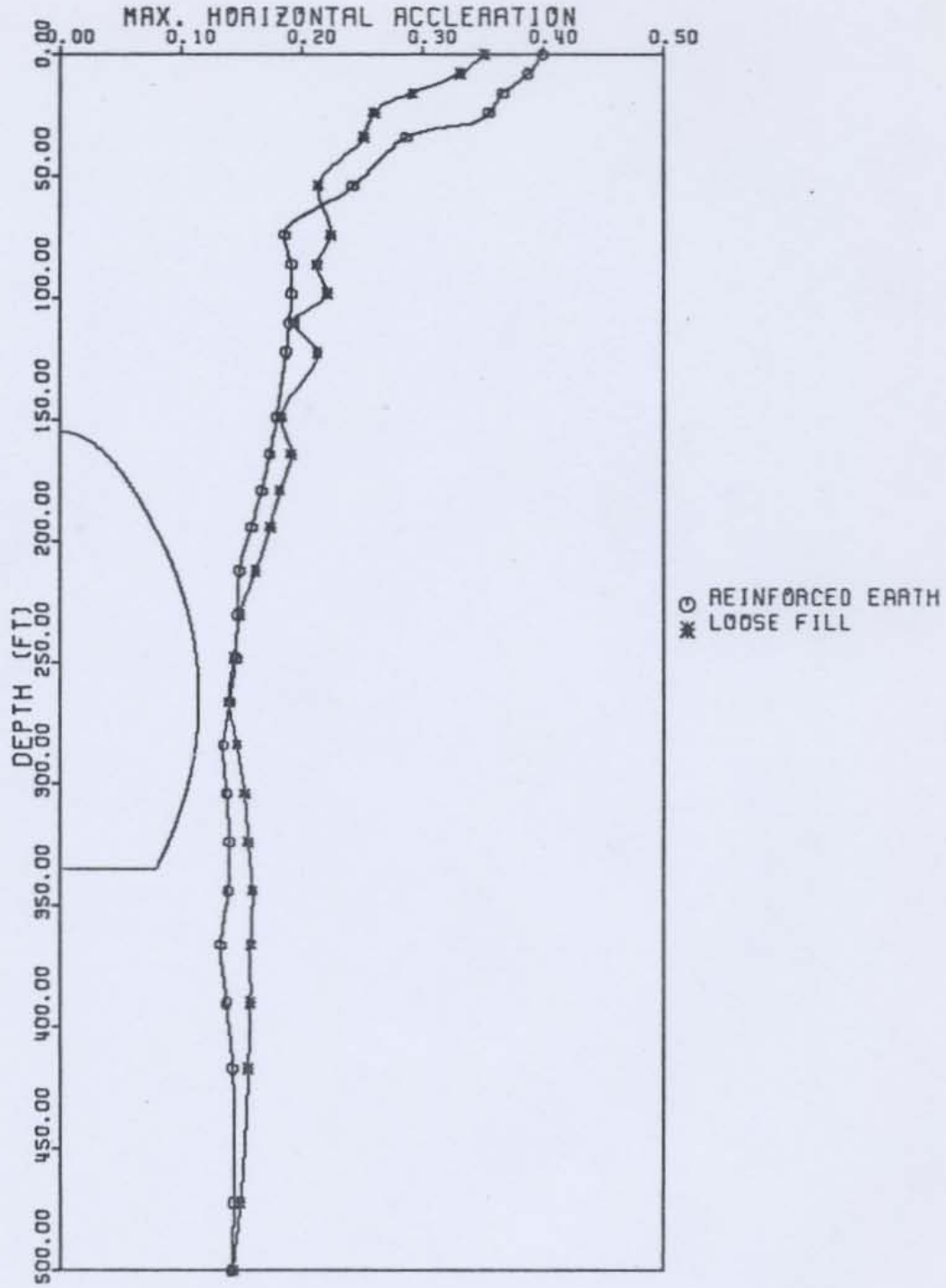

FIG. 4.58 MAXIMUM HORIZONTAL ACCELERATIONS IN THE SOIL AT A VERTICAL PLANE 10 FEET AWAY FROM THE CONTAINMENT - LOOSE FILL AND REINFORCED EARTH JACKET

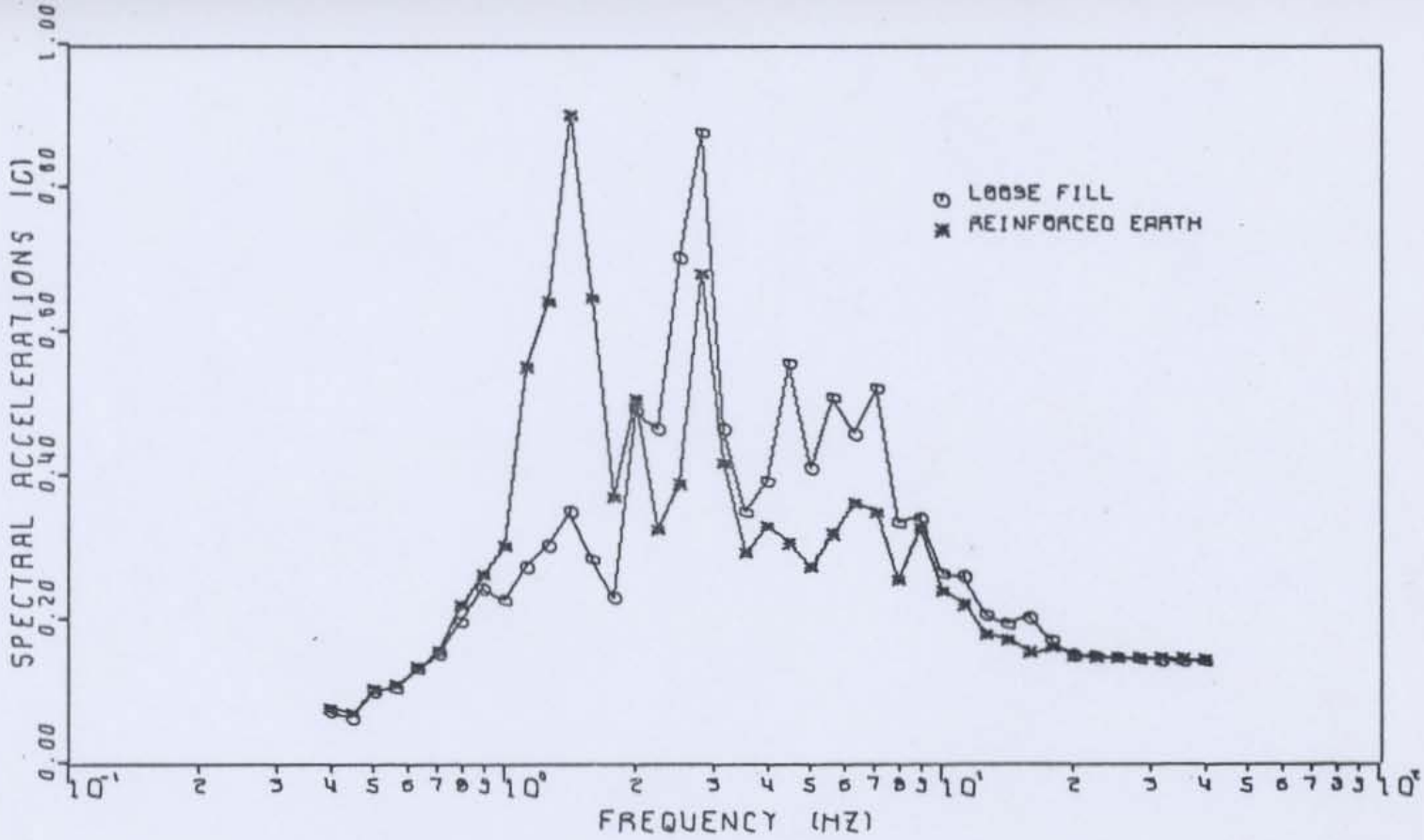

FIG. 4.59 ACCELERATION RESPONSE SPECTRA AT MID-HEIGHT OF THE CONTAINMENT WALL - LOOSE FILL AND REINFORCED EARTH JACKET. (SPECTRAL DAMPING = 2%)

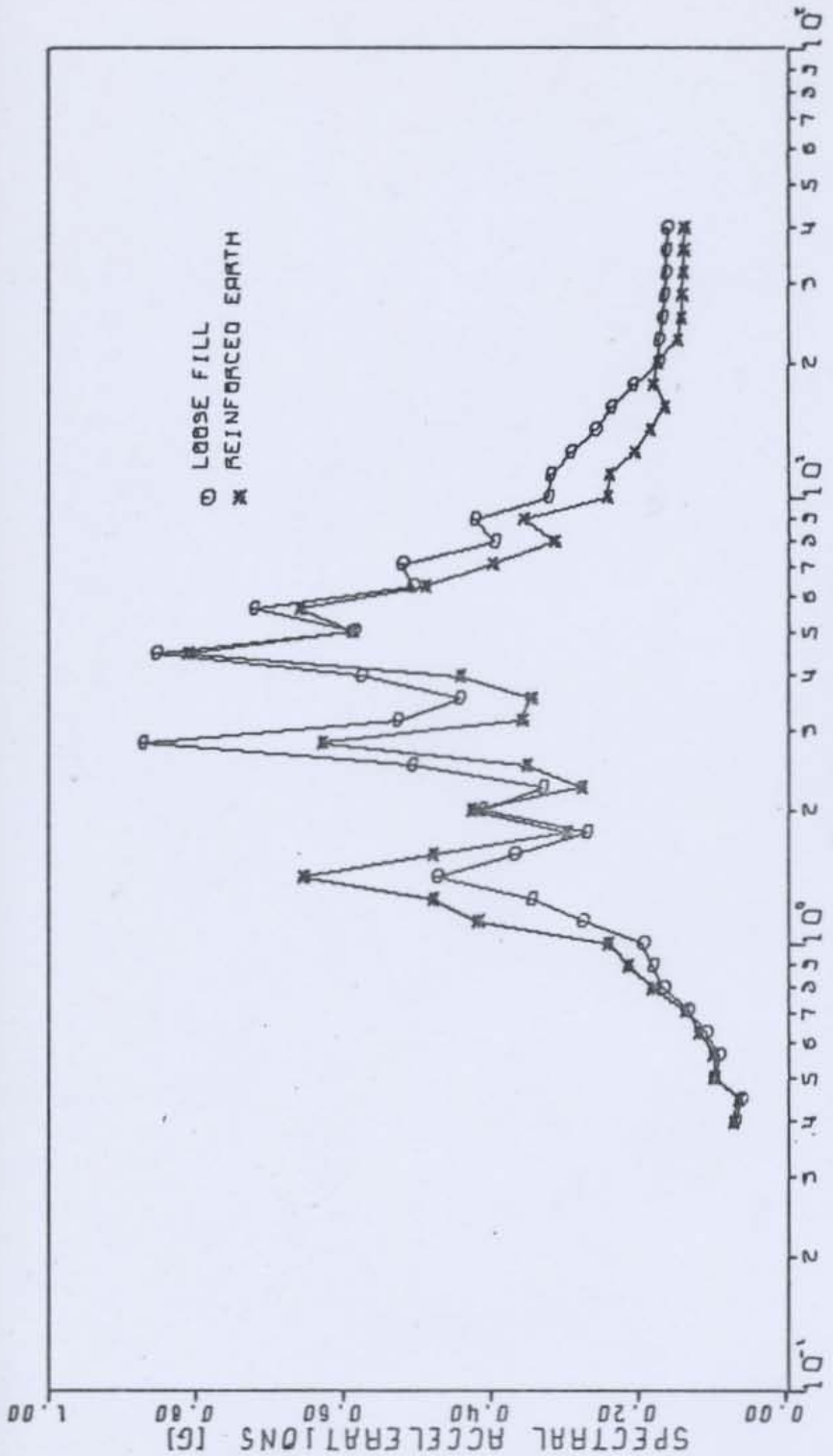

FIG. 4.60 ACCELERATION RESPONSE SPECTRA AT THE CONTAINMENT FOUNDATION MID-POINT - LOOSE FILL AND REINFORCED EARTH JACKET. (SPECTRAL DAMPING = 2%)

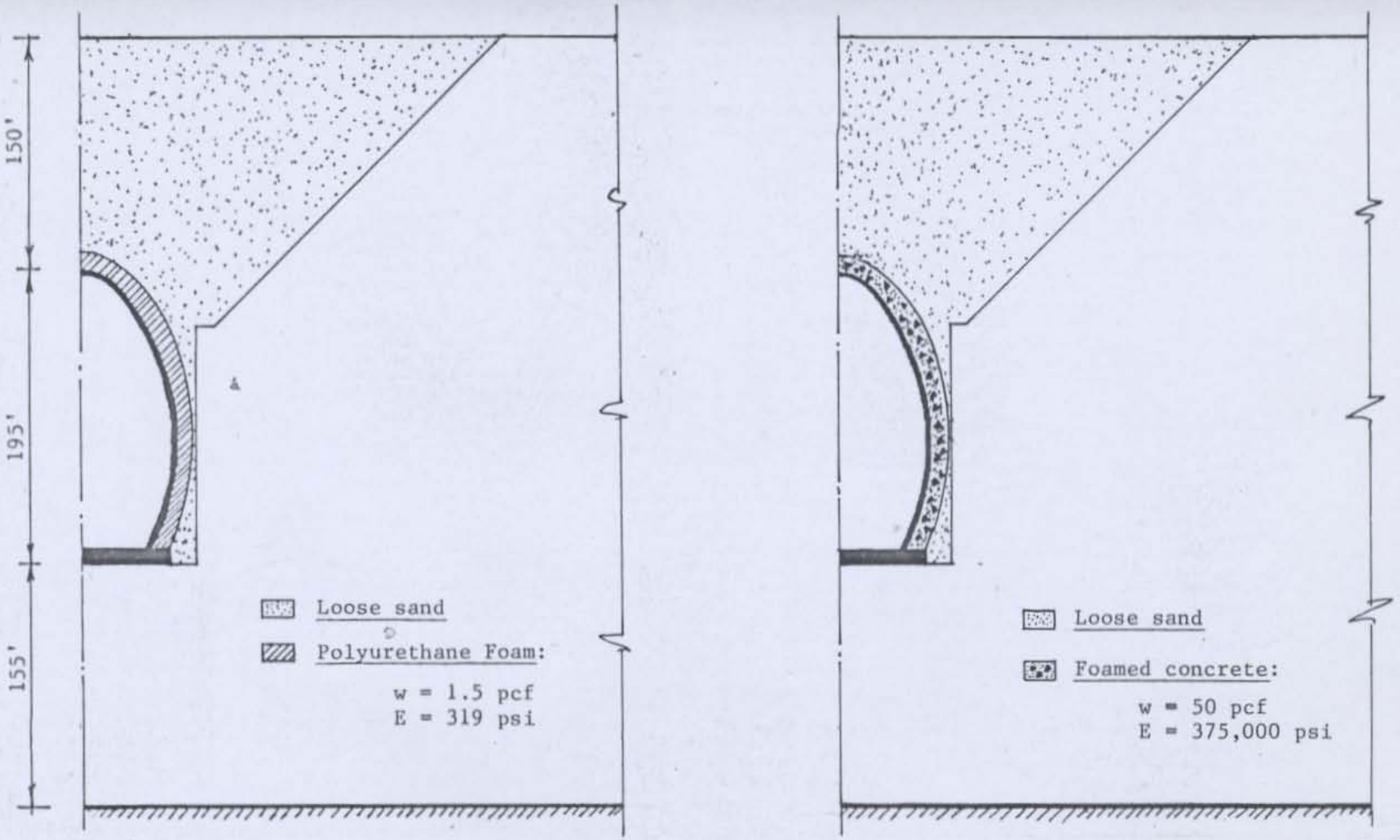

(I) POLYURETHANE FOAM JACKET

(II) FOAMED CONCRETE JACKET

FIG. 4.61 CONFIGURATION AND PROPERTIES OF THE ISOLATION JACKETS

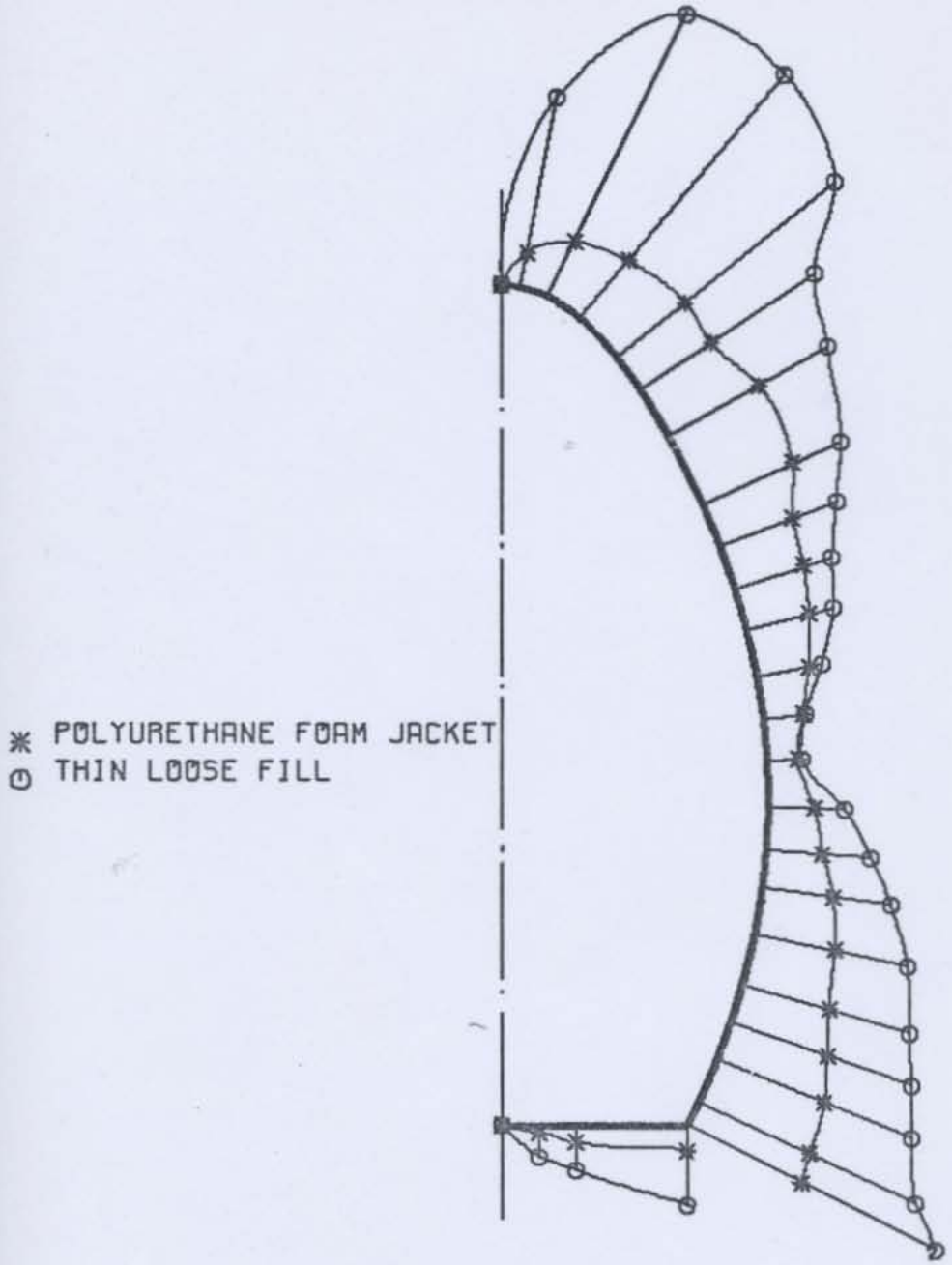

FIG. 4.62 EFFECT OF THE ENERGY ABSORBING JACKET (POLYURETHANE FOAM) ON MAXIMUM PRINCIPAL STRESSES IN THE CONTAINMENT (SCALE: 1 INCH = 400 P.S.I.)

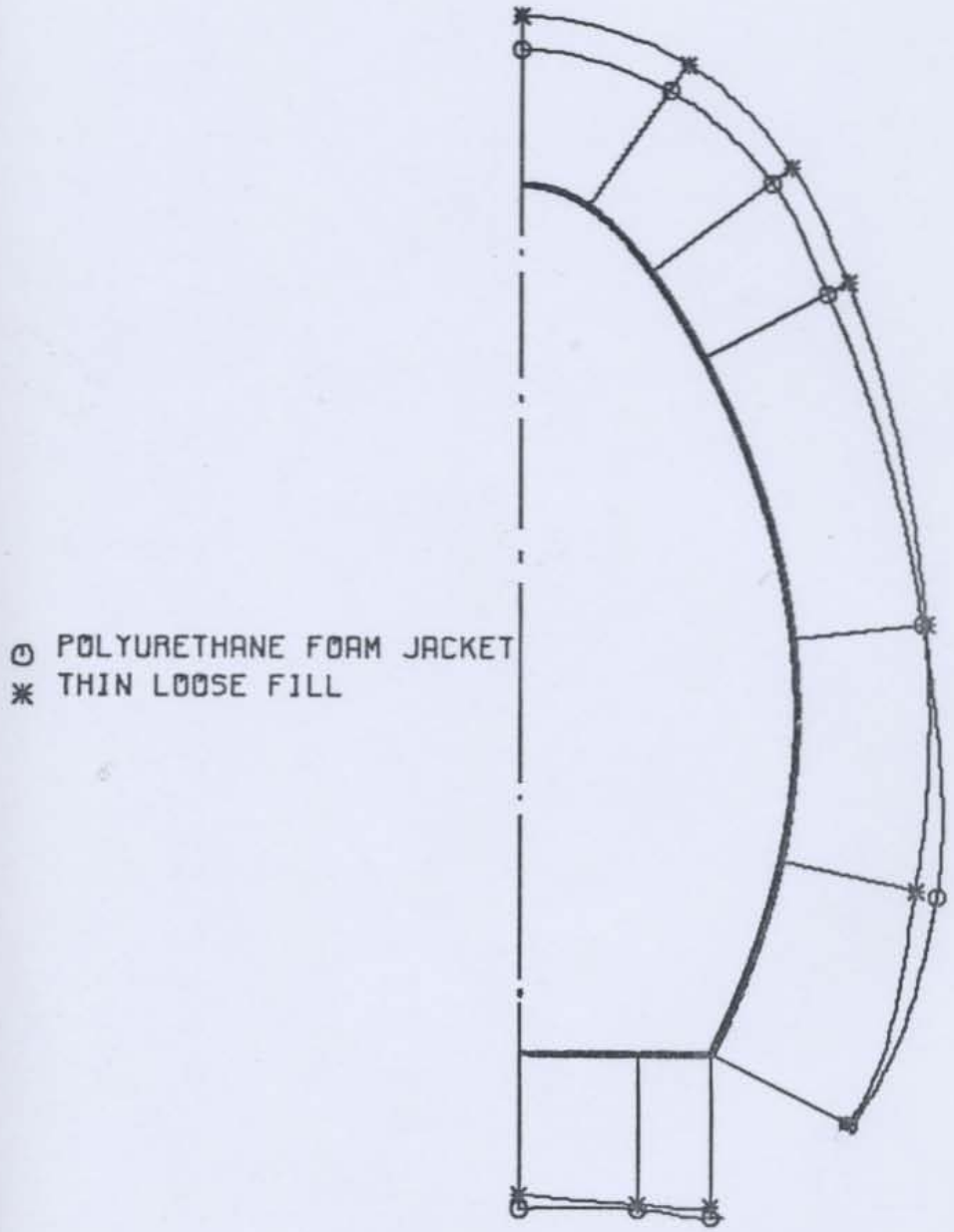

FIG. 4.63 EFFECT OF THE ENERGY ABSORBING JACKET (POLYURETHANE FOAM) ON MAXIMUM HORIZONTAL ACCELERATIONS IN THE CONTAINMENT (SCALE: 1 INCH=0.2G)

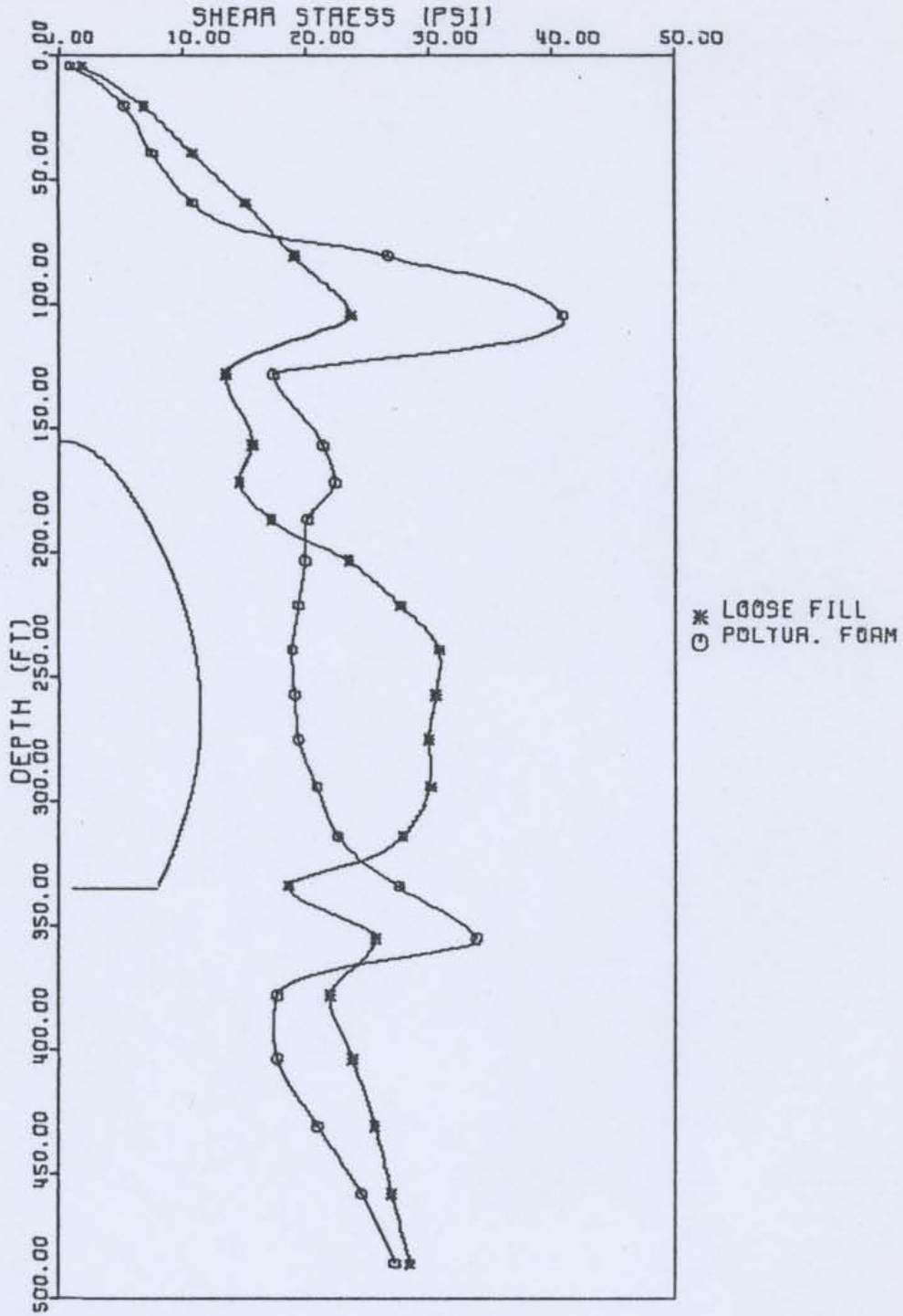

FIG. 4.64 MAXIMUM SHEAR STRESSES IN THE SOIL AT A VERTICAL PLANE 40 FT AWAY FROM THE CONTAINMENT - LOOSE FILL AND POLYURETHANE FOAM JACKET

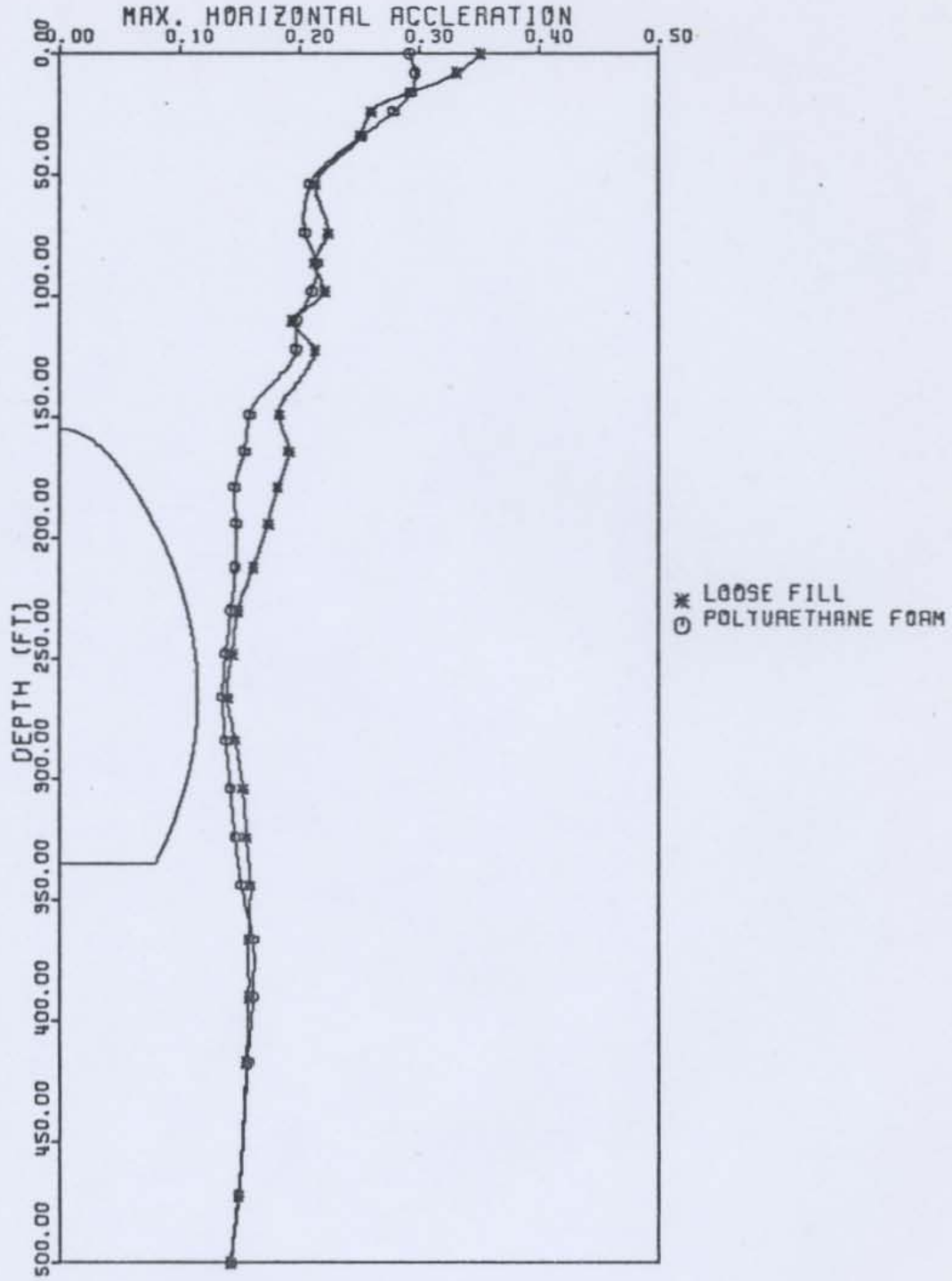

FIG. 4.65 MAXIMUM HORIZONTAL ACCELERATIONS IN THE SOIL AT A VERTICAL PLANE 10 FEET AWAY FROM THE CONTAINMENT - LOOSE FILL AND POLYURETHANE FOAM JACKET

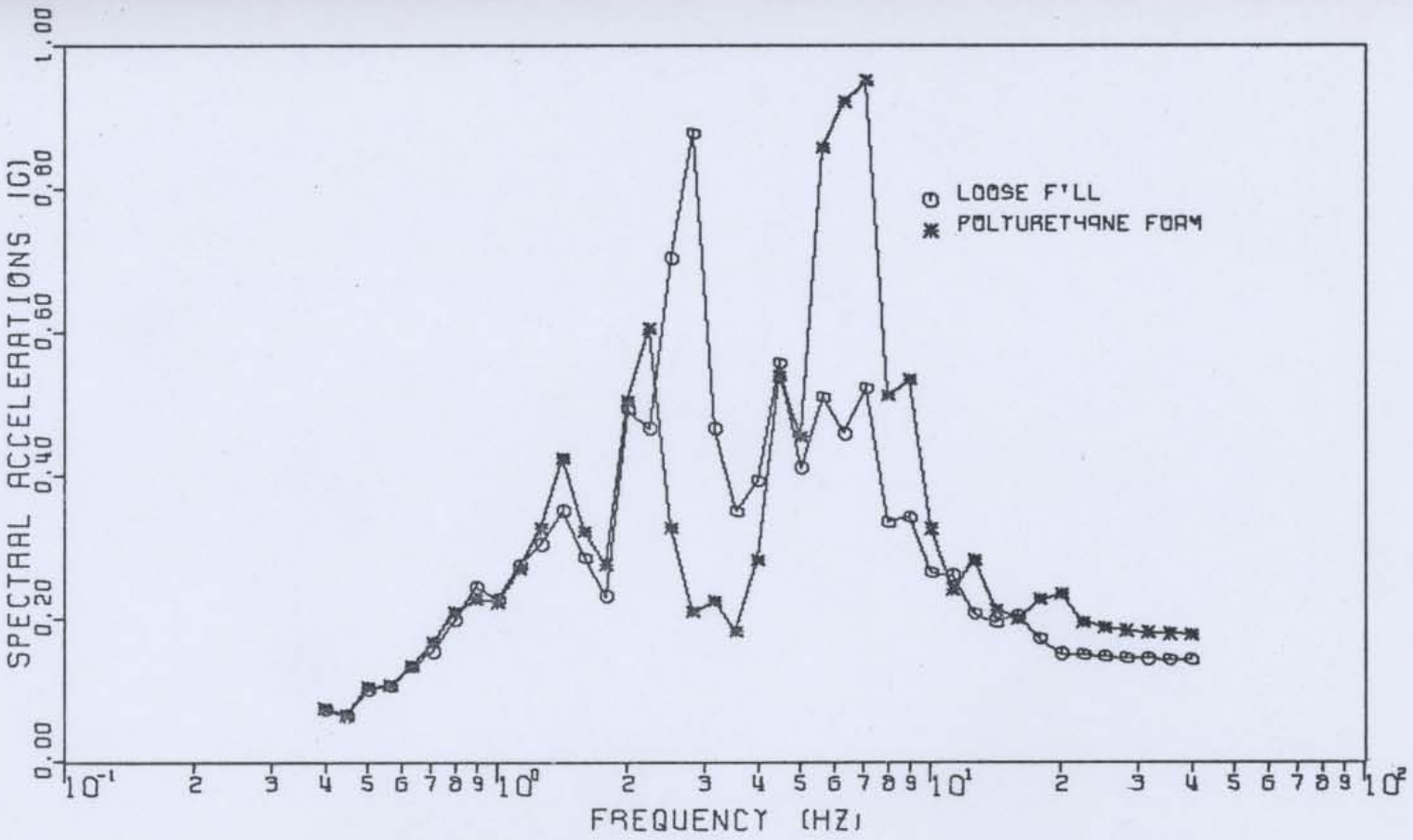

FIG. 4.66 ACCELERATION RESPONSE SPECTRA AT MID-HEIGHT OF THE CONTAINMENT WALL - LOOSE FILL AND ISOLATING POLYURETHANE FOAM JACKET
(SPECTRAL DAMPING = 2%)

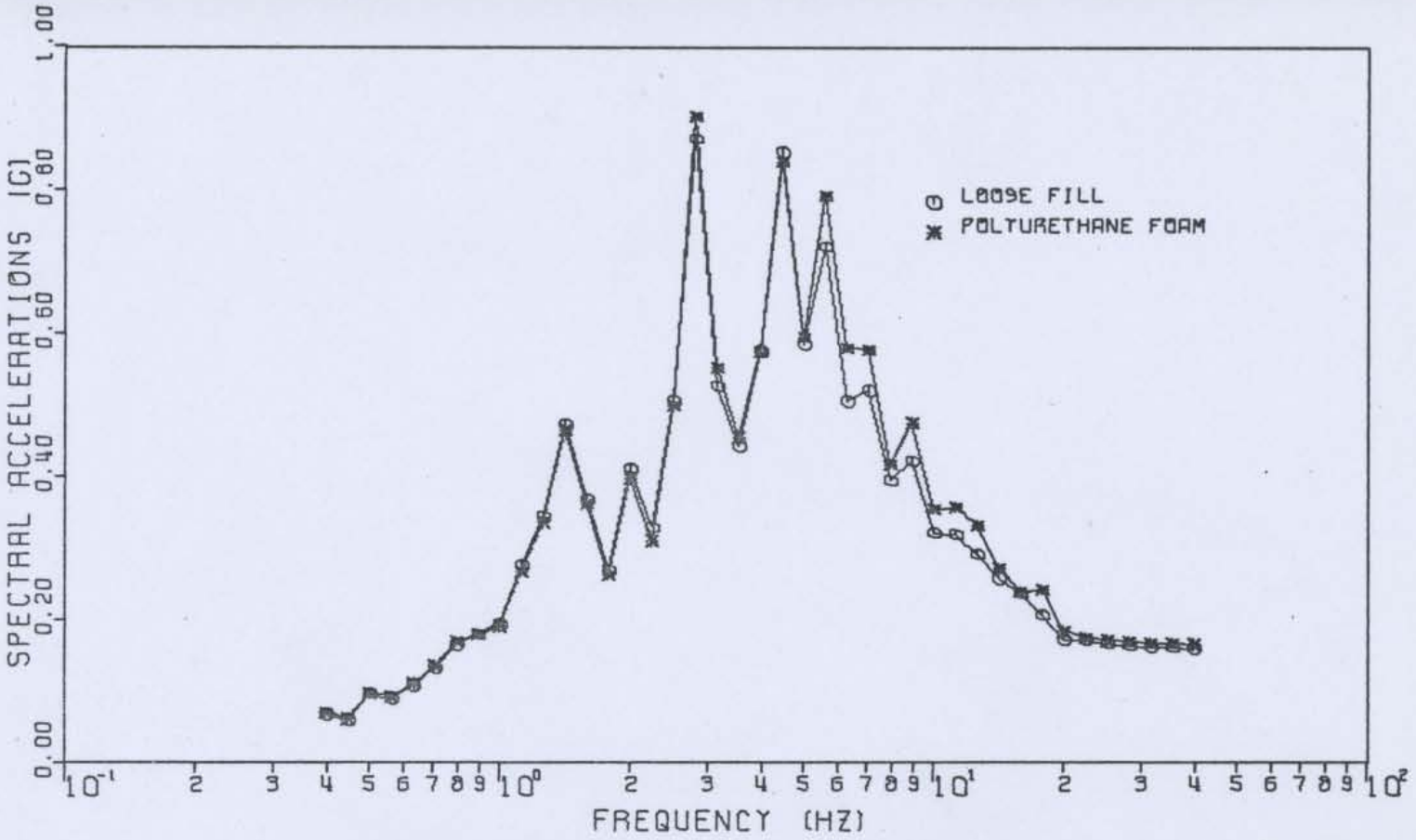

FIG. 4.67 ACCELERATION RESPONSE SPECTRA AT THE CONTAINMENT FOUNDATION MID-POINT - LOOSE FILL AND ISOLATING POLYURETHANE FOAM JACKET
(SPECTRAL DAMPING = 2%)

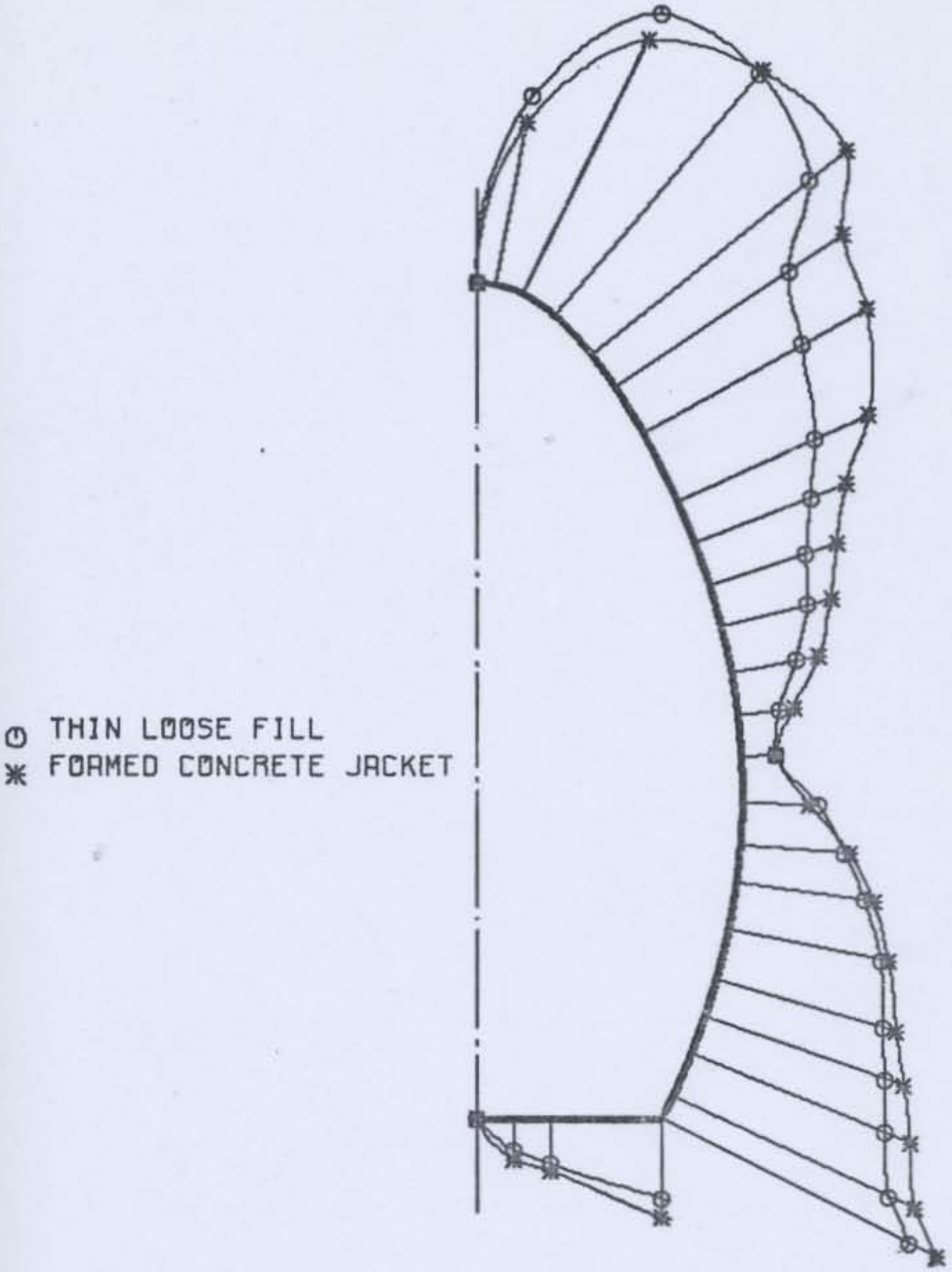

FIG. 4.68 EFFECT OF THE FORMED CONCRETE JACKET ON MAXIMUM PRINCIPAL STRESSES IN THE CONTAINMENT (SCALE: 1 INCH = 400 P.S.I.)

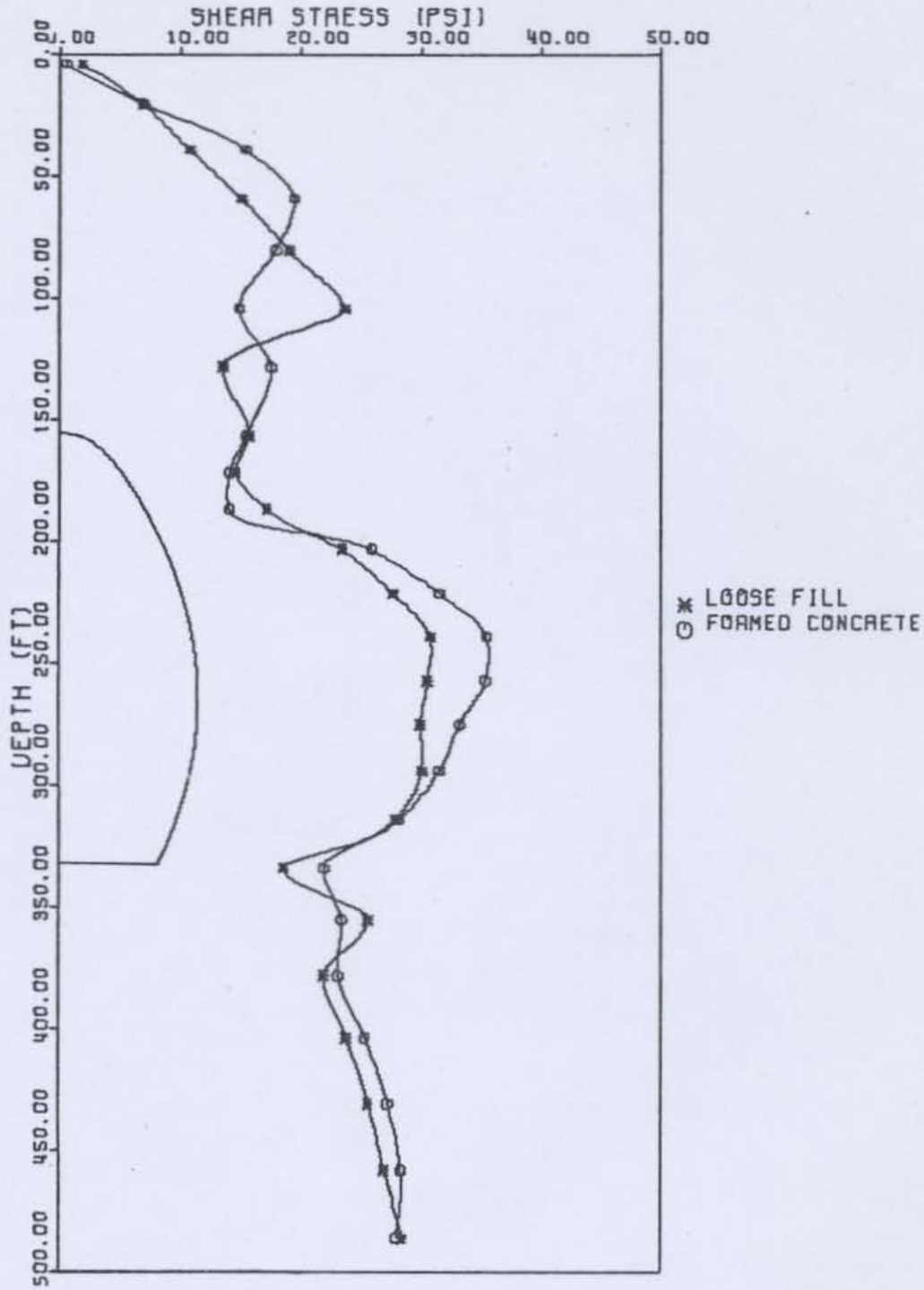

FIG. 4.69 MAXIMUM SHEAR STRESSES IN THE SOIL AT A VERTICAL PLANE 40 FT AWAY FROM THE CONTAINMENT - LOOSE FILL AND FOAMED CONCRETE JACKET

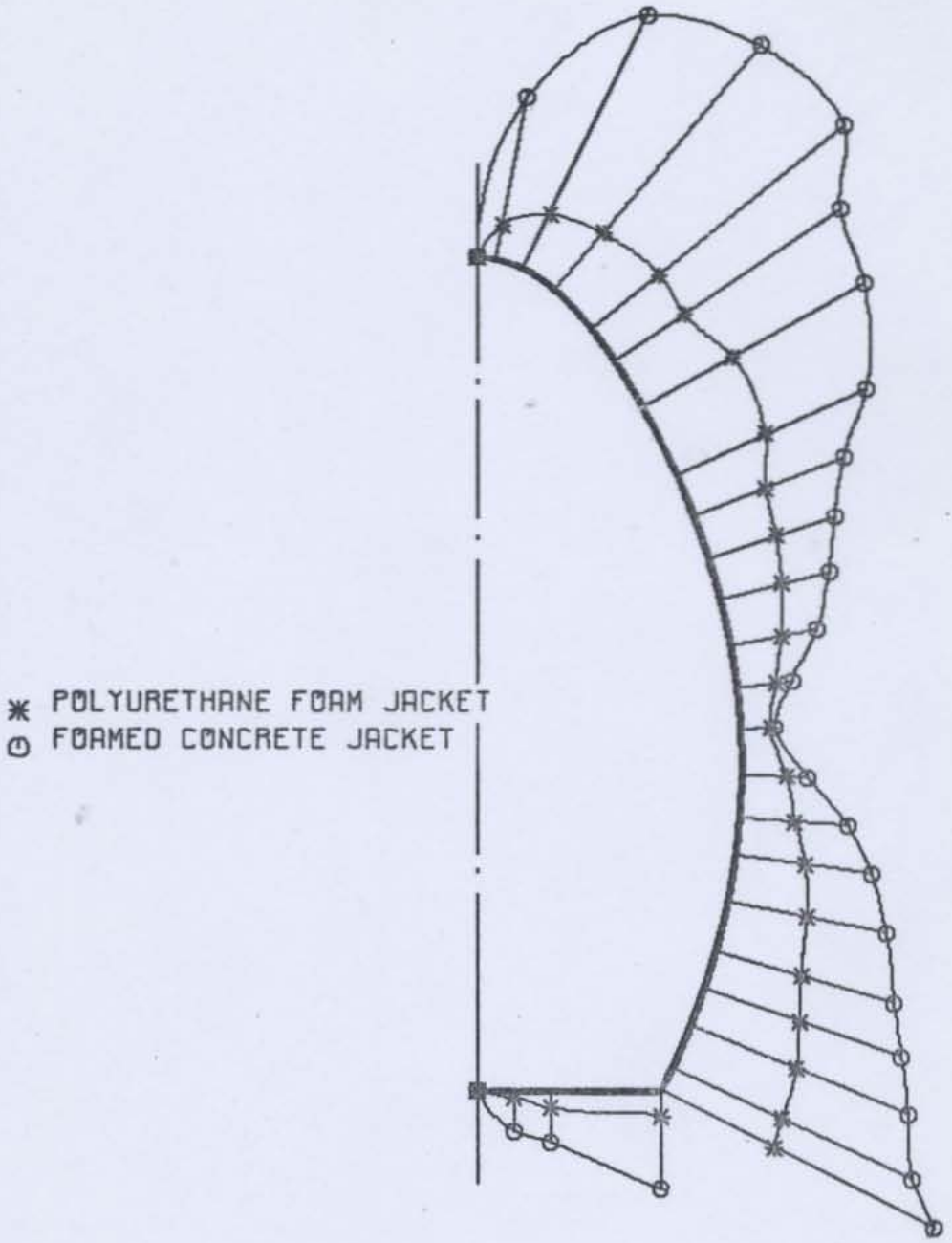

FIG. 4.70 MAXIMUM PRINCIPAL STRESSES IN THE CONTAINMENT FOR FOAMED CONCRETE AND POLYURETHANE FOAM JACKETS
(SCALE: 1 INCH = 400 P.S.I.)

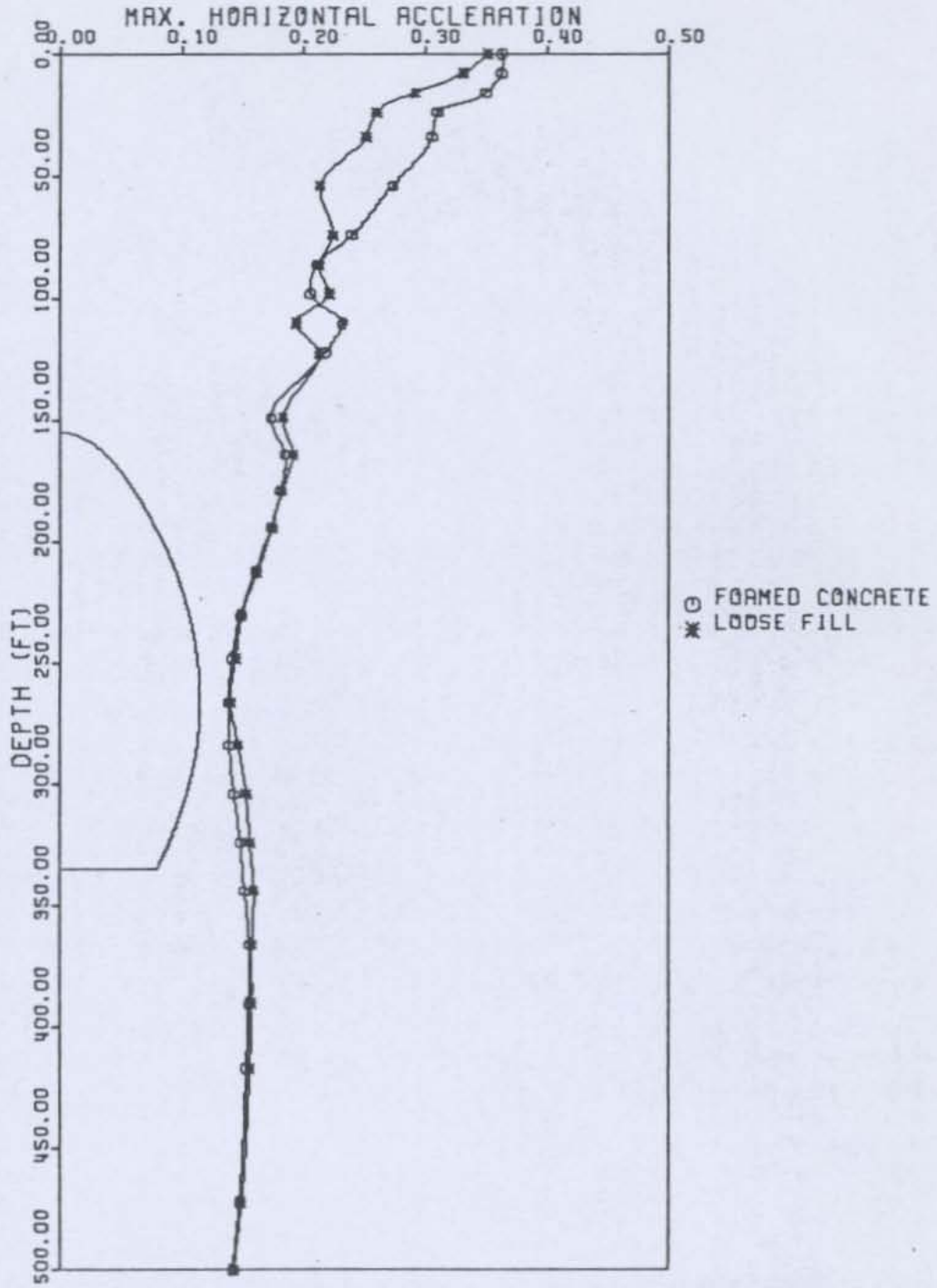

FIG. 4.71 MAXIMUM HORIZONTAL ACCELERATIONS IN THE SOIL AT A VERTICAL PLANE 10 FEET AWAY FROM THE CONTAINMENT - LOOSE FILL AND FOAMED CONCRETE JACKET

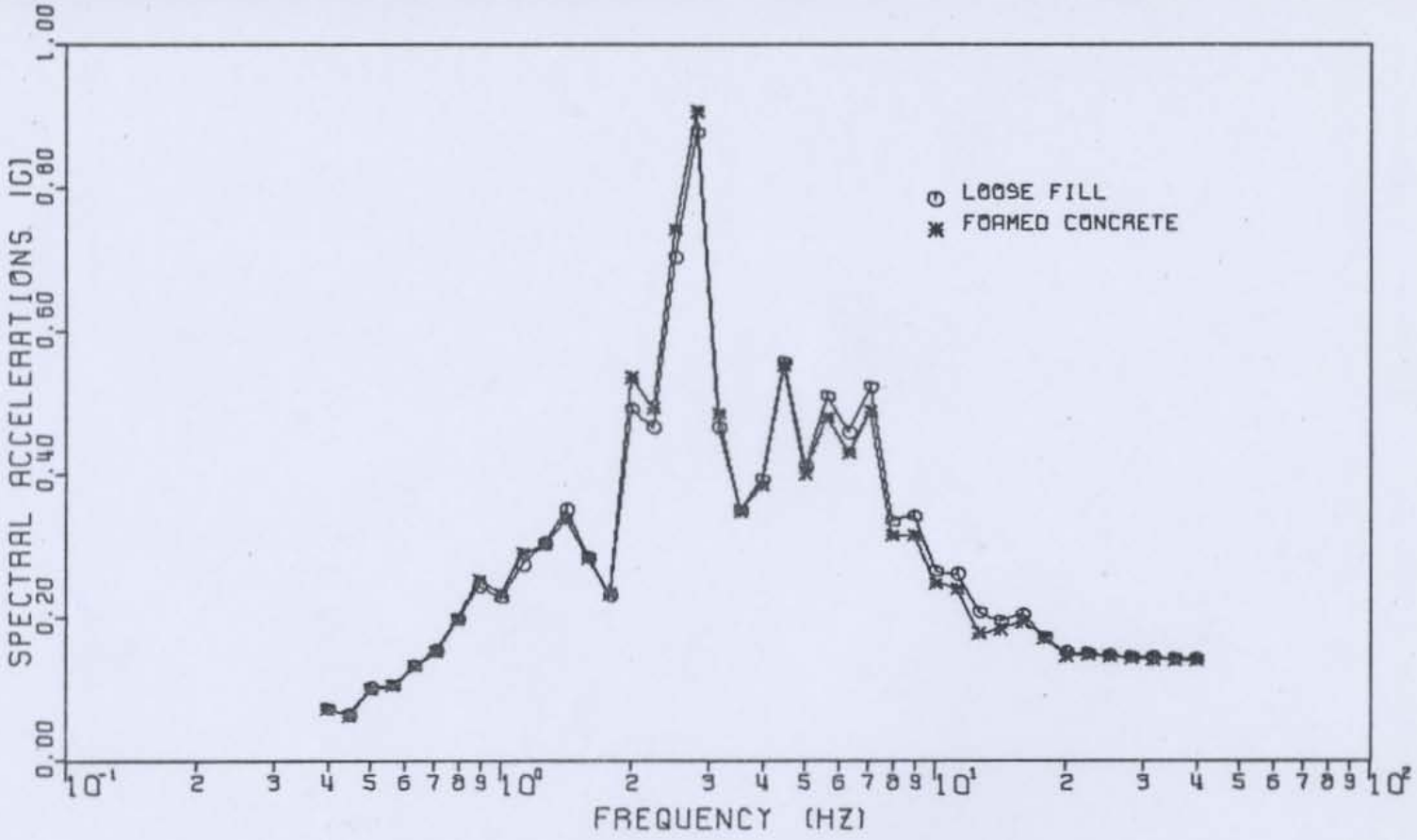

FIG. 4.72 ACCELERATION RESPONSE SPECTRA AT MID-HEIGHT OF THE CONTAINMENT WALL - LOOSE FILL AND FOAMED CONCRETE JACKET. (SPECTRAL DAMPING = 2%)

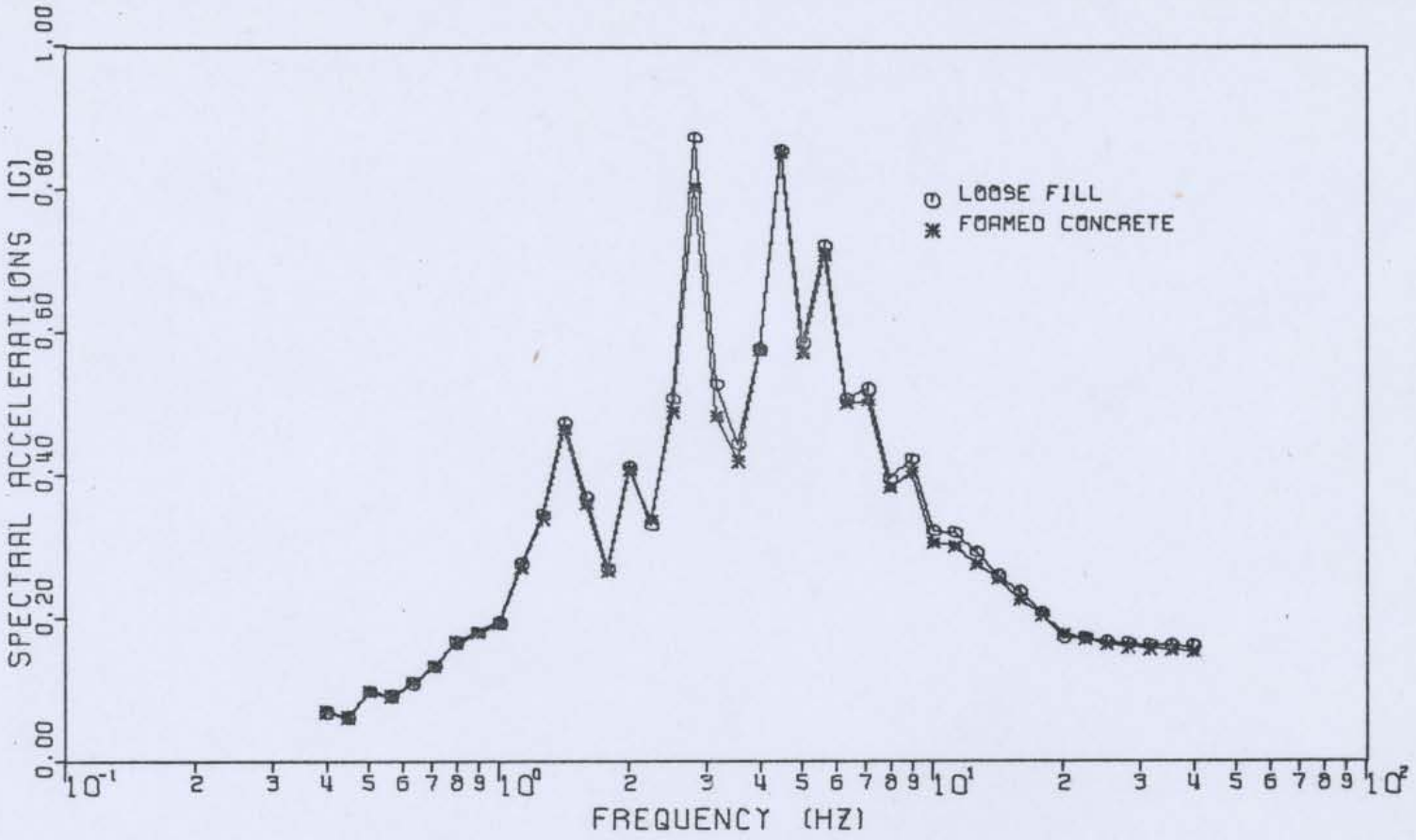

FIG. 4.73 ACCELERATION RESPONSE SPECTRA AT THE CONTAINMENT FOUNDATION MID-POINT - LOOSE FILL AND FOAMED CONCRETE JACKET. (SPECTRAL DAMPING = 2%)

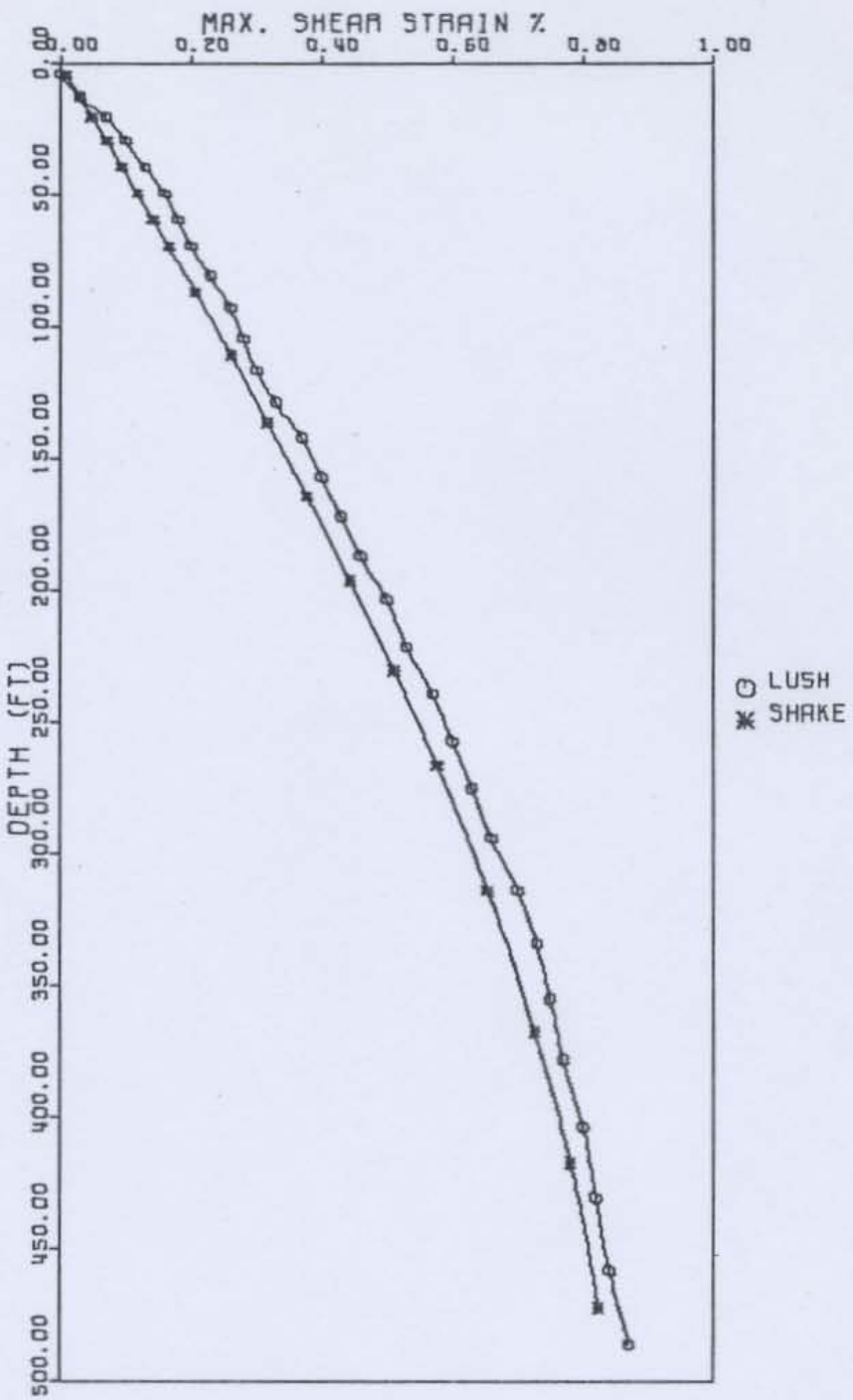

FIG. 4.74 MAXIMUM FREE FIELD SHEAR STRAIN IN ROCK COMPUTED FROM LUSH AND SHAKE

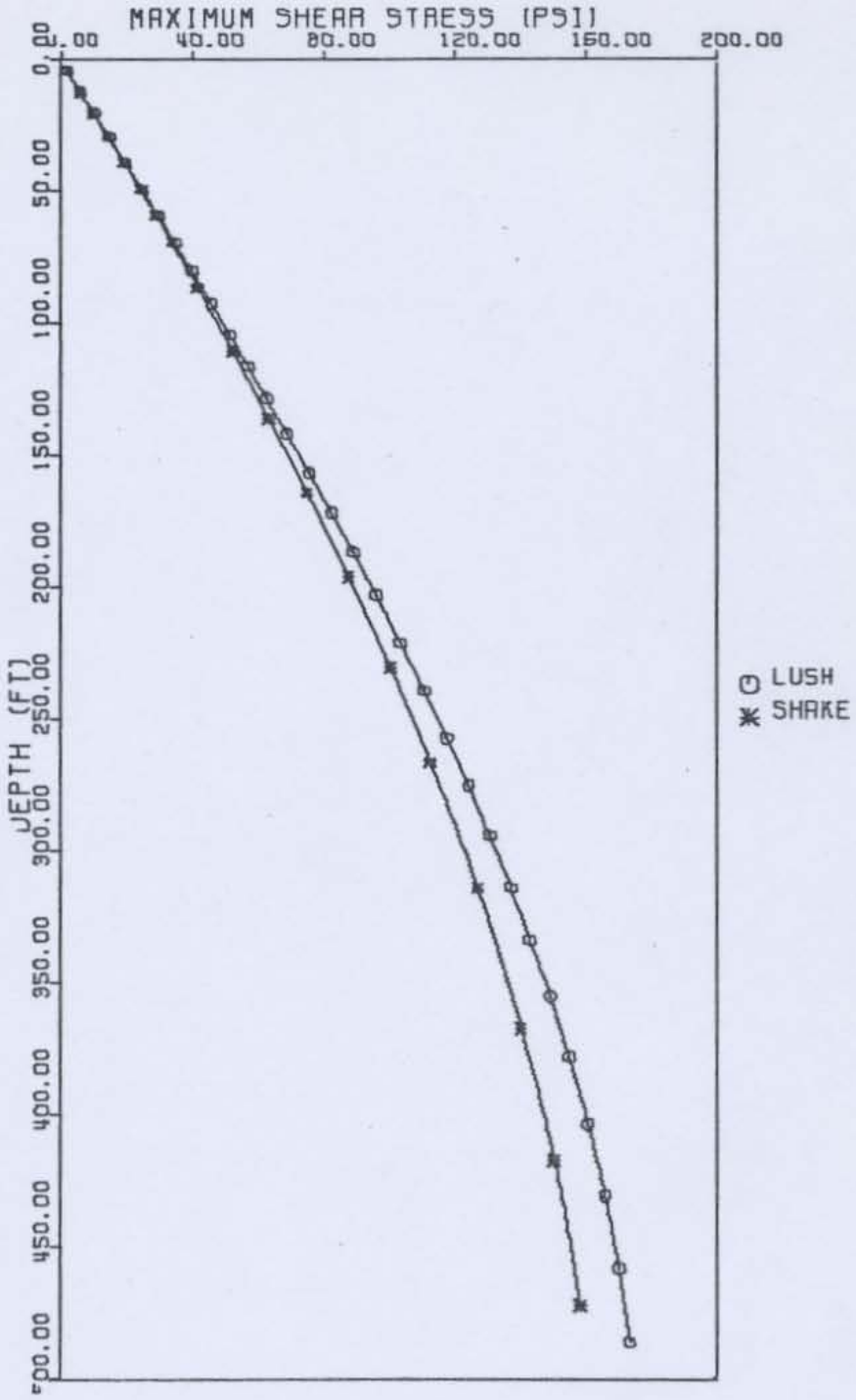

FIG. 4.75 MAXIMUM FREE FIELD SHEAR STRESSES IN ROCK - COMPUTED FROM LUSH AND SHAKE

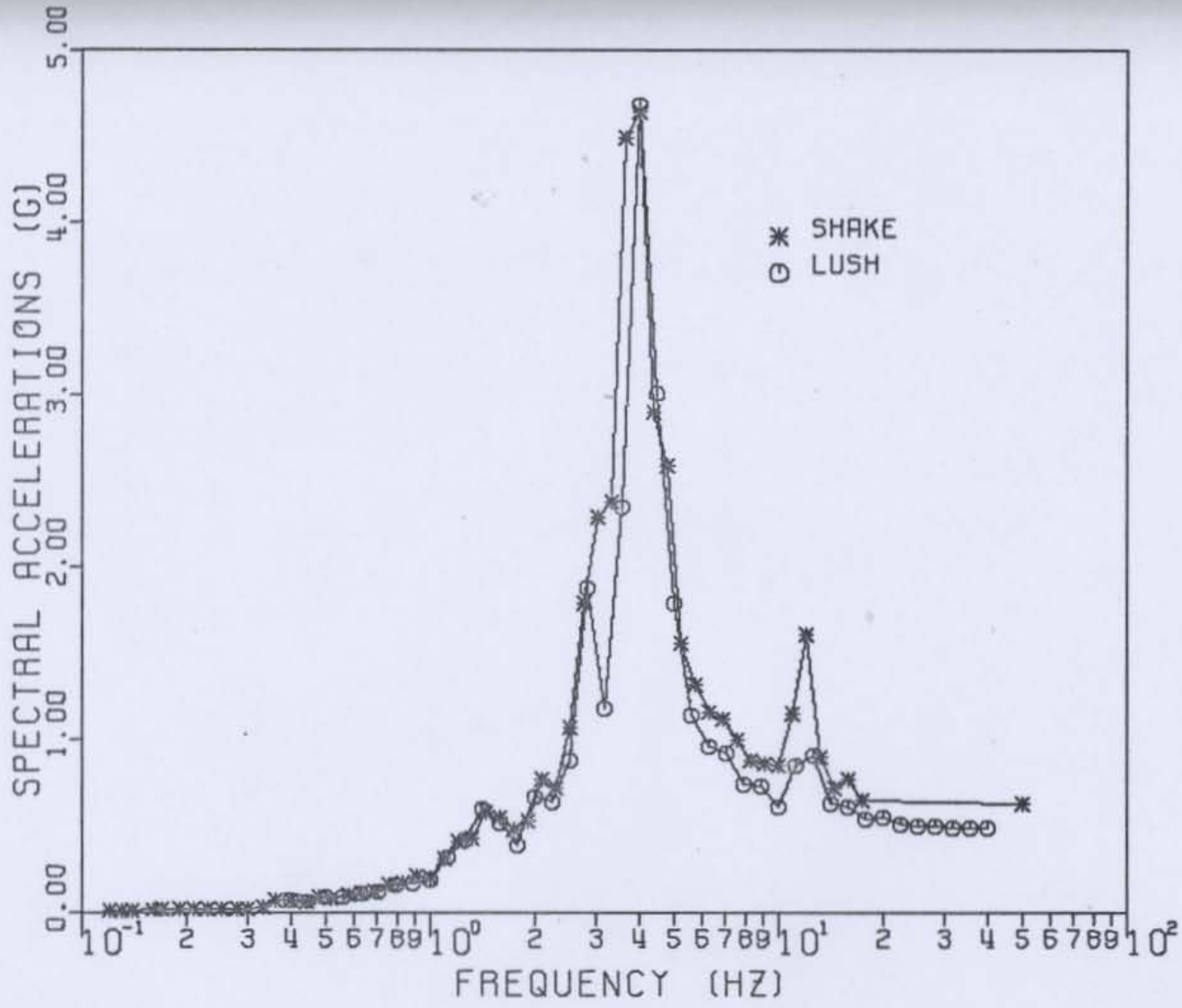

FIG. 4.76 FREE FIELD ACCELERATION SPECTRA AT A DEPTH OF 44 FT - COMPUTED FROM LUSH AND SHAKE - ROCK MEDIUM (SPECTRAL DAMPING=2%)

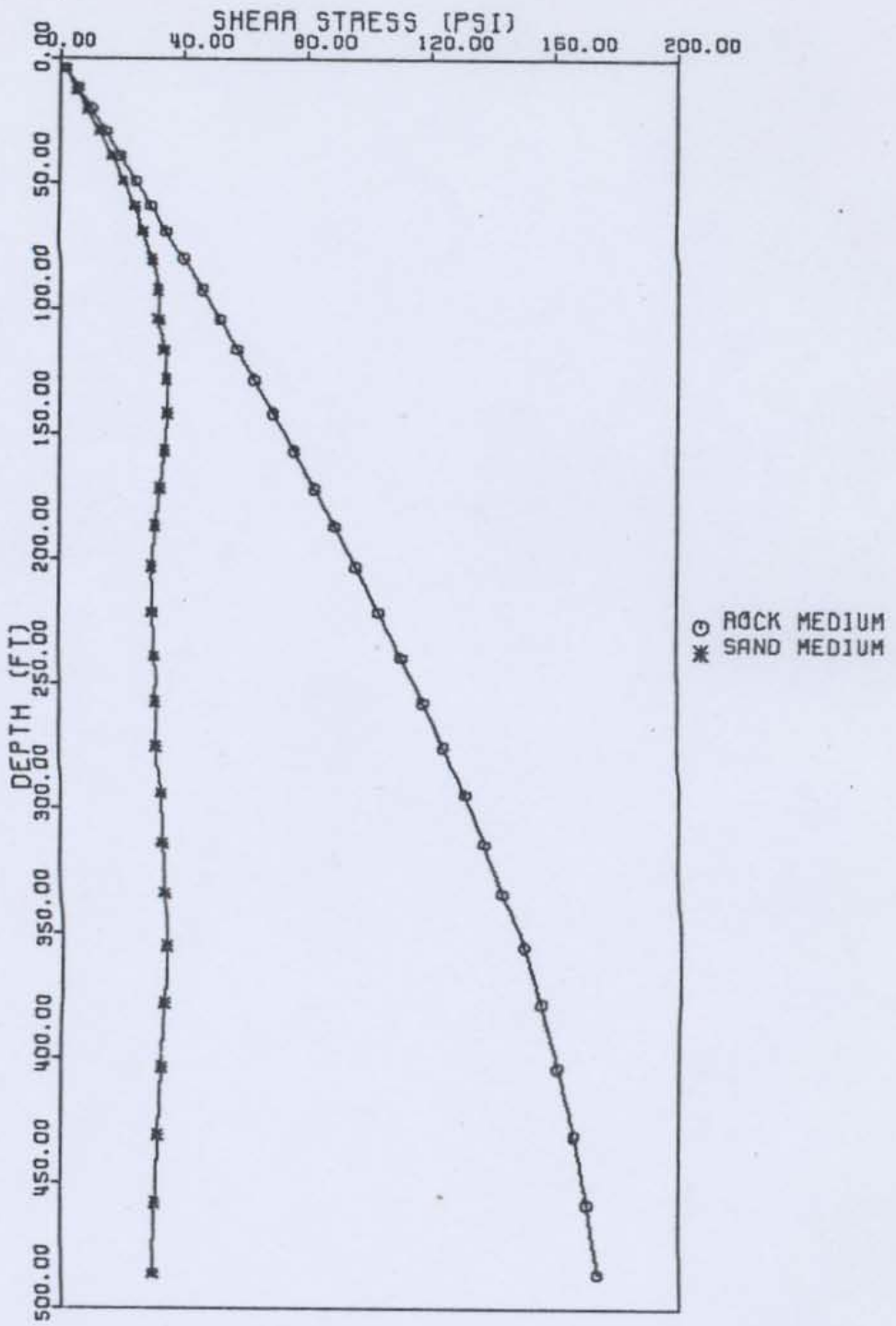

FIG. 4.77 MAXIMUM FREE FIELD SHEAR STRESSES IN ROCK AND SAND MEDIA

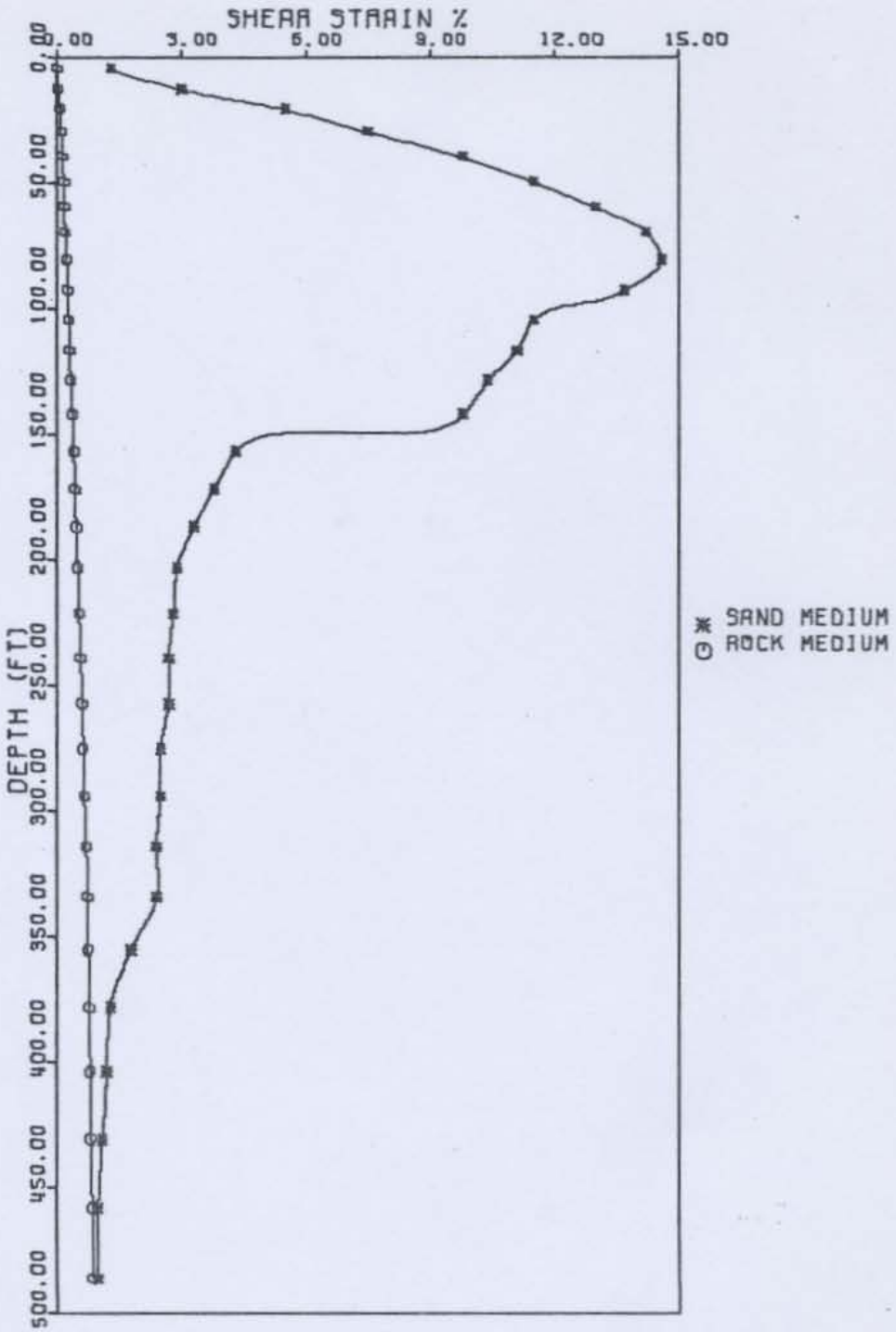

FIG. 4.78 MAXIMUM FREE FIELD SHEAR STRAINS IN ROCK AND SAND MEDIA

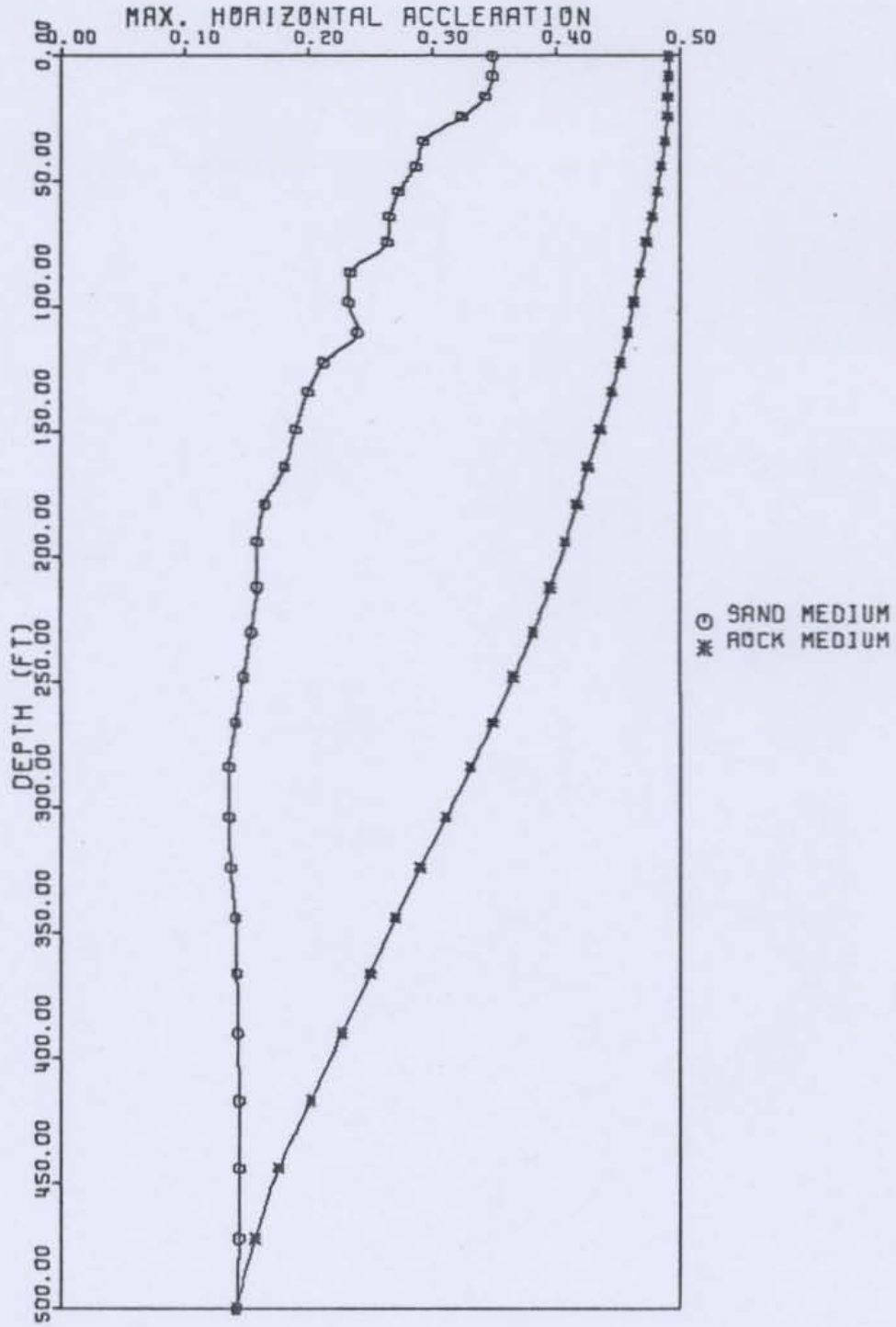

FIG. 4.79 FREE EIELD HORIZONTAL ACCELERATIONS IN THE SAND AND ROCK MEDIA

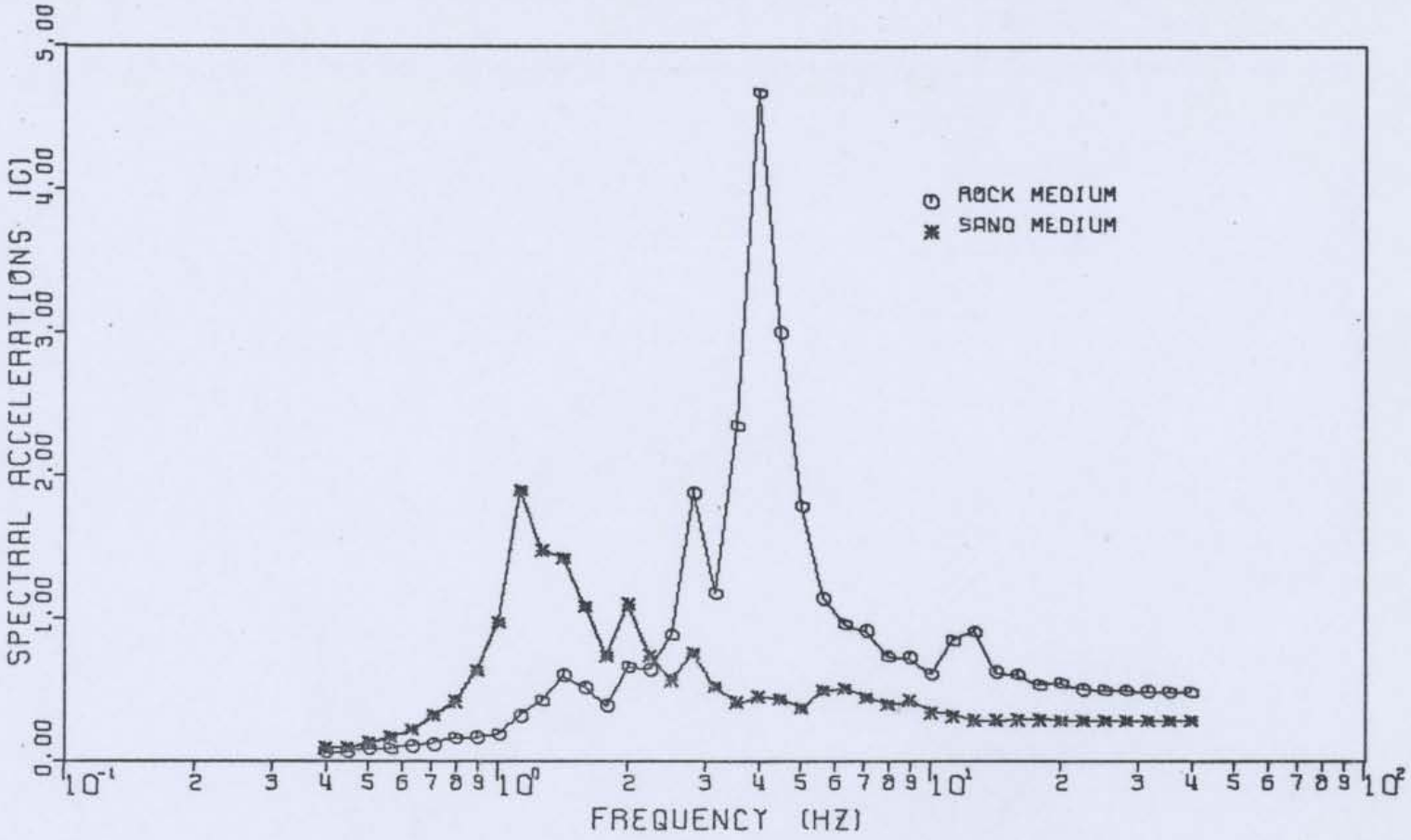

FIG. 4.80 FREE FIELD ACCELERATION RESPONSE SPECTRA AT A DEPTH OF 44 FT FOR ROCK AND SAND MEDIA
(SPECTRAL DAMPING = 2%)

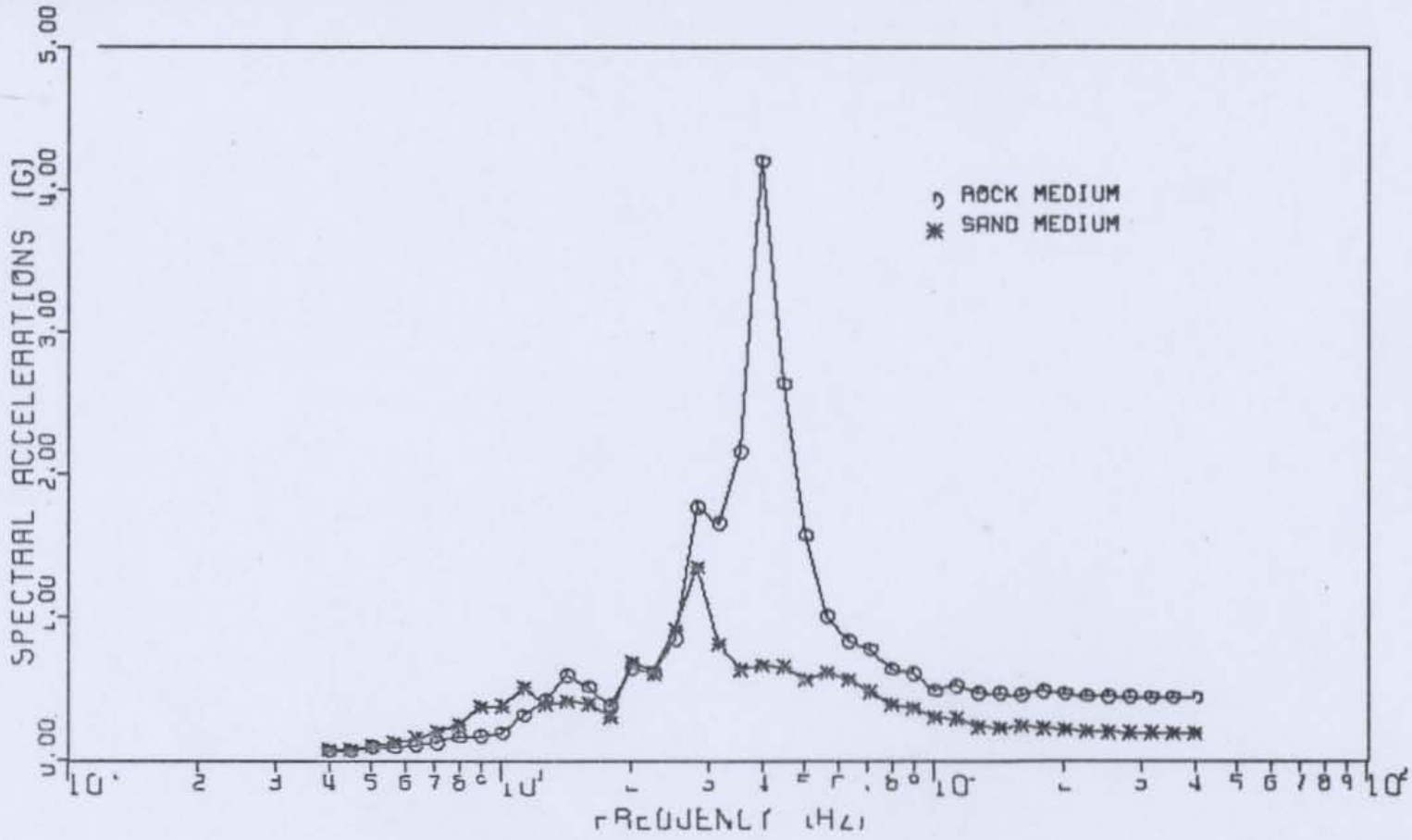

FIG. 4.81 FREE FIELD ACCELERATION RESPONSE SPECTRA AT A DEPTH OF 134 FT FOR ROCK AND SAND MEDIA
(SPECTRAL DAMPING = 2%)

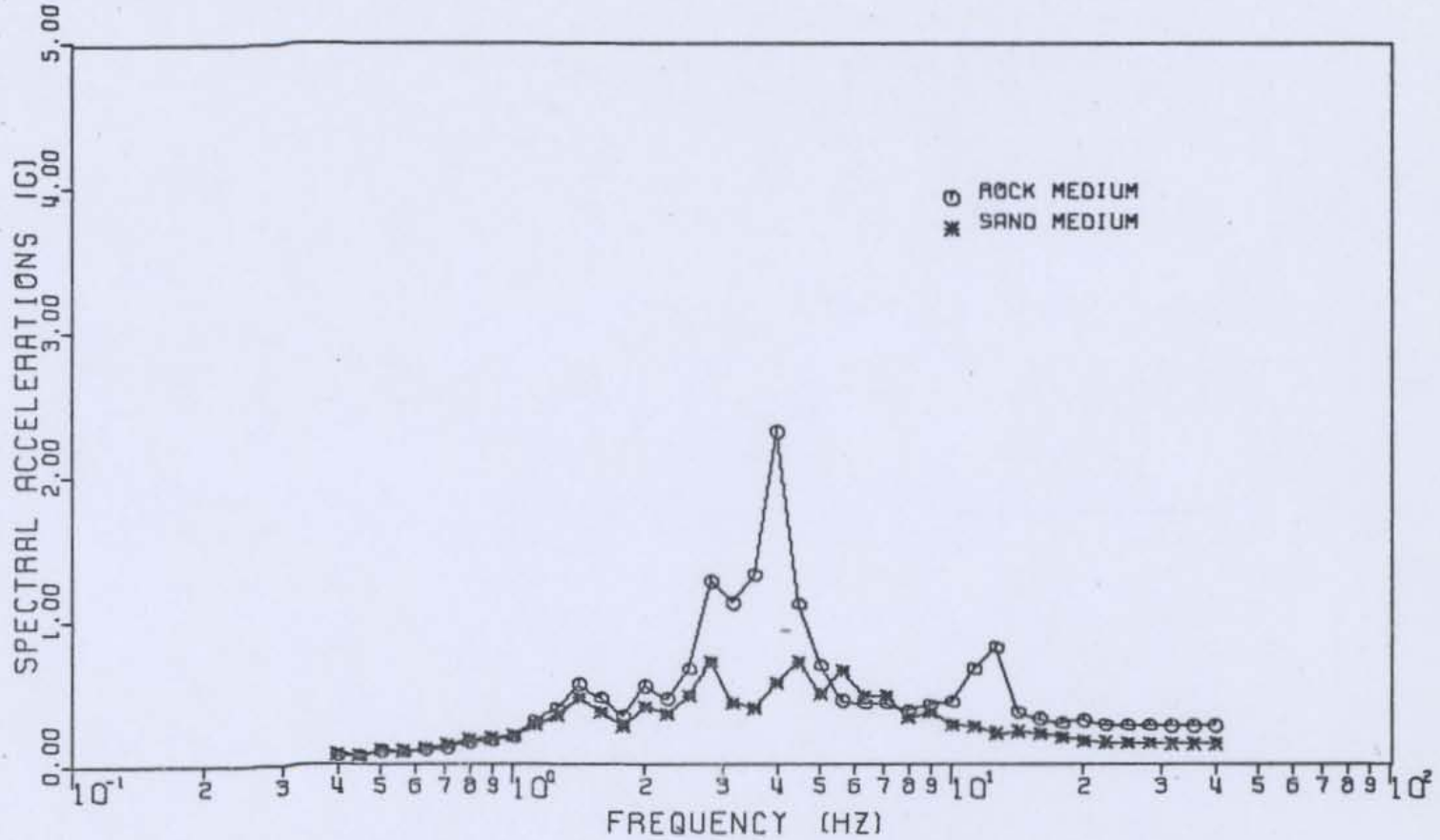

FIG. 4.82 FREE FIELD ACCELERATION RESPONSE SPECTRA AT A DEPTH OF 240 FT FOR ROCK AND SAND MEDIA
(SPECTRAL DAMPING = 2%)

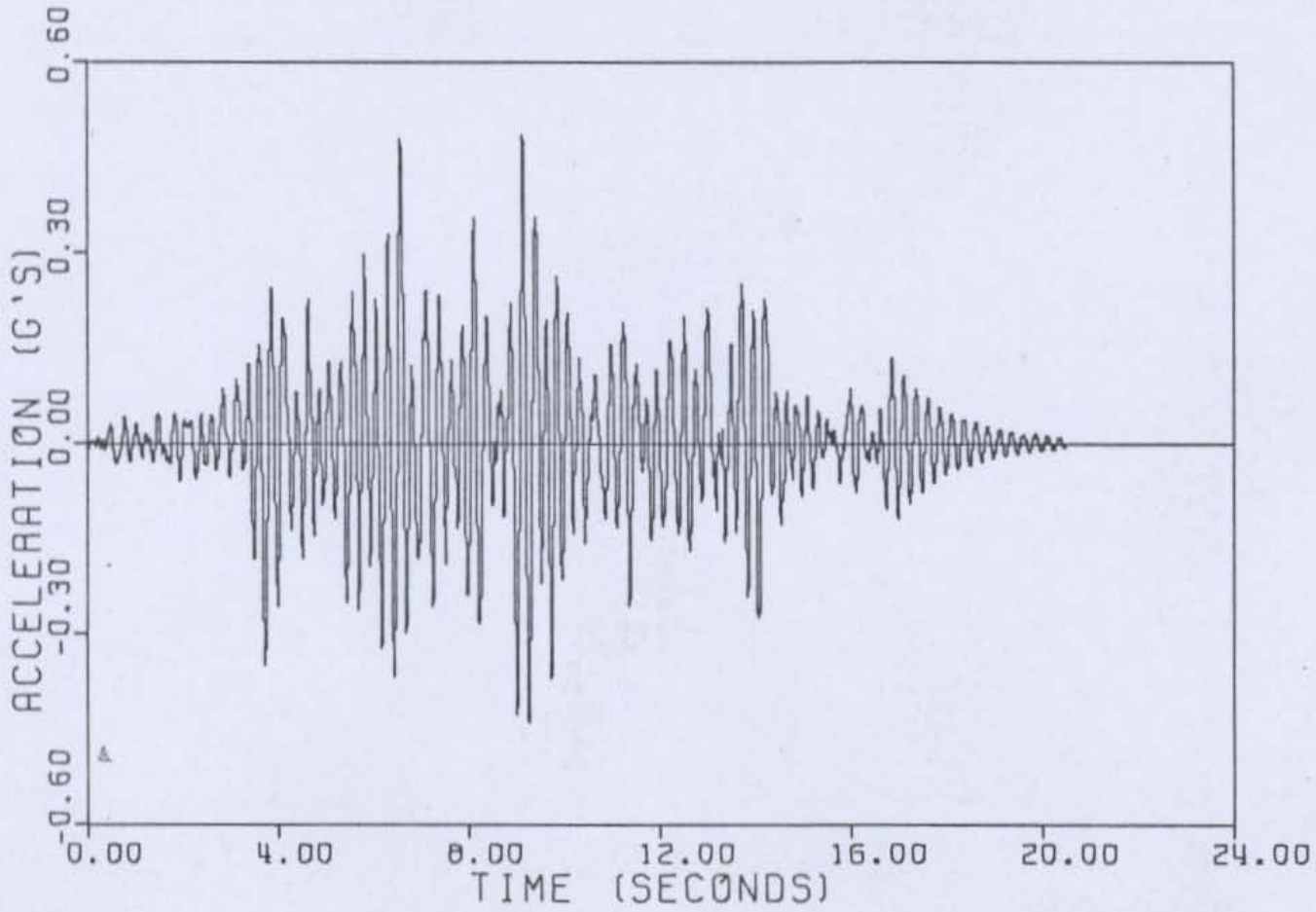

FIG. 4.83 OUTPUT FREE FIELD ACCELERATION AT 44 FT DEPTH IN ROCK MEDIUM

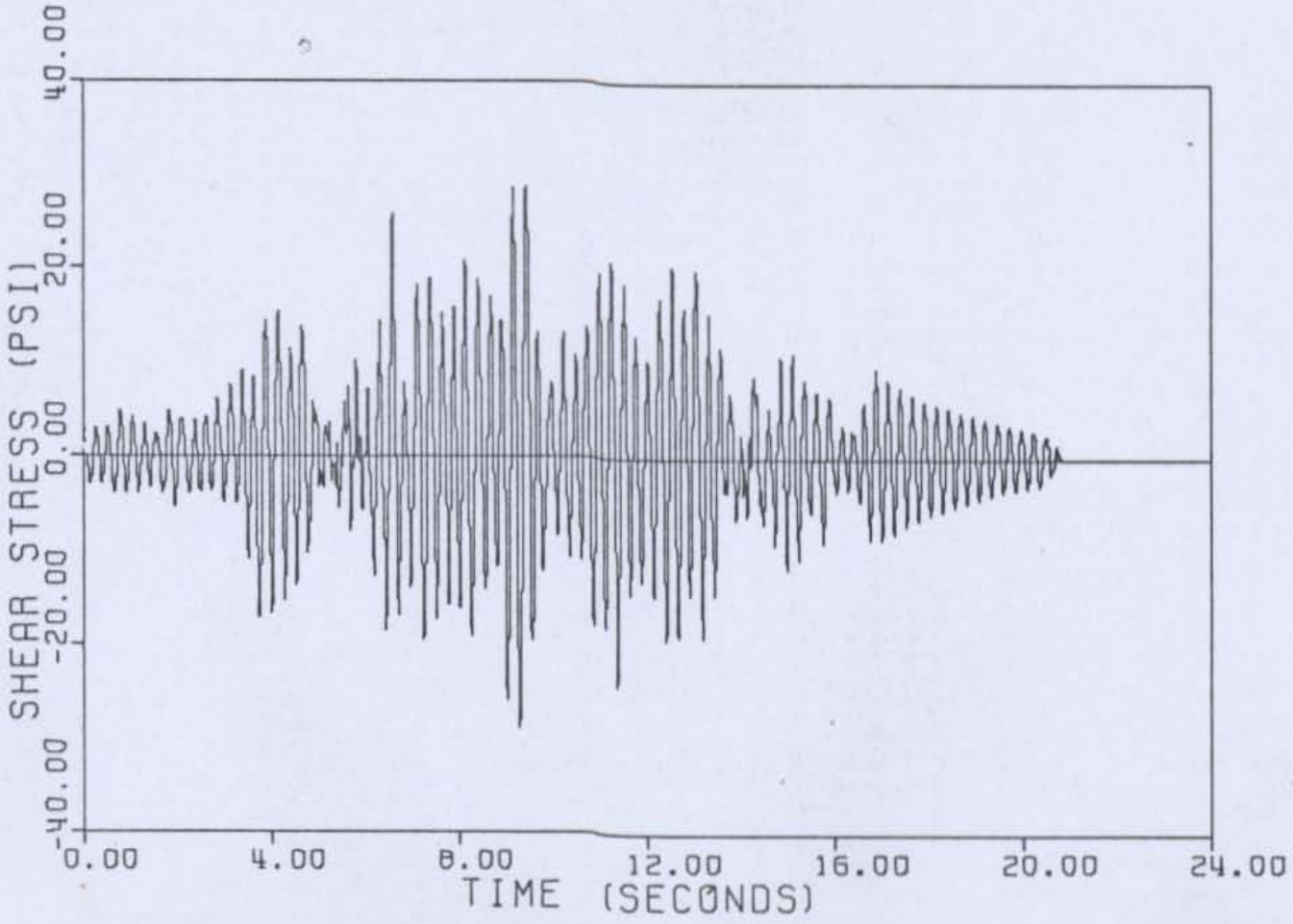

FIG. 4.84 FREE FIELD SHEAR STRESS TIME HISTORY
AT A DEPTH OF 44 FT IN ROCK

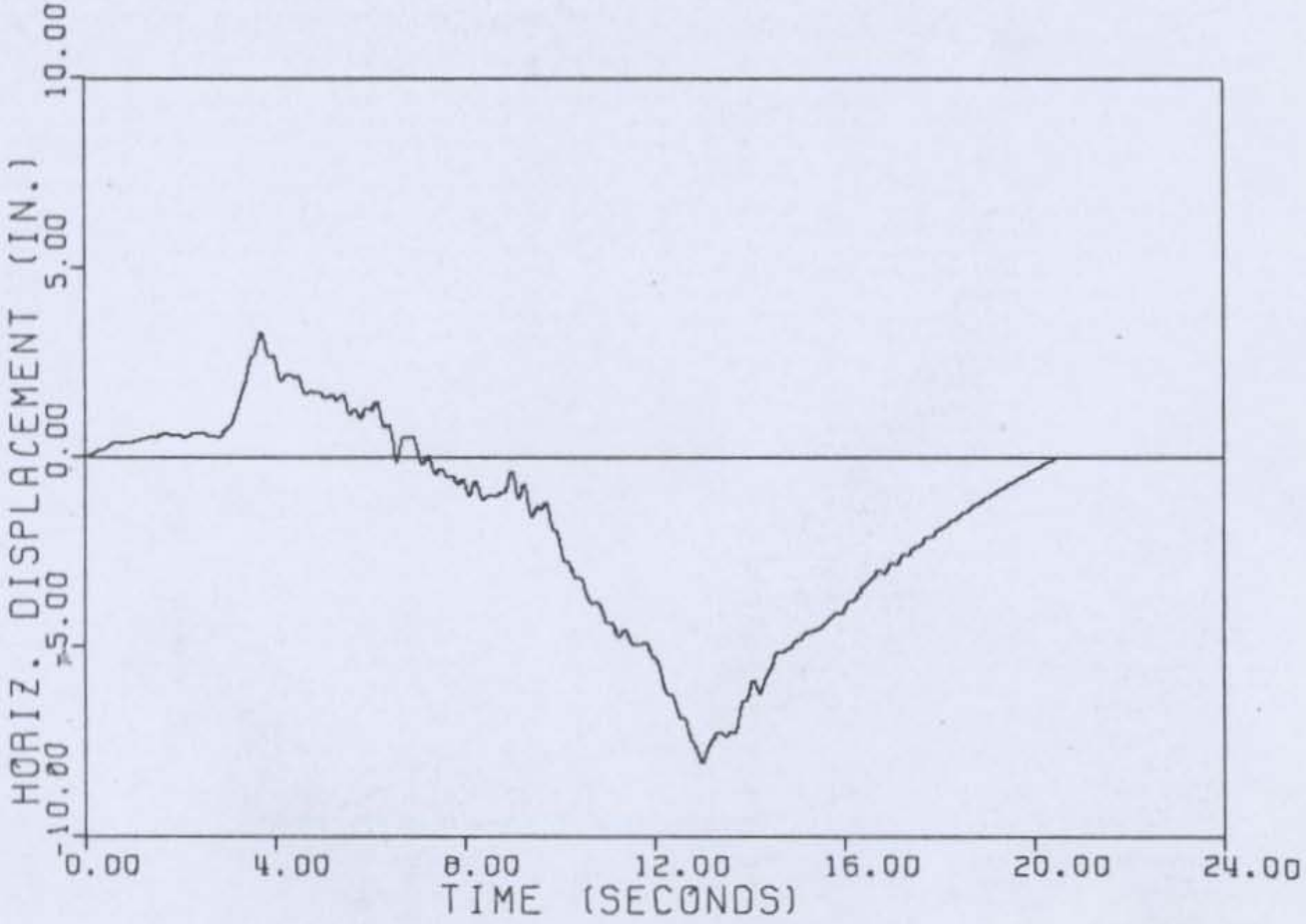

FIG. 4.85 FREE FIELD HORIZONTAL DISPLACEMENT
AT A DEPTH OF 44 FT IN ROCK

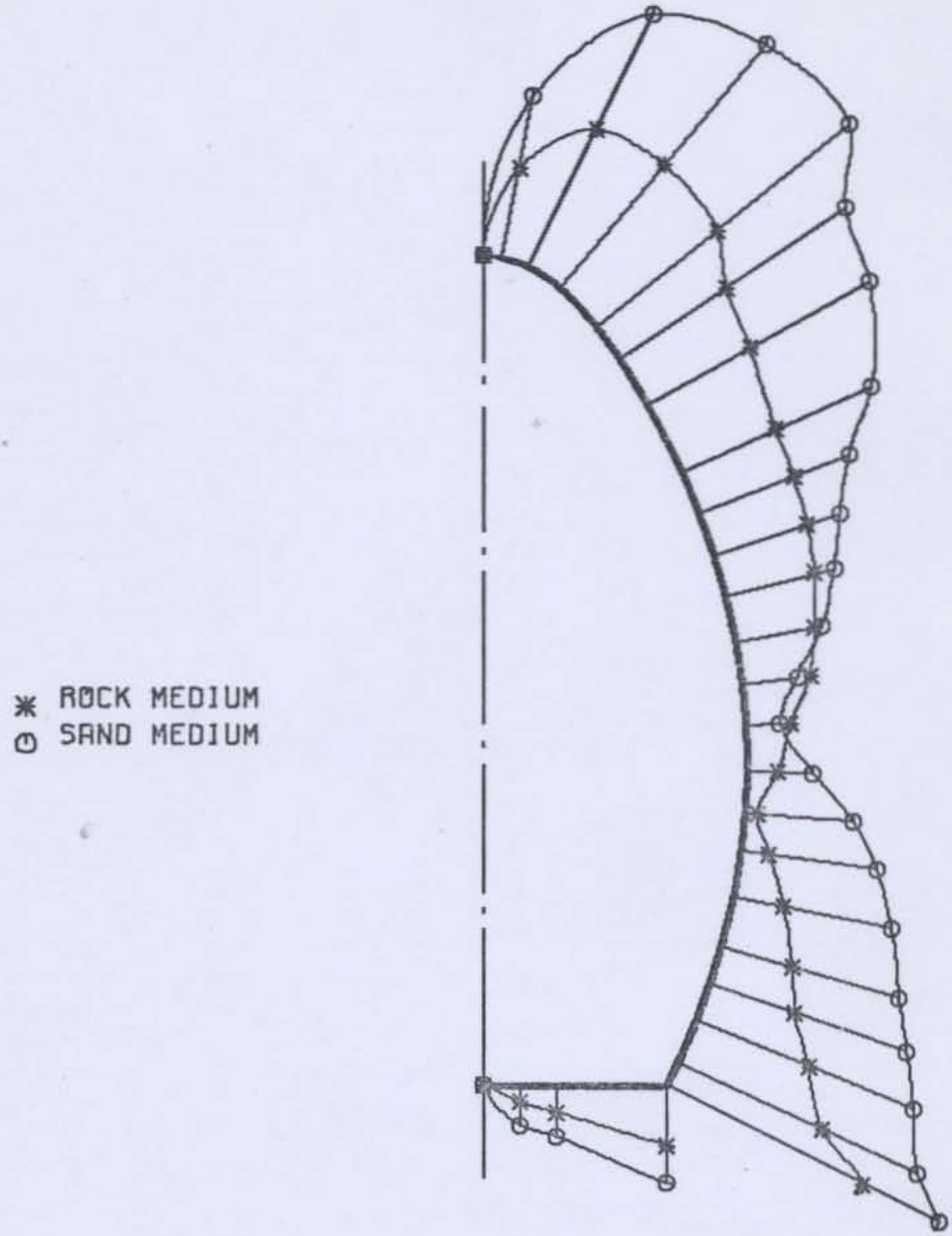

FIG. 4.86 MAXIMUM PRINCIPAL STRESSES IN THE CONTAINMENT FOR ROCK AND SAND MEDIA WITH FOAMED CONCRETE JACKETS
(SCALE: 1 INCH = 400 P.S.I.)

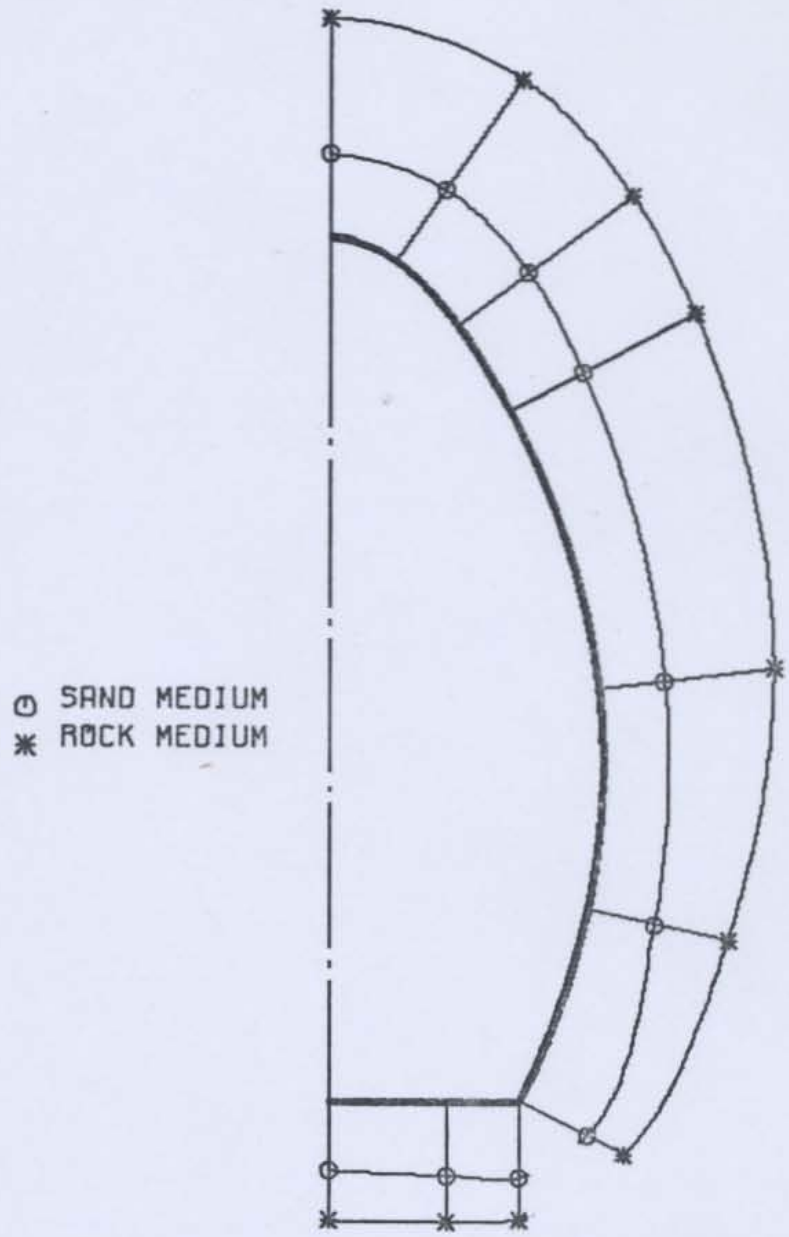

FIG. 4.87 MAXIMUM HORIZONTAL ACCELERATIONS FOR CONTAINMENTS IN ROCK AND SAND MEDIA (SCALE: 1 INCH=0.4G)

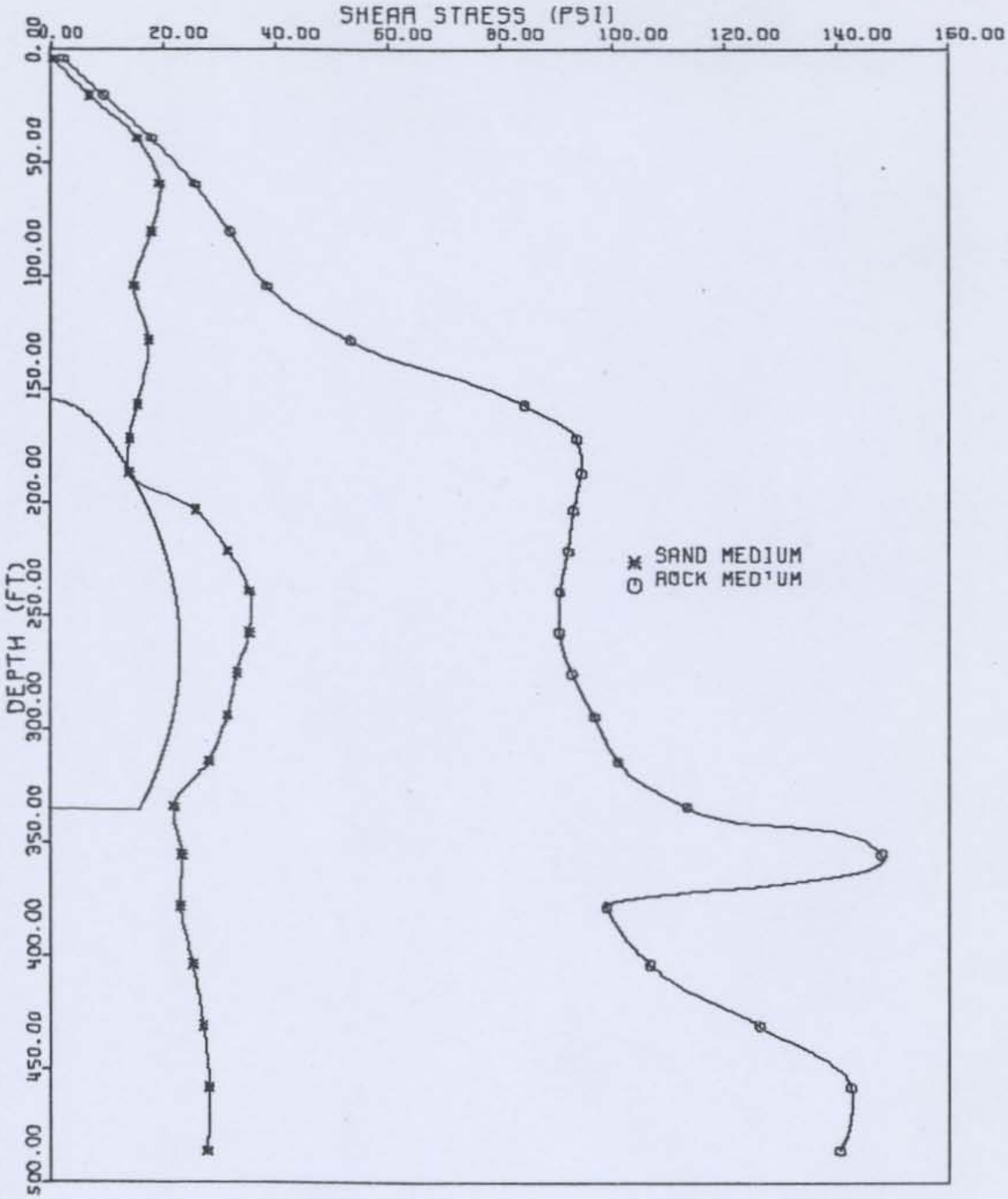

FIG. 4.88 MAXIMUM SHEAR STRESSES IN THE SAND AND ROCK MEDIA AT A VERTICAL PLANE 40 FT AWAY FROM THE CONTAINMENT - FOAMED CONCRETE JACKET

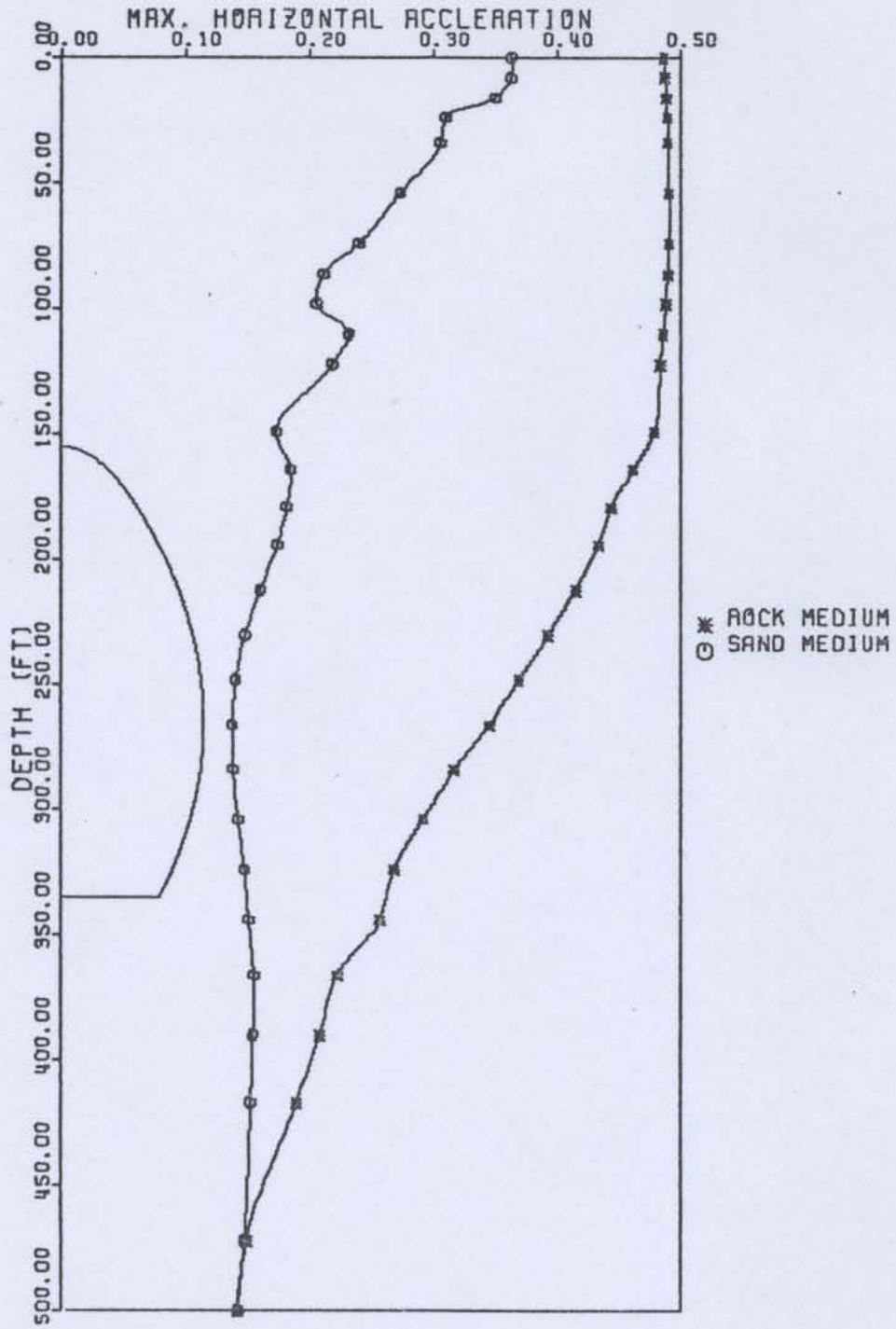

FIG. 4.89 MAXIMUM HORIZONTAL ACCELERATIONS IN SAND AND ROCK MEDIA AT A VERTICAL PLANE 10 FT AWAY FROM THE CONTAINMENT - FOAMED CONCRETE JACKET

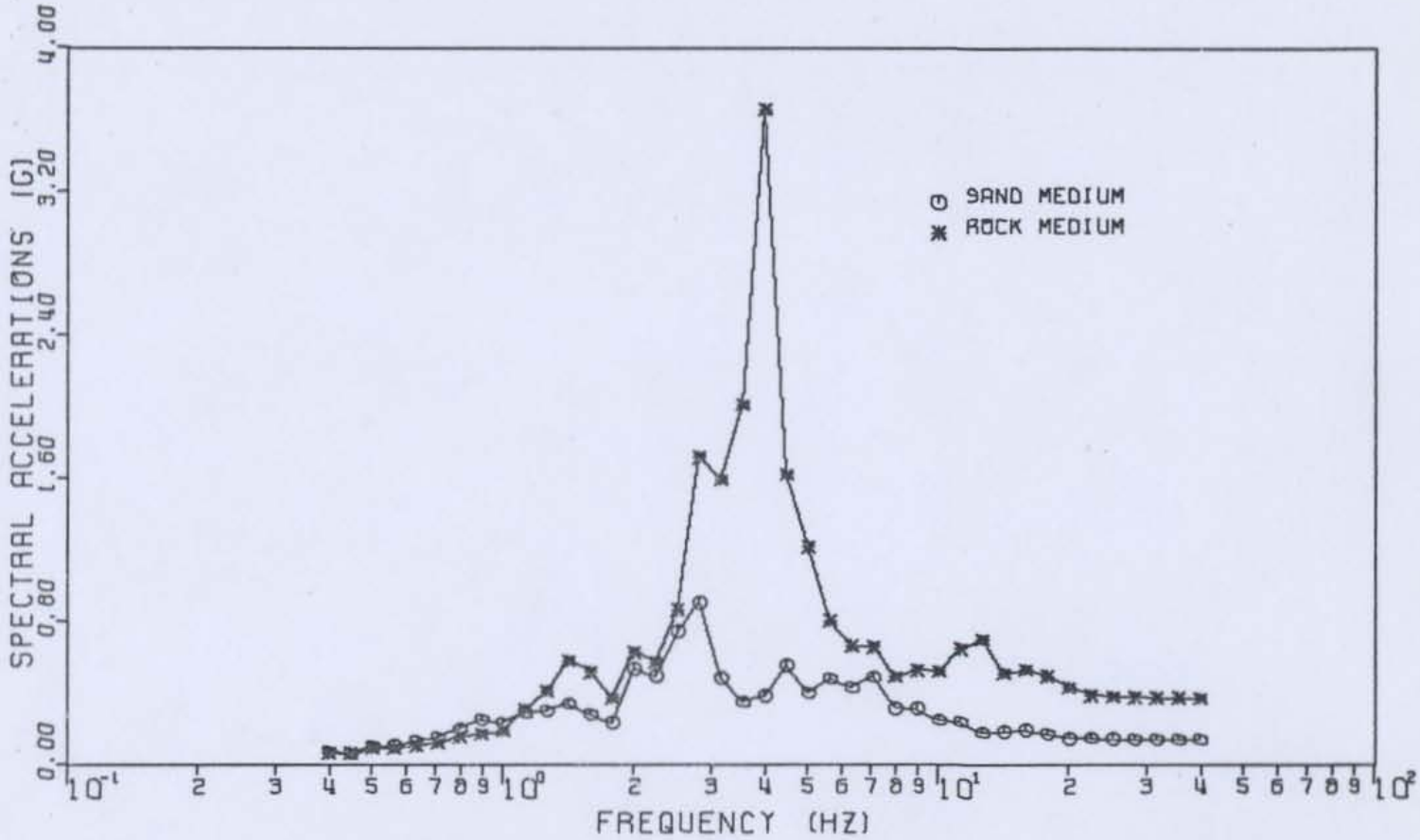

FIG. 4.90 ACCELERATION RESPONSE SPECTRA AT MID-HEIGHT OF THE CONTAINMENT WALL - SAND AND ROCK MEDIA
(SPECTRAL DAMPING = 2%)

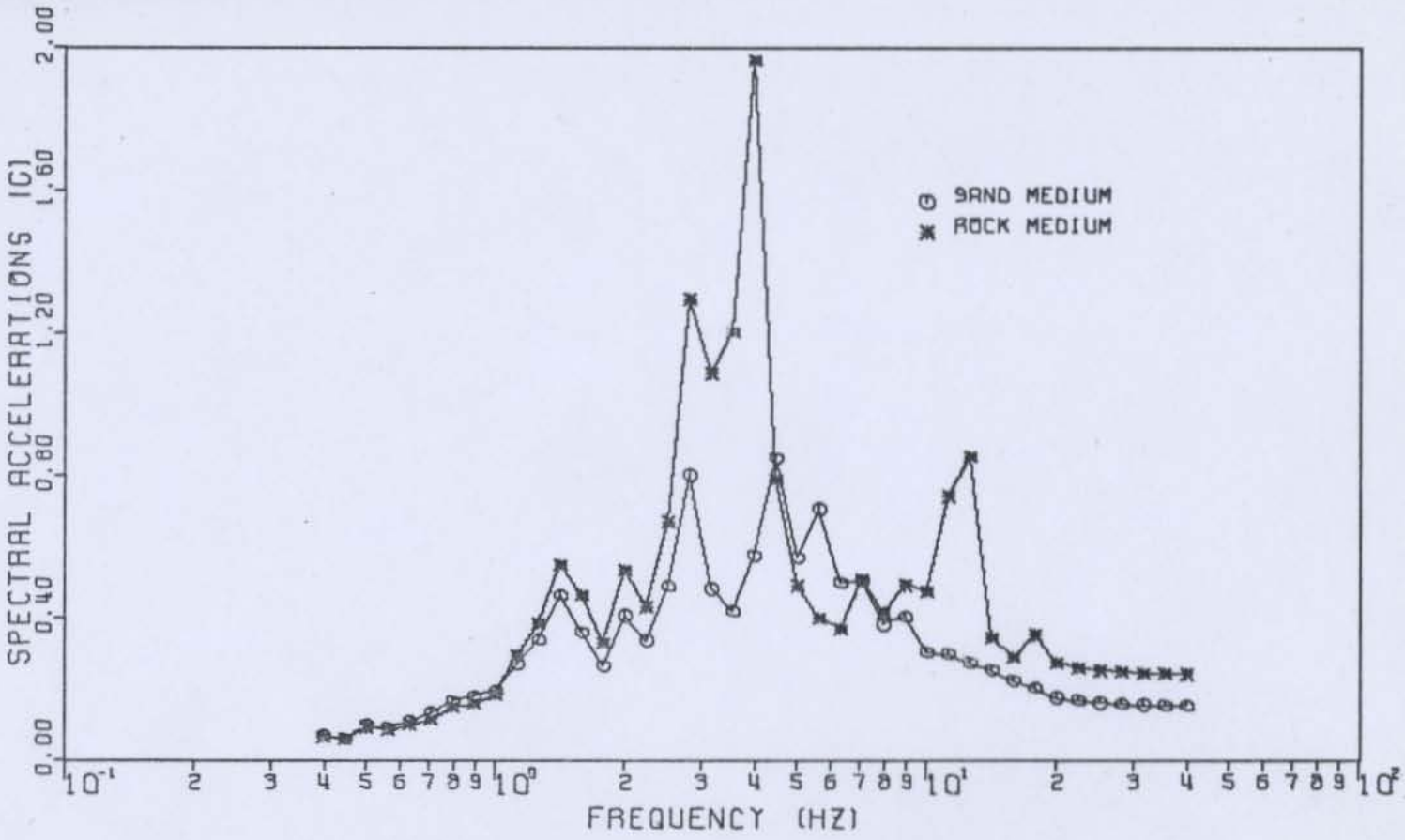

FIG. 4.91 ACCELERATION RESPONSE SPECTRA AT THE CONTAINMENT FOUNDATION MID-POINT - ROCK AND SAND MEDIA
(SPECTRAL DAMPING = 2%)

APPENDIX A

Listing of Sample Plotting Programmes

APPENDIX A

Listing of Sample Plotting Programmes

Twelve computer programmes have been written to plot the results of this investigation using the CALCOMP plotter. Listing of sample programmes used to plot the following results are presented in this Appendix:

1. Acceleration or displacement time history,
2. Acceleration response spectra,
3. Stresses and accelerations in the containment,
4. Stresses and accelerations in the medium, and
5. Finite element meshes.

```
C*********************************************************************
C    PLOTTING OF ACCELERATION OR DISPLACEMENT TIME HISTORY
C*********************************************************************



C*********************************************************************
C         DATA CARDS
C
C     CARD(1)  NO OF POINTS TO BE READ IN TIME HISTORY
C            1-5 NP
C
C     CARD (2) INFORMATION OF HORIZONTAL AXIS
C            1-10 LENGTH OF HORIZ.AXIS
C           11-20 FIRST VALUE ON HORIZ. AXIS
C           21-30 INTERVAL ON HORIZ. AXIS
C
C     CARD (3) TITLE OF HORIZ. AXIS
C            1-76 TITLE
C           77-83 NO OF CHARACTERS(-VE)
C
C     CARD(4) SAME AS CARD 2 FOR VERTICAL AXIS
C
C
C     CARD (5) SAME FOR VERTICAL AXIS (NO.OF CHARACTERS (+VE)
C
C     CARD(6)  1-5 NO OF CURVES TO BE DRAWN ON THE SAME GRAPH
C              16-25  AND 26-35  COORDINATES OF LEGEND
C
C     CARD(7) TITLE OF THE CURVE *** LEAVE IF NSAME=1
C            1-5 CODE FOR SHPE OF MARK
C            6-10 NO OF POINTS FOR SYMBOL
C           11-15 NO OF CHARACTERS IN TITLE
C           16-75 TITLE OF THE CURVE
C
C     CARD (8) AND FOLLOWING CARDS ----THE DATA OF VERTICAL AXIS
C
C     CARD(9)  1-5  NO OF LINES IN THE GRAPH TITLE
C
C     CARD(10)  TITLE OF THE GRAPH
C            1-5  NO OF CHARACTERS IN TITLE
C            6-77 TITLE OF THE GRAPH
C
C  ***************************************************************
C  FOLLOWING CARDS ARE FOR THE NEW PLOTTING (NEW GRAPH)
C*********************************************************************
C
      DIMENSION T(3020),G(3020),IBUF(1000)
      DIMENSION IVT(19),ISMB(15),IHT(19)     ,ICARD(500),ISMP(18)
      CALL PLOTS(IBUF,1000,6)
      CALL PLOT(0.0,0.0,-3)
    1 CONTINUE
      READ(5,100)NP
  100 FORMAT(I5)
      IF(NP.EQ.0)GOTO999
      N=NP
      T(1)=0.0
      DO20 I=2,N
```

```
      T(I)=T(I-1)+0.04883
   20 CONTINUE
C READ HORIZONTAL AXIS INFORMATION
      READ(5,200 ) HXL,FH,DH
  200 FORMAT (3F10.4)
      READ (5,300)IHT,NHT
  300 FORMAT(19A4,I4)
        NHT=-NHT
C READ VERTICAL AXIS INFORMATION
      READ (5,200) VXL,FV,DV
      READ(5,300) IVT,NVT
      CALL AXIS(0.0,0.0,IHT,NHT,HXL,0.0,FH,DH)
      CALL AXIS(0.0,0.0,IVT,NVT,VXL,90.0,FV,DV)
      READ (5,101) NSAME    ,DS ,DSY
  101 FORMAT(I5,2F10.4)
      NDRW=0
      ISM=0
      DO 800 I=1,NSAME
      IF(NSAME.EQ.1)GOTO600
      READ(5,500) ISM,NDRW,NCR,ISMB
  500 FORMAT (3I5,15A4)
  600 NCARD=(NP-1)/8+1
      JJ=0
      DO99IC=1,NCARD
      READ(5,10)(G(JJ+J),J=1,8)
   10 FORMAT(8F10.6 )
      JJ=JJ+8
   99 CONTINUE
      T(N+1)=FH
      G(N+1)=FV
      T(N+2)=DH
      G(N+2)=DV
  400 CALL LINE(T,G,N,1,NDRW,ISM)
      IF(NSAME.EQ.1)GOTO700
      DSX=DS
      DSY=DSY+0.21
      CALL SYMBOL(DSX,DSY,0.07,ISM,0.0,-1)
      DSX=DSX +0.2
  800 CALL SYMBOL(DSX,DSY,0.07,ISMB,0.0,NCR)
C  READ NAME OF EACH CURVE
  700 READ(5,100)NS
      DSY=-0.70
      DO 950 I=1,NS
      READ (5,900)NN,ISMP
  900 FORMAT(I5,18A4)
      DSX=(HXL-0.14*NN)/2.0
      DSY=DSY-0.2
      DIST=VXL/2.0
  950 CALL SYMBOL(DSX,DSY,0.14,ISMP,0.0,NN)
      CALL PLOT (0.0,VXL,3)
      CALL PLOT(HXL,VXL,2)
      CALL PLOT(HXL,0.0,2)
      DIST= HXL+10.0
      CALL PLOT (DIST,0.0,-3)
      GOTO1
  999 CALL PLOT(0.0,0.0,999)
      STOP
      END
```

```
C*****************************************************************
C     PLOTTING OF RESPONSE SPECTRA (LOG X AXIS & LINEAR Y AXIS)
C*****************************************************************



C*****************************************************************
C          DATA CARDS
C
C      CARD(0)  NO OF POINTS TO BE READ .
C             1-5 NP
C
C      CARD(1) VALUES OF FREQUENCY    8F10.4
C*****************************************************************
C THE ABOVE SET OF CARDS ARE TO BE PROVIDED ONLY ONCE EACH RUN
C
C THE FOLLOWING CARDS ARE TO BE REPEATED FOR EACH GRAPH
C*****************************************************************
C      CARD (2) INFORMATION OF HORIZONTAL AXIS
C             1-10 LENGTH OF HORIZ.AXIS
C            11-20 FIRST VALUE ON HORIZ. AXIS
C            21-30 INTERVAL ON HORIZ. AXIS
C
C      CARD (3) TITLE OF HORIZ. AXIS
C             1-76 TITLE
C            77-80 NO OF CHARACTERS(-VE)
C
C      CARD(4) SAME AS CARD 2 FOR VERTICAL AXIS
C
C
C      CARD (5) SAME FOR VERTICAL AXIS (NO.OF CHARACTERS (+VE)
C
C      CARD(6)  1-5 NO OF CURVES TO BE DRAWN ON THE SAME GRAPH
C
C      CARD(7) TITLE OF THE CURVE *** LEAVE IF NSAME=1
C             1-5 CODE FOR SHPE OF MARK
C             6-10 NO OF POINTS FOR SYMBOL
C            11-15 NO OF CHARACTERS IN TITLE
C            16-75 TITLE OF THE CURVE
C
C      CARD (8) AND FOLLOWING CARDS ----THE DATA OF VERTICAL AXIS
C
C      CARD(9)  1-5  NO OF LINES IN THE GRAPH TITLE
C
C      CARD(10)  TITLE OF THE GRAPH
C             1-5  NO OF CHARACTERS IN TITLE
C             6-77 TITLE OF THE GRAPH
C
C  *************************************************************
C  FOLLOWING CARDS ARE FOR THE NEW PLOTTING (NEW GRAPH)
C*****************************************************************
C
      DIMENSION T(3020),G(3020),IBUF(1000)
      DIMENSION IVT(19),ISMB(15),IHT(19)     ,ICARD(500),ISMP(18)
      CALL PLOTS(IBUF,1000,6)
      CALL PLOT(0.0,0.0,-3)
      READ(5,4444)N
 4444 FORMAT(I5)
```

```
      READ(5,330) (T(I),I=1,N)
  330 FORMAT(8F10.4)
C READ HORIZONTAL AXIS INFORMATION
    1 CONTINUE
      READ(5,200 ) HXL,FH,DH
      IF(HXL.EQ.0.0)GOTO999
  200 FORMAT (3F10.4)
      READ (5,300)IHT,NHT
      NHT=-NHT
  300 FORMAT(19A4,I4)
C READ VERTICAL AXIS INFORMATION
      READ (5,200) VXL,FV,DV
      READ(5,300) IVT,NVT
      CALLLGAXS(0.0,0.0,IHT,NHT,HXL,0.0,FH,DH)
       NCHECK=    1
        WRITE(6,1001) NCHECK
      CALL AXIS(0.0,0.0,IVT,NVT,VXL,90.0,FV,DV)
       NCHECK=        2
         WRITE(6,1001) NCHECK
      READ (5,101) NSAME    ,DS ,DSY
  101 FORMAT(I5,2F10.4)
      NDRW=2
      ISM=1
      DO 800II=1,NSAME
      IF(NSAME.EQ.1)GOTO600
      READ(5,500) ISM,NDRW,NCR,ISMB
  500 FORMAT (3I5,15A4)
  600 READ(5,330) (G(I),I=1,N)
   99 CONTINUE
      T(N+1)=FH
      G(N+1)=FV
      T(N+2)=DH
      G(N+2)=DV
      M=N+2
      WRITE(6,330)(T(I),I=1,M)
  400 CALLLGLIN(T,G,N,1,NDRW,ISM,-1)
       NCHECK=  3
         WRITE(6,1001) NCHECK
      IF(NSAME.EQ.1)GOTO700
      DSX=DS
      DSY=DSY+0.21
      CALL SYMBOL(DSX,DSY,0.10,ISM,0.0,-1)
       NCHECK=        4
         WRITE(6,1001) NCHECK
      DSX=DSX +0.2
  800 CALL SYMBOL(DSX,DSY,0.10,ISMB,0.0,NCR)
       NCHECK=        5
         WRITE(6,1001) NCHECK
C  READ NAME OF EACH CURVE
  700 READ(5,100)NS
  100 FORMAT(I5)
      DSY=-0.9
      DO 950 I=1,NS
      READ (5,900)NN,ISMP
  900 FORMAT(I5,18A4)
      DSX=(HXL-0.15*NN)/2.0
      DSY=DSY-0.24
      DIST=VXL/2.0
  950 CALL SYMBOL(DSX,DSY,0.15,ISMP,0.0,NN)
```

```
      NCHECK=        6
        WRITE(6,1001) NCHECK
      CALL PLOT (0.0,VXL,3)
       NCHECK=       7
        WRITE(6,1001) NCHECK
      CALL PLOT(HXL,VXL,2)
       NCHECK=       8
        WRITE(6,1001) NCHECK
      CALL PLOT(HXL,0.0,2)
       NCHECK=       9
        WRITE(6,1001) NCHECK
      DIST= HXL+10.0
      CALL PLOT (DIST,0.0,-3)
      GOTO1
  999 CALL PLOT(0.0,0.0,999)
 1001 FORMAT     ( '    NCHECK= ',I5)
      STOP
      END
```

```
C*****************************************************************
C   PLOTTING OF STRESSES IN THE HIGH HORSESHOE CONTAINMENT
C*****************************************************************
C
C
C
      DIMENSION IBUF(1000),ORD(30),X(30),Y(30),XN(32),YN(32),T(30),
     * IST(15)
      FX(X)=180. -0.025*X*X
      FX1(X)= -0.05*X
      FY(Y)= 40. +0.5*Y-1.0/280.0*Y*Y
      FY1(Y)= 1.0/(0.5-1.0/140.*Y)
      CALL PLOTS(IBUF,1000,6)
      CALL FACTOR(0.025)
      CALL PLOT(0.0,0.0,-3)
      READ (5,60) NPRB
      DO 333 IP=1,NPRB
      CALL PLOT (400.,0.0,-3)
      CALLCURVX(.01,40.0,180.0,0.0,-0.025,2.0,0.0,0.0,0.0,0.0,0.0,0.0)
      A=-1./280.0
      CALL CURVY(.01,140.0,40.0,0.0,0.0,0.5,1.0,A,2.0,0.0,0.0,0.0)
      CALLPLOT(0.0,0.0,3)
      CALL PLOT(40.0,0.0,2)
  333 CONTINUE
      CALL PLOT(0.0,0.0,-3)
  707 CONTINUE
      READ (5,5) NX,NY,NH
      IF(NX  .EQ.0) GOTO99
    5 FORMAT(3I5)
      READ(5,10) (X(I),I=1,NX)
   10 FORMAT(8F10.4)
      READ(5,10) (Y(I+NX),I=1,NY)
      READ(5,10)(X(I+NX+NY),I=1,NH)
      DO 20 I=1,NX
      T(I)=FX1(X(I))
   20 Y(I)= FX(X(I))
      DO30 J=1,NY
      I=J+NX
      T(I)=FY1(Y(I))
   30 X(I)=FY(Y(I))
    1 CONTINUE
      READ (5,40) FACT
   40 FORMAT(F10.4)
      IF(FACT.EQ.0.0)GOTO707
      CALL PLOT(0.0,200.0,3)
      CALL PLOT(0.0,-20.0,2)
      CALL FACTOR(1.00)
      N=NX+NY
      READ(5,60) NSAME
   60 FORMAT( I5)
      NDRW=1
      ISM=1
      DY=2.25
      DO 100 II=1,NSAME
      IF(NSAME.EQ.01) GOTO70
      READ(5,50) ISM,NDRW,NCR,IST
   50 FORMAT(3I5,15A4)
      DX=-0.1*(NCR)
   70 N1=N+NH
```

```
      READ(5,10)( CRD(I),I=1,N1)
      DO75I=1,N1
   75 CRD(I)=ORD(I)*FACT
      YN(1)= 180.0 + CRD(1)
      XN(1)=0.0
      DO 80J=2,N
      ALFA= ATAN2 (1.0,1./T(J))
      YN(J)= Y(J)- CRD(J)*COS(ALFA)
      XN(J) = X (J) +CRD(J)* SIN(ALFA)
   80 CONTINUE
      DO 120 I=1,NH
      J=I+N
      XN(J)= X(J)
      Y(J)=0.0
  120 YN(J) =-CRD(J)
      XN(N1+1)=0.0
      XN(N1+2)=40.0
      YN(N1+1)=0.0
      YN(N1+2)=40.0
      CALL FLINE(XN,YN,-N1,1,NDRW,ISM)
      IF(NSAME.EQ.1) GOTO130
      DY=DY-0.2
C
      CALL SYMBOL(DX,DY,0.1,ISM,0.,-1 )
      DX=DX+0.2000
      CALL SYMBOL(DX,DY,0.1,IST,0.0,NCR)
  100 CONTINUE
  130 CALL FACTOR(0.025)
      DO110I=1,N1
      CALL PLOT(X(I),Y(I),3)
  110 CALL PLOT(XN(I),YN(I),2)
      READ (5,60) NS
      IF(YN(N)-YN(N+1))289,289,288
  288 JL=N+1
      GOTO290
  289 JL=N
  290 CONTINUE
      DY=YN(JL)-20.0
      DO 205 I=1,NS
      READ (5,210) IST,NN
      WRITE(6,210) IST,NN
  210 FORMAT(15A4,I5)
      DX=-40.*(0.12*NN/2.0 )
      DY=DY-7.2
  205 CALL SYMBOL(DX,DY,4.8,IST,0.0,NN)
      CALL PLOT(-400.,0.0,-3)
      GOTO1
   99 CALL PLOT(0.0,0.0,999)
      STOP
      END
```

```
C*****************************************************************
C   PLOTTING OF SHEAR STRESSES AND ACCELERATIONS IN SOIL
C*****************************************************************
C
C
      DIMENSION T(3020),G(3020),IBUF(1000)
      DIMENSION IVT(19),ISMB(15),IHT(19)     ,ICARD(500),ISMP(18)
      CALL PLOTS(IBUF,1000,6)
      CALL PLOT(0.0,0.0,-3)
  777 CONTINUE
      READ(5,909)N,FFF
  909  FORMAT(I5,F10.5)
  100 FORMAT(I5)
      IF(N .EQ.0)GOTO999
      READ(5,20) (G(II),II=1,N)
   20 FORMAT (8F10.4)
C READ HORIZONTAL AXIS INFORMATION
      READ(5,200 ) HXL,FH,DH
  200 FORMAT (3F10.4)
      READ (5,300)IHT,NHT
  300 FORMAT(19A4,I4)
C READ VERTICAL AXIS INFORMATION
      READ (5,200) VXL,FV,DV
      READ(5,300) IVT,NVT
    1 CONTINUE
      CALL FACTOR(0.7)
      DIST= HXL+10.0
      CALL PLOT(DIST,0.00,-3)
      CALL AXIS(0.0,VXL,IHT,NHT,HXL,0.0,FH,DH)
      CALL AXIS(0.0,0.0,IVT,NVT,VXL,90.0,FV,DV)
      NDRW=1
      ISM=1
      READ (5,101) NSAME    ,DS ,DSY
      IF(NSAME.EQ.0)GOTO777
  101 FORMAT(I5,2F10.4)
      DO 800 I=1,NSAME
      IF(NSAME.EQ.1)GOTO600
      READ(5,500) ISM,NDRW,NCR,ISMB
  500 FORMAT (3I5,15A4)
  600 CONTINUE
      READ (5,20) (T(K),K=1,N)
      DO 292 JO=1,N
  292 T(JO)= T(JO)/FFF
   99 CONTINUE
      T(N+1)=FH
      G(N+1)=FV
      T(N+2)=DH
      G(N+2)=DV
      M=-N
  400 CALLFLINE(T,G,M,1,NDRW,ISM)
      IF(NSAME.EQ.1)GOTO700
      DSX=DS
      DSY=DSY-0.21
      CALL SYMBOL(DSX,DSY,0.12,ISM,0.0,-1)
      DSX=DSX +0.2
  800 CALL SYMBOL(DSX,DSY,0.12,ISMB,0.0,NCR)
C  READ NAME OF EACH CURVE
  700 READ(5,100)NS
      DSY=-0.70
```

```
      CALL PLOT (0.0,0.0,3)
      CALL PLOT(HXL,0.0,2)
      CALL PLOT(HXL,VXL,2)
      DO 950 I=1,NS
      READ (5,900)NN,ISMP
      WRITE(6,900)NN,ISMP
  900 FORMAT(I5,18A4)
      DSX=0.5*(HXL-0.17*NN)
      DSY=DSY-0.27
  950 CALL SYMBOL(DSX,DSY,0.17,ISMP,0.0,NN)
      CALL FACTOR(.014)
      CALL PLOT(0.,165.,-3)
      CALLCURVX(.01,40.0,180.0,0.0,-0.025,2.0,0.0,0.0,0.0,0.0,0.0,0.0)
      A=-1./280.0
      CALL CURVY(.01,140.0,40.0,0.0,0.5,1.0,A,2.0,0.0,0.0)
      CALLPLOT(0.0,0.0,3)
      CALL PLOT(40.0,0.0,2)
      CALL PLOT(0.0,-165.,3)
      GOTO1
  999 CALL PLOT(0.0,0.0,999)
      STOP
      END
```

```
C*********************************************************************
C    PLOTTING OF FINITE ELEMENT MESH OF THE MODEL
C*********************************************************************



      DIMENSION IBUF(1000)
      CALL PLOTS(IBUF,1000,6)
      CALL PLOT(0.,0.,-3)
    1 CONTINUE
      READ(5,10)N,FACT,ICODE,DDD
   10 FORMAT(I5,F10.5,I5,F10.5)
      IF(N.EQ.0) GOTO99
      CALL FACTOR(FACT)
      IF(ICODE.EQ.2) GOTO 333
      DO 20 I=1,N
      READ(5,30) X1,Y1
      READ(5,30) X2,Y2
   30 FORMAT(5X,2F10.3)
      IF(X1.EQ.1050.)X1=1010.
      IF(X2.EQ.1050.0) X2=1010.
      IF(ICODE.EQ.0) X2=1.5*X2
      CALL PLOT(X1,Y1,3)
      CALL PLOT(X2,Y2,2)
20    CONTINUE
      IF (ICODE.NE.1) GOTO88
40    CALL PLOT(0.,DDD ,-3)
      CALLCURVX(.01,40.0,180.0,0.0,-0.025,2.0,0.0,0.0,0.0,0.0,0.0)
      A=-1./280.0
      CALL CURVY(.01,140.0,40.0,0.0,0.5,1.0,A,2.0,0.0,0.0)
      CALLPLOT(0.0,0.0,3)
      CALL PLOT(40.0,0.0,2)
   88 CONTINUE
      CALL PLOT(2000.,-DDD,-3)
      GOTO1
  333 CONTINUE
      DO 444I=1,N
      CALLCURVX(.01,40.0,180.0,0.0,-0.025,2.0,0.0,0.0,0.0,0.0,0.0)
      A=-1./280.0
      CALL CURVY(.01,140.0,40.0,0.0,0.5,1.0,A,2.0,0.0,0.0)
      CALLPLOT(0.0,0.0,3)
      CALL PLOT(40.0,0.0,2)
      CALLPLOT(600.0,0.,-3)
444   CONTINUE
      GOTO1
   99 CONTINUE
      CALL PLOT(0.,0.,999)
      STOP
      END
```

APPENDIX B

Brief Description of LUSH and SHAKE

(Summarized from Refs. 62 and 81)

B.1 PROGRAMME LUSH [62]

General

The computer programme LUSH was developed in the Department of Civil Engineering at the University of California, Berkeley, California by a group of faculty members and graduate students of geotechnical engineering. LUSH is basically a finite element programme designed for earthquake analysis of plane structures of the type shown in Fig. B.1. The programme, in an approximate manner, takes into account the strong nonlinear effects which occur in soil masses subjected to strong earthquake motions. This is achieved by a combination of the equivalent linear method described by Ref. 45 and the method of complex response with complex moduli. The latter method makes it possible to work with different damping properties in all elements of the finite element model, even in the high frequency ranges which must be considered in the study of soil-structure interaction for nuclear power plants.

The physical problem which can be solved by LUSH is illustrated by Fig. B.1. The mathematical model consists of plane quadrilateral or triangular elements. The model is excited by a specified acceleration time history at the rigid base. The base does not have to be horizontal and the specified motion can have any direction in the plane of the model. A special provision makes it possible to specify that selected nodal points can move only in the horizontal or the vertical direction and it is also possible to connect any pair of nodal points by a rigid element such that they will have the same displacement at all times.

The stiffness and damping of the materials in the model can be chosen to be constant or to vary with the effective shear strain

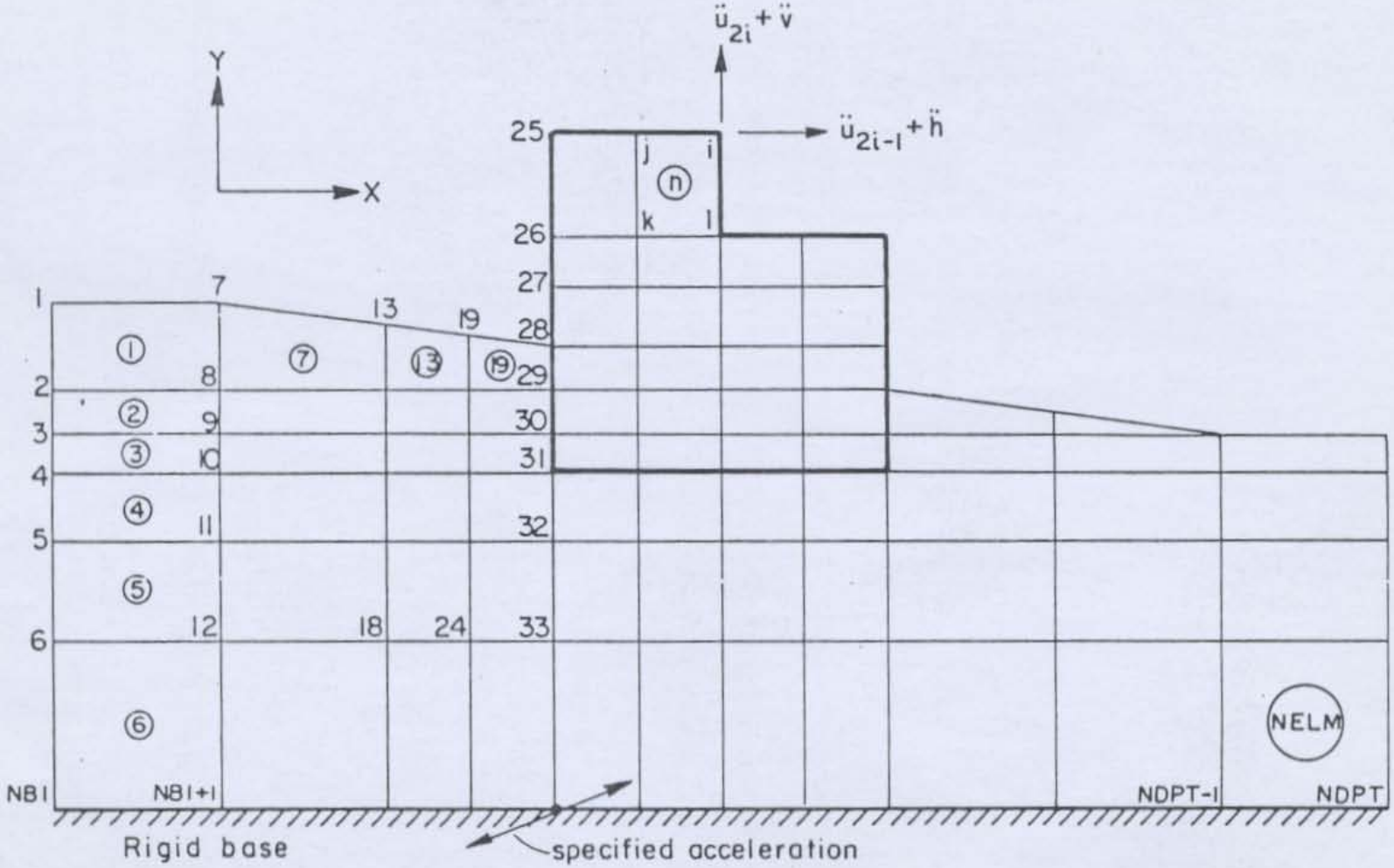

FIG. B.1 TYPICAL FINITE ELEMENT MODEL FOR LUSH [62]

amplitude in each element. Typical relationships between stiffness, damping and effective shear strains for sand and clay are provided within the programme (Table B.1).

The mass distribution within the model can be either distributed (consistent mass matrix) or concentrated at the nodal points (lumped mass matrix), or it can be any combination of these choices.

Many options are available for output which may consist of time histories or response spectra for selected nodal points. A special option provides for a permanent record on magnetic tape of both input and basic information on the complete solution.

Equations of Motion

Equations of motion and the numerical procedure followed by LUSH to solve these equations are described in Chapter III.

Summary of Numerical Procedure

The following is a summary of the procedure as it is used in LUSH. Only the most basic operations are included.

A. Define input motion

   Transform to frequency domain

B. Define finite element model

   1. Nodal points

   2. Boundary conditions

   3. Elements

   4. Estimate material properties

C. Form mass matrix

D. Form stiffness matrix

E. Determine amplification functions

Table B.1 - Strain-compatible Soil Properties. [45]

Effective Shear Strain γ_{eff} (%)	log (γ_{eff})	Shear Modulus Reduction Factor*		Fraction of Critical Damping (%)	
		Clay	Sand	Clay	Sand
$\leq 1. \times 10^{-4}$	-4.0	1.000	1.000	2.50	0.50
3.16×10^{-4}	-3.5	0.913	0.984	2.50	0.80
1.00×10^{-3}	-3.0	0.761	0.934	2.50	1.70
3.16×10^{-3}	-2.5	0.565	0.826	3.50	3.20
1.00×10^{-2}	-2.0	0.400	0.656	4.75	5.60
3.16×10^{-2}	-1.5	0.261	0.443	6.50	10.0
1.00×10^{-1}	-1.0	0.152	0.246	9.25	15.5
0.316	-0.5	0.076	0.115	13.8	21.0
1.00	0.	0.037	0.049	20.0	24.6
3.16	0.5	0.013	0.049	26.0	24.6
≥ 10.00	1.0	0.004	0.049	29.0	24.6

*This is the factor which has to be applied to the shear modulus at low shear strain amplitudes (here defined as 10^{-4} percent) to obtain the modulus at higher strain levels.

1. Solve Eqn. 3.12 for required frequencies
2. Interpolate in frequency domain

F. Determine effective shear strains in all elements
1. Compute strains in frequency domain
2. Convert to time domain
3. Determine γ_{eff} = factor x γ_{max}

G. Compute strain-compatible soil properties
1. Enter Table B.1 for all elements
2. Compare with properties used in analysis
a. If differences too large, repeat analysis from D. with new properties
b. If differences small, go to H.

H. Convert displacements to time domain

I. End of analysis.

B.2 PROGRAMME SHAKE [81]

Programme SHAKE computes the responses in a system of homogeneous, viscoelastic layers of infinite horizontal extent subjected to vertically travelling shear waves. The system is shown in Fig. B.2. The programme is based on the continuous solution to the wave-equation adapted for use with transient motions through the Fast Fourier Transform algorithm [24] is accounted for by the use of equivalent linear soil properties [82] using an iterative procedure to obtain values for modulus and damping compatible with the effective strains in each layer. The following assumptions are implied in the analysis:

1. The soil system extends infinitely in the horizontal direction.
2. Each layer in the system is completely defined by its value of

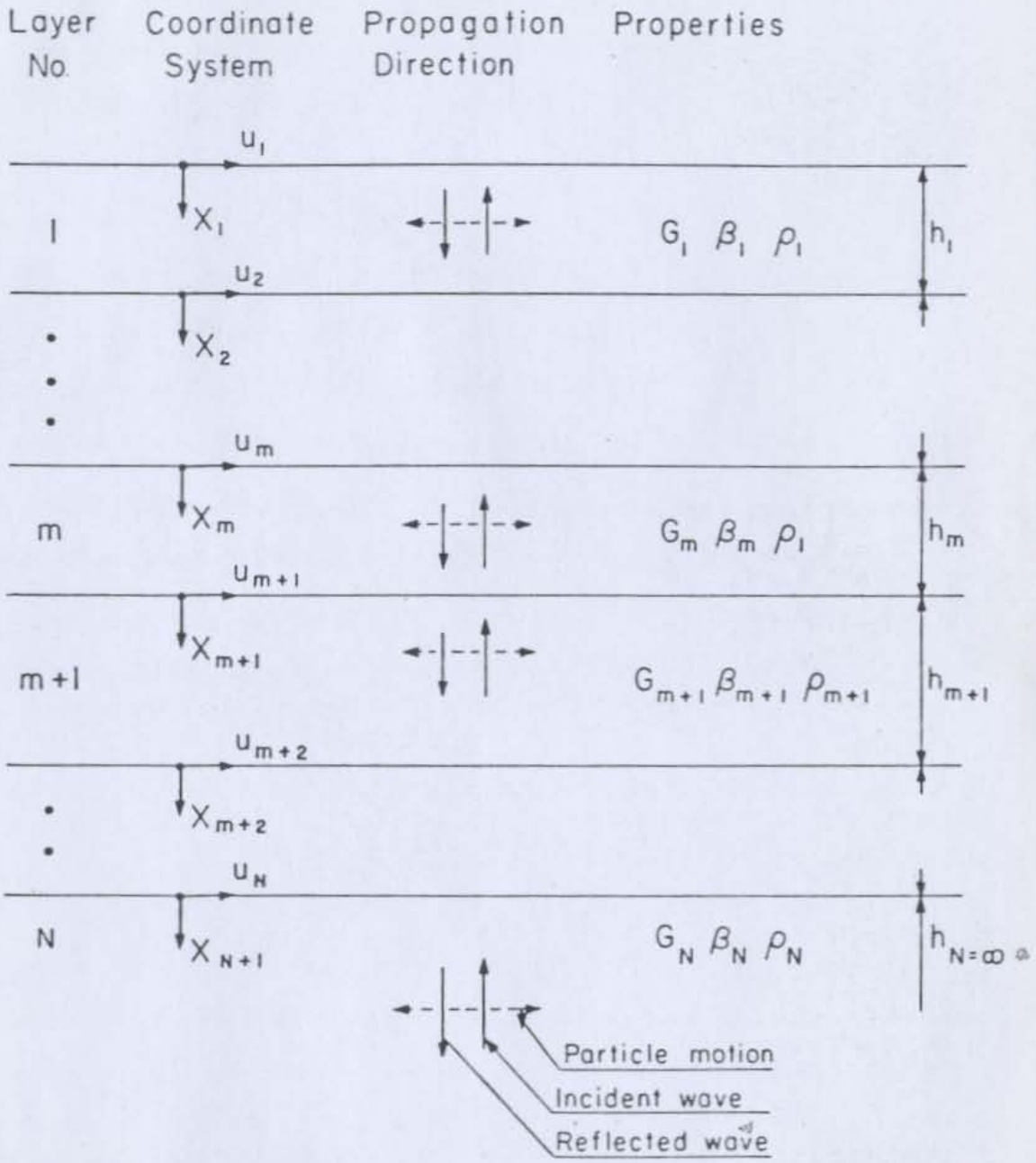

FIG. B.2 ONE DIMENSIONAL SYSTEM FOR SHAKE [81].

shear modulus, critical damping ratio, density, and thickness. These values are independent of frequency.

3. The responses in the system are caused by the upward propagation of shear waves from the underlying rock formation.
4. The shear waves are given as acceleration values of equally spaced time intervals. Cyclic repetition of the acceleration time history is implied in the solution.
5. The strain dependence of modulus and damping is accounted for by an equivalent linear procedure based on an average effective strain level computed for each layer.

The programme is able to handle systems with variation in both moduli and damping and takes into account the effect of the elastic base. The motion used as a basis for the analysis, the object motion, can be given in any one layer in the system and new motions can be computed in any other layer.

The following set of operations can be performed by SHAKE:

1. Read the input motion, find the maximum acceleration, scale the values up or down, and compute the predominant period.
2. Read data for the soil deposit and compute the fundamental period of the deposit.
3. Compute the maximum stresses and strains in the middle of each sublayer and obtain new values for modulus and damping compatible with a specified percentage of the maximum strain.
4. Compute new motions at the top of any sublayer inside the system or outcropping from the system.
5. Print, plot and punch the motions developed at the top of any sublayer.

6. Plot Fourier Spectra for the motions.
7. Compute, print and plot response spectra for motions.
8. Compute, print and plot the amplification function between any two sublayers.
9. Increase or decrease the time interval without changing the predominant period or duration of the record.
10. Set a computed motion as a new object motion. Change the acceleration level and predominant period of the object motion.
11. Compute, print and plot the stress or strain time-history in the middle of any sublayer.

These operations are performed by exercising the various available options in the programme.

REFERENCES

1. Agbabian-Jackson Associates, "A Study of Earthquake Input Motion for Seismic Design", Los Angeles, June 1970.

2. Ali-Akbarian, M., and Johnson, J., University of Illinois, Technical Report No. AFWL-TR-69-56, Air Force Weapons Laboratory, New Mexico, July 1969.

3. Allgood, J.R., "Structure in Soil Under High Loads", American Society of Civil Engineers, Proceedings, Journal of the Soil Mechanics and Foundations Division, Vol. 97, No. SM3, Mar. 1971, pp. 565-579.

4. Allgood, J.R., "Balanced Design and Finite Element Analysis of Culverts", paper presented at 51st Annual Meeting, Highway Research Board, Washington, D.C., Jan. 17-21, 1972.

5. Allgood, J.R., "Summary of Soil-Structure Interaction", Technical Report R-771, Y-F008-08-02-108, DNA 13.018, Naval Civil Eng. Laboratory, Port Hueneme, California 93043, July 1972.

6. Atkinson, J.H., and Cairncross, A.M., "Collapse of a Shallow Tunnel in a Mohr-Coulomb Material", Proc. Symp. on the Role of Plasticity in Soil Mechanics, Cambridge, 1973, pp. 202-206.

7. Atkinson, E.T., Brown, E., and Potts, M., "Collapse of Shallow unlined Tunnels in Dense Sand", Tunnel and Tunnelling, May 1975, pp. 81-87.

8. Beck, C., "Engineering Study on Underground Construction of Nuclear Power Reactors", USAEC, AECU-3779, April 15, 1958.

9. Benson, R.P., Kierans, T.W., and Sigvaldason, O.T., "In situ and Induced Stresses at the Churchill Falls Underground Powerhouse", Labrador, Second Congress of the International Society of Rock Mechanics, Belgrade, Yugoslavia, Sept. 1970.

10. Berger, E., Lysmer, J., and Seed, H.B., "Comparison of Plane Strain and Axisymmetric Soil-Structure Interaction Analyses", Proc. 2. ASCE Spec. Conf. on Struc. Design of Nuclear Plant Facilities, New Orleans (1975), Vol. 1-A, pp. 809-825.

11. Bielak, J., "Dynamic Behaviour of Structures with Embedded Foundations", Earthquake Eng. Struct. Dyn. 3, (1975), pp. 259-274.

12. Bjerrum, L., Frimann Clausen, C.J., and Duncan, J.M., "Earth Pressures on Flexible Structures", (A State-of-the-art Report), Norwegian Geotech. Inst. Pub. No. 91, Oslo, 1972, pp. 1-28.

13. Blake, A., Karpenko, V.N., McCauley, E.W., and Walter, C.E., "A Concept for Underground Siting of Nuclear Power Reactors", Lawrence Livermore Lab., Rep. UCRL-51408, 1973.

14. Blakey, L.H., "Dynamic Response of Reinforced Openings in Rock", Ph.D. Thesis, The Catholic University of America, 1971.

15. Brekke, T.L., and Glass, C.E., "Some Considerations Related to Underground Siting of Nuclear Power Plants in Rock", Department of Soil Engineering, University of California, March 1973.

16. Buclin, J.C., "Comments re the Article on Underground Nuclear Plant Siting", Nuclear Safety, Vol. 16, No. 4, July-August 1975, pp. 434-435.

17 Bulson, P.S., "Blast Loading of Buried Square Tubes", Vib. in Civil Engineering, (Proc. Sym), Butterworths, London, 1966, pp. 229-234.

18. Burns, J.Q., "An Analysis of Circular Cylindrical Shells embedded in elastic media", Ph.D. Thesis, University of Arizona, Tucson, Ariz., 1965.

19. Castellani, A., "Boundary Conditions to Simulate an Infinite Space", Meccanica, Journal of the Italian Association of Theoretical and Applied Mechanics AIMETA, Vol. 9, No. 3, Sept. 1974, pp. 188-205.

20. Chang, C.Y., Nair, K., and Karwoski, W.J., Proc. Conf. Appl. Finite Element Method in Geotech. Eng., Vicksburg, Miss., 1972, pp. 457-504.

21. Chester, R.O., and Chester, C.V., "A protective Containment System for Large Nuclear Power Plants", 18th Annual Health Physics Society, Paper 20, June 17, 1973-Also CONF-730603.

22. Czéchy, K., "The Art of Tunnelling", Second English Edition, Akademiai Kindo, Budapest, 1973.

23. Clough, G.W., "Application of the Finite Element Method to Earth-Structure Interaction", Proc. of the Symposium held at Vicksburg, Mississippi, May 1972, pp. 1057-1116.

24. Cooley, J.W., and Tukey, J.W., "An Algorithm for the Machine Calculation of Complex Fourier Series", Mathematics of Computation, Vol. 19, No. 90, 1965, pp. 297-301.

25. Costantino, C.J., and Mariano, R.L. Jr., "Response of Cylindrical Shells Encompassed with Isolation Material to a Plane Pressure Pulse", Illinois Institute of Technology, Chicago, Illinois, Report No. AFWL-TR-65-122, Feb. 1966.

26. Costantino, C.J., and Lvfrano, L., "Finite Element Analysis for Soil Amplification Studies", ASCE Spec. Conf. on Struct. Design of Nuclear Plant Facilities, Chicago, Dec. 1973.

27. Costantino, C.J., Miller, C.A., and Lufrano, L.A., "Soil-Structrue Interaction Parameters from Finite Element Analysis", Nuclear Eng. and Design, Vol. 38, No. 2, August 1976, pp. 289-302.

28. Coulomb, C.A., "Esai sur une Application des Ragles de Maximis et Mininis a quelques Problems du Statique", Memories Academic Royal des Science, Vol. 7, Paris, 1776.

29. Crowley, D., and McCreath, "Underground Nuclear Plant Siting", Nuclear Safety, Vol. 15, No. 5, pp. 519-534.

30. Dawkins, W.P., "Dynamic Response of a Tunnel liner-packing system", Ph.D. Thesis, University of Illinois, Urbana, 1966.

31. Deere, D.V., Peck, R.B., Monsees, J.E., and Schmidt, B., "Design of Tunnel Liners and Support Systems", Report for V.S. Dept. of Transportation, OHSGT Contract 3-0152, No. PB 183-799, 1969, pp. 287.

32. Drucker, D.C., "Limit Analysis of Two and Three Dimensional Soil Mechanics Problems", Journal Mechanics and Physics of Solids, Vol. 1, 1953, pp. 217-226.

33. Farhoomand, I., "Nonlinear Dynamic Stress Analysis of two-dimensional Solids", Ph.D. Thesis, Dept. of Civil Eng., University of California, Berkeley, Calif., Sept. 1970.

34. Finn, W.D.L., "Boundary Value Problems of Soil Mechanics", Journal of the Soil Mechanics and Foundations Division, ASCE, Vol. 89, No. SM5, 1963, pp. 39-72.

35. Forrestal, M.J., Reddy, D.V., and Herrmann, G., American Society of Civil Engineering, EMD 91, Proc. Paper 4354, 1965, pp. 1-11.

36. Ghaboussi, J., Wilson, E.L., and Isenberg, J., J. Soil Mechanics Foundation Division, Proc. ASCE 99 (SM10), Oct. 1973, pp. 833-848.

37. Ghaboussi, J., and Ranken, R.E., Final Report for Dept. Transportation, Fedral Railroad Admn. No. FRA-ORDFO 75-24, Nov. 1974.

38. Glass, C.E., "Seismic Considerations in Siting Large Underground Openings in Rock", Ph.D. Thesis, University of California, Berkeley, 1974.

39. Hall, J.R., Jr., and Kissenpfennig, J.F., "Special Topics on Soil-Structure Interaction", Nuclear Engineering and Design, Vol. 38, No. 2, August 1976, pp. 273-288.

40. Hansen, J.B., Earth Pressure Calculation, The Danish Technical Press, The Institution of Danish Civil Engineers, Copenhagen, 1953.

41. Heale, D.G., and Reddy, D.V., "Response of a Spherical Cavity to a Plane Wave", Proc. Fifth Can. Cong. App. Mech., Fredericton, May 1975, pp. 307-308.

42. Hentenyi, M., Beams on Elastic Foundations, University of Michigan Press, Ann Arbor, Michigan, 7th Ed., 1964.

43. Holmes and Narver, Inc., "California Power Plant Siting", HN-81452, Anaheim, California 1973 - also Nuclear News. Oct. 1973.

44. Howard, G.E., Ibàñez, P., and Smith, C.B., "Seismic Design of Nuclear Power Plants - An Assessment", Nuclear Engineering and Design, Vol. 38, No. 3, Sept. 1976, pp. 385-462.

45. Idriss, I.M., Dezfulian, H., and Seed, H.B., "Computer Programes for Evaluating the Seismic Response of Soil Deposits with Non-Liner Characterisitics Using Equivalent Linear Procedure", Research Report Geotechnical Engineering, University of California, Berkeley, Calif., 1969.

46. Idriss, I.M., Lysmer, J., Hwang, R., and Seed, H.B., "QUAD-4, A Computer Program for Evaluating the Seismic Response of Soil-Structures by Variable Damping Finite Element Procedures", Report No. EERC 73-16, Col. of Engg., Univ. of Calif., Berkeley, Calif., July 1973.

47. Idriss, I.M., and Khosrow Sadigh, A.M., "Seismic SSI of Nuclear Power Plant Structures", Journal of the Geotechnical Engineering Division, ASCE, Vol. 102, No. GT7, July 1976, pp. 663-682.

48. James, R.G., and Bransby, P.L., "Experimental and Theoritical Investigations of a Passive Earth Pressure Problem", Geotechnique, Vol. 20, No. 1, 1970.

49. Kanai, K., "Observation of Strong Earthquake Motion in Matsushiro Area", Part I, Bull. ERI, Vol. 44, 1966, pp. 1269-1296.

50. Kanai, K., Osada, K., and Yoshizawa, S., "Observational Study of Earthquake Motion in depth of Ground", V, Bulletin, Earthquake Research Institute, Tokyo University, Vol. 32, 1954, pp. 361-371.

51. Kierans, T.W., Reddy, D.V., and Heale, D.G., "Dynamic Analysis and Structural Design of Primary Underground Nuclear Facilities", Draft for the Seismic Task Group of the ASCE Committe for Nuclear Facilities, Meeting at Atlanta, Georgia, October 1973.

52. Krishna, J., and Arya, A.S., "Building Construction in Seismic Zones of India", Proceedings, Second Symposium on Earthquake Engineering, November 10-12, 1962.

53. Kröger, W., Altes, J., and Schwarzer, K., "Underground Siting of Nuclear Power Plants with Emphasis on the 'cut-and-cover' Technique", Nuclear Engineering and Design, Vol. 38, No. 2, August 1976.

54. Kröger, W., Altes, J., Escherich, K.H., and Kasper, K., "Cut-and-Cover' Design of a Commercial Nuclear Power Plants", 4th International Conference on Structural Mechanics in Reactor Technology, San Francisco, August 14-19, 1977.

55. Kuhlemeyer, R.L., and Lysmer, J., "Finite Element Method Accuracy for Wave Propagation Problems", Journal of the soil Mechanics and Foundations Division, ASCE, Vol. 99, No. SM5, May 1973, pp. 421-471.

56. Kuhlemeyer, R.L., "Vertical Vibrations of Footings Embedded in Layered Media", Ph.D. Thesis, University of California, Berkeley, 1969.

57. Kulhawy, F.H., "Finite Element Modeling Criteria for Underground Opening in Rock", Int. J. Rock Mech. Min. Sci. & Geomech. Abst. Vol. II, December 1974, pp. 465-472.

58. Kulhawy, F.H., "Stresses and Displacements around Openings in Homogeneous Rock", Int. J. Rock Mech. Min. Sci. & Geomech. Abst., Vol. 12, 1975, pp. 43-57.

59. Kulhawy, F.H., "Stresses and Displacements around Openings in Rock Containing an Inelastic Discontinuity", Int. J. Mech. Min. Sci. & Geomech. Abst., Vol. 12, 1975, pp.73-78.

60. Lee, K.L., Adams, B.D., and Vagheron, J.J., "Reinforced Earth Retaining Walls", Journal of the Soil Mechanics and Foundations Division, ASCE, Vol. 99, No. SM10, Proc. Paper 10068, Oct. 1973, pp. 745-763.

61. Luco, J.E., and Hadjian, A.H., "Two Dimensional Approximation to the Three-Dimensional Soil-Structure Interaction Problem", Nuclear Engineering and Design, Vol. 31, 1974, pp. 195-203.

62. Lysmer, J., Udaka, T., Seed, H.B., and Hwang, R., "LUSH-A Computer Program for Complex Response Analysis of Soil-Structure Systems", Report No EERC 74-4, Earthquake Engineering Research Center, University of California, Berkeley, Calif., April 1974.

63. Mithal, R.S., and Srivastava, L.S., "Behaviour of Soils During Seismic Disturbance", Proceeding of Second Symposium on Earthquake Engineering, November 1962, pp. 131-152.

64. Moselhi, O.E., "Finite Element Analysis of Dynamic Structure-Medium Interaction with some Reference to Underground Nuclear Reactor

Containment", M. Eng. Thesis, Memorial Univ., St. John's, Newfoundland, August 1975.

65. Murthy, G.K.N., and Reddy, D.V., Nuclear Engineering and Design, Vol. 5, No. 4, 1967, pp. 426-432.

66. Nasu, N., "Comparative Studies of Earthquake Motions Aboveground and in a Tunnel", Bull. ERI, Vol. 9, 1931, pp. 454-472.

67. Norsk Hydro, "Nuclear Power Plant in Norway - A Project Study", NVE-Statskraftver Kene, Institute for Atomenergi, Vol. 1, Summary Report.

68. Nosseir, A.B., Takahashi, S.K., and Crawford, J.E., "Stress Analysis of Multicomponent Structures", Tech. Report R-743, Port Hueneme, Calif., Oct. 1971.

69. Novak, M., and Beredugo, Y., "The Effect of Embedment on Footing Vibrations", Proc. 1st Can. Conf. Earthquake Eng. Res., Univeristy of British Columbia, Vancouver, 1971, pp. 111-125.

70. Oak Ridge National Laboratory, "Preliminary Concepts of Subsurface Reactor Containment Structure to Withstand Differential Earth Displacement", SD-71-66 (R)-587, August 1966.

71. Okamoto, S., "Introduction to Earthquake Engineering", University of Tokyo Press, Tokyo, Japan, 1973.

72. Peck, R.B., "Deep Excavations and Tunneling in Soft Ground", Proceedings, 7th International Conference on Soil Mechanics and Foundation Engineering, State-of-the-Art-Volume, 1969, pp. 225-290.

73. Rankine, W.J., "On the Stability of Loose Earth", Transactions, Royal Society, London, Vol. 147, 1857.

74. Reddy, D.V., and Heale, D.G., "Interaction of Plane Elastic Waves with an Embedded Circular Cylindrical Shell", Proc. 13th Int. Congr. of Theoritical and Applied Mechanics, Moscow, August 1972.

75. Reddy, D.V., and Kierans, T.W., "Dynamic Analysis for Design Criteria For Underground Nuclear Reactor Containment", Nuclear Engineering and Design, Vol. 38, No. 2, August 1976, pp. 177-206.

76. Richardson, G.N., and Lee, K.L., "Seismic Design of Reinforced Earth Walls", Journal of the Geotechnical Eng. Division, ASCE, Vol. 101, No. GT2, Proc. Paper 11143, Feb. 1975, pp. 167-188.

77. Rogers, F.C., "Underground Nuclear Power Plant: Environmental and Economic Aspects", Nuclear News, May 1971.

78. Romstad, K.M., Herrmann, L.R., and Shen, C.K., "An Integrated Study of Reinforced Earth - I: Theoritical Formulation", Journal of the Geotechnical Eng. Division, ASCE, Vol. 102, No. GT5, Proc. Paper 12144, May 1976, pp. 457-471.

79. Rowe, P.W., and Peaker, K., "Passive Earth Pressure Measurements", Geotechnique, Vol. XV, No. 1, March 1965.

80. Saita, T., and Suzuki, M., "On the Upper Surface and Underground Seismic Disturbance at the Downtown in Tokyo", Bull., ERI, Vol. 12, 1934, pp. 517-526.

81. Schnabel, P.B., Lysmer, J., and Seed, H.B., "SHAKE-A Computer Program for Earthquake Response Analysis of Horizontally Layered Sites", Report No. EERC 72-12, Earthquake Engineering Research Center, University of California, Berkeley, Calif., Dec. 1972.

82. Seed, H.B., and Idriss, I.M., "Soil Moduli and Damping Factors For Dynamic Response Analysis", Report No. EERC 70-10, Earthquake Engineering Research Center, College of Eng., Univ. of California, Berkeley, Calif., 1970.

83. Seed, H.B., Lysmer, J., and Hwang, R., "Soil-Structure Interaction Analyses for Seismic Response", Journal of the Geotechnical Engineering Division, ASCE, Vol. 101, No. GT5, Proc. Paper 11318, May 1975, pp. 439-457.

84. Sheha, S.A., "Static and Dynamic Analysis of Underground Cavities with some reference to Nuclear Reactor Containments", M. Eng. Thesis, Memorial University of Newfoundland, St. John's, August 1975.

85. Shen, C., Romstad, F.M., and Herrmann, L.R., "Integrated Study of Reinforced Earth-II", Journal of the Geotechnical Eng. Division, ASCE, Vol. 102, No. GT6, Proc. Paper 12210, June 1976, pp. 577-590.

86. Sigvaldason, O.T., Benson, R.P., and Thomson, M.V., "Stress Analysis of Underground Openings in Rock Using the Finite Element Method", Ann. Conf. of the Engineering Institute of Canada, Halifax, May 1968.

87. Smernoff, B.J., "Underground Siting of the LMFBR Demonstration Plant: A Serious Alternative", HI-1686/2-p, Hudson Institute, Sept. 12, 1972. Also Hearings before the Joint Committee on Atomic Energy, Sept. 7, 8 and 12, 1972, pp. 131-141 and 259-263.

88. Sokolovski, V.V., Statics of Granular Media, Translated from Russian by J.K. Luscher, Pergamon Press, London, 1965.

89. Swiger, V.F., "Can We Place Nuclear Power Plants Underground?", Presented at the Geological Society of America, Washington, D.C., No. 1971.

90. Tajimi, H., "Dynamic Analysis of a Structure Embedded in an Elastic Stratum", Proc. 4th World Conf. on Earthquake Eng. Santiago, Chile, 1969, Session A-6, pp. 53-69.

91. Tandon, A.N., "Assessement of Maximum Seismic Intensity and Ground Acceleration", Proceeding, Second Symposium on Earthquake Engineering, University of Roorkee, India, 1962.

92. Terzaghi, K., "Record Earth-Pressure Testing Machine", Engineering News Record, Vol. 109, Sept. 1932.

93. Terzaghi, K., "Large Retaining Wall Tests. I. Pressure of Dry Sand", Engineering News Reocrd, Vol. III, Feb. 1934.

94. Terzaghi, K., "A Fundamental Fallacy in Earth Pressure Computations", Journal of the Boston Society of Civil Engineers, Vol. 23, 1936.

95. Trulio, AFWL-TR-66-19, Air Force Weapons Testing Laboratory, June 1966.

96. United Engineers and Acres American, "Underground Nuclear Power Plants - A Preliminary Evaluation", July 1971.

97. United Engineers and Acres American, "Review of Underground siting of Nuclear Power Plants", UEC-AEC-740/07, January 1974.

98. Watson, M.B., Kammer, W.A., Langley, N.P., Selzer, L.A., and Beck, R.L., "Underground Nuclear Power Plant Siting", Report No. 6, Cal. Tech. Sept. 1972; also Nucl. Eng. Design Vol. 33, 1975, pp. 269-307.

99. Wilson, E.L., "A Computer Program for the Dynamic Stress Analysis of Underground Structures", Report No. 68-1, Structural Eng. Laboratory, Univ. of California, Berkeley, Calif., Jan. 1968.

100. Wilson, E.W., "A General Structural Analysis Program", Structural Eng. Laboratory, Univ. of California, Berkeley, Calif., Sept. 1970.

101. Yoshihara, T., Robinson, R.A., and Merritt, J.L., Civil Eng. Stud., S.R.S. No. 261, Univ. Ill., 1963.

102. Yu, Y.S., and Coates, D.F., Research Report R.198, Department of Energy, Mines and Resources, Ottawa, July 1969.